Intracellular ROS Generation under Adrenergic Stimulation and its Effect on Downstream Events

Thesis submitted to Jawaharlal Nehru University
for the award of the degree of

Doctor of Philosophy

NIKHAT SALEEM

Molecular Cardiology Laboratory
School of Life Sciences
Jawaharlal Nehru University
New Delhi –110067

2017

SCHOOL OF LIFE SCIENCES
JAWAHARLAL NEHRU UNIVERSITY
NEW DELHI-110067
INDIA

CERTIFICATE

I hereby declare that the research work embodied in this thesis entitled **"Intracellular ROS Generation under Adrenergic Stimulation and its Effect on Downstream Events"** has been carried out by myself under the supervision of Professor Shyamal K. Goswami, at the School of Life Sciences, Jawaharlal Nehru University, New Delhi, India. This work is original and has not been submitted so far, in part or full, for the award of any degree or diploma of any university.

Nikhat

Nikhat Saleem
(Candidate)

13.6.17

Prof. Shyamal K. Goswami
(Supervisor)

(Dean)

2017

To

My Parents……

CONTENTS

"So indeed, with the hardship, there is relief" Quran 94:5

First and foremost, I would thank the Almighty ALLAH for all HIS blessings and giving me the patience and strength I needed to carry on.

This work would not have been possible without the invaluable academic, environmental and psychological support provided by people around me.

I am grateful to my family for their myriad love, belief and tolerance. Thank you Ammi and Papa ji, the angels of my life. Thanks to my wonderful brothers who are forever set to take my wishes. I am grateful to my sisters- in- law and the kids of our family.

I express my sincerest gratitude to my supervisor Prof. Shyamal K. Goswami for giving me the opportunity to encounter with the real world of life science. Thank you Sir for your constant guidance, motivation, patience and for the freedom you give us during the work. Thanks a lot sir for everything.

I thank the current Dean, SLS, Prof. Shyamal K. Goswami and the previous Deans, Prof. R. Madhubala, Prof. Neera Bhalla Sarin, Prof. B. N. Mallick and Prof. B. C. Tripathy for providing me the necessary infrastructure and facilities to carry out this work.

I thank all the teachers at School of Life Sciences, JNU.

I am thankful to Dr. Manish Sharma (DIPAS, DRDO, New Delhi) for his valuable suggestions and providing the opportunity to work with him. Thank you sir for making me feel as I am working in my own lab.

I would like to extend my gratitude to Prof. S. K. Maulik (AIIMS, New Delhi) for providing the Echocardiography facility.

I would also like to acknowledge all the previous and current staff of SLS administrative office. I am thankful to the members of Central Instrument Facility (CIF) and Advanced Instrumentation Research Facility (AIRF), JNU specially Joginder ji for all his help. A special thanks to Tripti (CIF) for helping me in operating fluorescence microscope and solving my queries about.

Thanks is inadequate to extend my gratitude towards all my lab members. I would like to thanks my seniors Anita di, Indrani di, Ekta di, Pooja di, Goutam

sir, Santosh sir, Sangeeta di and Jahangir sir, my batchmate and friend Shweta and the juniors Buddhi, Arti, Anamika, Richa and Padmini for all their help. I am in-depth of the unconditional affection shown by Ekta di. You are one of the most amazing persons I have ever met. A very special thanks to Pooja di for all her care and precious advices. My heartfelt thanks to Goutam sir for introducing me with the lab techniques and all his support. I am grateful to Jahangir sir for all his help whenever I needed to resolve the problems during this work. Thank you so much sir. Thank you very much Buddhi for the valuable discussion we had. A special thanks to Anamika for always being there to support me. I am very much thankful to my chatter box partner Richa for accompanying me whenever I needed. I would like to extend my thanks to Anupam sir for his suggestions and technical tricks.

I would also like to acknowledge the dissertation students; Neetu, Arshdeep, Manoj, Purnima, Richa, Sagrika, Ankita, Srujana, Tripti, Mamta, Himanshi and specially Rashmi and Sukhman for their help.

I would also like to thank Suresh ji, Ramkripal ji, Amlendu and Rajiv ji for all their help to carry out my work.

I am grateful to Pankaj sir for assisting in Echocardiography at AIIMS and solving my queries about. I am very much thankful to Aastha for her help, discussion and the light moments we shared during my work at DIPAS.

I take this opportunity to acknowledge the gems of my life, 'my friends'. Loads of thanks to Savita and Maher for always being there to bear my frustration and encouraging me and making me believe that everything is going to be alright. A special thanks to my childhood friend Meenakshi for all the memories we share. I am highly thankful to my 'tapori gang'- Meghna, Nilofer, Munazah, Tapan and Nitesh. You people made my stay in JNU a memorable one. I will miss all our Delhi darshan trips, the conferences and our surprise dinner treats.
I am running out of words to express my gratitude towards you Munazah. You were there as a rock solid support during the toughest time I had here. I will always cherish the thick and thin moments we shared.

Acknowledgements

I am thankful to my hostelmates; caring and affectionate Vijeta di and Noor aapi, my dear friend Shilpi, loving juniors Sumita and Nalini and my 'humnaam' Nikhat.

I would also like to thanks my 'Halqah' friends Juveria, Aina, Shabista, Farah, Fauzia and Putri and 'Ramzan' partners Munazah, Razeena, Nazia and Benhar.

I thank Indian Council of Medical Research for providing me fellowship during my work.

Last but not the least, my sincere acknowledgement to Jawaharlal Nehru Univeristy, for the beautiful environment it provides to all its inhabitants.

I apologize to those whom I have missed to mention and acknowledge by name.

Nikhat

%	Percentage
˚C	Degree Celsius
α-MHC	α-Myosin heavy chain
β-MHC	β-Myosin heavy chain
µg	Micro gram
µL	Micro liter
µm	Micro meter
µM	Micro molar
ACTA-1	Actin, alpha skeletal muscle
ANP	Atrial natriuretic peptide
AP-1	Activator protein-1
Apo	Apocynin
APS	Ammonium persulphate
ATP	Adenosine Tri Phosphate
BNP	Brain/ventricular natriuretic peptide
bp	base pairs
BSA	Bovine Serum Albumin
cDNA	complementary DNA
CREB	cAMP response element-binding protein
DCFH-DA	2',7'-dichlorfluorescein-diacetate
DEPC	Diethyl pyrocarbobate
DHE	Dihydroethidium
DMEM	Dulbecco's Modified Eagle's Medium
DMSO	Dimethyl sulfoxide
DNA	Deoxyribonucleic Acid
dNTP	deoxyribonucleoside Triphosphate
DTT	Dithiothreitol
ECL	Enhanced chemiluminscence
EDTA	Ethylene diamine tetra acetic Acid
ER	Endoplasmic reticulum
ERK	Extracellular regulated kinase
ETC	Electron transport chain

FAD	Flavin adenine dinucleotide
FBS	Fetal Bovine Serum
FosB	FBJ murine osteosarcoma viral oncogene homolog B
g	Gram
GAPDH	Glyceraldehyde-3-phosphate dehydrogenase
hr	Hours
H_2O_2	Hydrogen peroxide
HRP	Horseradish peroxidase
Iso	Isoproterenol
kb	Kilo base pairs
kDa	kilo Dalton
kg	Kilo gram
L	Liter
LB	Lysogeny Broth
LV	Left ventricle
MALDI	Matrix associated laser desorption/ionisation
MAPK	Mitogen activated protein kinase
mg	Mili gram
min	Minutes
mL	Milli liter
mm	Milli meter
mM	Milli molar
mRNA	Messenger RNA
NaCl	Sodium chloride
NADPH	Nicotineamide adenine dinucleotide phosphate
NaOH	Sodium hydroxide
NE	Norepinephrine
ng	Nanogram
nm	nano-meter
nM	nano Molar
NOS	Nitric oxide synthase
Nox	NADPH oxidase

$O_2^{\bullet-}$	Superoxide
OD	Optical density
ORF	Open reading frame
PAGE	Poly Acrylamide Gel Electrophorosis
PBS	Phosphate Buffered Saline
PCR	Polymerase chain reaction
PMSF	Phenyl Methyl Sulfonyl Fluoride
PKA	Protein kinase A
PVDF	Polyvinylidene fluoride
ROS	Reactive oxygen species
RNA	Ribonucleic Acid
rpm	Revolutions per minute
sec	Seconds
SDS	Sodium Dodecyl Sulfate
SOD	Superoxide dismutase
TAE	Tris acetate EDTA buffer
TBS	Tris Buffered Saline
TEMED	N,N,N,N-Tetramethylethylenediamine
Tris	Tris (hydroxymethyl)-aminomethane
UV	Ultra violet
v/v	Volume/volume
w/v	Weight/volume

Introduction

Cardiovascular diseases (CVDs) are the leading cause of death worldwide. An estimated ~17.3 million people died from CVDs in 2013, which represents 31% of all global deaths. By 2030, the number is expected to grow to >23.6 million. CVDs are a group of disorders of the heart and blood vessels that include coronary (ischemic) heart disease, rheumatic heart disease, hypertension, diseases of pulmonary circulation, stroke, atherosclerosis and other arterial diseases etc (Mozaffarian *et al.*, 2016).

A. Sympathetic nervous system and heart failure

The final common pathway of many of the CVDs is heart failure. Heart failure is a pathological condition in which there is impairment in the ability of the ventricle to fill with or eject blood. It is thus unable to pump enough blood to meet the metabolic demands of the body. To preserve the cardiac output, the heart manifests a robust plasticity response termed "cardiac remodeling", which is a complex series of structural and functional reorganization leading to changes in shape and volume of the heart. Cardiac remodeling involves altered transcriptional, electrophysiological, and signaling activities. Although, initially these changes are compensatory but eventually it becomes part of the disease process itself, further worsening the cardiac dysfunctions (Figure 1) (Hill & Olson, 2008; Burchfield *et al.*, 2013).

Among the compensatory neurohumoral mechanisms, activation of sympathetic nervous system (SNS) and inhibition of parasympathetic nervous system (PSNS) have long been attributed to cardiac dysfunctions. The sympathetic and parasympathetic systems (collectively termed autonomic nervous system [ANS]), work in a fine-tuned, yet opposing fashion in the heart (Lymperopoulos *et al.*, 2013). The contrasting effects are mediated by release of catecholamines such as norepinephrine (NE) and epinephrine (EPI). Sympathetic nerve endings release NE directly into the synaptic cleft while chromaffin cells of adrenal medulla synthesize, store and release EPI and NE predominantly upon stimulation. NE transporter 1 recycle ~80% of NE released by the synaptic nerve endings and the remainder clears into circulation. In response to increased cardiac load, there is increased release and decreased uptake of NE at nerve endings, thus help maintaining the cardiac output. However, long term SNS hyperactivity may account for further increase in cardiovascular risk (Leineweber *et al.*, 2002; Triposkiadis *et al.*, 2009; Florea & Cohn, 2014). Plasma NE level provides a better index of cardiac performance and ~50-fold increase in NE spillover is found in heart failure patients. Increased circulating NE may result in hypertension, myocardial infarction, shock and multisystem failure (Meredith *et*

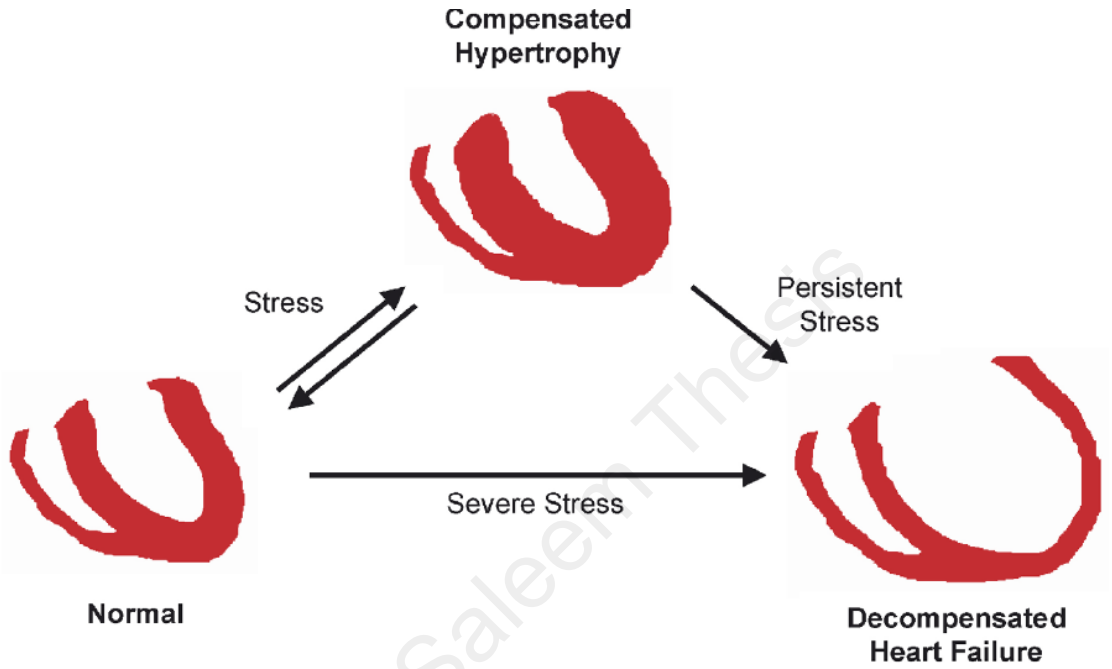

Figure 1. Paradigm of left ventricular remodeling: Moderate stress triggers compensatory hypertrophic response, which eventually may lead to heart failure under prolonged stress.

Adapted from Berry et al., (2007) Drug Discovery Today: Disease Models

al., 1993; Morris *et al.*, 1997; Grassi *et al.*, 2009; Prejbisz *et al.*, 2011). Evidences also suggest significant downregulation in SNS activity at certain stages in heart failure. A reduction of approximately 30% in NE level along with a decreased density of sympathetic nerve endings and impaired NE reuptake has been reported in heart failure (Kimura *et al.*, 2010; Baker, 2014).

B. Adrenergic Receptors in cardiac function and heart failure

The interface between the SNS and cardiac function is formed by the adrenergic receptors (ARs) that are responsive to the endogenous catecholamines (Capote *et al.*, 2015). ARs belong to the superfamily of integral membrane proteins known as G-protein-coupled receptors (GPCRs) and are involved in pathophysiology of cardiac functions. GPCRs are comprised of seven conserved transmembrane α-helices, an extracellular amino terminus and an intracellular carboxyl terminus. A wide variety of extracellular signals such as ambient physical and chemical stimuli, endogenous hormones, neurotransmitters and growth factors, as well as exogenous therapeutic agents initiate the transmembrane signaling by GPCRs. Following ligand (hormones or neurotransmitters) binding, there is a conformational change in the GPCRs that in turn causes coupling with guanine nucleotide regulatory proteins (G-proteins) (Lefkowitz, 2000; Pierce *et al.*, 2002; Salazar *et al.*, 2007).

G-proteins are heterotrimeric proteins comprising of α, β, and γ subunits. Coupling with GPCR induces exchange of G-protein-bound GDP for GTP, followed by its dissociation and resulting in active Gα and Gβγ subunits. According to their amino acid sequences and function, Gα subunits are classified into four subfamilies viz., Gαs (stimulatory), Gαi (inhibitory), Gαq and Gα12. Receptors coupled to Gs, Gi, Gαq and Gα12 proteins lead to the activation of adenylyl cyclases (ACs), inhibition of ACs, activation of phospholipase C β (PLC β) and the activation of Rho guanine nucleotide exchange factors (Rho GEFs) respectively (Neves *et al.*, 2002; Galés *et al.*, 2005; Boularan & Kehrl, 2014). These intracellular effector molecules in turn regulate the concentration of second messengers (cAMP; cyclic adenosine monophosphate, IP3; inositol 1,4,5-triphosphate, DAG; diacylglycerol) followed by the activation of a number of different downstream signaling molecules, including protein kinase A (PKA) and protein kinase C (PKC). The dissociated Gβγ subunit targets a range of signaling pathways involved in desensitization and downregulation of receptors, apoptosis, and ion-channel activation. Apart from canonical G protein signaling, GPCR activation also mediates G protein-independent signaling

through β-arrestin, which was originally identified for its role in receptor desensitization and internalization (Salazar *et al.*, 2007; Tilley, 2011).

Based on pharmacological properties, the AR family is comprised of nine subtypes: three α1-ARs, three α2-ARs and three β-ARs. About 90% of ARs in the human heart is represented by β-ARs and ~10 % by α1-ARs (Bylund *et al.*, 1994; Montgomery *et al.*, 2017).

B.I. α- Adrenergic Receptors

α1-ARs are the most abundant α-ARs in the heart, located in cardiac myocytes and in the coronary vasculature. In contrast, α2-ARs are of much lower abundance and are located within the coronary microvasculature and on nerve terminals to mediate presynaptic inhibition of NE release. α1-ARs are further divided into three subtypes; α1A-AR, α1B-AR, and α1D-AR. While α1D-AR is absent in cardiac myocytes at protein level, the abundance of α1B-AR is ~ 2- to 4-fold higher than that of α1A-AR. α1-ARs couple to the Gq proteins to activate downstream signaling pathways. Both α1A- and α1B-AR subtypes localize and initiate signal at the nuclear membrane towards the plasma membrane ("inside-out" signaling). (Turnbull *et al.*, 2003; Wright *et al.*, 2008; O'Connell *et al.*, 2014).

A large number of studies involving the molecular events underlying α1-AR induced cardiac hypertrophy and heart failure have suggested its role in mediating adaptive physiological hypertrophy and playing a protective role in the stressed heart. The conventional α1-AR-Gq/PLC/calcium pathway induces calcineurin-mediated activation of NFAT (nuclear factor of activated T-cells) and calcium calmodulin-mediated nuclear export of class II HDAC; both contributing to heart growth (Pu *et al.*, 2003; Backs *et al.*, 2006; Bossuyt *et al.*, 2008). Cardiomyocyte growth is also promoted through the Gq mediated activation of ERK1/2, JNK, and PKC-PKD (Xiao *et al.*, 2001; Braz *et al.*, 2002; Wright *et al.*, 2008). Further, receptor interaction with G12/13 proteins activate RhoA signaling leading to receptor-induced cytoskeletal reorganization and the activation of certain key transcription factors like GATA-4 followed by enhanced fetal gene expression (Liang, De Windt, *et al.*, 2001; Liang, Wiese, *et al.*, 2001; Suzuki, 2011). Also, the activation of the transcription factor NF-κB through a mechanism involving AKAP-Lbc and RhoA leads to the production of interleukin-6, a pro-inflammatory cytokine contributing to cardiac hypertrophy. α1-AR stimulation in isolated heart induces "ischemic preconditioning", thus preventing ischemia–reperfusion induced cell death (Banerjee *et al.*, 1993; Lanzafame *et al.*, 2006; Amirahmadi *et al.*, 2008). Study of α1A/α1B double

knockout mice showed a pronounced decrease in postnatal heart size and increased mortality under pressure overload marking the importance of α1-ARs to maintain heart function. Also, α1A/α1B double knockout mice derived cardiomyocytes exhibit more pronounced necrosis after exposure to a number of toxic stimuli (McCloskey *et al.*, 2003; O'Connell *et al.*, 2003, 2006; de Lucia *et al.*, 2014).

B.II. β- Adrenergic Receptors

β-ARs are divided into three subtypes- β1, β2 and β3. Of these, β1-AR is the predominant subtype in heart representing ~80% of receptor population. β2-AR comprise ~20% of the β receptors in heart (primarily it is expressed in lung, kidney and blood vessels). β3-AR is mainly found in adipose tissues and minimally in the heart. However in failing hearts, a 2- to 3-fold increase in β3-AR has been reported (Bristow *et al.*, 1986; Brodde & Michel, 1999; Moniotte *et al.*, 2001; Tilley, 2011; Balligand, 2016). The principal agonists for all the β-ARs are EPI and NE, though their downstream signaling pathways and physiological consequences are significantly different. Activation of β1-AR and to a lesser extent of β2-AR exerts positive inotropic effect (increase in cardiac contractility), positive chronotropic effect (increase in heart rate), positive lusitropic effect (increase in rate of relaxation) and positive dromotropic effect (impulse conduction through the atrioventricular node). On the contrary, stimulation of β2- and β3-ARs produces a negative inotropic effect, thus playing as a "safety valve" during intense adrenergic stimulation. Upon stimulation, β1-AR primarily couple to the Gs protein, while depending on the developmental or pathophysiological state of the heart, β2-AR can be coupled to both Gs and Gi proteins (Madamanchi, 2007; Najafi *et al.*, 2016). Cardiac performance is tightly regulated via PSNS and SNS to maintain the balance between the demands of the body and supply (cardiac output). In heart failure, pathological remodeling of the heart results in decreased cardiac output. In order to meet the demands of the body, the SNS is activated and the released catecholamines increase contractile performance via stimulation of β-ARs (Figure 2) (Esler *et al.*, 1997; Triposkiadis *et al.*, 2009). Although this phenomenon is beneficial in the acute phase, chronic β-ARs stimulation via sustained and elevated catecholamines level leads to severely irregular β-AR signaling cascades. This is reflected by the decrease in the β1-AR levels by 50% (β2-AR levels remain constant), a sharp induction (up to 200%) in the level of Gαi and significant elevation in G-protein-coupled receptor kinase-2 (GRK2) activity, further worsening the development of heart failure. Studies using transgenic mice models have reported that the cardiac specific overexpression of β1-AR

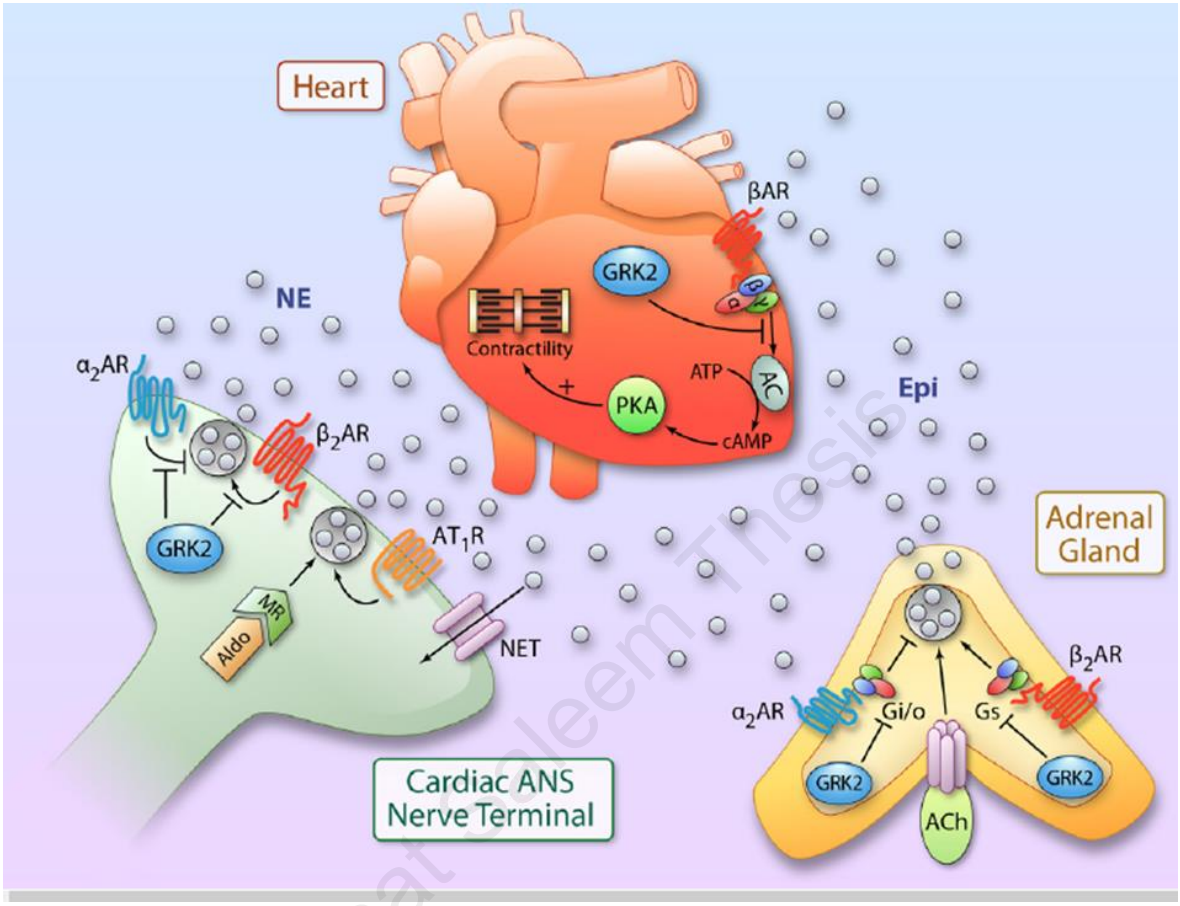

Figure 2. Autonomic nervous system (ANS) in heart pathophysiology: ANS activation translate into the release of catecholamines (NE, norepinephrine; EPI, epinephrine) from sympathetic nerve terminals and adrenal medulla. These catecholamines bind to the cardiac adrenergic receptors and .increase the contractile performance of the heart. NET (NE transporter) recycle the NE released from the nerve endings. GRK2 (GPCR kinase-2) desensitize the adrenergic receptor to prevent the persistent receptor stimulation.

Adapted from Lymperopoulos et al., (2013) Ciculation Reserach

by 5-15 fold leads to the development of dilated cardiomyopathy (DCM) and heart failure at young age, reiterating the view that increased β1-AR is ultimately detrimental to cardiac function. On the other hand, cardiac specific overexpression of β2-AR showed improved basal contractility and cardiac function with minimal pathology. Further, β1-AR knockout mice were largely embryonically lethal while that of β2-AR knockout showed no significant difference in cardiovascular phenotype suggesting that β1-AR is the dominant β-AR involved in the cardiac contractility (Milano *et al.*, 1994; Chruscinski *et al.*, 1999; Engelhardt *et al.*, 1999; Madamanchi, 2007; Baker, 2014). β2-AR signaling via Gi protein enhances heart failure as it attenuates the positive inotropic effects of β1-AR stimulation. In β2-ARs knockout mice, chronic stimulation with isoproterenol (β-AR agonist) displayed enhanced myocyte apoptosis and thus mortality. In summary, chronic β1-AR signaling have cardiotoxic effects while chronic β2-AR signaling exert cardioprotective effects in heart failure, although the effects also depend on the underlying diseases (Woo & Xiao, 2012; Lymperopoulos *et al.*, 2013).

Receptor desensitization

Persistent stimulation of ARs by catecholamines overwhelms the G-protein signal cycle (active/inactive form) and prompt further negative feedback regulation of GPCR activity. The receptor desensitization mechanism includes homologous and heterologous desensitization. Homologous desensitization of receptors initiates within minutes of agonist stimulation, through binding of Gβγ subunit of the activated G-protein with the active form of GRK (Barak *et al.*, 1999; Ferguson, 2001; Auman *et al.*, 2002; Madamanchi, 2007; Zhang & Kim, 2017). Seven isoforms of GRK (GRK1 to 7) are known and GRK2 (also termed β-AR kinase 1 [βARK1]) is the most prominent cardiac isoform. GRK3 and GRK5 are also present in heart at a minimal level (Madamanchi, 2007). After Gβγ subunit binding, GRK2 translocates to the stimulated receptor and phosphorylate it at the carboxy terminus. Heterologous desensitization of receptors involves phosphorylation of receptor through its downstream signaling product (e.g. cAMP) regulated kinase (e.g. PKA). Unlike GRK, PKA phosphorylates both stimulated and unstimulated receptors. Independent of phosphorylation mechanism, the phosphorylated receptor gets targeted to bind β-arrestin which functionally uncouple the receptor from the G-protein. The affinity of the receptor for AP2 and clathrin is increased via binding of β-arrestin resulting in rapid receptor internalization via clathrin-coated vesicles and transportation to endosomes. Under persistent receptor stimulation, the receptors can either be recycled back to the

plasma membrane or be degraded in the liposome (Freedman *et al.*, 1995; Claing *et al.*, 2002; Perry & Lefkowitz, 2002; Kelly *et al.*, 2008).

GRK2 thus maintains the adequate cardiac output in the healthy myocardium via fine tuning of adrenergic signaling. However, disturbed AR signaling in the injured and failing heart results due to increased GRK2 activity followed by attenuation of β-AR catecholamine sensitivity by receptor desensitization and downregulation. Enhanced GRK2 expression has been associated with hypertension, cardiac hypertrophy, post-myocardial infarction and heart failure. It is thus a potential biomarker of cardiac function and it is an attractive therapeutic target for heart failure treatment (Lymperopoulos *et al.*, 2012; Reinkober *et al.*, 2012).

C. Reactive oxygen species in cardiac function and diseases

Increased oxidative/nitrosative stress is one of the most evidenced marker of cardiovascular diseases, including atherosclerosis, hypertension, cardiac hypertrophy, heart failure, and ischemia-reperfusion injury (Belch *et al.*, 1991; Hill & Singal, 1996; Takimoto & Kass, 2007; Münzel *et al.*, 2015). Oxidative/nitrosative stress is defined as the pathological imbalance towards excess generation of reactive oxygen/nitrogen species ($R^O/_NS$) relative to antioxidant defense, disturbing the "redox state" of a cell. $R^O/_NS$ are oxygen/nitrogen based chemical species which include free radicals such as superoxide anion ($O_2^{\cdot -}$), hydroxyl- ($HO^{\cdot}$), lipid- (ROO^-) and nitric oxide ($NO^{\cdot}$) radicals as well as non-radicals such as hydrogen peroxide (H_2O_2), peroxynitrite ($ONOO^-$) and hypochlorous acid (HOCl). ROS scavenging systems/antioxidants, including superoxide dismutase (SOD), catalase, glutathione peroxidase (GPx), and peroxiredoxin (Prx) tightly regulate the level of ROS. Reduced pools of glutathione, glutaredoxin, and thioredoxin (Trx) is maintained by NADPH-regenerating reactions, primarily the pentose phosphate pathway in the cytosol and the activity of mitochondrial Ca^{2+}-dependent Krebs cycle dehydrogenases (Aon *et al.*, 2010). $R^O/_NS$ induce discrete, site specific and reversible modifications of proteins that mediate spatially and temporally regulated redox signaling to generate crucial effects. Oxidative/nitrosative stress causes cellular damage by free radical-induced irreversible oxidation of lipids, proteins and DNA leading to changes in molecular pathways and result in pathogenesis of several diseases, including neurological diseases, cancer, heart diseases and so on. In the heart, redox signaling is involved in physiological processes (e.g., excitation-contraction coupling [ECC], cell differentiation) stress response pathways (e.g., adaptation to hypoxia/ischemia), pathological conditions (e.g., adverse

cardiac remodeling, fibrosis) and cellular homeostatsis. Excess in $R^{O}/_{N}S$ generation disturbs a wide range of cellular events and therefore underpins cardiac dysfunctions such as direct modification of proteins central to ECC, impairing the contractile functions, activating a number of hypertrophic signaling kinases and transcription factors, stimulation of fibroblasts proliferation and activation of matrix metalloproteinases (MMPs) leading to extracellular matrix remodeling (Figure 3) (Vassalle *et al.*, 2008; Elahi *et al.*, 2009; Tsutsui *et al.*, 2011; Madamanchi & Runge, 2013; Byon *et al.*, 2016).

C.I. Sources of ROS

The cellular sources of ROS production in heart are cardiomyocytes, endothelial cells and neutrophils while that of subcellular sources include mitochondrial electron transport chain (ETC), NADPH oxidases, xanthine oxidase and uncoupled nitric oxide synthases.

1. Mitochondria

About 30% of the cardiomyocyte volume is constituted by mitochondria which is a major source of ROS. Mitochondria produce ROS through a single electron leakage in the ETC, causing reduction of molecular oxygen (O_2) to superoxide ($O_2^{\cdot -}$). Under normal condition, approximately 2–5% of electrons escape to react with O_2 resulting in the production of small quantities of ROS, which contribute to homeostatic redox signals and excess ROS, if any, get detoxified by the endogenous scavenging enzymes like superoxide dismutase and catalase. Electron leakage mainly occurs at the NADH dehydrogenase (complex I) and CoQH2-cytochrome *c* reductase (complex III) of ETC (Ide *et al.*, 1999; Sawyer & Colucci, 2000; Kovacic *et al.*, 2005; Burgoyne *et al.*, 2012). Additionally, ETC-dependent ROS production can couple to a transient opening of the mitochondrial permeability transition pore (MPTP), thereby generating superoxide flashes, which may modulate local signaling (Wang *et al.*, 2008). In the failing heart, the enzyme activities in the mitochondrial ETC decrease and the $O_2^{\cdot -}$ production increase. Moreover, under pathological conditions such as ischemia or hypoxia, the availability of oxygen is reduced and the generation of ROS increases, resulting in myocyte damage or myocardial infarction. Additionally, during ischemia–reperfusion, MPTP opening can be triggered by ROS, leading to a burst of further ROS release, which results in cell injury (Zorov *et al.*, 2000; Perrelli *et al.*, 2011). Other sources of mitochondrial ROS include 2-oxoglutarate dehydrogenase, pyruvate dehydrogenase, and flavoprotein acyl-CoA dehydrogenase (Brand, 2010). Mitochondrial monoamine oxidase-A (MAO-A) enzymes are involved in oxidative deamination of catecholamines resulting in the production of pro-hypertrophic neurotransmitters like NE

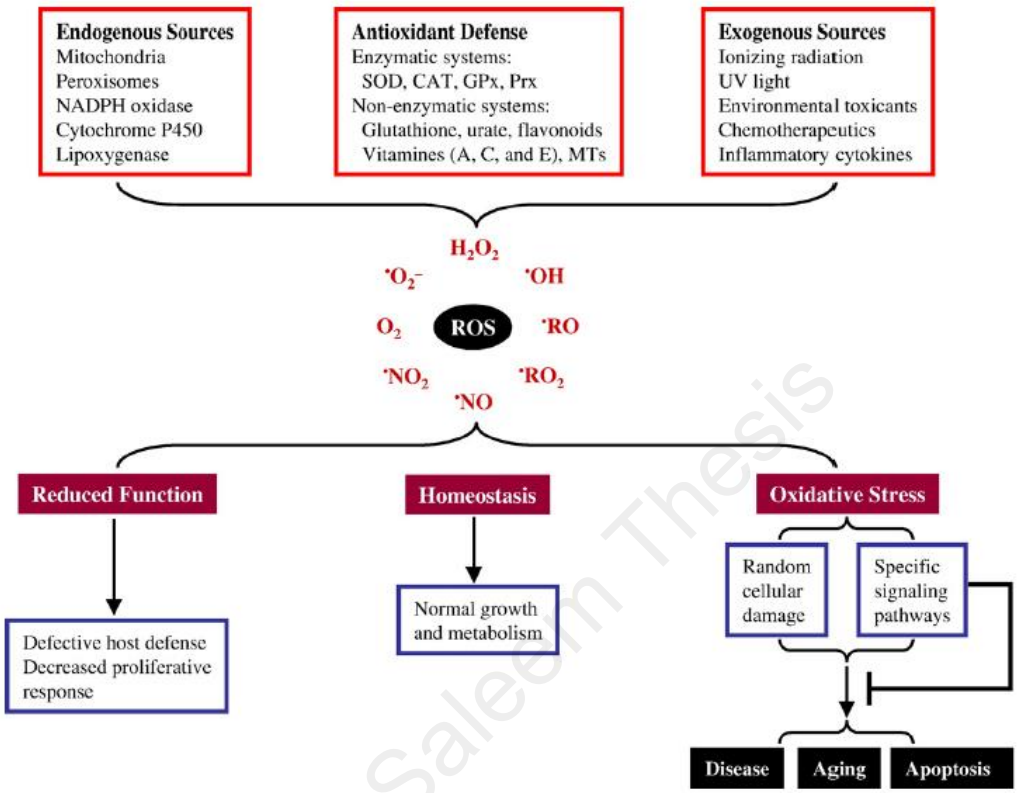

Figure 3. Metabolism and biological effects of ROS: ROS is diverse group of molecules generated from endogenous and exogenous sources. Several specific and non-specific antioxidant defense system attenuates excess of ROS and maintains the redox homeostasis. While ROS within a physiological range is necessary for normal function, its over-production leads to oxidative stress with pathological consequences.

Adapted from Ma et al., (2010) Pharmacology and Therapeutics

and serotonin along with H_2O_2. In mice with pressure overload-induced heart failure, MAO-A inhibitor clorgyline, or dominant-negative mutant of MAO-A reduces oxidative stress, inhibits MMP and caspase-3 activation, thus ameliorating the contractile dysfunction (Kaludercic *et al.*, 2010, 2014).

2. Xanthine Oxidase

Of the two interconvertible isoforms of xanthine oxidoreductase i.e. xanthine oxidase (XO) and xanthine dehydrogenase (XDH), only XO generates ROS. Quantity and type of ROS production depends on various conditions, e.g. during hypoxia, substantially more H_2O_2 (than $O_2^{\bullet-}$) is produced. Upregulation of XO has been seen in experimental models of heart failure as well as in end-stage failing human myocardium (Cappola *et al.*, 2001; Borges *et al.*, 2002; Vorbach *et al.*, 2003; Tsutsui *et al.*, 2011). Level of serum uric acid, a product of XO, is increased during the development of heart failure and is used as a diagnostics marker for the disease (Higgins *et al.*, 2009; Harzand *et al.*, 2012). Allopurinol, a XO inhibitor, improves LV contractile function and myocardial efficiency in animal models of heart failure. In addition, inhibition of XO by allopurinol in animals with experimentally induced MI significantly reduces adverse LV remodeling. A link between XO and nNOS has been reported wherein XO-derived ROS increases under nNOS deficiency (Ukai *et al.*, 2001; Saavedra *et al.*, 2002; Minhas *et al.*, 2006; Schuchardt *et al.*, 2017).

3. Nitric Oxide synthase

There are three isoforms of nitric oxide synthase (NOS) of which neuronal (nNOS) and endothelial (eNOS) isoforms are constitutively expressed in cardiomyocytes whereas expression of the third isoform i.e., inducible NOS (iNOS) occurs under pathological situations. Nitric oxide (NO) released from eNOS and nNOS play a crucial part in myocardial contractile function (Grobe *et al.*, 2006; Elahi *et al.*, 2009; Simon *et al.*, 2014). NO-mediated nitrosylation of cysteine residues are involved in cell signaling cascades. In the deficiency of essential NOS cofactor tetrahydrobiopterin (BH4), NOSs can uncouple and generate $O_2^{\bullet-}$, which in turn further degrade BH4 and thus act as an amplifier of ROS generation (Schulz *et al.*, 2008; Alkaitis & Crabtree, 2012). Reduced BH4 level and uncoupling of eNOS is associated with LV dilatation and contractile dysfunction in mice subjected to transverse thoracic aortic constriction (TAC). Further, if NOS are partially uncoupled, $O_2^{\bullet-}$and NO may be concomitantly produced and they spontaneously combine

and generate highly reactive peroxynitrite ($ONOO^-$). Peroxynitrite causes nitrooxidative stress with deleterious effects on cell functions. Markers for NO-associated stress viz., total NO, 3-Nitrotyrosine, nitrite are elevated in failing hearts (Eleuteri *et al.*, 2009; Cipak Gasparovic *et al.*, 2017).

4. NADPH Oxidases

NADPH oxidases (Noxes) are a family of membrane bound enzyme complexes, solely dedicated for ROS generation. Nox was identified for its role in the respiratory burst-dependent microbicidal activity (phagocytosis) in neutrophils (Bedard & Krause, 2007). Later on, it became clear that the Nox involved in the phagocytosis is only one member of the family of homologous enzymes and was termed Nox2. Noxes are present in a variety of cell types including endothelial cells (ECs), vascular smooth muscle cells (VSMCs), macrophages, adipocytes, stem cells, fibroblasts and cardiac myocytes (Bedard & Krause, 2007; Lassègue *et al.*, 2012). The Nox family is comprised of 7 isoforms termed Nox1-5 and Duox1 and Duox2 (for Dual Oxidase), each encoded by separate genes. Each isoform differs in requirement of additional partner subunits for activation, the mode of regulation, tissue expression, types of ROS generated and physiological functions. For their activation, one or more of the regulatory subunits; i.e., p22phox, p47phox, Noxo1, p67phox, Noxa1, p40phox, and the major binding partner Rac is required. The conserved catalytic subunit of Noxes comprise of six amino-terminus transmembrane α-helices (helices I-VI) connected by 5 loops (Biberstine-Kinkade *et al.*, 2001). The cytosolic carboxy-terminal moiety of all Nox contains one multimodular NADPH binding site and a bimodular FAD binding site. Upon activation, 2 electrons are transferred from NADPH to FAD and sequentially to the heme groups and finally to molecular oxygen, generating $O_2^{\cdot -}$ (Figure 4 & 5). Availability of NADPH and FAD also regulate Nox activity and ROS generation and this relationship between NADPH and ROS levels seems complex and dependent on the Nox isoform and the subcellular localization (Sumimoto, 2008; Lassègue *et al.*, 2012). Although in cardiovascular tissues, Nox1, 2, 4 and 5 are expressed, Nox2 and Nox4 are the predominant isoforms. They are involved in normal vascular and cardiac function including cell proliferation, differentiation, contraction, migration and survival. Upon acute or chronic upregulation, they are implicated in the development of cardiovascular diseases such as hypertension, atherosclerosis, ischemia reperfusion injury, cardiac remodeling, and heart failure. Nox5 is found only in higher mammals and adequate

	NOX1	NOX2	NOX4	NOX5
Agonist stimulation requirement	+	+	Constitutive	+
Cardiovascular distribution	EC, VSMC, Cardiomyocytes	EC, Cardiomyocytes	EC, VSMC, cardiac fibroblasts	EC, VSMC, cardiac fibroblasts
Intracellular distribution	Plasma membrane, Caveolae, Endosomes, Perinuclear	Plasma membrane, Perinuclear, Nuclear pore	ER, Perinuclear, Nucleus, Mitochondria, Focal adhesions, Stress fibers, Cytoplasm	Plasma membrane, Intracellular
Pathophysiological function	Hypertension, hypertrophy	VEGF signaling	H_2O_2 signaling	Atherosclerosis, Hypertension, post myocardial infarction

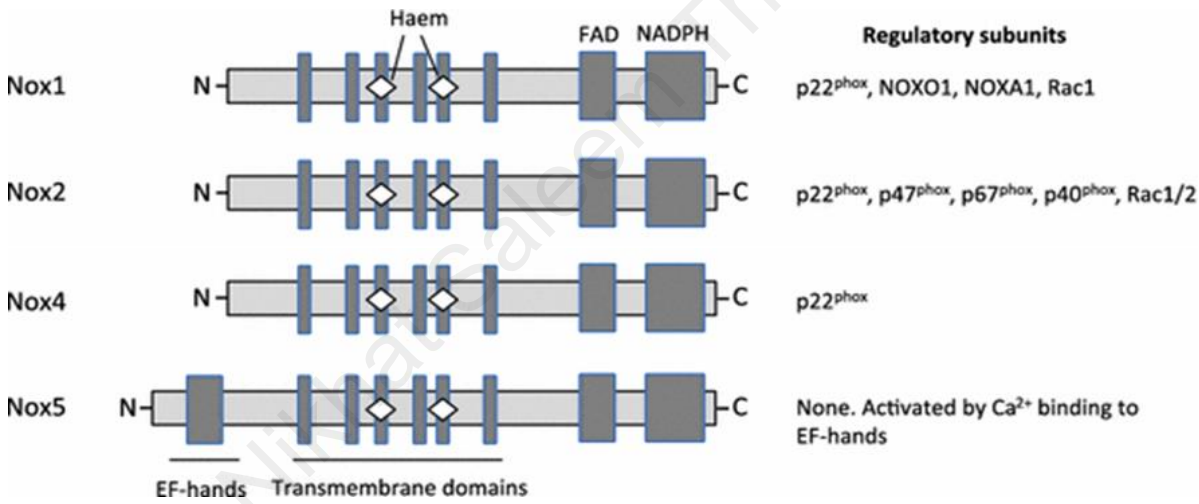

Figure 4. NADPH oxidases isoform specificity: Nox display isoform specific activation mechanism, cellular and subcellular distribution leading to diverse pathophysiological function. It comprised of six transmembrane α-helices containing NADPH and FAD binding site at the carboxyl-terminus. Nox activation involve assembly of isoform specific regulatory subunits. The electron is transfereed from NADPH and FAD to molecular oxygen via two heme groups to generate superoxide.

Adapted from Nabeebaccus A et al., (2011) Heart Failure Review

information is not available for its function (Cave *et al.*, 2006; Burgoyne *et al.*, 2012; Lassègue *et al.*, 2012; Zhang *et al.*, 2013; Gray & Jandeleit-Dahm, 2015).

4.1. Nox2

Also known as gp91-phox, Nox2 is the first discovered member of the Nox family and has been extensively studied in phagocytes. Non-phagocytic Nox2 activation is slower than the phagocytic Nox2 and it produces substantially less ROS than the neutrophil complex. It is present in endothelial cells, vascular smooth muscle cells, adventitial fibroblasts and cardiomyocytes. It is localized at the plasma membrane, perinuclear space and nuclear pores. In the resting state, Nox2 forms an inactive membrane complex with p22phox termed cytochrome b558, whereas the cytosolic subunits p67phox, p47phox and p40phox form a trimer. A number of stimuli including GPCR agonists (Angiotensin II, Endotelin-1), growth factors, cytokines, mechanical and metabolic forces initiate the signaling cascades involving Rac, p47phox and p40phox subunit activation followed by their translocation to the membrane and association with the cytochrome b558 to form the active holoenzyme (Hwang *et al.*, 2003; Lassègue & Clempus, 2003; Pietrowski *et al.*, 2011; Lassègue *et al.*, 2012). p47phox is termed as the "organizer subunit" of Nox2 since its phosphorylation by kinases, such as PKC, PKD, PI3K, PLA2 and MAPKs actuate the assembly of Nox2 (Ago *et al.*, 2003). p67phox plays as an "activator subunit" and triggers activation process upon binding to a specific domain of p47phox (Uhlinger *et al.*, 1994). The interaction of Rac with p67phox and Nox2 is promoted by GTP/GDP exchange on Rac and is regulated by PI3K generated 3-phosphorylated phosphoinositides including PIP3. PIP3 recruits several PH-domain containing activators of Rac to the plasma membrane, such as the GEFs, P-Rex and Vav1 (Diekmann *et al.*, 1994; Welch *et al.*, 2002; Aguirre & Lambeth, 2010; Zhang *et al.*, 2013).

Nox2 activation is implicated in the vessel contraction (through neutralization of NO by $O_2^{\cdot -}$ and subsequent impairment in NO mediated relaxation), inflammatory response (through release of IL-6, G-CSF, GM-CSF and MCP-1), EC proliferation (involving p38MAPK and Akt), prevention of apoptosis (through inhibition of caspase 3/7 activity) and in AngII/AT1R-induced senescence in endothelial progenitor cells (EPCs), thereby suggesting cell and context specific regulation of Nox2 (Zhang *et al.*, 2013; Murdoch *et al.*, 2014; Sirker *et al.*, 2016). Nox2 is reported to be involved in AngII induced cardiac hypertrophy, atrial fibrillation and interstitial fibrosis and the effect are attenuated in $Nox2^{-/y}$ mice. Parajuli *et al.* have reported the association of increased Nox2 levels with adverse

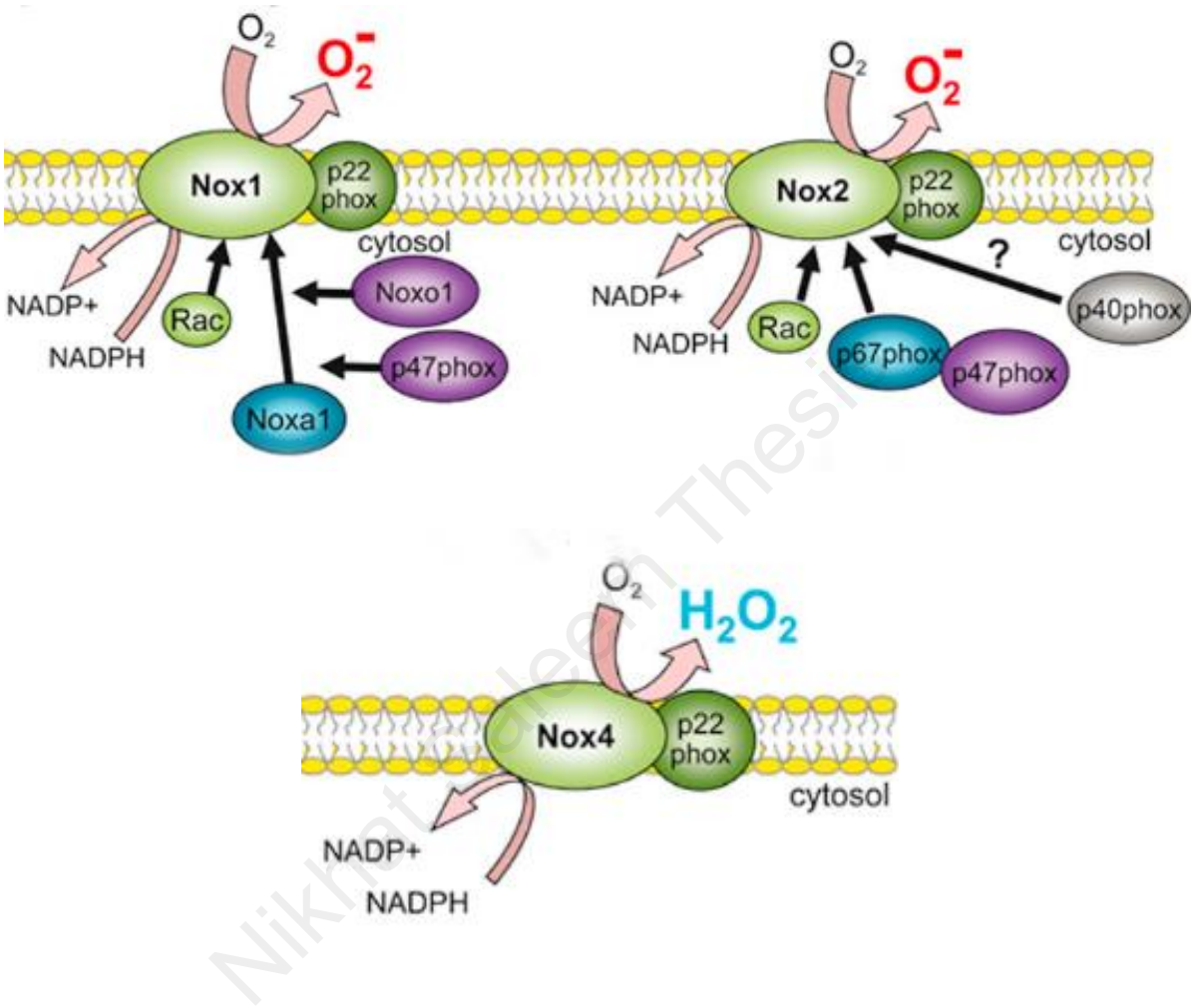

Figure 5. Structural and molecular organisation of cardiac specific NADPH oxidase isoforms: All Nox proteins form a complex with p22phox, but the cytosolic subunits needed for their activation differ between the isoforms. While activation of Nox1 and Nox2 require assembly with cytosolic factors to generate superoxide, Nox4 is constitutively active isoform and generate primarily hydrogen peroxide.

Adapted from Brandes RP et al., (2014) Free Radical Biology and Medicine

myocardial remodeling and increased oxidative stress in human dilated cardiomyopathy (Parajuli *et al.*, 2014). In Post-acute MI, Nox2 is up-regulated in the infarcted myocardium and loss of Nox2 in mice is protective against LV dilatation, hypertrophy, apoptosis and interstitial fibrosis, weeks after MI (Fukui *et al.*, 2001; Looi *et al.*, 2008; Bache & Chen, 2014).

4.2. Nox4

Nox4 is the most highly expressed Nox family member in the cardiovascular system. It is localized in intracellular membranes viz., ER, mitochondria and nucleus, the perinuclear space and at focal adhesions. Although Nox4 binds to p22phox subunit for its activity, the cytosolic subunits are not required for the activation suggesting its constitutive activity mostly regulated at the level of gene expression (Ellmark *et al.*, 2005; Martyn *et al.*, 2006; Lassègue *et al.*, 2012). Unlike Nox2, the predominant product of Nox4 is H_2O_2 (Serrander *et al.*, 2007; Dikalov *et al.*, 2008; Takac *et al.*, 2011). H_2O_2 may even enhance NOS activity and signaling, thereby inducing angiogenesis (Craige *et al.*, 2011). A wide array of stimuli such as TGF-β, TNF-α, IFN-γ, urokinase, oscillatory shear stress, hypoxia, hyperoxia and vascular injury, upregulate Nox4 suggesting that it mediates many different cellular responses. Nox4 activation is implicated in proinflammatory responses, differentiation, migration, proliferation, apoptosis, senescence and oxygen sensing (Ellmark *et al.*, 2005; Lee *et al.*, 2006; Sturrock *et al.*, 2006; Clempus *et al.*, 2007; Basuroy *et al.*, 2009; Lyle *et al.*, 2009; Murray *et al.*, 2013; Sciarretta *et al.*, 2013). Several studies have proposed the role of Nox4 in pressure overload induced cardiac hypertrophy. However, it was reported to have a protective role during chronic pressure overload through the induction of HIF-VEGF signaling in cardiomyocytes, resulting in a higher myocardial capillary density. Moreover, under the setting of starvation, NOX4 has been shown to enhance the expression of cytoprotective genes (Kuroda *et al.*, 2010; Sag *et al.*, 2014; Sciarretta *et al.*, 2014; Nabeebaccus *et al.*, 2015).

4.3. Nox1

Similar to Nox2, Nox1 also associates with p22phox to form a membrane-bound cytochrome complex b558, whereas the cytosolic subunits p47phox and p67phox are replaced by Noxo1 and Noxa1 respectively. In addition, Nox1 also requires Rac1 for its activity like Nox2 (Bánfi *et al.*, 2003; Hanna *et al.*, 2004; Lassègue *et al.*, 2012). Interestingly, Nox1 appeared to be activated in specific locations resulting in site specific

$O_2^{\cdot-}$ generation which rapidly converts to H_2O_2: both inside and outside the cells by Ang-II, extracellular generation by muscarinic agonists; endosomal generation by IL-1β and TNF-α (Dikalova *et al.*, 2005; Szanto *et al.*, 2005; Miller *et al.*, 2007; Zhang *et al.*, 2007, 2013). Further, chaperones Hsp90 and PDI also regulate Nox1 activity by mediating protein folding and enzyme stability (Janiszewski *et al.*, 2005; Chen *et al.*, 2011). Nox1 is involved in moderate physiological activity and has been implicated in multiple vascular diseases, including hypertension, restenosis and atherosclerosis. However, due to its low expression in cardiac tissues, its role in cardiac disease is poorly understood. Matsuno *et al.* have reported Nox1 upregulation in endotoxin-induced apoptosis in cardiomyocytes, thereby affecting the risk of mortality under systemic inflammatory conditions (Matsuno *et al.*, 2012). Following ischemic preconditioning, Nox1 level increases in the myocardium and provide protective effects involving TNF-α expression and the activation of NF-κB (Jiang *et al.*, 2014).

C.II. Redox regulated signaling proteins and their targets:

The signaling effects of $R^O/_NS$ (redox signaling) bring about site specific, discrete and mostly reversible oxidation-reduction modifications in the cellular proteins. The effect is accounted by its site of generation, particular species, local concentration, and cell compartment–specific antioxidant pools.

Although $O_2^{\bullet-}$ are slow reacting radicals, they are involved in important signaling reactions involved in growth factor and hormonal responses (Buetler *et al.*, 2004). It also reacts rapidly with NO to generate $ONOO^-$, which itself is a powerful oxidant. Most of the $O_2^{\bullet-}$ get converted to H_2O_2 either via SOD catalyzed reaction or spontaneously (Bedard & Krause, 2007; Brandes *et al.*, 2014a). H_2O_2 is a predominant signaling ROS in biological system and mediate majority of its effect by directly oxidizing cysteine or methionine thiols. H_2O_2 degradation (by peroxidases and catalases) may generate more powerful oxidants such as $HO^{\cdot}$, which are highly reactive its effects are nonspecific and irreversible. A range of proteins including receptors, kinases, phosphatases, transcription factors and structural proteins act as protein sensors. They sense alterations in local redox state with a change in conformation, stability, molecular interactions, and activity to transduce the signals via specific posttranslational modifications (Burgoyne *et al.*, 2012; Brandes *et al.*, 2014a; Brown & Griendling, 2015).

However, there is great heterogeneity regarding the Nox enzymes involved in various cells and stimuli. There are differences in cell type specific expression of Nox homologues,

their subcellular compartmentalization and the underlying activated pathways making one of the most complex signaling system (Chen *et al.*, 2008).

1. Small G proteins

Small GTPases are in active state when bound to GTP and are inactive when bound to GDP. They regulate cell proliferation, differentiation, movement, and lipid vesicle transport (Bar-Sagi & Hall, 2000). The activity of the small GTPase, a member of Ras family, located at the entry level of the Ras-Raf-MEK-MAP pathway, is governed by its redox-sensitive cysteines. ROS target the cysteine 118 and facilitates replacement of GDP with GTP, thus leading to increased GTPase activity (Heo & Campbell, 2005). Ras, as a downstream target of Nox derived ROS, is involved in many signaling cascade leading to increased protein synthesis in skeletal myoblasts, renal myofibroblasts and Ang II-induced smooth muscle cell hypertrophy (Adachi, Pimentel, *et al.*, 2004; Wu *et al.*, 2007; Mitchell *et al.*, 2013; Sedeek *et al.*, 2013).

2. Peroxiredoxins

The Prxs are highly conserved family of peroxidases which exist as homodimers and catalyze the reduction of peroxides. Oxidation of a conserved cysteine residue at the amino-terminus by H_2O_2 is followed by the oxidation of another carboxy-terminal cysteine present in the homodimeric primer leading to the formation of an intermolecular disulfide bond. Under high H_2O_2 stress, further oxidation of cysteine to sulfinic form (RSO_2H) leads to the formation of Prx aggregates inactivating it. Thioredoxin (Trx)-mediated reduction reconstitutes the reduced Prx (Rhee *et al.*, 2005; Hoyle & O'Neill, 2015). Peroxiredoxin plays a role in controlling Nox signaling (induced by growth factors, insulin etc) by localizing H_2O_2 in a microdomain that inhibits phosphatases including PTP and PTEN (Choi *et al.*, 2005; Chen *et al.*, 2009).

3. Protein kinases/phosphatases

Redox regulated molecular targets in the cell include protein kinases and protein phosphatases, which mediate phosphorylation and dephosphorylation of the target proteins involved in a wide spectrum of cellular processes. These modifications typically occur at serine and threonine or tyrosine residues of the target proteins by the respective kinases and phophatases.

3.1. Protein kinase A

PKA is a serine/threonine specific kinase involved in the regulation of cardiac contractility and performance by targeting the ryanodine receptor 2 (RyR2), L-type Ca^{2+} channel and phospholamban (PLN) (Li *et al.*, 2004; Jones *et al.*, 2008). Activation of PKA by β-AR regulates myocardial ECC and vasodilation. PKA-mediated phosphorylation of RyR2 partially influences spontaneous release of Ca^{2+} from sarcoplasmic reticulum causing ventricular tachycardia during chronic heart failure (Phrommintikul & Chattipakorn, 2006; Dhalla & Müller, 2010; Burgoyne *et al.*, 2012). Redox regulation of PKA occurs through two interprotein disulfides bond formation in the regulatory R1α subunits (Brennan *et al.*, 2006; Corcoran & Cotter, 2013).

3.2. Protein kinase G

Protein kinase G (PKG) is a serine/threonine specific kinase activated by c-GMP. It is implicated in the regulation of vascular tone, cardiomyocyte contraction and hypertrophy. PKG is comprised of two identical subunits held together at the N-terminus by leucine zipper interaction to form a homodimer, which get activated by allosteric binding of cGMP. Under oxidizing condition, an intermolecular disulfide between the two Cys-42 residues is formed within the dimerization domain, thus activating the enzyme independent of the NO-cGMP pathway. Disulfide activation increases its substrate affinity, resulting in its translocation to subcellular compartments (Burgoyne *et al.*, 2007). In knock in mouse with C42S ('redox-dead' version of PKGI-α), the vasodilatory action of oxidation is blocked leading to hypertension (Prysyazhna *et al.*, 2012). Additionally, the trans-nitrosylating agent such as nitrosocysteine bring disulfide bond formation in PKG causing vasorelaxation (Burgoyne & Eaton, 2009; Corcoran & Cotter, 2013).

3.3. *Protein Kinase C*

Protein kinase C (PKC) is a superfamily of structurally related serine-threonine kinase involved in cell signaling. Cysteine rich regions present in both the catalytic and regulatory domains make it susceptible to redox regulation. Low dose of oxidant stimulates PKC activation whereas higher dose inactivates it by reacting with crucial cysteine residues (Steinberg, 2015). There are twelve isoforms of PKC involved in distinct signaling effects associated with cardiac functions. Isoform specific increase in PKC activity leads to pressure or volume overload induced left ventricular hypertrophy, right ventricular hypertrophy and transition to heart failure (Gu & Bishop, 1994; Bayer *et al.*, 2003; Braun *et al.*, 2004; Dhalla & Müller, 2010; Steinberg, 2012).

3.4 Mitogen activated protein kinases (MAPKs)

MAPKs are highly conserved and ubiquitous Ser/Thr kinases involved in various cellular processes including cell cycle, growth, differentiation, development, survival, and cell death. It consists of three main subfamilies; extracellular signal-regulated kinases (ERK1/2), c-Jun NH_2-terminal kinases (JNK1, -2 and -3) and p38 kinase (α, β, γ, δ) (Widmann *et al.*, 1999; Johnson & Lapadat, 2002; Qi & Elion, 2005). MAPKs are activated by dual phosphorylation of a Thr-X-Tyr motif in their regulatory loop by MAPK kinases (MAPKK) which are phosphorylated by MAPK kinase kinase (MAPKKK) making the phosphorelay system (Rose *et al.*, 2010). The activated MAPKs can phosphorylate Ser or Thr residues in a specific Pro-X-Thr/Ser-Pro motif on their target proteins. While ERK1/2 is activated mainly by growth factors (FGF, EGF, PDGF) and cytokines (IL-1β and TNF-α), JNK and p38 are activated in response to stress. Phosphorylation of p38 MAPK and JNK is modulated by Nox1 and Nox2. Certain redox sensitive kinases viz Src, PKC and PLCγ are upstream of the MAP kinase pathway. In VSMCs, stimuli including AngII, thrombin, FGF-2 increase Nox mediated phosphorylation of p38 MAP kinase and JNK (Viedt *et al.*, 2000; Brandes *et al.*, 2001; Schröder *et al.*, 2007; Asrih *et al.*, 2013). Further, MEK kinase kinase ASK-1 (Apoptosis signaling kinase-1) is upstream to JNK/p38 MAPK and under basal condition it is inactive through the interaction with reduced thioredoxin. Increase in ROS level oxidizes thioredoxin and ASK-1 which act as a prime cellular redox sensor followed by the activation of JNK and p38 kinase (Liu *et al.*, 2000; Brandes *et al.*, 2014a). It has been reported that some growth factor receptors are independently activated by ROS followed by the activation of ERK (Rose *et al.*, 2010).

3.5 PI3 Kinase-Protein kinase B (PI3K-PKB)

PI3K-Akt pathway gets activated in response to growth factors, hormones and cytokines and is involved in the regulation of protein synthesis, cell cycle progression, proliferation, autophagy and apoptosis. Ligand-activated receptor triggers the PI3K activation which catalyzes the synthesis of PIP3 followed by the recruitment of PDK-1 to the membrane where it phosphorylates and activates Akt (PKB) (Brandes et al., 2014). There are some studies which directly address the role of Nox enzymes in this process. In serum starved photoreceptor cells, phosphorylation of Akt was found to increase in a Nox2-dependent manner thus limiting apoptosis (Mackey *et al.*, 2008), whereas in C2C12 murine myocytes, IGF-I induced Akt phosphorylation and subsequent hypertrophy is Nox4 dependent

(Handayaningsih *et al.*, 2011). Under certain conditions, Nox diminishes Akt phosphorylation; thereby promoting apoptosis. In LPS-mediated cardiac injury, Nox1 mediates Akt oxidation followed by its dephosphorylation by PP2A (Kwon *et al.*, 2004; Matsuno *et al.*, 2012; Nakanishi *et al.*, 2014).

3.6 Ca2+/Calmodulin-dependent Protein Kinase II (CaMKII)

CaMKII is a highly conserved Ser/Thr protein kinase with multiple catalytic and regulatory domains. Under enhanced intracellular Ca^{2+}/CaM level, the autoinhibitory effect of regulatory domain is relieved, followed by activation of catalytic (kinase) domain. CaMKII activation is implicated in modulation of excitation-contraction coupling, gene transcription and apoptosis through phosphorylation of respective cardiac Ca^{2+}-handling proteins. In the presence of sustained Ca^{2+}/CaM, activated CaMKII undergo inter subunit autophosphorylation at Thr-287 in the autoinhibitory domain, which prevent its reassociation with the catalytic domain and thus sustain kinase activity even after removal of Ca^{2+} (Hook & Means, 2001; Tombes *et al.*, 2003; Erickson, 2014). Pro-oxidant conditions also enhance the CaMKII activity. It has been shown that oxidation of redox active Met-281 and Met-282 residues at regulatory domain sustain CaMKII activity even after decline of Ca^{2+}/calmodulin (Dietrich *et al.*, 2005). In the heart, the CaMKII oxidation is mediated by Nox2 derived ROS. It is reported that chronic AngII stimulation or MI promote Met-281/Met-282 oxidation of CaMKII that is hindered in p47phox-null hearts (Hudmon & Schulman, 2002; Zhu *et al.*, 2007; Erickson *et al.*, 2008; Mollova *et al.*, 2015).

3.7 Protein Tyrosine Kinases

Most of the tyrosine kinases contain conserved cysteine residues at the carboxy-terminal, and their oxidation activates the tyrosine kinase activities. On the other hand, they are also involved in Nox activation, thereby forming a positive feedback loop of ROS production. Moreover, receptor transactivation of tyrosine kinases such as Src, which itself is redox regulated and promotes Nox activation (Seshiah *et al.*, 2002; Gianni *et al.*, 2008; Chignalia *et al.*, 2012; Brandes *et al.*, 2014a). In mesangial cells, Angiotensin II-induced Nox4 expression and concomitant ROS generation resulted in the activation Src, a critical step in angiotensin II–induced expression of fibronectin (Block *et al.*, 2008).

Protein phosphatases

The phosphate groups from proteins phosphorylated by kinases are removed by the protein phosphatases. The superfamily of phosphatases is characterized by the presence of

cysteine in their active centers. Under oxidizing environment, oxidation of cysteine abolishes the phosphatase activity, accentuating the activity of kinases (Boivin *et al.*, 2010). Initial studies showing that Nox2 in phagocytes inactivates PTPs during the respiratory burst, suggested regulation of protein tyrosine phosphatases (PTPs) by NADPH oxidases (Zor *et al.*, 1993). Nox4 is reported to have inhibitory effect on phosphatase PTP1B, thereby modulating a spectrum of PTP1B targeted cellular processes including insulin signaling, EGF signaling, cytoskeletal protein phosphorylation and the endothelial barrier functions (Mahadev *et al.*, 2001; Chen *et al.*, 2008; Mondol *et al.*, 2014). IL-4 receptor activation by stimuli TNFα and IL-3 induces Nox1 and Nox5 dependent inhibition of PTP1B leading to increase in the activity of signal transducer and activator-6 (STAT-6) transcription factor (Sharma *et al.*, 2008). Receptor-associated phosphatase VE-PTP or DEP-1 involved in Src inactivation and receptor dephosphorylation have is inactivated by Nox-derived ROS (Chabot *et al.*, 2009; Vockel & Vestweber, 2013).

4. Calcium channels and pumps

Excitation-contraction coupling in cardiac myocytes involves Ca^{2+} release and subsequent reuptake through Ca^{2+} channels and pumps. The ryanodine receptor (RyR2, cardiac isoform) mediates Ca^{2+} release from sarcoplasmic reticulum (SR) store, essential for contraction of cardiac and skeletal muscle. It is a tetrameric complex containing 364 cysteines, of which ~84 residues are basally reduced, suggesting its redox regulation (Zima & Blatter, 2006; Prosser *et al.*, 2010). These receptors are regulated by redox dependent kinases such as PKA and CaMKII. Further, NO-induced S-nitrosylation at multiple cysteines activates the receptor, independent of cGMP formation. RyR2 S-nitrosylation is reported to protect against detrimental oxidation, suggesting close interrelationship between the effects of ROS and NO (Xu *et al.*, 1998; Burgoyne *et al.*, 2012). The sarcoendoplasmic reticulum Ca^{2+}-ATPase (SERCA) sequesters the Ca^{2+} into SR for the relaxation of cardiac muscles. There is inverse relation between the oxidation levels and SERCA activity (Periasamy & Kalyanasundaram, 2007). It is directly regulated by thiol oxidation, whereas its indirect redox regulation is mediated by phosphorylation of its regulatory protein phospholamban by PKA (at Ser16) or CaMKII (at Thr17) (Johnston *et al.*, 2015). In smooth muscle, SERCA2 is directly activated by peroxynitrite-induced S-glutathiolation of Cys-674 (Adachi, Weisbrod, *et al.*, 2004; Ying *et al.*, 2008). Cardiac SERCA2a can also get activated by nitroxyl mediated increased glutathionylation

(Tocchetti *et al.*, 2007; Lancel *et al.*, 2009). Other redox regulated channels and pumps include L-type Ca^{2+} channels, the plasmalemmal Ca^{2+} -ATPase, the Na^{+}/Ca^{2+} exchanger, Na^{+}channels and K^{+}channels (Santos *et al.*, 2011). The Na^{+}-K^{+}ATPase (sodium pump) is directly regulated via oxidation of sensitive cysteines and is indirectly phosphoregulated by PKA and PKC. PKCε-dependent Nox activation and subsequent inhibitory S-glutathionylation of Cys-46 in the β1 subunit results in inhibition of pump activity under AngII-stimulation and in MI model (White *et al.*, 2009).

5. Histone deacetylases

Histone acetyltransferases (HATs) and histone deacetylases (HDACs) mediate histone acetylation and deacetylation and thereby promote and inhibit gene expression respectively. There are number of reports which highlight redox regulation of HDAC localization and subsequent cardiomyocyte hypertrophy (Yoon & Eom, 2016). Phenylephrine induced intramolecular disulfide formation in HDAC4 leads to its phosphorylation-independent nuclear export resulting in hypertrophy (Matsushima *et al.*, 2013). Isoproterenol-induced nuclear export of HDAC5 in cardiomyocyte is mediated by oxidation (Haworth *et al.*, 2012). Sirtuins (SIRTs) are NAD^{+}-dependent histone deacetylase which deacetylate histones as well as nonhistone proteins. SIRT isoforms are also redox regulated. Natural cardioprotective polyphenol resveratrol and other oxidants activate SIRT1 (Zee *et al.*, 2010).

C.III. Redox regulated transcription factors

Transcription factors involved in the regulation of gene expression pattern are also regulated by redox status of the cell.

1. Nuclear factor κB (NF-κB)

NF-κB is a family of inducible transcription factors, first described as B-lymphocyte specific nuclear protein needed for immunoglobulin kappa light chain transcription. It regulates transcription of more than 200 genes involved in stress responses, cytokine release, cell adhesion, inflammation, immune response and programmed cell death (Madamanchi & Runge, 2013). NF-κB is a dimeric transcription factor formed by homo- or hetero-dimerization of members of Rel family of protein which include Rel-A (p65), Rel-B, c-Rel, p50 and p52. All the Rel family members contain a Rel homology domain which carry a nuclear localization signal (NLS). Unstimulated homo- and hetero-dimers are kept inactive in the cytoplasm by association with IκB family of inhibitory proteins

which include IκB-a, IκB-b, IκB-e, and p105 and p100 (precursors of p50 and p52 respectively) (Hayden & Ghosh, 2008). Under oxidative stress, the inhibitory protein IκB get phosphorylated (at Ser-32 and Ser-36) by ubiquitin-dependent protein kinases resulting in its ubiquitination (at Lys-21 and Lys-22) and proteolytic degradation. The dissociated/activated NF-κB translocate rapidly to the nucleus to regulate NF-κB responsive genes (Traenckner *et al.*, 1995). Also, reduction of Cys-62 of the p50 subunit by thioredoxin or Ref-1 is essential for its DNA binding in the nucleus (Matthews *et al.*, 1992; Madamanchi & Runge, 2013). NF-κB signaling may be both "good" and "bad" depending on the duration and cellular context (Gordon *et al.*, 2011). Under chronic pressure overload or Ang-II stimulation in male mice, the initial LV hypertrophy is attenuated by NF-κB inhibition, but the course of LV remodeling does not alter indicating its role in adaptive cardiac hypertrophy (Zelarayan *et al.*, 2009; Dhingra *et al.*, 2010). NF-κB signaling pathways protect cardiomyocytes from apoptosis induced by acute myocardial infarction (Misra *et al.*, 2003). However, chronic NF-κB activation, under heart failure settings, exacerbates cardiac remodeling by stimulating proinflammatory and profibrotic genes inducing myocytes apoptosis (Hamid *et al.*, 2011).

2. Activator protein-1 (AP-1)

AP-1 is a family of basic domain/leucine zipper (bZIP) transcription factors comprised of homo- hetero-dimers of members of Jun (c-Jun, JunB, JunD), Fos (c-Fos, FosB, Fra-1, and Fra-2), Maf (c-Maf, MafB, MafA, MafG/F/K, and Nrl), and ATF (ATF2, ATF3/LRF1, BATF, JDP1, JDP2). In response to variety of extracellular signals such as H_2O_2, UV, ionizing radiation as well as intracellular stimulus such as arachidonic acid metabolite concentration and redox sensitive MAPK pathway activity, the expression of c-Jun and c-Fos get induced resulting in activation of AP-1 (Turner & Tjian, 1989; Elahi *et al.*, 2009; Madamanchi & Runge, 2013). It is also activated by a number of antioxidants such as cysteine based redox regulators of glutathione and thioredoxin pathways, which hint towards its complex regulation (Winyard *et al.*, 2005). The DNA binding domain of Fos and Jun protein possesses an oxidation susceptible conserved cysteine residue making it redox sensitive (Abate *et al.*, 1990). AP-1 activity is at the basal level in adapted myocardium, whereas in isolated hearts, the duration of ischemia and reperfusion correlates with an increase in AP-1 activity, suggesting that AP-1 stimulates oxidative stress-induced apoptosis (Maulik *et al.*, 2000; Madamanchi & Runge, 2013).

3. Nuclear factor erythroid 2 (NFE2)-related factor 2 (Nrf2)

Nrf2 belongs to the bZIP subfamily of transcription factors. Under basal conditions, a cysteine rich Kelch-like ECH-associated protein 1 (Keap1) binds Nrf2 and targets it for ubiquitin-dependent proteasomal degradation. Oxidation disrupts the Nrf2-Keap1 complex resulting in Nrf2 stabilization thereby its activation leading to increased transcription of genes such as heme oxygenase-1 (HO-1), glutathione S-transferase, and NAD(P)H:quinineoxidoreductase 1, thus helps to maintain the cellular redox homeostasis (Itoh *et al.*, 1999, 2003; Ma, 2013; Madamanchi & Runge, 2013). Nrf2 activation protects cardiomyocytes, VSMCs and endothelium against oxidative stress (Levonen *et al.*, 2007; Dreger *et al.*, 2009; He, Siow, *et al.*, 2011). Furthermore, atheroprotective laminar flow activates whereas proatherogenic oscillatory flow inhibits Nrf2 activity in human endothelial cells, underlying the importance of Nrf2 regulated gene expression in vascular homeostasis (Hosoya *et al.*, 2005; Madamanchi & Runge, 2013).

Cardiac hypertrophy and the activation of fetal gene expression.

In the fetus, the predominant source of energy is carbohydrate metabolism, which after birth switches to fatty acid oxidation accompanied by expression of "adult" isoforms of metabolic enzymes and other proteins. However, in response to hemodynamic or metabolic stress conditions including hypoxia, ischemia, hypertrophy and atrophy, there is reactivation of fetal gene program in the heart. As a result, there is re-emergence of features of fetal heart metabolism and carbohydrates are preferably used as substrates for energy generation in a relatively hypoxic environment (Goodwin *et al.*, 1998; Bartelds *et al.*, 2000; Rajabi *et al.*, 2007). Additional features of the reprogramming include the re-expression of genes crucial for fetal development such as atrial natriuretic factor (ANF), transforming growth factor β (TGF-β), early response genes (c-myc and c-fos), and also there is isoform switches of many other proteins including sarcomeric proteins (myosin heavy chains and α-actins) (Schwartz *et al.*, 1992; Taegtmeyer *et al.*, 2010; Nandi & Mishra, 2015).

C.IV. Pathological roles of cardiac redox signaling

Redox signaling plays a crucial part in modulating the complex phenotype associated with heart failure, including contractile dysfunction, arrhythmia, cardiac hypertrophy, fibrosis and myocyte death (Figure 6).

1. Abnormal Ca^{2+} regulation, contractile dysfunction and arrhythmia

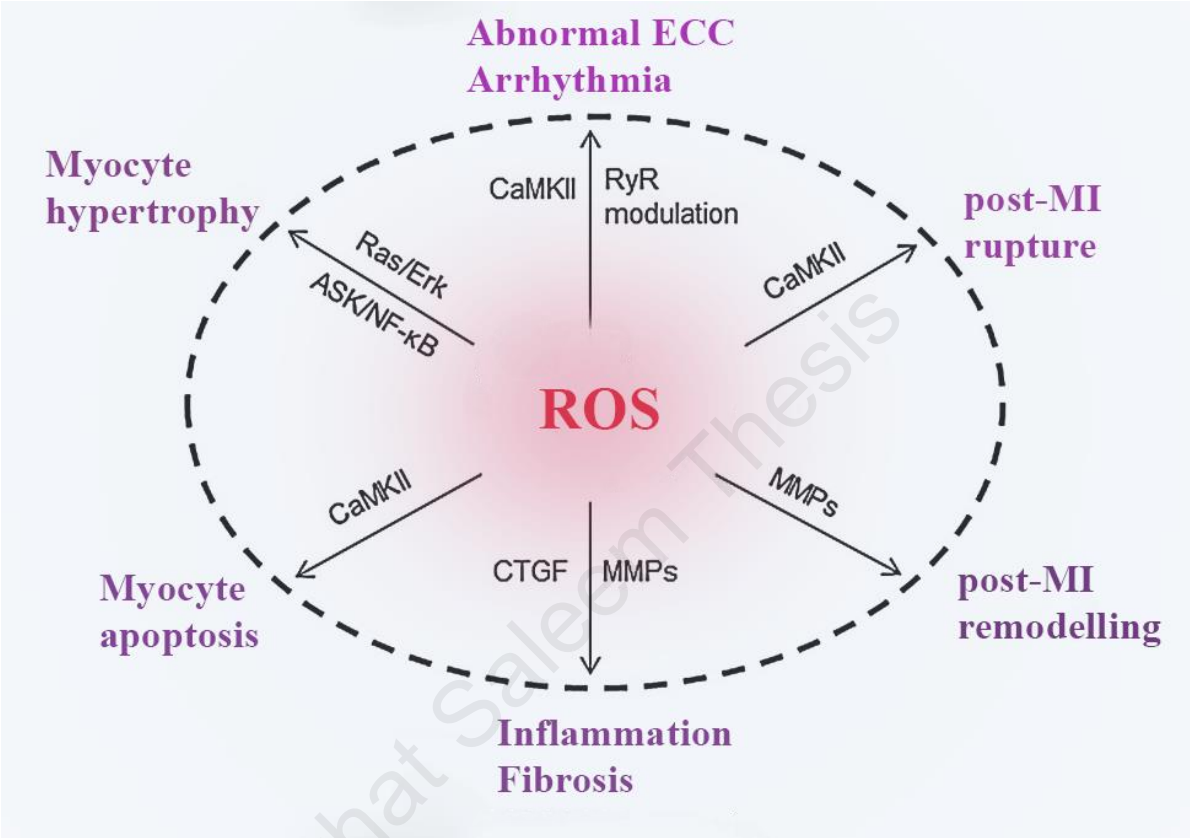

Figure 6. Pathological roles of redox signaling in heart: The excess of ROS generated from NADPH oxidases induce diverse signaling partners contributing to various pathological consequences.

Adapted from Zhang M et al., (2013) Antioxidants and Redox Signaling

Redox signaling plays a significant role in Ca^{2+} homeostasis and disturbances in this homeostasis is the fundamental characteristics of heart failure (Zima & Blatter, 2006). PKA or CaMKII mediated hyperphosphorylation of RyR2 or its direct oxidation contributes to RyR2 dysfunction leading to diastolic Ca^{2+} leak from SR thereby increasing diastolic Ca^{2+} as well as reduced systolic force associated with arrhythmia (Terentyev *et al.*, 2008; Sag *et al.*, 2011). Under chronic Ang II stimulation, Nox-generated ROS hyperactivate the RyR2 mediated Ca^{2+} leak which results in aberrant Ca^{2+} release and arrhythmogenic waves (Prosser *et al.*, 2011). In the mouse model of AngII-induced dysrhythmia, Nox2-dependent CaMKII oxidation leads to apoptosis of sinoatrial cells and thus promotes sinus node dysfunction (Swaminathan *et al.*, 2011; Mollova *et al.*, 2015). Increased SERCA2a oxidation is also reported to be involved in contractile dysfunction. Sulfination (irreversible oxidation of sulfenic acid; R-SOH) of SERCA2a at Cys674 and nitration at Tyr294/295 were noted in transgenic mice overexpressing Gαq (heart failure model) (Lancel *et al.*, 2010; Salazar-Cantú *et al.*, 2016).

2. Myocyte death and ischemia reperfusion

Cardiomyocyte death add in ischemia-reperfusion injury and development of chronic heart failure (Dorn, 2009). Both the extrinsic and intrinsic apoptotic pathways are redox regulated. The mechanisms involved in ROS mediated intrinsic pathway activation include promotion of Ca^{2+}-dependent/direct opening of MPTP or translocation of pro-apoptotic proteins Bax/Bad to mitochondria. Also, ROS mediates extrinsic pathway activation and further activation of ligands of death receptor superfamily (Burgoyne *et al.*, 2012). Furthermore, β-AR activation contributes to ROS-dependent c-JNK activation which in turn activates mitochondrial death pathway in adult cardiomyocytes (Remondino *et al.*, 2003). Downstream to GPCRs, ROS-activated MAPKKK Ask-1 activates p38MAPK/c-Jun N-terminal kinase and the mitochondrial pathway. Cardiomyocyte apoptosis is induced in transgenic mice overexpressing ASK-1, whereas ASK-1 null mice exhibited attenuation of ventricular remodeling after pressure overload and decrease in apoptosis. The ASK-1/p38MAPK pro-apoptotic pathway is also activated with AngII stimulated Nox2 derived ROS (Hirotani *et al.*, 2002; Yamaguchi *et al.*, 2003; Burgoyne *et al.*, 2012). Early after MI, the Nox2 level increases in cardiomyocytes and inflammatory cells (Fukui *et al.*, 2001; Krijnen *et al.*, 2003). The elevated level of Nox2 mediates oxidation of CaMKII that leads to enhanced matrix metalloproteinase (MMP)-9 activity resulting in early cardiac rupture (He, Joiner, *et al.*, 2011). Moreover, $Nox2^{-/-}$ and $p47phox^{-/-}$mice

have shown compromised adverse post-MI remodeling (Doerries *et al.*, 2007; Zhang *et al.*, 2013).

3. Interstitial Fibrosis and Extracellular Matrix Remodeling

Increased mechanical load or local tissue injury trigger fibrosis via activation of RAAS and inflammatory pathways. Redox regulation contribute to fibrosis, involving fibroblasts, cardiomyocytes, endothelial cells, inflammatory cells and other circulating cells. (Chen & Frangogiannis, 2010; Burgoyne *et al.*, 2012). ROS activate latent TGF-β, which promote transformation of interstitial fibroblast into myofibroblasts (Barcellos-Hoff & Dix, 1996). In addition to TGF-β, ROS also promote transcription of other profibrotic factors such as CTGF (connective tissue growth factor), in fibroblasts and cardiomyocytes (Park *et al.*, 2001). TGF-β–induced cardiac myofibroblast differentiation involves Nox4 regulated Smad2/3 signaling (Cucoranu *et al.*, 2005). Further, AngII-induced myofibroblast transformation is Nox2-dependent and involves activation of c-JNK and calcineurin/NFAT. Significantly reduced interstitial fibrosis was found in $Nox2^{-/-}$ mice under AngII or aldosterone infusion, chronic RAAS activation or aortic banding (Burgoyne *et al.*, 2012; Zhang *et al.*, 2013). Although Nox4 too is reported to be profibrotic *in vitro* but *in vivo* models did not mimic the effect as under chronic pressure overload, rather, global Nox4 knockout mice developed more (not less) fibrosis (Zhang *et al.*, 2010). MMPs expression and activation is redox sensitive and depending on context its activation may release profibrotic/antifibrotic factors. In cardiomyocytes, β-adrenergic stimulation induces the H_2O_2/c-JNK-dependent expression of MMP inducer, which in turn aggravate MMP-2 activity (Li *et al.*, 2000; Spinale, 2007; Siwik *et al.*, 2008; Sawicki, 2013).

4. Cardiac hypertrophy and failure

Cardiac hypertrophy is an adaptive response to increased cardiac workload. It accompanies many forms of cardiac dysfunction including ischemia, hypertension and heart failure. In the setting of hypertrophy, changes in the heart was divided into three stages by Meerson and colleagues in 1960 viz., (1) developing hypertrophy, where the cardiac work load exceeds the cardiac output, (2) compensatory hypertrophy, where the load/mass ratio is normalized with resting cardiac output and (3) overt heart failure, where the ventricle dilation and progressive decline in cardiac output occur despite of continuous activation of the hypertrophic program (Meerson, 1961; Frey *et al.*, 2004; Madamanchi & Runge, 2013).

Cell size increase, enhanced protein synthesis, and heightened organization of the sarcomere derive cardiomyocyte hypertrophy at cellular level while at molecular level these changes are accompanied by fetal gene re-induction. Phenotypically, cardiac hypertrophy can be divided into two types: concentric hypertrophy in response to pressure overload, which involves addition of sarcomeres in parallel resulting in lateral cell growth, and (2) eccentric hypertrophy in response to volume overload which involves addition of sarcomeres in series resulting in longitudinal cell growth (Dorn *et al.*, 2003; Fernandes *et al.*, 2011).

Cardiomyocyte hypertrophy involves multiple overlapping signaling pathways and many of these pathways are redox modulated (Mudd & Kass, 2008; Sag *et al.*, 2014). GPCR agonists (AngII, ET-1 and α-AR agonists)-induced cardiac hypertrophy is reported to be mediated by Nox2 generated ROS and involves activation of redox regulated kinase i.e. Erk1/2 and the transcription factor NF-κB (Xiao *et al.*, 2002; Hingtgen *et al.*, 2006). LV hypertrophy was shown to be abrogated in Nox2 or ASK1 knockout mice under the stimulation of AngII (Bendall *et al.*, 2002; Izumiya *et al.*, 2003).

An array of stimuli such as mechanical strain and natriuretic peptide, and activation of receptors like GPCRs and receptor tyrosine kinase are involved in pressure overload hypertrophy. In cultured myocytes, mechanical strain leads to hypertrophy through induction of Rac1/Nox2-dependent Erk-1/2 and p38MAPK activation (Pimentel *et al.*, 2001; Li *et al.*, 2002; Burgoyne *et al.*, 2012; Zhang *et al.*, 2013; Tham *et al.*, 2015). $ACE2^{-/-}$/$p47phox^{-/-}$ double knockout mice have shown significantly reduced susceptibility to pressure overload–induced LVH and heart failure as compared to only ACE2 null mice (Bodiga *et al.*, 2011). Pressure-overload-induced hypertrophy also involves redox regulated components of several signaling pathways such as PI3K/Akt, PKD, PKA, JAK-STAT, and calcineurin/NFAT. Prolonged, severe pressure-overload leads to development of heart failure which may involve an elevated level of mitochondrial ROS and its associated mitochondrial DNA damage and protein oxidation. It was reported that cardiomyocyte-specific Nox4 overexpression promoted pressure overload–induced heart failure, however, hypertrophy was not affected (Ago *et al.*, 2010; Kuroda *et al.*, 2010). Mice with chronic pressure overload, infusion of AngII or cardiomyocyte-targeted Gq overexpression develop heart failure in long term whereas mitochondrial-targeted catalase overexpression in mice significantly ameliorated it (Dai *et al.*, 2011). Although Nox4-derived ROS promote detrimental effects during pressure overload but a number of reports suggests its beneficial proangiogenic effects as well. Also, recent evidence shown

protection of the heart from dilation, contractile depression and pressure overload-induced hypertrophy after cardiac-specific overexpression of Nox4 (Zhang *et al.*, 2010).

D. Models to study the pathophysiology of cardiac hypertrophy and failure

Cardiovascular diseases are the leading cause of death worldwide. Therefore, a number of *in vitro* as well as *in vivo* models mimicking the vast array of clinical phenotypes have been developed to understand the pathophysiology of the disease and to target pathological remodeling of the heart with the intent to prevent, arrest or possibly reverse the progression of disease (Figure 7).

D.1. *In vitro* models

Neonatal cardiomyocytes in primary culture is widely used for cell culture based studies because of the lack of a true 'cardiac' cell line. These cells are isolated from rat and after about one division in cell culture, they can be maintained for about a week in healthy state. Although adult ventricular myocytes are also isolated and maintained for some period in culture, but they start dedifferentiating with time and lose crucial features of adult cardiomyocyte phenotype ("Berry: Models of cardiac hypertrophy and transition... - Google Scholar," 2017). Cell culture based studies using rat ventricular myocytes (NRVMs) elucidated molecular mechanisms of myocardial hypertrophy and failure. Exposure of isoproterenol (β-AR agonist), AngII or phenylephrine (α-AR agonist), triggers increase in NRVMs size *in vitro* and have been used to develop a model of hypertrophy (Ding *et al.*, 2014; Wang *et al.*, 2014; Medzikovic *et al.*, 2015). Other cell lines which are alternatively used for cardiac hypertrophy related experiments and are easier to maintain include H9c2 myoblasts and C2C12 myoblasts. H9c2 myoblasts are isolated from embryonic rat hearts and proliferate in culture. For studies, these can also be induced to differentiate into myotubes (Watkins *et al.*, 2011; Purushothaman & Nair, 2016). C2C12 myoblasts are derived from skeletal muscle and used for molecular studies (Montesano *et al.*, 2013).

D.2. *In vivo* models

Based on stress and growth signals observed in cardiac diseases in human, cardiac hypertrophy and failure animal models have been generated.

1. Pressure-overload induced hypertrophy

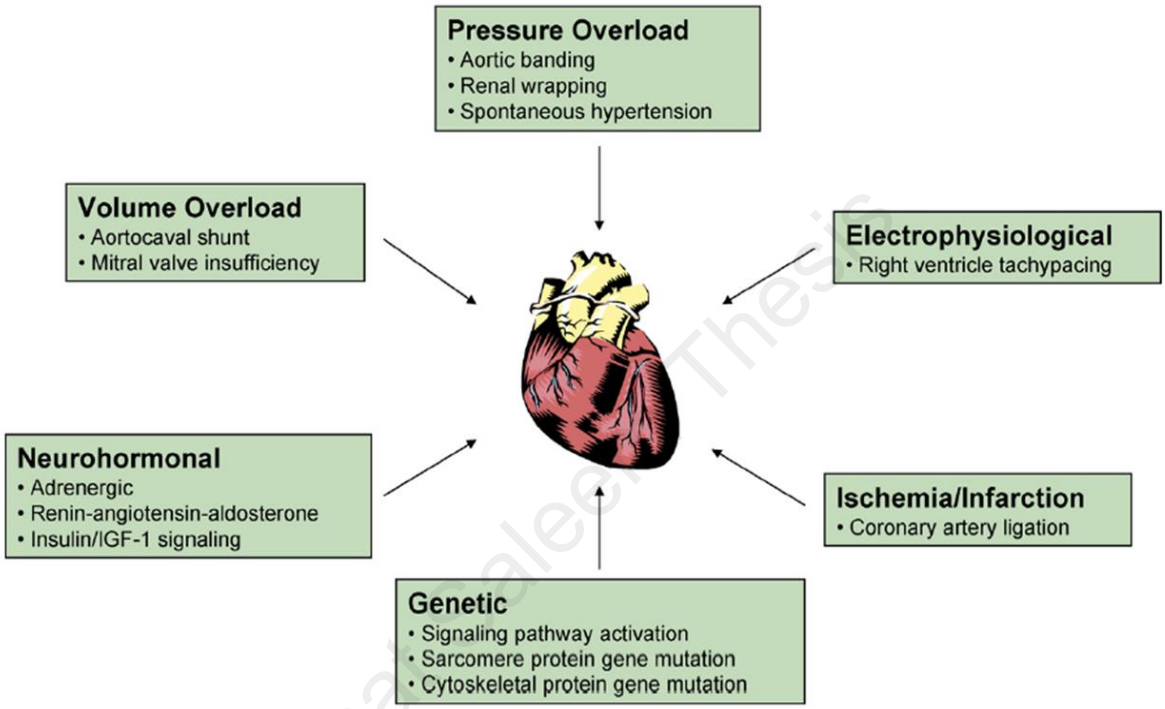

Figure 7. Stressors leading to cardiac hypertrophy: Models for studying hypertrophy and failure are developed by imposing one or more of the stresses which lead to diseased condition.

Adapted from Berry et al., (2007) Drug Discovery Today: Disease Models

To manage the persistently increased afterload (left ventricle wall pressure during ejection) in heart diseases such as hypertension and aortic stenosis, the left ventricle generates a higher systolic blood pressure so that an adequate stroke volume can be ejected, referred as pressure overload. Methods adopted for modeling the pressure overload stress (and thus cardiac hypertrophy and heart failure) for experimental purposes include surgical banding of ascending (Weinberg *et al.*, 1994), transverse (Rockman *et al.*, 1991), or descending aorta, renal wrapping to produce persistent hypertension (Munagala *et al.*, 2005) and feeding high salt diet for weeks to develop significant increase in blood pressure (Dahl salt sensitive model) (Iwanaga *et al.*, 2002; Rysä *et al.*, 2005; Patten & Hall-Porter, 2009). Moreover, variation in animal strain and banding technique can results in varying phenotype due to differential activation of stress-response signaling pathways. Adult male C57BL6 mice with moderate aortic banding, develop ventricular hypertrophy with a normal ejection fraction (termed compensated ventricular hypertrophy) while, with slightly more severe banding leads to dilated heart, compromised systolic function, heart failure and increase in mortality (termed decompensated ventricular hypertrophy) (Rothermel *et al.*, 2005).

2. Volume-overload induced hypertrophy

Another pathological stress is continuous increase in preload (end diastolic volume which stretches the left/right ventricle to its largest dimensions) which occurs in patients with aortic regurgitation, chronic mitral regurgitation, arteriovenous malformations and specific kinds of congenital heart disease. Therefore, there is a setting of increase in stroke volume to maintain the forward cardiac output, termed volume overload. Volume-overload induced hypertrophy model is developed by creating an aortocaval shunt which results in animal with significantly dilated heart over several months (Cantor *et al.*, 2005).

Several studies have been performed on animal model of combined pressure and volume overload, which is developed by rupturing the aortic valve followed by surgical constriction of abdominal aorta. Myocardial infarction animal model is developed by surgical ligation of a coronary artery (Ai *et al.*, 2005).

3. Neurohormonal stress

Cardiac hypertrophy and heart failure is associated with increase in sympathetic activity and thereby a cardiac hypertrophy and heart failure model can be developed by stimulation of adrenergic signaling pathways. Isoproterenol induced cardiac hypertrophy is well

established in animal model. Another neurohumoral stress induced model can be developed by continuous administration of angiotensin II causing activation of Renin-Angiotensin-Aldosterone system (RAAS) leading to pathological ventricular remodeling and heart failure (Leenen *et al.*, 2001; Matsumoto *et al.*, 2013; Chen *et al.*, 2014).

E. Clinical and translational implications

With the emergence of role of redox signaling in the development of cardiovascular diseases, clinical trials are being addressed to combat risk factors associated with ROS (Burgoyne *et al.*, 2012). The nonspecific antioxidant approaches have mostly proven unsuccessful in combating the risk factors, thus better strategies are needed including targeting specific ROS sources and redox modulated pathways (Sawyer, 2011). In recent years, great interest has been shifted towards the development and use of specific Nox inhibitors. The complex signaling mechanisms of disease progression involve Nox and therefore, inhibition of Nox activity can be done at several different points including the inhibition of catalytic or regulatory subunits, blockage of translocation of cytosolic subunits to the membrane and by inhibition of the signal transduction pathways upstream of NADPH oxidase activation (Figure 8) (Cai *et al.*, 2003; Streeter *et al.*, 2013). Generally, small-molecule inhibitors are opted for their hydrosolubility and oral bioavailability. The trial of peptide-based Nox inhibitors is currently an area of intense research.

Peptide based Nox specific inhibitor gp91ds-tat, developed by Pagano and coworkers, is a chimeric peptide composed of nine amino acids of gp91phox and nine amino acids from HIV coat protein (Rey *et al.*, 2001). The coat protein TAT allows the peptide to enter cells readily (Fawell *et al.*, 1994), then gp91phox portion binds with p47phox and interferes its assembly with endogenous gp91phox, which ultimately leads to Nox activation in the heart (Nox2) (Streeter *et al.*, 2013). Although this peptide inhibitor is useful and effective, it possesses limited potency for clinical therapeutics because its oral administration cannot be done.

Several small molecules are also used as Nox inhibitors. Extensive study has been done using apocynin as an inhibitor in animal models of inflammation and cardiovascular diseases. This molecule is extracted from the leaves of *Picrorhiza kurroa* and can be given orally too. Apocynin blocks oxidase assembly (Stolk *et al.*, 1994) but it is also reported as an antioxidant and thus it might not be a Nox specific inhibitor (Heumüller *et al.*, 2008). However, whether these effects are nonspecific or downstream to Nox generated ROS is

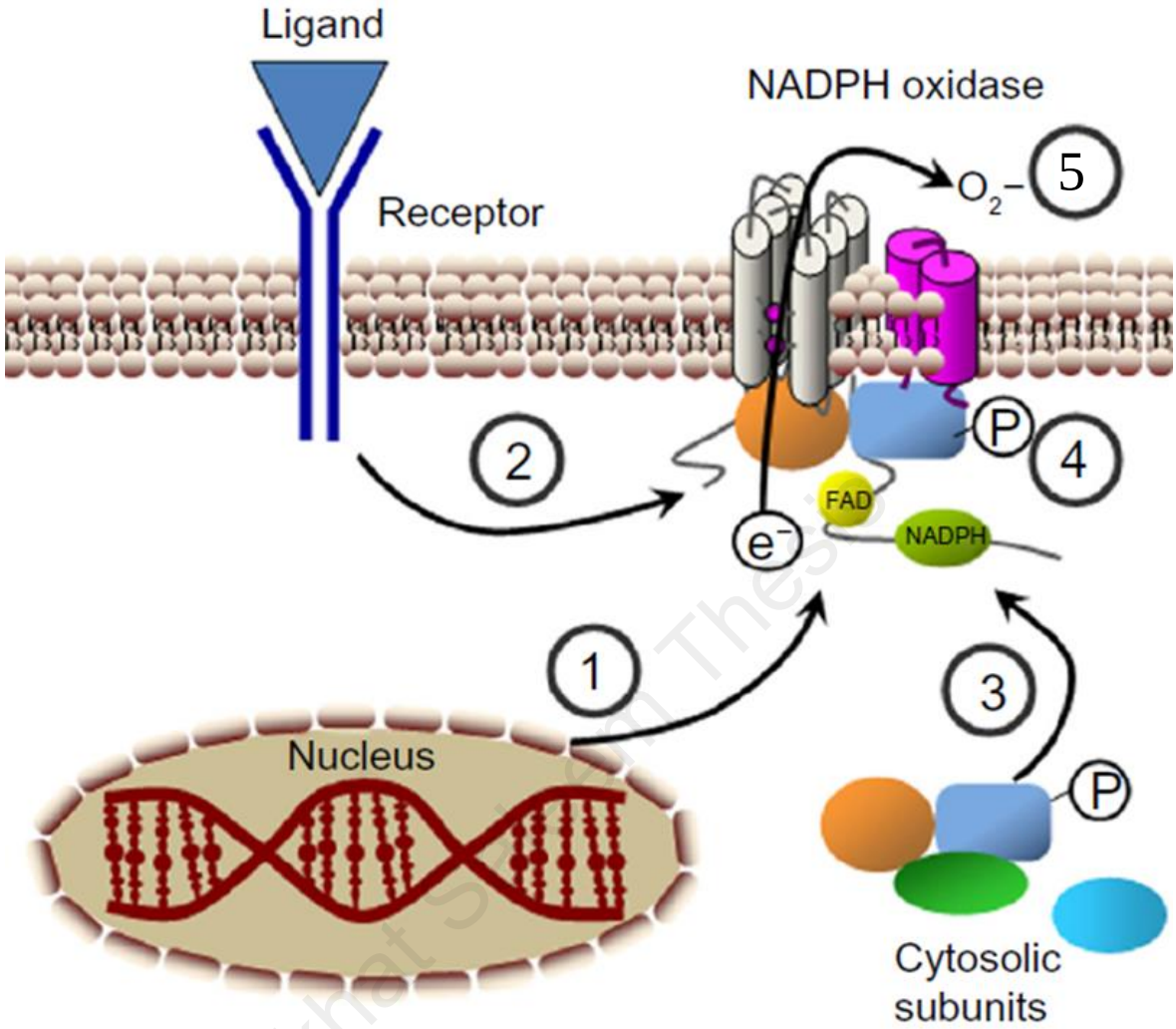

Figure 8. Potential targets for NADPH oxidase inhibition: The activation of Noxes can be prevented by targeting (1) the expression of Nox subunits, (2) the signaling upstream to Nox activation, (3) translocation and assembly of cytosolic subunits, (4) phosphorylation and activation of subunits and (5) electron transfer through the enzyme complex.

Rodiño-Janeiro BK et al., (2013) Vascular Health and Risk Management

not clear but apocynin is still the most employed inhibitor of Nox (Williams & Griendling, 2007; Petrônio *et al.*, 2013).

Pefabloce [aminoethylbenzenesulfono fluoride (AEBSF)] is another agent which inhibits assembly of p47phox to cytochrome b558, but as this is a serine protease inhibitor, it has many other nonspecific effects too (Diatchuk *et al.*, 1997; Streeter *et al.*, 2013).

Aims and Objectives

Cardiovascular diseases encompass dysfunction of heart and blood vessels leading to highest number of death worldwide (Mozaffarian *et al.*, 2016). Many of the cardiac insults such as ischemic heart disease, myocardial infarction, cardiomyopathy, and hypertension lead to heart failure. Although, initial cardiac overload elicit adaptive response characterized by cardiac remodeling that involves reprogramming of gene expression in both myocytes and non-myocytes resulting in increased cardiac volume termed hypertrophy. However under prolonged stress, it leads to maladaptation followed by cardiomyocyte loss by apoptosis causing heart failure (Burchfield *et al.*, 2013). These responses are mediated by a plethora of signal transducing kinases, phosphatases, and transcriptional regulators, often with paradoxical interconnections (Arad *et al.*, 2007; Kass *et al.*, 2007). Further, the compensatory neurohumoral response involves activation of sympathetic nervous system as depicted by increased level of catecholamines (de Lucia *et al.*, 2014).

Catecholamine binding activate its cognate receptors (α and β adrenergic receptors with several subtypes) which in turn activate downstream signalling cascades (Capote *et al.*, 2015). Norepinephrine (NE) induce hypertrophy at a lower concentration and apoptosis at a higher dose (Gupta *et al.*, 2006). However, the underlying mechanism of such concentration dependent response is not fully understood as yet. Oxidative stress is implicated in the pathogenesis of a plethora of cardiovascular diseases including interstitial fibrosis, contractile dysfunction, ischemia-reperfusion injury and cardiac remodelling (Murray *et al.*, 2014; Münzel *et al.*, 2015). Further, studies have depicted that both low and high doses of NE elicit their respective effects via generation of ROS (Clerk, 2003). However, the precise mechanism by which ROS leads to differential response is largely unknown.

Our laboratory have been investigating differential adrenergic signaling as a paradigm of understanding how ROS differentially direct cardiac myocytes towards hypertrophic or apoptotic pathways. It was demonstrated in our laboratory that in H9c2 cardiac myoblasts, both the hypertrophic response; elicited by limited adrenergic stimulation (≤10 μM NE), and apoptotic response; induced by higher dose (≥50 μM NE), is prompted through distinct but comparable repertoire of ROS at the onset followed by respective gene expression programs (Gupta *et al.*, 2006; Jindal & Goswami, 2011; Thakur *et al.*, 2015).

In the present study, we primarily intended to understand the redox signalling under adrenergic stress.

In recent years, NADPH oxidases (Noxes) have emerged as an important player in cardiovascular pathophysiology (Bedard & Krause, 2007; Brandes *et al.*, 2010; Nabeebaccus *et al.*, 2011; Lassègue *et al.*, 2012). Despite the growing evidences on the role of specific Nox isoforms; mechanisms of their activation, targets of reactive oxygen species (ROS) generated and their downstream effects are poorly understood as yet. Agonist (NE, Isoproterenol etc.) binding stimulate adrenergic receptors and generate ROS from membrane associated NADPH oxidases (Brandes *et al.*, 2014b). However, due to high reactivity and extremely short half-life of ROS, their precise nature, subcellular origin and the extent of involvement in the downstream signalling is unknown. We intend to investigate differential adrenergic-Nox signaling as a paradigm of understanding how ROS drive cardiac myocytes towards hypertrophic pathways.

In pursuing this broad objective, the specific objectives that were pursued in this study are:

1. *To study the spatio-temporal generation of H_2O_2 in H9c2 cardiac myoblasts under norepinephrine treatment.*
2. *To study the role of H_2O_2 generated by NADPH oxidase in mediating redox signaling induced by NE.*
3. *To investigate the mechanisms of modulation of aderenergic signaling by ROS.*

Materials and Methods

MATERIALS

All biochemicals were procured from Sigma-Aldrich, St Louis, USA or Fisher Scientific unless mentioned otherwise.

H9c2 cardiac myoblasts were procured from Sigma Aldrich, USA (originally from ECACC, UK).

Dulbecco's Modified Eagle's Medium (DMEM), Penicillin Streptomycin solution, Amphotericin B, Sodium bicarbonate, Norepinephrine, Isoproterenol, Apocynin and Fetal Bovine Serum were purchased from Sigma Aldrich, USA. Peptide inhibitor gp91ds-tat (RKKRRQRRRCSTRIRRQL-NH2) was obtained from AnaSpec, Inc. Trypsin-EDTA solution was purchased from Invitrogen Life Technologies, USA. The filter unit for medium filtration was purchased from Nalgene International, Denmark and filter membranes (0.22 μm pore size) were from Millipore. Tissue culture plastic ware was from Corning International, USA and Greiner, Germany. All other plastic wares were from Tarsons, Germany.

All restriction enzymes, DNA modifying enzymes and DNA ladder (100 bp and 1 kb) were procured from Thermo Fisher Scientific USA or New England Biolabs, USA. Bacterial growth media (LB and Agar) was purchased from HiMedia. Plasmid Isolation kit and gel extraction kit were from Qiagen, Germany. Pre-stained protein molecular weight marker was obtained from Puregene, Genetix, India. RNA Isolation reagent was TRI reagent from Sigma, USA. Reverse Transcription kit and Power SYBR® Green Master Mix was procured from Applied Biosystems, Inc., USA. Escort (IV) Transfection Reagent was purchased from Sigma, USA. Luciferase Assay System was bought from Promega Corporation, Madison, USA.

PVDF membranes were purchased from Amersham Biosciences, USA. X-Ray Films were purchased from Kodak. Filter Papers were purchased from Whatman Ltd. (Madistone, England). Enhanced Chemiluminiscence (ECL) detection reagent was purchased from Sigma-Aldrich, USA.

Plasmid Constructs: pHyPer-Cyto and pHyPer-Mito constructs were obtained from Evrogen (Moscow, Russia). The human ANF reporter plasmid containing luciferase reporter gene (ANF-luc) was a kind gift from Dr. KR Chein, Department of Medicine, Center for Molecular Genetics, University of California at San Diego, School of Medicine, La Jolla, California (Knowlton *et al.*, 1991). p22-phox-Wt and p22-phox-DN constructs were kind gift from Dr. Jaharul Haque, Cleveland Clinic, USA (Kawahara *et al.*, 2005).

Antibodies: List of antibodies used in the experiments.

	Antibody	Host	Catalogue No.	Dilution used
1.	Akt (pan)	Rabbit	CST; 4685	1:2000 (WB)
2.	phospho-Akt (Ser473)	Rabbit	CST; 4060	1:1000 (WB)
3.	ANP	Mouse	sc 515701	1:500 (WB) 1:50 (ICC)
4.	β-MHC	Rabbit	Biorbyt; orb1206	1:50 (ICC)
5.	CREB	Rabbit	ab 32515	1:1000 (WB)
6.	phospho-CREB (Ser133)	Rabbit	ab 32096	1:1000 (WB)
7.	Erk1/2	Rabbit	CST; 4695	1:2000 (WB)
8.	phospho-Erk1/2 (Thr202/Tyr204)	Rabbit	CST; 4370	1:1500 (WB)
9.	FosB	Rabbit	CST; 2251	1:500 (WB) 1:100 (ICC)
10.	GAPDH	Rabbit	CST; 5174	1:5000 (WB)
11.	c-Jun	Rabbit	CST; 9165	1:1500 (WB)
12.	pospho-c-Jun (Ser73)	Rabbit	CST; 3270	1:1500 (WB)
13.	PKA	Rabbit	sc 28895	1:1000 (WB)
14.	phospho-PKA (Ser96)	Rabbit	sc 21901-R	1:500 (WB)
15.	HRP-conjugated anti-Mouse IgG	Goat	sc 2005	1:10000 (WB)
16.	HRP-conjugated anti-Rabbit IgG	Goat	sc 2004	1:10000 (WB)
17.	Alexa fluor-488 anti-Mouse	Goat	TFS; A11029	1:500 (ICC)
18.	Alexa fluor-555 anti-Rabbit	Goat	TFS; A21429	1:500 (ICC)

CST; Cell Signaling Technologies, USA.
sc; Santa Cruz Biotechnology, USA.
ab; Abcam, UK.
TFS; Thermo Fisher Scientific
WB; Western blot
ICC; Immunocytochemistry

Table 1s. List of oligonucleotides used in the experiments (synthesized from Sigma Aldrich, USA)

Name	Sequence
For cloning of pHyPer-ER	
ER signal	Forward 5' TACCGCTAGCATGAACAGCCAAGTGTCAG 3'
ER signal	Reverse 5' TACCGCTAGCGGTCTGCACATTTTGGCAG 3'
ER retrieval	Forward 5' AAGGACGAGCTCTAAAAGCTTCGAATTCTGC 3'
ER retrieval	Reverse 5' GAGCTCGTCCTTAACCGCCTGTTTTAAAACTTTATC 3'
For real time PCR	
ANP	Forward 5' CAGGCCATATTGGAGCAAATC 3'
ANP	Reverse 5' CTCATCTTCTACCGGCATCTT 3'
BNP	Forward 5' CTAGCCAGTCTCCAGAACAATC 3'
BNP	Reverse 5' AGCTGTCTCTGAGCCATTTC 3'
α-MHC	Forward 5' TGGAGAACGACAAGCTTCAG 3'
α-MHC	Reverse 5' GGCCTGCTCATCCTCTATTT 3'
β-MHC	Forward 5' TCCAGCTGAAAGCAGAAAGAG 3'
β-MHC	Reverse 5'CCTGGGAGATGAACGCATAAT 3'
ACTA-1	Forward 5' TATTCAGGCGGTGCTGTCT 3'
ACTA-1	Reverse 5' TCCCCAGAATCCAACACGAT 3'
GAPDH	Forward 5' GACATGCCGCCTGGAGAAAC 3'
GAPDH	Reverse 5' AGCCCAGGATGCCCTTTAGT 3'

METHODS

Cell culture:

H9c2, rat cardiac myoblasts were cultured as monolayer in Dulbecco's modified Eagle medium (DMEM) supplemented with 10% fetal bovine serum (FBS), 90 U/mL Penicillin, 90 µg/mL streptomycin and 5 µg/mL amphotericin B in humidified, 5% CO2 containing incubator at 37 °C. Upon reaching confluence, cells were washed with 1X PBS (phosphate buffered saline) and sub-cultured in the ratio 1:3 with 0.025% trypsin-EDTA solution.

1X PBS (phosphate buffered saline)		
Component		*Amount/1000 mL (w/v)*
1.	Sodium chloride	8.0 g
2.	Potassium chloride	0.2 g
3.	Di-sodium hydrogen phosphate	1.44 g
4.	Potassium di-hydrogen phosphate	0.24 g

ROS/$O^{2\bullet-}$ measurement:

H9c2 cells were grown in 35 mm dishes to 70% confluence and kept in serum free media for 12-14 hr followed by treatment with 2 µM NE for 10 min. Wherever necessary, cells were pretreated with gp91ds-tat peptide (5 µM), 30 min prior to NE treatment. Thirty min prior to imaging, cells were labeled with the fluoroprobes Dichloro-dihydro-fluorescein diacetate (DCFH-DA, 5 µM) or Dihydroethidium (DHE, 10 µM), kept in dark at 37˚C. Cells were then washed in 1XPBS and the images were captured in Nikon Eclipse Ti-E fluorescence microscope using excitation/emission at 504/529 nm and 535/610 nm respectively. For quantification, the mean intensity of fluorescence was measured by NIS-Elements software (Nikon).

Isolation of RNA:

Following requisite treatments and time periods, 1 mL Tri Reagent (Sigma) was added to the H9c2 cells (in 100 mm dish) or the tissue (100 mg; homogenized using tissue tearer followed by centrifugation at 10,000g for 15 min). The lysate was then incubated at room temperature for 5 min and 200 µL of chloroform was added followed by a brief but vigorous shaking. Following incubation at room temperature for 10 min, the mixture was centrifuged at 10,000g for 15 min at 4°C. The upper aqueous phase was carefully removed in a clean RNAse free tube and one starting volume of chilled isopropanol was added and the mixture was then incubated at RT for 10 min. Thereafter, the samples were centrifuged

at 10,000g for 20 min at 4°C to pellet down the RNA. The pellet was then washed with 75% ethanol followed by centrifugation at 10,000g for 5 min at 4ºC. The pellet was air dried and resuspended in appropriate amount of nuclease free water.

Spectrophotometric estimation of nucleic acids:

The quantity and purity of plasmid DNA and RNA were determined by measuring absorbance at 260 nm and 280 nm. The concentration of dsDNA was calculated by taking the Abs260 = 1 = 50 µg/mL. The concentration of ssRNA was calculated by taking the Abs260 = 1 = 40 µg/mL.

Reverse transcription polymerase chain reaction (RT-PCR):

First strand cDNA was synthesized from 1 µg of RNA using Applied Biosystems reverse transcription kit as per manufacturer's instructions. PCR reactions were performed using the Taq DNA polymerase (NEB) and gene-specific primers (Table 1s).

Polymerase Chain Reaction:

Polymerase chain reaction was carried out in 50 µL reaction volume with 1X buffer, 0.2 mM dNTPs, 2 ng/µL primers, 5 ng of template and 1U of Taq Polymerase (NEB).

Cycling condition was as follows:

1. 95° C for 5 min	Initial Denaturation
2. 95° C for 1 min	Denaturation
3. 55° C -60° C for 1 min	Annealing
4. 68° C for 1-6 min	Extension
5. Step 2-4 30- 35 times	
6. 68° C for 5 min	Final Extension

Restriction digestion:

Restriction digestion was carried out in the appropriate buffer according to the manufactures instructions (Thermo Fisher Scientific, USA or NEB, USA).

Ligation reaction:

Restriction digested vector and insert DNA were purified from agarose gel and ligated according to : [Amount of insert = (Size of insert/Size of vector) X 100 ng of vector] in 20 µL volume in 1X Ligase buffer and 5U of T4 DNA ligase (NEB, USA) at 16°C overnight.

Transformation of competent DH5α Cells with plasmid DNA:

Five to ten ng of plasmid DNA or equivalent quantity of ligation reaction was added to 100 µL of DH5α competent cells, mixed well by gentle tapping and incubated on ice for 30 min. Heat shock was given for 90 sec at 42ºC followed by a rapid chilling for 5 min. LB medium (900 µL) was added and the transformation mix was allowed to revive for 1 hr at 37ºC. Appropriate volume of the transformation culture plated on LB agar plate supplemented with appropriate antibiotic. Plates were incubated at 37ºC for 12-16 hr until the colonies were apparent.

Plasmid DNA isolation (Mini Preparation):

Single colony culture was grown in 2 mL of 2% LB medium with appropriate antibiotic (100 µg/mL ampicillin or 25 µg/mL kanamycin) at 37ºC overnight with vigorous shaking. The culture was then pelleted at 5000 rpm for 10 min; the supernatant was drained out by leaving about 50 µL of LB. The cell pellet was then resuspended in the remaining LB by vortexing followed by the addition of 225 µL of solution II. The suspension was mixed by inversion and incubated on ice for 5 min. 115 µL of ice-cold solution III was added, incubated on ice for 5 min and then centrifuged for 15 min at 13,000 rpm. The supernatant was transferred in to a fresh tube and the plasmid DNA was precipitated by adding 1 mL of 100% ethanol. After incubation at room temperature for 15 min, DNA was collected by centrifugation at 13,000 rpm for 15 min. The pellet was washed with 70% ethanol, dried and resuspended in 30 µL of nuclease free water.

Solution II				
Component		*Stock conc*	*Working conc*	*Amount/10 mL (v/v)*
1.	Sodium hydroxide	1 N	0.2 N	2 mL
2.	SDS	10%	1%	1 mL

Solution III				
Component		*Stock conc*	*Working conc*	*Amount/100 mL (v/v)*
1.	Potassium acetate	5 M	3 M	60 mL
2.	Glacial acetic acid			11.5 mL

Agarose gel electrophoresis of DNA:

Agarose gel electrophoresis was done as described in Sambrook et al., 1989. Routinely 1% agarose gels prepared in 1 X TAE buffer containing 0.5 µg/mL ethidium bromide were used.

50X TAE (Tris acetate EDTA buffer)				
Component		*Stock conc*	*Working conc*	*Amount/100 mL (w/v) or (v/v)*
1.	Tris base		40 mM	24.2 g
2.	EDTA	0.5 M; pH 8.0	1 mM	10 mL
3.	Glacial acetic acid			5.7 mL

Construction of pHyPer-ER:

For targeting HyPer to endoplasmic reticulum (ER), the HyPer-ER was reconstituted from HyPer-Cyto essentially as described by Malinouski et al (Malinouski *et al.*, 2011). Briefly, an 87 nucleotide long oligonucleotide harboring the ER signal peptide sequence of 29 amino acids was generated from the total RNA isolated from the pituitary gland of rat by using appropriate primers (Table 1s). The PCR product was then cloned in frame at the N-terminal of pHyPer-Cyto. Also, in the C-terminal, a synthetic 12 nucleotide long sequence harboring the ER retention signal (KDEL) was inserted (Figure 1s).

Transient transfection:

H9c2 cardiac myoblasts were grown up to 60-70% confluence and transiently transfected with plasmids using Escort IV transfection reagent. Briefly, plasmid DNA and transfection reagent were mixed in 1:2 ratio (in DMEM) per well. Cells were incubated with the transfection reagent in serum- and antibiotic-free medium for 10-12 hr, followed by incubation in medium containing twice the concentration of serum and antibiotics for 6 hr. Cells were then kept in 10% serum containing medium for 6 hr. Finally, cells were kept in serum-free medium for 12 hr, treated with inhibitor and/or agonist and proceeded as per the requirement of experiment. For promoter reporter assay using p22-phox-Wt/DN constructs, cells were co-transfected with p22-phox-Wt/DN plasmid and reporter plasmids.

Measurement of cell compartment specific H2O2 generation:

H9c2 cells were grown in 35 mm glass bottom dish to 70% confluence followed by transient transfection. After 24 hr of transfection, cells were kept in serum free media for

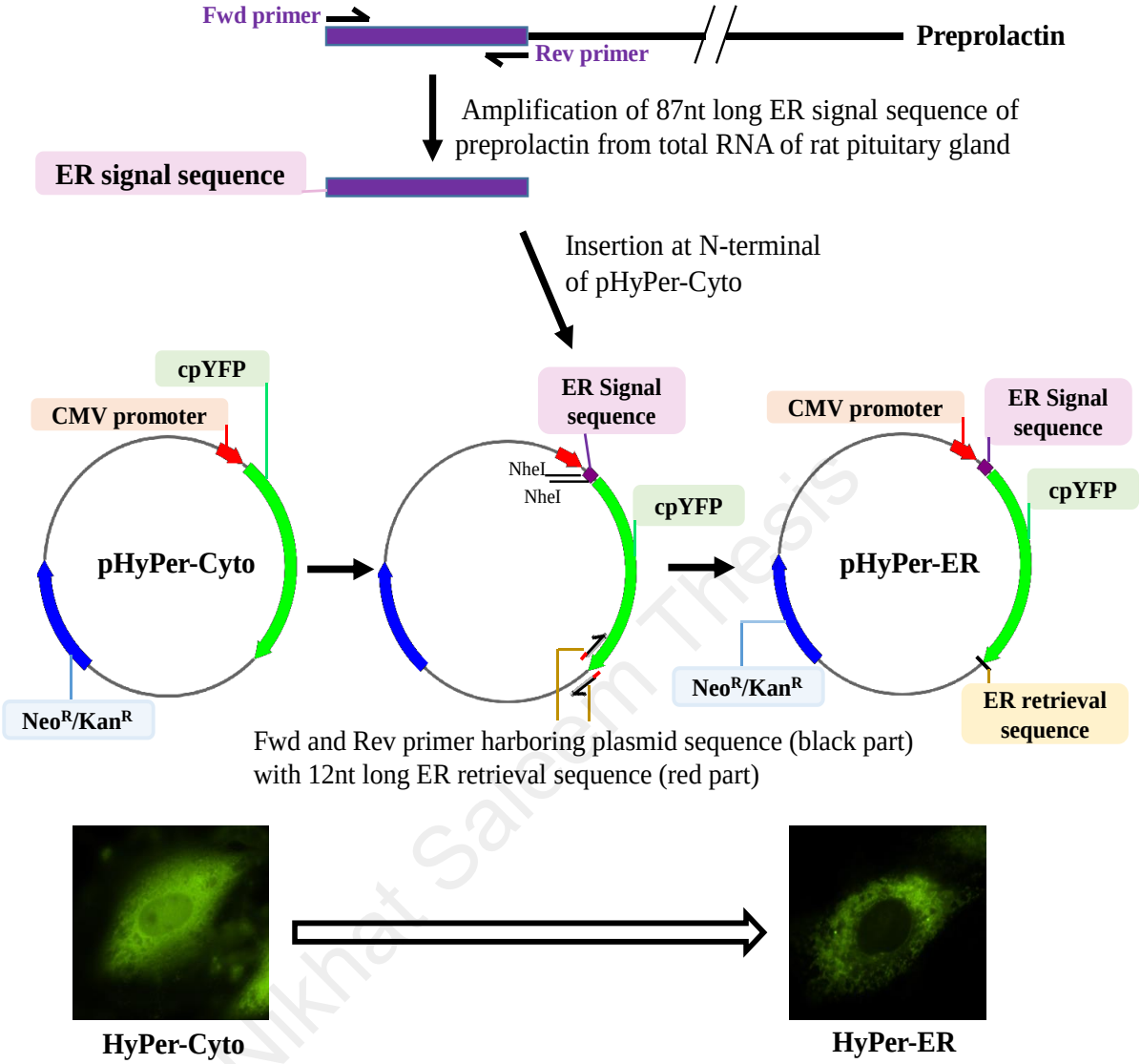

Figure 1s. Schematic representation of construction of HyPer-ER: ER signal sequence and retrieval sequence were inserted in-frame at N-terminal and C-terminal of pHyPer-Cyto ORF (open reading frame) to generate pHyPer-ER (details given in materials and methods). Then pHyper-Cyto and pHyPer-ER constructs were transiently transfected in H9c2 cells. After 36 hr of transfection, images were captured at Ex max of 488nm by Nikon Eclipse Ti-E fluorescence microscope.

12-14 hr followed by treatment with 2µM NE in phenol red free DMEM. Fluorescence of live cells were captured while in a live cell chamber with 5% CO_2 at 37˚C by Andor spinning disc confocal microscope (Olympus) with excitation using 488 nm laser line. The intensity of fluorescence was quantified by NIS-Elements AR-ver 4.000 software.

Luciferase reporter assays:

Following experimental treatments, cells were lysed in 1X lysis buffer (Promega). Cell lysates were analyzed for luciferase activity using the Luciferase Reagent Assay Kit (Promega) in accordance with the manufacturer's instructions in a GLOMAX Multi JR detection system (Promega). Normalization of transfection efficiency was done by the estimation of total protein used for the luciferase assay (Burch *et al.*, 2004; Jindal & Goswami, 2011).

Immunocytochemistry:

Following experimental treatments, cells were washed with 1XPBS twice and fixed with chilled methanol for 20 min followed by three PBS washes. Cells were then blocked with PBS containing 1% BSA, 1% bovine serum and 0.1% Triton-X-100 for 1 hr. Then, after three PBS washes the coverslips were incubated overnight at 4°C with respective primary antibodies at appropriate dilution in blocking solution. After washing three times with PBS, coverslips were incubated with respective Alexa-fluor secondary antibodies (1:500 dilution) for 1 hr. The cover slips were then washed thrice in PBS and mounted on glass slides over 80% glycerol (in PBS) containing cell nuclei stain Hoechst (1:1000) and sealed at the corners with nail paint. The images were captured in Nikon Eclipse Ti-E fluorescence microscope at 60X magnification.

Animal model of cardiac hypertrophy:

Animal studies were carried out using male Wistar rats of 6-8 weeks. Animal were kept under standard laboratory conditions (temperature; 25 ± 2^{o}C, relative humidity; 50 ± 15% and 12 hr dark/12 hr light period) and provided feed and water ad libitum. All animal procedures were reviewed and approved by Institutional Animal Ethics Committee (IAEC code 09/2014) of the Jawaharlal Nehru University, New Delhi (Registration No. 19/GO/ReBi/S/99/CPCSEA Dated: 10.03.1999).

Rats were randomly divided into five groups;

(i) Control groups were administered subcutaneously with saline,

(ii) Iso groups were subcutaneously injected with isoproterenol (5 mg/kg body weight; in saline),

(iii) Iso+Apo groups were administered intraperitonially with apocynin (10 mg/kg body weight; in 10% DMSO) followed by isoproterenol (5 mg/kg body weight; in saline),

(iv) Apo groups were administered intraperitonially with apocynin (10 mg/kg body weight; in 10% DMSO) and

(v) DMSO groups were administered intraperitonially with DMSO (10%; in saline).

All the drugs were freshly prepared and given once daily for 14 days.

After 14 days, body weight and tail length were measured and rats were sacrificed. The hearts were carefully excised, washed in ice cold PBS, blotted dry with tissue paper and weighed. The ratio of heart weight to body weight and the ratio of heart weight to tail length was taken as a parameter of cardiac hypertrophy. Tissues were snap frozen in liquid nitrogen, and stored at -80^{o}C for later analysis.

Echocardiography:

Rats were anaesthetized with ketamine (50 mg/kg) and xylazine (10 mg/kg) and the chest hair was shaved. Transthoracic echocardiography was performed using a fully digitized Philips, USA system (Vivid 7 dimension) with a 10-11.5 MHz neonatal cardiac probe transducer. The transducer was placed on the left hemithorax. Two dimensional M-mode images of left ventricle (LV) at the papillary muscle level were obtained from the parasternal short axis view. LV posterior wall thickness (LVPWd), interventricular septal thicknesses (IVSd), and LV internal dimensions at end of diastole (LVIDd) and systole (LVIDs) were measured from M-mode images. Based on these measurements, various other parameters were also calculated using the following formula:

Fractional Shortening (FS %) = {(LVIDd-LVIDs)/LVIDd}*100

Ejection Fraction (EF %) = [{(LVIDd)3-(LVIDs)3}/(LVIDd)3]*100

Left Ventricle Mass (LVM gm) = 0.8[1.04{(LVIDd+IVSd+LVPWd)3-(LVIDd)3}]+0.6

Real time PCR:

First strand cDNA was generated using 1 µg of total RNA, oligo (dT) primer, dNTPs and reverse transcriptase (Applied Biosystems) in a total volume of 20 µL as per the

manufacturer's protocol. Real-time PCR was done in 20 µL volume using 1X SYBR Green Master Mix (Applied Biosystems), 1.0 picomole of gene specific primers (Table 1s) and 20-50 ng of cDNA to amplify the specific transcripts. Reaction was performed in an Applied Biosystems 7500 Real- Time PCR System (50^{o}C, 2 min; 95^{o}C, 10 min, 1 cycle; 95^{o}C, 15 sec; 60^{o}C 1 min, 40 cycles). Modulation of transcript levels were quantified using Ct values. GAPDH quantification was used as an internal control for normalization. Fold differences of mRNA levels over control values were calculated.

Preparation of total protein lysate for Western analysis:

Following experimental treatments, adhering cells (washed with ice cold PBS, scrapped and collected by low speed centrifugation; 3000 rpm at 4^{o}C were lysed) or 100 mg of heart tissue (left ventricle section, homogenized with tissue tearer) in ice-cold 1X RIPA buffer with phosphatase inhibitor cocktail, 1 mM phenylmethylsulphonyl fluoride (PMSF) and protease inhibitor cocktail followed by sonication. Cell lysates were then centrifuged at 13,000 rpm (at 4^{o}C) and supernatant were saved at -80^{o}C. Protein concentrations in the extracts were estimated by modified Bradford method (Bradford, 1976; Kruger, 1994).

2X RIPA buffer				
Component		*Stock conc*	*Working conc*	*Amount/10 mL (w/v) or (v/v)*
1.	Tris-Cl	1.5 M; pH7.4	50 mM	0.66 mL
2.	Sodium chloride	1 M	150 mM	3 mL
3.	EDTA	0.5 M; pH 8.0	1 mM	0.04 mL
4.	Sodium deoxycholate		1%	0.2 g
5.	SDS	10%	0.1%	0.2 mL
6.	Triton X-100		1%	0.2 mL

Bradford's Reagent		
Component		*Amount/1000 mL (w/v) or (v/v)*
1.	Coomassie brilliant blue (CBB) G-250	0.1 g
2.	Ethanol	50 mL
3.	Orthophosphoric acid	100 mL

Immunoblot analysis:

Equal quantities of protein samples (50-80 µg) were resolved by 10% or 12% SDS-PAGE as described in Sambrook et al., 1989. Part of the protein gel (selected based on the

molecular weight of the protein of interest) were sliced out and transferred to PVDF membranes in Towbin's buffer. Following transfer, the membranes were blocked for 2 hr at RT with 3% BSA (Bovine Serum Albumin) in TBS containing 0.1% Tween-20 (TBST). Blots were then incubated overnight at 4°C with respective primary antibodies at appropriate dilutions in blocking solution. Next day the blots were washed on a rocker with TBST (3 washes with each wash of 10 min) and incubated for 1 hr at RT with respective secondary antibody (at appropriate dilutions) in TBST. Following removal of the secondary antibody, blots were extensively washed (3 washes with each wash of 10 min and one wash with TBS) and developed using the Enhanced Chemiluminescence detection system (ECL).

Quantification of band intensities was performed with the Image-J software system. The signal intensity of each protein was normalized with the corresponding GAPDH signal and fold change over control was calculated.

The remaining part of the gels (which was not transferred) containing separated proteins were visualized by CBB (Coomassie brilliant blue) staining whenever required.

SDS PAGE gel				
Component		*Stock conc*	*Amount/10 mL (v/v)*	
Resolving			*10%*	*12%*
1.	Acrylamide	30%	3.3 mL	4.0 mL
2.	Tris-Cl	1.5 M; pH 8.8	2.5 mL	2.5 mL
3.	SDS	10%	0.1 mL	0.1 mL
4.	APS	10%	0.1 mL	0.1 mL
5.	TEMED		0.004 mL	0.004 mL
Stacking			*5%*	
1.	Acrylamide	30%	1.66 mL	
2.	Tris-Cl	1 M; pH 6.8	1.26 mL	
3.	SDS	10%	0.1 mL	
4.	APS	10%	0.1 mL	
5.	TEMED		0.01 mL	

6X protein loading buffer			
Component		*Working conc*	*Amount/10 mL (v/v) or (w/v)*
1.	1 M Tris-Cl; pH 6.8	300 mM	3.0 mL

2.	DTT	600 mM	0.925 g
3.	SDS	12%	1.2 g
4.	Glycerol	60%	6.0 mL
5.	Bromophenol blue	0.6%	0.06 g

Component		*Amount/1000 mL (w/v) or (v/v)*
10X Tris-glycine		
1.	Tris base	30.3 g
2.	Glycine	144 g
SDS PAGE running buffer		
1.	10X Tris glycine	100 mL
2.	10% SDS	10 mL
Towbin's buffer (transfer buffer)		
1.	10X Tris glycine	100 mL
2.	Methanol	100 mL
3.	10% SDS	5 mL

TBS (Tris buffered saline)				
Component		*Stock conc*	*Working conc*	*Amount/1000 mL (v/v)*
1.	Tris-Cl	1.5 M; pH 7.6	10 mM	6.66 mL
2.	Sodium chloride	4 M	150 mM	37.5 mL

Two-dimensional gel electrophoresis (2-DE):

Sample preparation, isoelectric focusing and SDS-PAGE

Total protein extract from heart's LV section was prepared in RIPA buffer with phosphatase inhibitor cocktail, 1 mM phenylmethylsulphonyl fluoride (PMSF) and protease inhibitor cocktail followed by sonication. The extract was centrifuged at 13000 rpm for 20 min at 4°C to remove debris. The supernatant was acetone precipitated at -20°C overnight followed by centrifugation at 13000 rpm for 20 min at 4°C. The protein pellet so obtained was dissolved in sample buffer. Protein concentration was determined by Bradford assay using BSA as standard. Protein samples (250 µg) diluted in rehydration buffer were applied to a 24 cm strip holder containing an immobilized pH gradient (IPG)

strip (13 cm, pH 3–10, linear) (GE Healthcare, UK) using a passive rehydration method (for 16 hr at room temperature). The IPG strips were then transferred to an isoelectric focusing (IEF) cell and IEF was performed according to the manufacturer's instructions (GE Healthcare, UK). Prior to second dimension, the gel strips were equilibrated for 15 min each in equilibration buffer I and equilibration buffer II. The strips were then washed in SDS running buffer and applied to the top of a 12% SDS polyacrylamide gel at 80 Volt. The gels were then stained with silver nitrate.

Sample buffer			
Component		*Working conc*	*Amount/1.0 mL (v/v) or (w/v)*
1.	1 M Tris-Cl; pH 6.8	40 mM	0.04 µL
2.	Urea	8.0 M	0.48 g
3.	Thiourea	2.5 M	0.19 g
4.	CHAPS	3.0%	0.015 g
Rehydration buffer			
Component		*Working conc*	*Amount/1.0 mL (v/v) or (w/v)*
1.	Urea	7.0 M	0.42 g
2.	Thiourea	2.0 M	0.152 g
3.	CHAPS	1.2%	0.006 g
4.	DTT		
5.	IPG buffer		5.0 µL
6.	Bromophenol blue		

Equilibration buffer				
Component		*Working conc*	*Amount/10 mL (v/v) or (w/v)*	
			I	***II***
1.	1.5 M Tris-Cl; pH 8.8	0.05 M	0.335 mL	0.335 mL
2.	Urea	6.0 M	3.6 g	3.6 g
3.	10% SDS	2.0%	2.0 mL	2.0 mL
4.	Glycerol	30%	3.0 mL	3.0 mL
5.	DTT	1.0%	0.1 g	--

6.	Iodoacetamide	2.5%	--	0.25 g

Silver staining

After fixing the gels in fixative solution (30% ethanol, 12% acetic acid and 0.05% formaldehyde) for 2 hr followed by washing in 20% methanol for 20 min, gels were silver stained through following three steps.

Step1: Sensitization: Gels were treated with sodium thiosulfate solution (0.02%) for 2 min and washed with autoclaved water (2 X 30 sec).

Step 2: Staining: Gels were immersed in the staining solution (0.2% silver nitrate and 0.076% formalin) for 30 min and washed with autoclaved water (2 X 30 sec).

Step 3: Developing: Developing solution (6% sodium carbonate, 0.004% sodium thiosulfate and 0.05% formalin) was added to the gels and kept shaking for 2-5 min till the time no more spots appear. The reaction was stopped by adding terminating solution (12% acetic acid).

The silver stained gel was then scanned and image analysis was performed using 'Samespot Analysis for 2-D Gels', Totallab Systems, as per the manufacturer's instructions.

Sample preparation for Mass spectrometric analysis

The selected differentially expressed protein spots were individually excised into new tubes, and the isolated protein spots were destained twice with destaining solution (100 mM sodium thiosulfate and 30 mM potassium ferricyanide in 1:1 ratio) followed by three washes with water for 10 min each. Then the gel pieces were incubated in acetonitrile : 10 mM ammonium bicarbonate : water (1:1:2) for 15 min at room temperature followed by addition of acetonitrile to cover the gel pieces. As the gel pieces shrink, acetonitrile was removed followed by drying in speed vacuum. Then the protein gel pieces were digested with trypsin (MS-grade from Promega, USA) with 25 mM ammonium bicarbonate at 37° C for 16 hr. The resulting peptide mixtures were extracted with 200 µL of 50% acetonitrile and 0.1% trifluoroacetic acid (TFA) for 15 min with sonication and the supernatant was collected. After pooling the supernatant into new tubes, peptide samples were dried completely using speed vacuum system at room temperature. Samples were dissolved in 50% acetonitrile 0.1% TFA, co-crystallized by mixing with matrix (α-cyano-4-hydroxy-cinnamic acid saturated with 0.1% TFA/50% acetonitrile) and loaded on the silicon-coated 396 well microtiter ground plate (Bruker Daltonics).

Mass spectrometry (MALDI-TOF/MS analysis)

Trypsin digested peptide fragments were analyzed on a Matrix-assisted Laser Desorption Ionization Time of Flight Mass Spectrometry (MALDI-TOF MS) with a Bruker Autoflex II TOF/TOF mass spectrometer (Bruker Daltonics) working in positive ion reflector mode. The spectra were processed by the Flex control TOF/TOF software (Bruker Daltonics) and the peaks annotated automatically and checked manually. A list of the corrected mass peaks was the peptide mass fingerprint (PMF). The peptide mass data were searched against NCBI database with the Mascot search engine (Matrix Science Ltd., UK, http://www.matrixscience.com/) and with *Rattus norvegicus* as the species searched. This software creates a peak list from the raw spectra with a given threshold after removal of trypsin, polymer peaks, noise peaks and subjected to database interrogation for protein identification.

Statistical analysis:

Statistical analyses were performed using GraphPad Prism, PC version 5 (GraphPad software). Data are expressed as mean ± SEM. Experimental groups were compared with the use of one-way ANOVA if there was one independent variable (Tukey's test) or two-way ANOVA if there were two independent variables. Values of $P < 0.05$ were considered statistically significant.

Results and Discussion

Chapter I

Norepinephrine signaling in H9c2 cardiac myoblasts involve activation of NADPH oxidase

Introduction:

Oxidative stress has long been attributed to cardiovascular diseases like endothelial dysfunction, cardiac hypertrophy, cardiomyocyte apoptosis, ischemia reperfusion injury and heart failure (Zhang *et al.*, 2012; Ho *et al.*, 2013; Murray *et al.*, 2014). Paradoxically, alleviating those conditions by antioxidants have largely been unsuccessful (Sawyer, 2011). Recent years have seen paradigm shifts wherein apart from their deleterious effects, reactive oxygen species (ROS) have emerged as the mediator of intracellular signals (Wadley *et al.*, 2016). Such regulatory roles of ROS is fast evolving (Forman *et al.*, 2014; Latimer & Veal, 2016). Superoxide ($O_2^{\bullet-}$), a prevalent ROS, is generated from a number of redox enzymes and mitochondrial electron transport complexes in distinct cellular locations. It is also converted into hydrogen peroxide (H_2O_2), a potent signaling molecule (Latimer & Veal, 2016). Their effects on the cellular constituents depend on the duration of generation, steady state concentrations, subcellular locations and surrounding antioxidants etc (Lee *et al.*, 2013; Stangherlin & Reddy, 2013). $O_2^{\bullet-}$ and H_2O_2 may oxidize, nitrosylate or glutathionylate the cysteine thiols in adjoining proteins, affecting their conformation, stability and functions (Forman *et al.*, 2014; Groitl & Jakob, 2014).

The response of the cardiovascular system to the pathological stimuli leading to the development of hypertrophy and heart failure is complex and involves all known modes of regulations including phosphorylation–dephosphorylation, intracellular trafficking, protein and mRNA turnover and oxidative modifications of the cellular proteome (Madamanchi & Runge, 2013). While the other modes of regulation are better understood, those by the oxidative and nitrosative modifications of various proteins are least investigated till date (Madamanchi & Runge, 2013; Forman *et al.*, 2014).

Norepinephrine (NE) is released from the sympathetic nervous system and targets α- and β- adrenergic receptors, regulating cardiac performance (Ciccarelli *et al.*, 2013; Ferrara *et al.*, 2014). Cardiac myocytes in culture when treated with a lower dose of NE (≤10 µM NE) elicit hypertrophic response, while at a higher dose (≥50 µM NE) induces apoptosis. These two responses are the hallmark of heart failure (Clerk, 2003; Fu *et al.*, 2004). We have demonstrated earlier that although ROS is the common denominator of both the responses, its mechanism of actions are far more nuanced and complex than simple threshold dependent effects as perceived earlier (Gupta *et al.*, 2006; Thakur *et al.*, 2015).

NADPH oxidases (Nox1-5) are enzymes solely dedicated for the production of $O_2^{\bullet-}$ and H_2O_2 in various tissues in a context specific manner (Sirokmány *et al.*, 2016). Except Nox4

which is constitutive, all other Noxes are activated by various mechanisms (von Löhneysen *et al.*, 2010). Apart from their activation by intracellular mechanisms like calcium flux and by protein-protein interactions, they are also co-activated by the engagement of various growth factors, peptide hormones and cytokines to their cognate receptors though the mechanisms not fully understood (Brandes *et al.*, 2014b; Spencer & Engelhardt, 2014; Heppner & van der Vliet, 2016). Three of its isoforms viz., Nox1/2/4 are expressed in heart and ROS generated from them have been attributed to interstitial fibrosis, contractile dysfunction, ischemia-reperfusion injury and cardiac remodeling (Lassègue *et al.*, 2012; Madamanchi & Runge, 2013; Forman *et al.*, 2014; Granger & Kvietys, 2015).

Nox2, the prototype member of the family, is primarily localized in the plasma membrane and it is involved in redox signaling from cell exterior to interior (Fisher, 2009). In heart, several pathophysiological stimuli i.e., hypoxia, membrane depolarization (endothelial cells), induction of platelet activating factor (PAF), arachidonic acid, tumor necrosis factor- α (TNF-α), interleukin-1β (IL-1β) etc activate Nox2 (Granger & Kvietys, 2015). Despite evidences that generation of ROS is an integral part of adrenergic signaling, their source, nature and mode of actions are largely unknown (Gupta *et al.*, 2006; Thakur *et al.*, 2015; Theccanat *et al.*, 2016). In the present study, we demonstrate that in H9c2 cardiac myoblasts, stimulation of adrenergic receptor by NE co-stimulates Nox2 generating $O_2^{\bullet-}$ and H_2O_2. ROS generated from Nox2 is an integral part of the adrenergic signaling as the inhibition of Nox2 attenuates the hemodynamic parameters of hypertrophy, prevents the activation of transcription factors mediating those responses and the induction of a number of marker genes considered as the hallmarks of hypertrophy.

Results:

NE treated cardiac myoblast generates ROS from Nox2

We have demonstrated earlier that that cardiac myoblasts upon stimulation with NE generates a complex repertoire of ROS that contribute towards the downstream responses viz., hypertrophy and apoptosis (Gupta *et al.*, 2006; Jindal & Goswami, 2011; Thakur *et al.*, 2015). Since such generation of ROS is an immediate (< 1 min) response and includes both $O_2^{\bullet-}$ and H_2O_2, involvement of Nox2 is anticipated. To test this possibility, H9c2 cardiac myoblasts were kept in serum free medium overnight and stimulated with NE (2 µM) for 10 min. Generation of ROS was monitored by the general ROS sensitive fluoroprobe Dichloro-dihydro-fluorescein diacetate (DCFH-DA) and $O_2^{\bullet-}$specific fluoroprobe Dihydroethidium (DHE). To test the involvement of Nox2, its specific peptide inhibitor gp91ds-tat (5 µM) was added. As shown in Figure I.1A, NE induced ROS (DCFH-DA) generation was completely blocked by the specific inhibition of Nox2. In agreement with our previous report, part of the ROS was $O_2^{\bullet-}$ (DHE sensitive) that was also completely blocked by the specific inhibition of Nox2 by gp91ds-tat as well as the general inhibition of all Noxes by apocynin (Figure I.1B). These results strongly corroborated with our hypothesis that stimulation of adrenergic receptor by NE co-activates Nox2 and generates $O_2^{\bullet-}$and other associated ROS.

NE induces ROS generation primarily in the cytosol

We have demonstrated earlier that treatment of H9c2 cardiac myoblasts with 2 µM of NE leads to the sustained but oscillating generation of ROS (Gupta *et al.*, 2006; Jindal & Goswami, 2011; Thakur *et al.*, 2015). Since redox signaling is specified by the cellular microdomain where it is generated, we also tested the subcellular location of the ROS generated by NE. Cells were transfected with the H_2O_2 sensitive cpYFP (circularly permuted-yellow fluorescent protein) based ratiometric fluorescent probe HyPer plasmids (Belousov *et al.*, 2006) that monitors the H_2O_2 generation in the cytoplasm, mitochondria and endoplasmic reticulum (ER). After 24 hr of transfection, cells were kept overnight in serum free media followed by treatment with 2µM NE and live cell imaging was done at Ex_{max} 488nm. As shown in Figure I.2A, snapshots of a single living cell showed treatment with NE resulted in a sharp and rapid increase in H_2O_2 generation in the cytosol, that sustained till 2 hr, the last time point tested (further analysis was not possible as the cells started crumbling, presumably due to the repeated exposure to the light). Although there was a gradual decrease (~20%) in fluorescence with time, it was still well above the

(A)

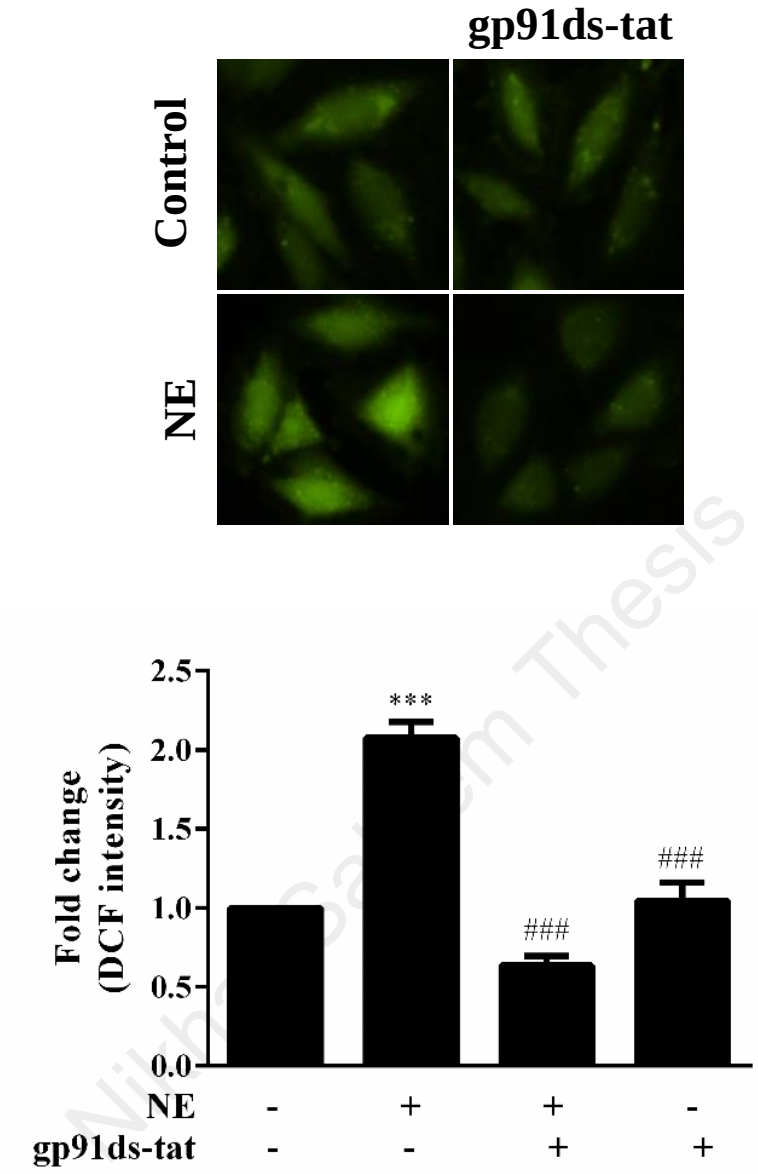

Figure I.1 Nox2 is the source of ROS in NE treated cardiac myoblasts: (A) Upper panel: H9c2 cells were serum starved overnight followed by treatment with 2µM NE for 10 min. 5µM gp91ds-tat was added 30 min before NE treatment wherever marked. Cells were labeled with redox sensitive fluoroprobe DCFH-DA (5µM) 30 min prior to imaging. Lower Panel: Quantification of the fluorescence intensity normalized to control. ***P $\leq$ 0.001 vs control; ###P $\leq$ 0.001 vs NE.

(B)

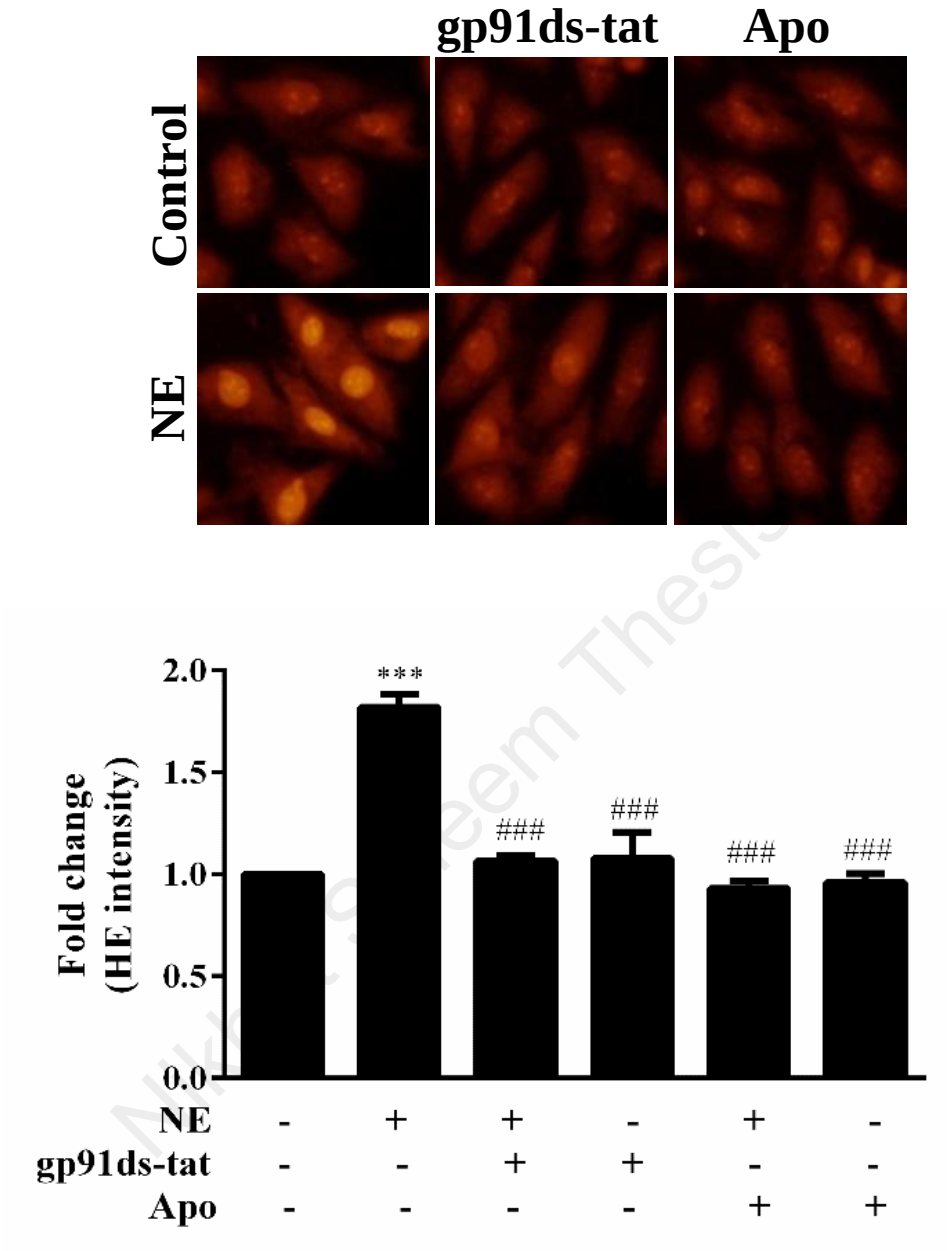

(B) Upper panel: H9c2 cells were serum starved overnight followed by treatment with 2µM NE for 10 min. 5µM gp91ds-tat or 10 µM Apo was added 30 min before NE treatment wherever marked. Cells were labeled with superoxide sensitive fluoroprobe DHE (10µM) 30 min prior to imaging. Lower Panel: Quantification of the fluorescence intensity normalized to control. ***P $\leq$ 0.001 vs control; ###P $\leq$ 0.001 vs NE.

(A)

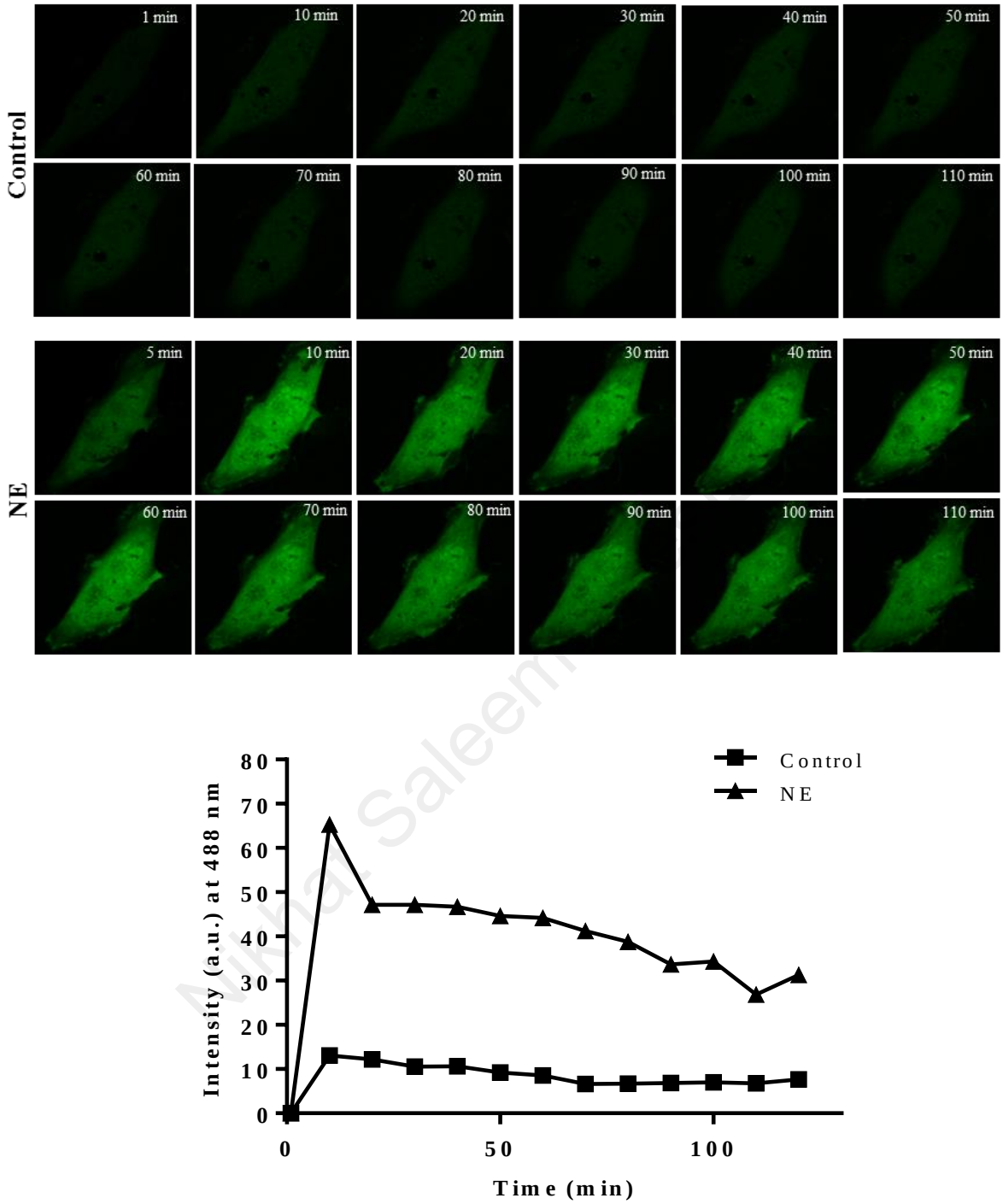

Figure I.2 NE induces generation of hydrogen peroxide primarily in the cytosol:

(A) Upper panel: H9c2 cells were transfected with pHyPer-Cyto. After 24 hr of transfection, cells were kept overnight in serum free media followed by treatment with 2µM NE as marked. Live single cell imaging was done at 60X for 1 hr at Ex_{max} 488 nm and most representative image is shown. Lower panel: Quantification of the fluorescence intensity normalized to intensity at 1 min.

(B)

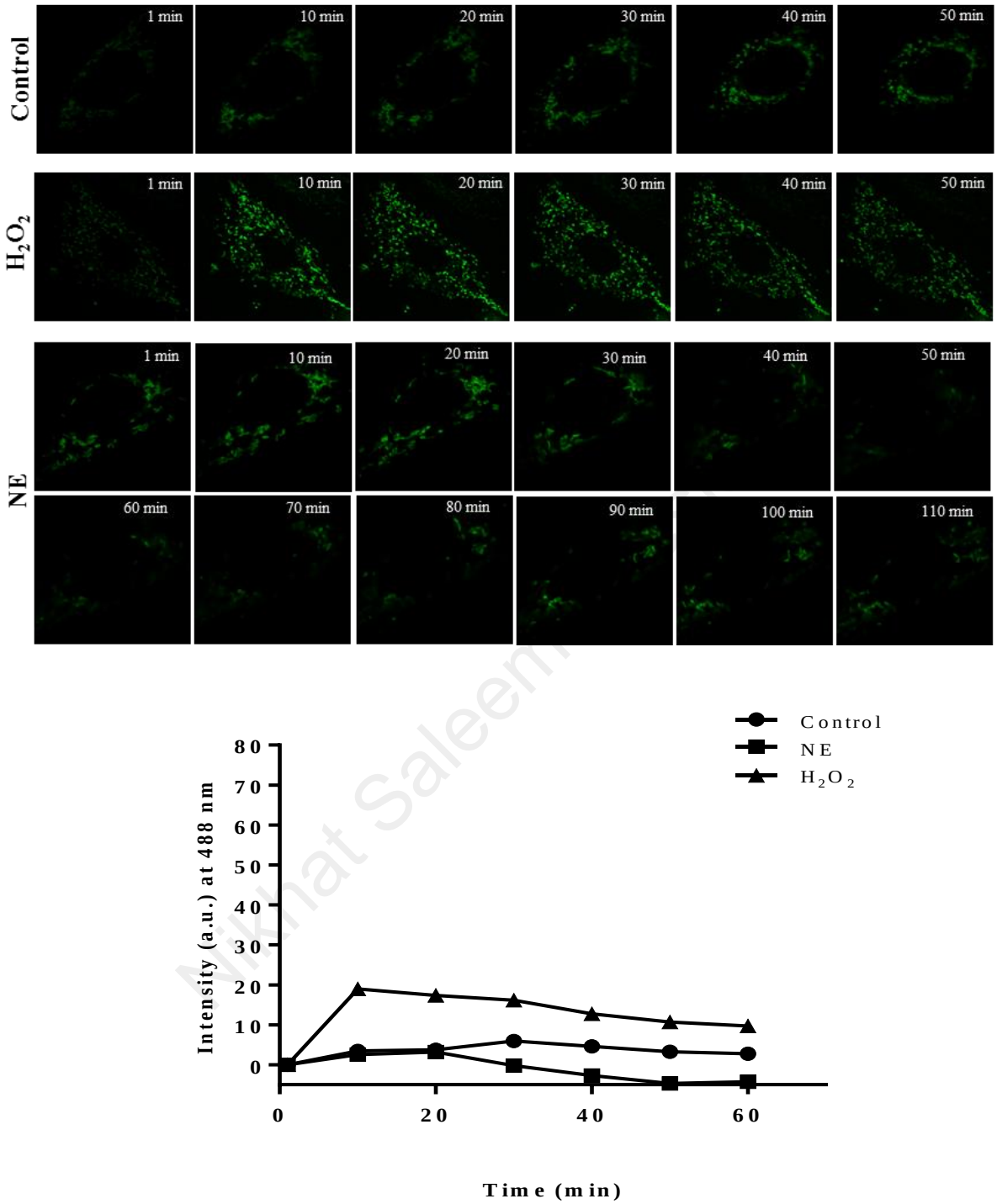

(B) Upper panel: H9c2 cells were transfected with pHyPer-Mito. After 24 hr of transfection, cells were kept overnight in serum free media followed by treatment with 2µM NE or 20µM H_2O_2 treatment as marked. Live single cell imaging was done at 60X for 1 hr at Ex_{max} 488 nm and most representative image is shown. Lower panel: Quantification of the fluorescence intensity normalized to intensity at 1 min.

(C)

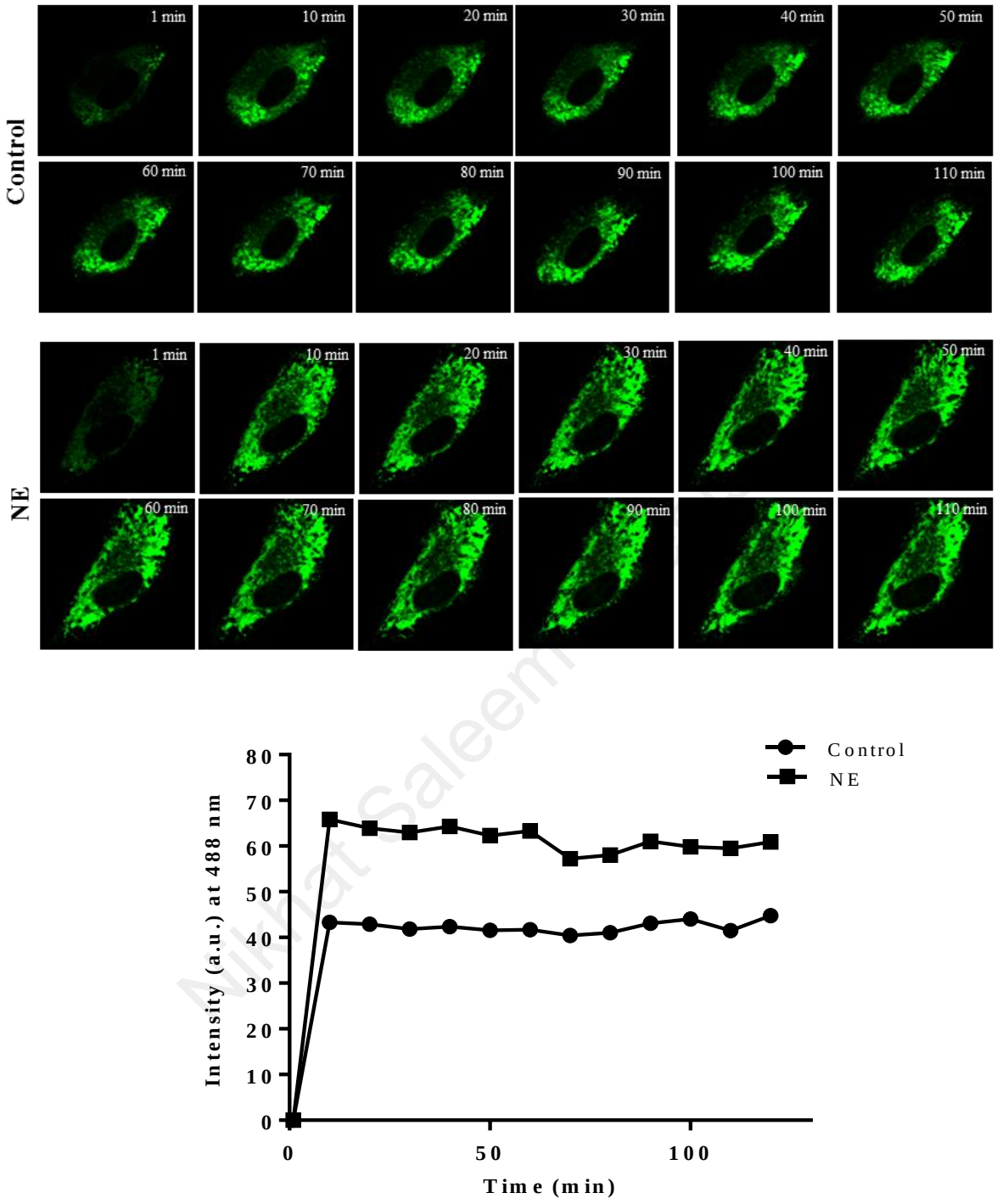

(C) Upper panel: H9c2 cells were transfected with pHyPer-ER. After 24 hr of transfection, cells were kept overnight in serum free media followed by treatment with 2µM NE or 20µM H_2O_2 treatment as marked. Live single cell imaging was done at 60X for 1 hr at Ex_{max} 488 nm and most representative image is shown. Lower panel: Quantification of the fluorescence intensity normalized to intensity at 1 min.

baseline (untreated cells). Noticeably, no increase in fluorescence was seen in the mitochondria in NE treated cells as monitored by the HyPer-Mito (Figure I.2B). Rather, the signal was below the baseline (untreated control) after 30 min, though the reason is not clear. The efficacy of the assay was evident from the increase in fluorescence in cells treated with 20 µM H_2O_2. Unlike the mitochondria, some increase in fluorescence was seen in ER upon NE treatment (Figure I.2C), though the response was not as intense as in cytosol. The higher baseline intensity of HyPer-ER reflects the oxidizing environment of ER. Together, these data suggest that cytosol is the primary and the ER is the secondary location of H_2O_2 generation in NE treated cells. Due to the lack of organelle specific probes, similar assay for superoxide generation in those organelles could not be done.

Induction of fetal gene expression by NE is prevented by the inhibition of Nox2.

Re-induction of fetal gene expression program is a characteristic feature of cardiac hypertrophy and it is faithfully reproduced by treating cultured myocytes *ex vivo* with adrenergic agonists (Banerjee & Bandyopadhyay, 2014; Yariswamy *et al.*, 2016). To analyze the role of Nox2 induced ROS in the induction of fetal gene program, if any; we estimated the mRNA levels of three established markers viz., ANP (atrial natriuretic peptide), α-MHC (α-myosin heavy chain) and β-MHC (β-myosin heavy chain). As expected, upon treatment with 2 µM NE, the transcript levels of ANP and β-MHC increased by ~1.7 and 2.0 fold respectively and that of α-MHC decreased by ~0.4 fold. Pretreatment of cells with gp91ds-tat (5 µM) prevented the modulation of transcript levels by NE (Figure I.3A). We further confirmed such modulation of hypertrophic markers at the protein levels by immunocytochemistry. As shown in Figure I.3B & C, treatment with NE (2 µM) increased the levels of both ANP and β-MHC that were attenuated by the inhibition of Nox2 by gp91ds-tat (5 µM). These results not only strengthened our previous observation that ROS induced by NE treatment play a direct role in regulation of gene expression in hypertrophied heart (Gupta *et al.*, 2006; Jindal & Goswami, 2011; Thakur *et al.*, 2015), it also established that Nox2 is the primary source of this regulatory ROS (Figure I.1 & 2).

Nox2 induced ROS modulates the activities of transcription factors mediating hypertrophic responses:

Heterodimeric transcription factor AP-1 has long been identified as the key mediator of hypertrophic signals elicited by several agonists (Yan *et al.*, 2013). Also, depending on the pathophysiological stimuli, the role of AP-1 can be divergent (Windak *et al.*, 2013). We

(A)

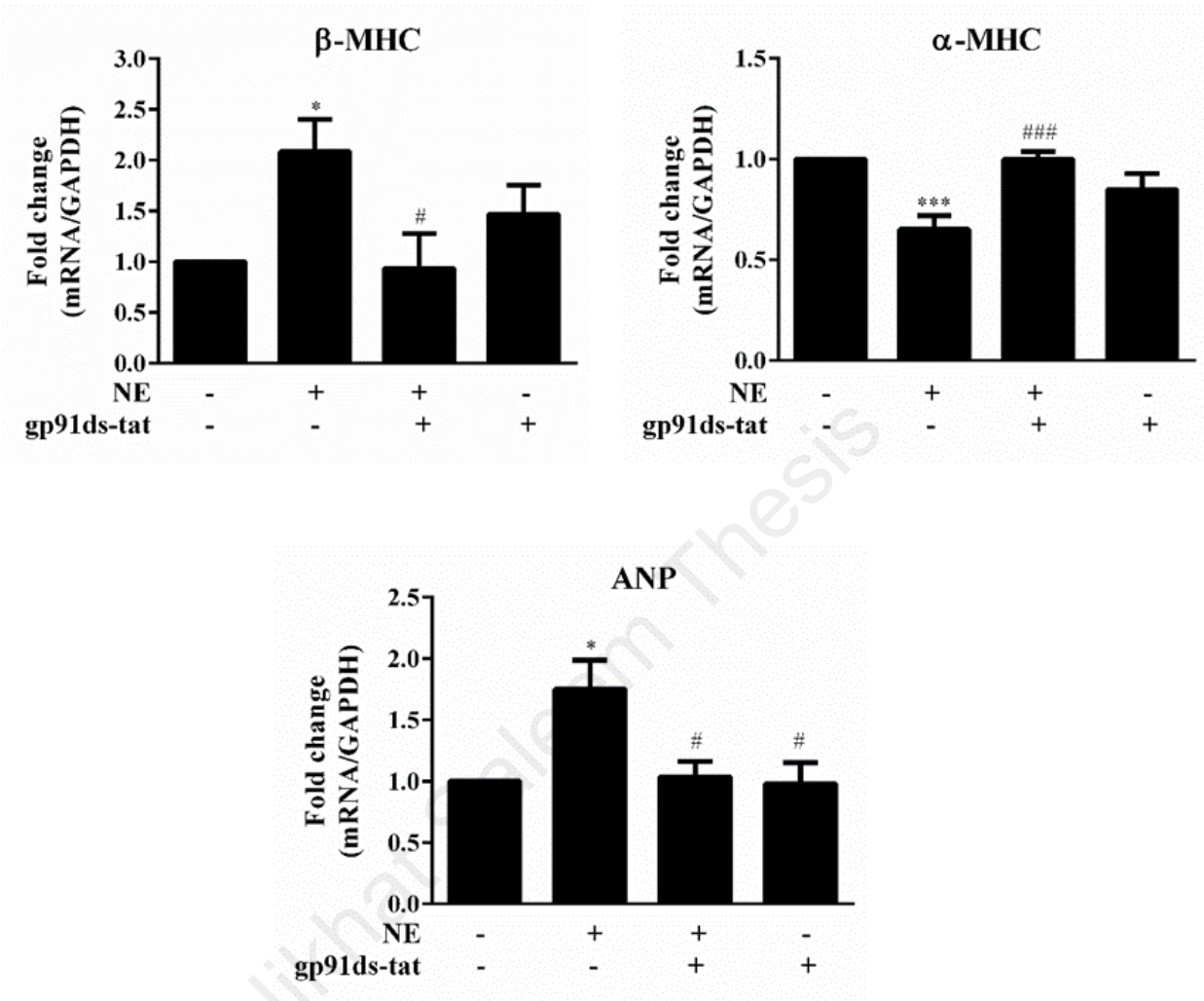

Figure I.3 Induction of fetal gene expression by NE is prevented by the inhibition of Nox2: (A) H9c2 cells were serum starved overnight followed by treatment with 2μM NE for 24 hr. 5μM gp91ds-tat was added 30 min before NE treatment wherever marked. Total RNA was assayed for ANP, β-MHC and α-MHC transcripts using gene specific primers by Real-time PCR. Normalization of input RNA was done by using GAPDH level as an internal control. Fold differences of mRNA levels over control were calculated. *P $\leq$ 0.05 vs control; ***P $\leq$ 0.001 vs control; #P $\leq$ 0.05 vs NE; ###P $\leq$ 0.001 vs NE.

(B)

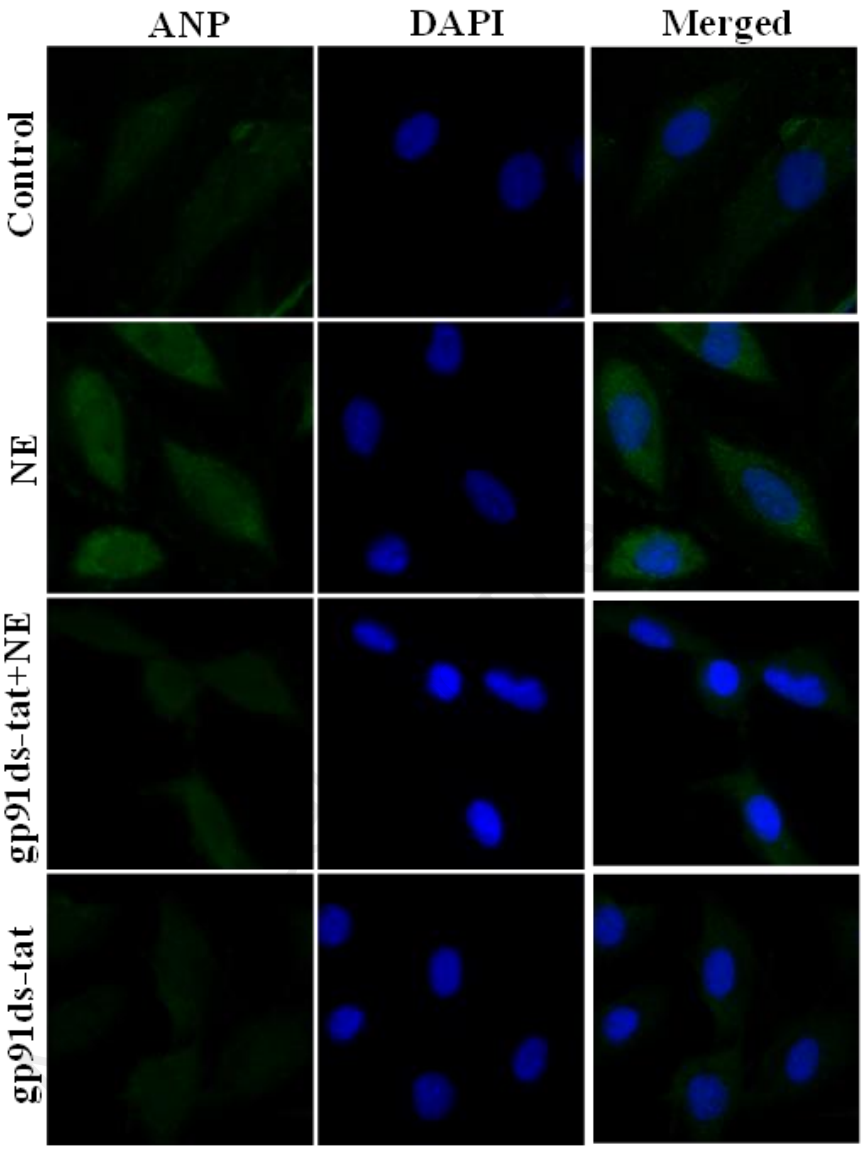

(B) H9c2 cells were serum starved overnight followed by treatment with 2μM NE for 24 hr. 5μM gp91ds-tat was added 30 min before NE treatment wherever marked. Immunostaining was done using antibody specific for ANP. The images were captured at 60X magnification by Nikon Eclipse Ti-E fluorescence microscope.

(C)

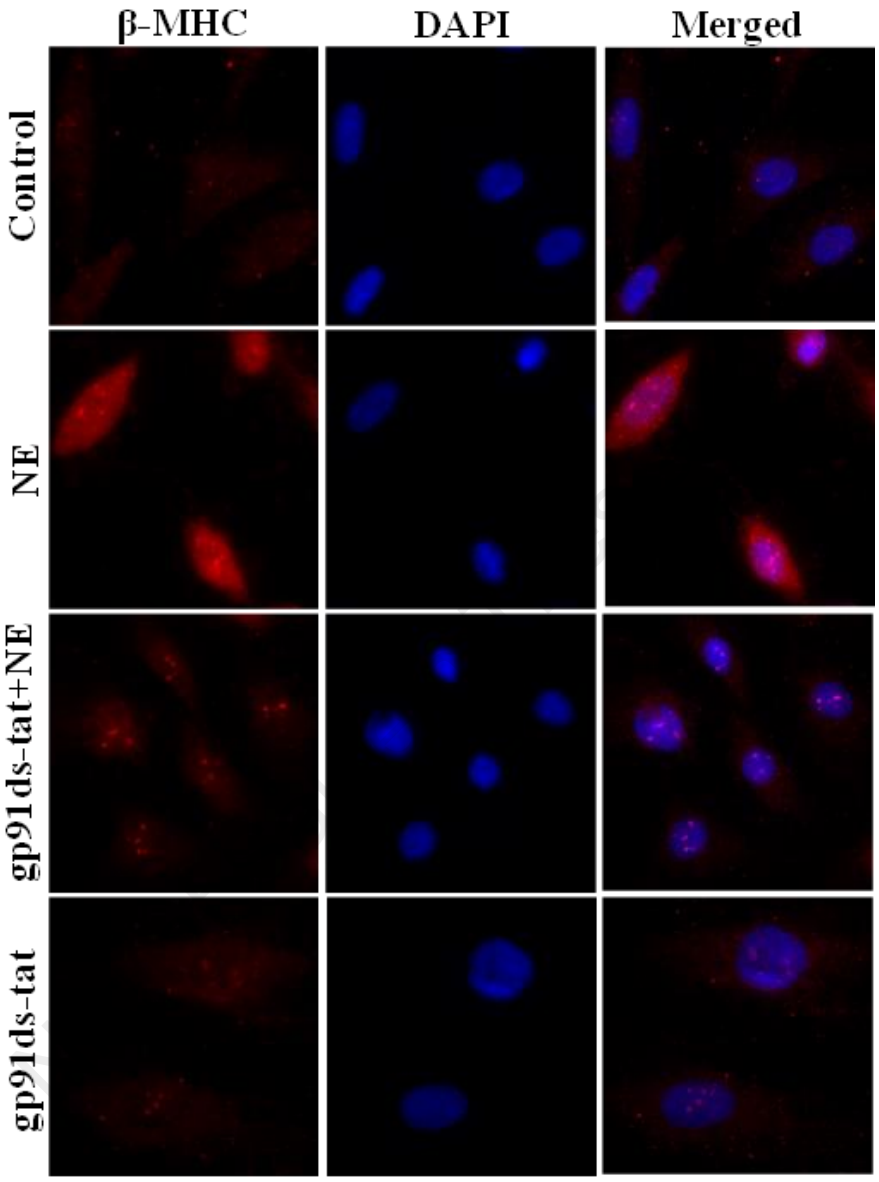

(C) H9c2 cells were serum starved overnight followed by treatment with 2μM NE for 24 hr. 5μM gp91ds-tat was added 30 min before NE treatment wherever marked. Immunostaining was done using antibody specific for β-MHC. The images were captured at 60X magnification by Nikon Eclipse Ti-E fluorescence microscope.

have demonstrated earlier that in NE treated cardiac myoblasts, the redox and kinase signals integrate at various transcription factors viz, AP-1, SP-1 and CREB, which then mediate their effects through the cognate *cis*-regulatory elements in the responsive gene promoters, specifying the transcriptional output (Gupta *et al.*, 2006; Jindal & Goswami, 2011). To reiterate that observation in the context of ROS generated from Nox2, the expression levels of two members of the AP-1 family that is c-Jun and FosB were assayed by Western analyses. As shown in Figure I.4A, upon treatment with NE, c-Jun level was induced by 1.25 and 1.38 fold at 2 hr and 4 hr of NE treatment respectively and that were attenuated by gp91ds-tat treatment. Although, gp91ds-tat itself also showed some induction of c-Jun, it was less than that able to suppress the c-Jun level below base line at 4 hr. Similar observations were also made for FosB (FBJ murine osteosarcoma viral oncogene homolog B), a member of the AP-1 family and the dimerization partner of c-Jun. As shown in Figure I.4A, level of FosB was increased by 1.45 fold in NE treated cells at 2 hr but diminished thereafter at 4 hr. This kinetic is in agreement with our earlier study with the FosB transcript (Jindal & Goswami, 2011). As expected, the induction of FosB was also abrogated by treatment with gp91ds-tat. In view with the low intensity of the signal with the FosB antibody in the Western blot (possibly, a reflection of the low abundance), we also confirmed its modulation by immunocytochemistry as shown in the Figure I.4B. Immunocytochemistry not only reiterated the pattern of modulation seen in the Western blot, it also showed the nuclear localization of FosB. We also examined the level of phospho-c-Jun in NE treated cells and its modulation by gp91ds-tat. As shown in Figure I.4A, treatment with NE rather decreased the level of phospho-c-Jun (thus effectively decreasing the phospho-c-Jun/c-Jun ratio) while treatment with gp91ds-tat partially restored that reduction. Although, phosphorylation of c-jun is known for its activation (in addition to the increase in its expression level), its cellular function is highly context specific with multiple layers of a regulatory networks wherein it integrates different signals (Meng & Xia, 2011). It is thus difficult to assess the implication of increase in c-Jun expression with concurrent decrease in its state of phosphorylation upon NE treatment. Nevertheless, this data unequivocally reiterates that Nox2 plays a role in modulating the AP-1 activity by NE.

Subsequent to analyzing the expression of c-Jun and FosB, we also assayed a number of promoter reporter (luciferase) constructs regulated by AP-1 in cardiac myocytes treated with adrenergic agonists. We tested one synthetic promoter harboring three consecutive AP-1 binding sites, and two endogenous promoters *viz* that of FosB and ANP genes. The

(A)

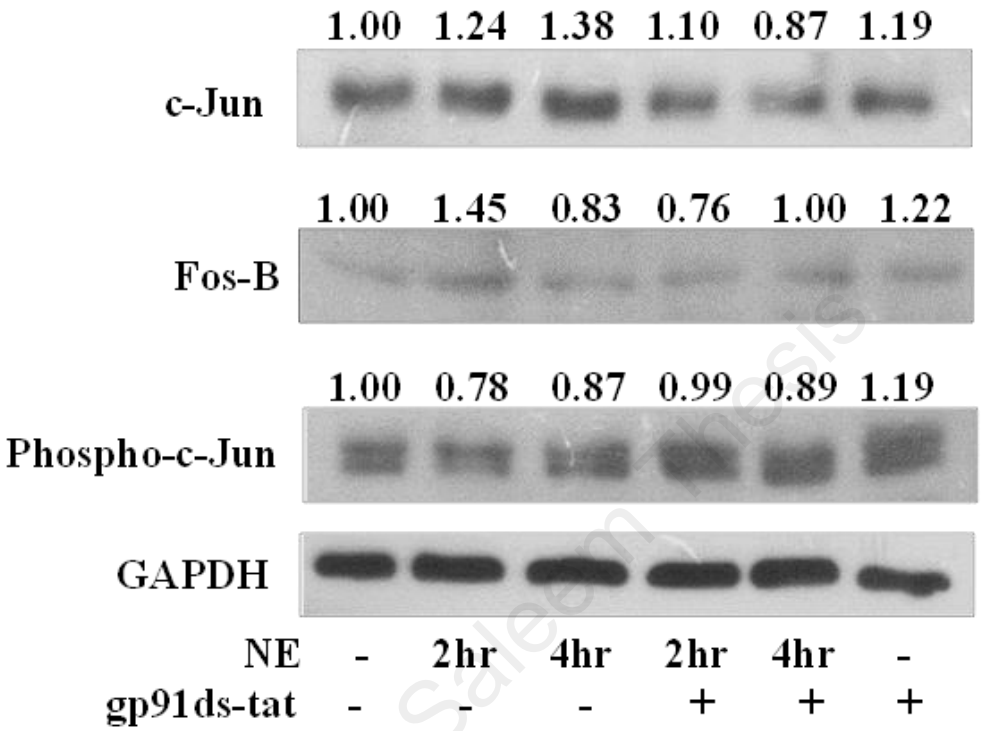

Figure I.4 Nox2 induced ROS modulates the activities of transcription factors mediating the hypertrophic response: (A) H9c2 cells were serum starved overnight followed by treatment with 2µM NE for 2 hr or 4 hr as indicated. 5µM gp91ds-tat was added 30 min before NE treatment wherever marked. Total protein was isolated and equal amount (50µg) of lysates were assayed by Western blot analysis using antibody specific for FosB, Phospho-c-Jun and c-Jun. GAPDH level was the loading control. The intensity of bands were evaluated as a ratio relative to that of GAPDH and values are written above the respective bands.

(B)

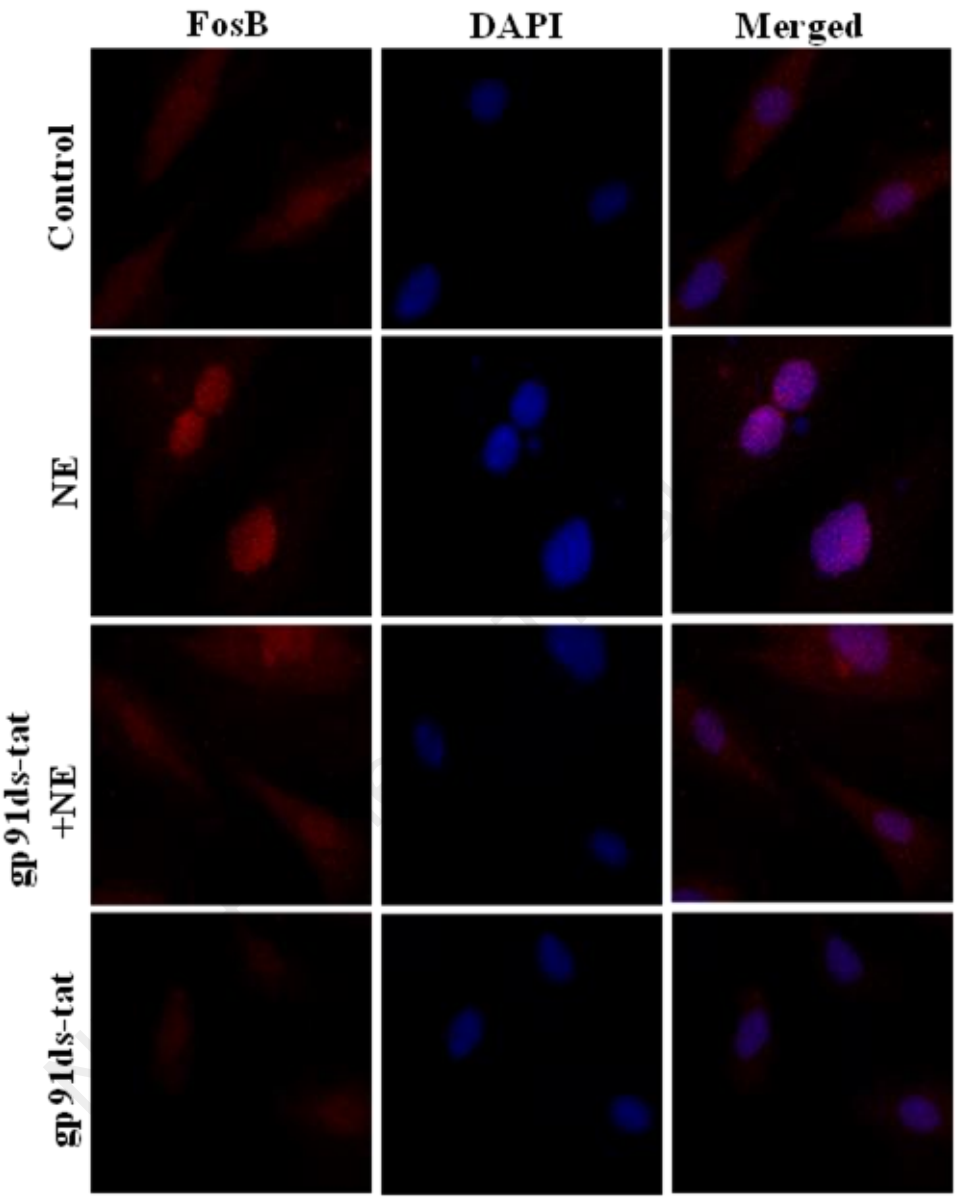

(B) H9c2 cells were serum starved overnight followed by treatment with 2µM NE for 2 hr. 5µM gp91ds-tat was added 30 min before NE treatment wherever marked. Immunostaining was done using antibody specific for FosB. The images were captured at 60X magnification by Nikon Eclipse Ti-E fluorescence microscope.

endogenous promoter of ANP gene has been extensively studied for analyzing the signal transduction pathways mediating hypertrophic response (Wang *et al.*, 2005) and it harbors an AP-1 site along with other cis-elements (Knowlton *et al.*, 1991). Although the FosB promoter has not been studied in details, we have demonstrated that it is selectively activated by the hypertrophic dose of NE and have used it as a paradigm of understanding how redox and kinase signals integrate at the gene level regulating its expression (Gupta *et al.*, 2006; Jindal & Goswami, 2011). When we tested the effects of NE on these promoters, there was increase by ~1.45 fold for AP-1, ~1.6 fold for FosB and ~1.5 fold for ANP. Pretreatment of cells with the Nox2 inhibitor gp91ds-tat (5μM) prevented the induction of all three (Figure I.4C).

To further confirm the role of Nox2 in regulating the expression of these promoters in NE treated cells, we co-transfected the wild type (Wt) and the dominant negative (DN) variant of p22-phox subunit of Nox. Although the activation of both Nox2/4 isoforms require p22-phox, its DN variant (P156Q) prevents ROS generation from Nox2 only (Kawahara *et al.*, 2005; von Löhneysen *et al.*, 2010). We argued that if the upregulation of these promoters are Nox2 dependent, it would be compromised by the over-expression by the DN mutant of p22-phox. As shown in Figure I.4D, expression of p22-phox-DN subunit of Nox compromised the stimulatory effect of NE seen in control, that is promoters transfected with the p22-phox-Wt, confirming the involvement of Nox2 in mediating NE response. Taken together, these data reiterates the involvement of Nox2 in modulating the gene network involved in hypertrophic signaling by NE.

(C)

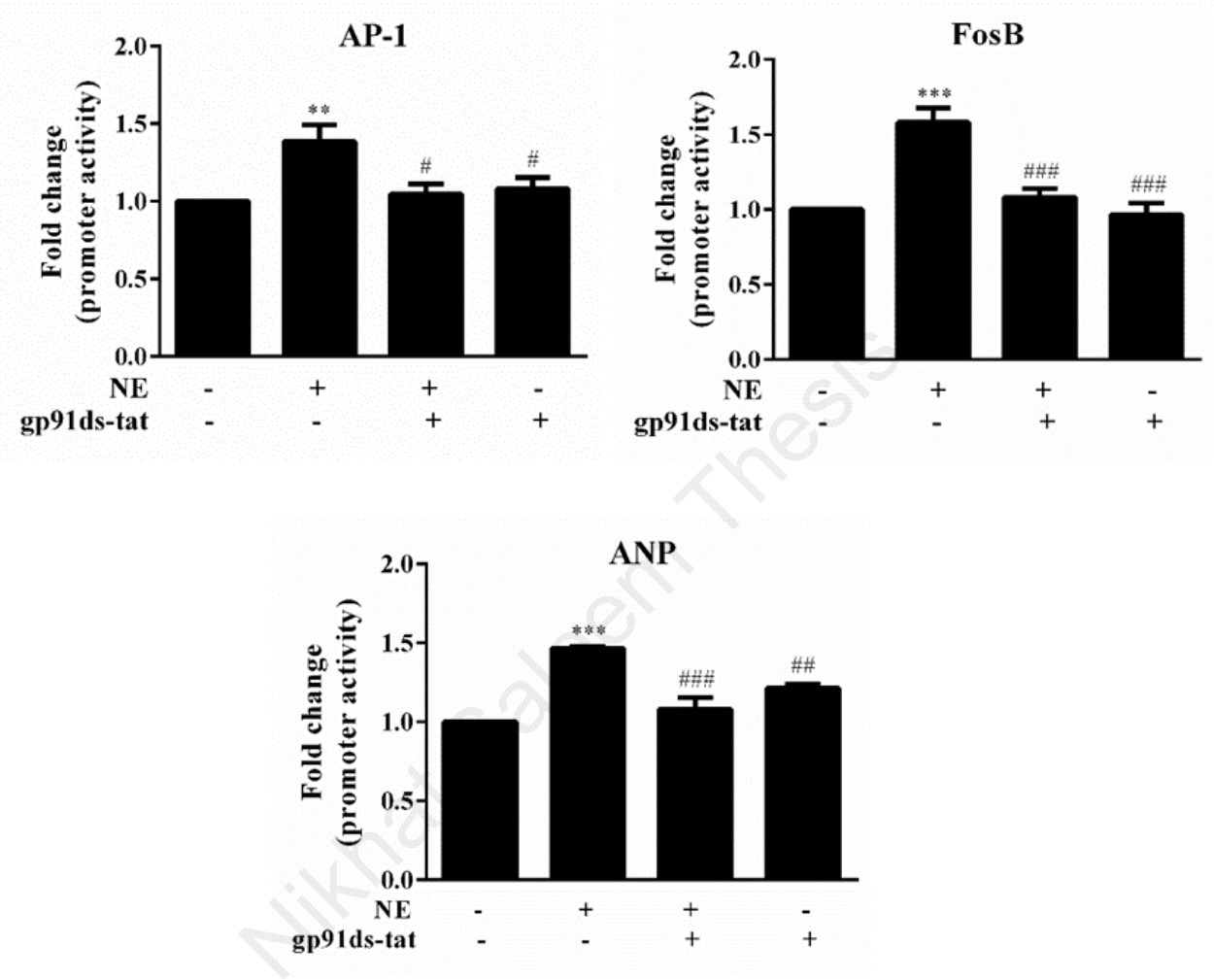

(C) H9c2 cells were transfected with AP-1, FosB and ANP promoter reporter constructs. After 24 hr of transfection, cells were kept overnight in serum free media followed by treatment with 2µM NE for 4 hr. 5µM gp91ds-tat was added 30 min before NE treatment wherever marked. Cell lysates were assayed for reporter luciferase activity. Normalization of luminescence was done against total protein concentration. Fold differences of promoter activity over control were calculated. **P $\leq$ 0.01 vs control; ***P $\leq$ 0.001 vs control; #P $\leq$ 0.05 vs NE; ##P $\leq$ 0.01 vs NE; ###P $\leq$ 0.001 vs NE.

(D)

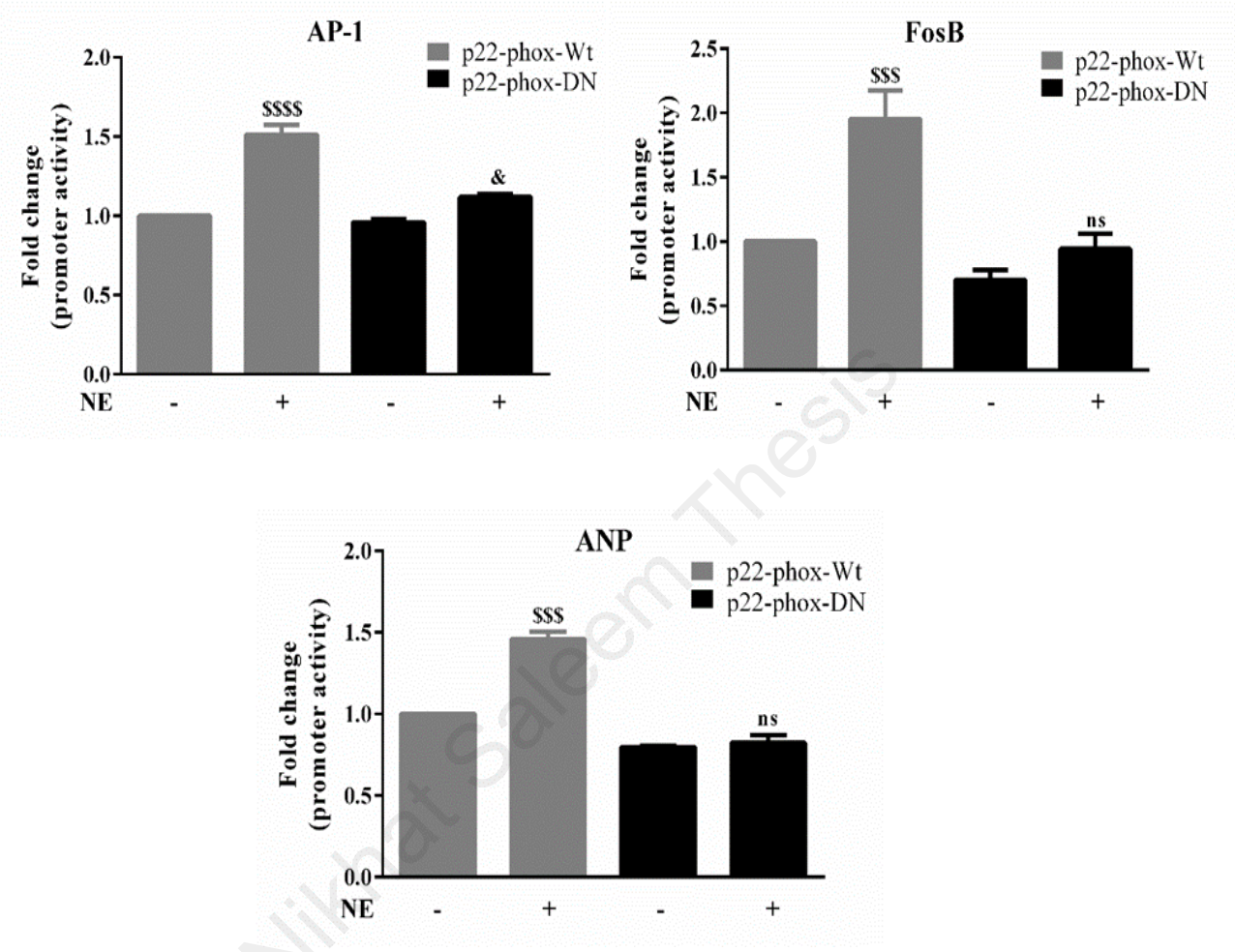

(D) H9c2 cells were co-transfected with p22-phox-Wt or p22-phox-DN constructs and AP-1, FosB or ANP promoter reporter constructs. After 24 hr of transfection, cells were kept overnight in serum free media followed by treatment with 2µM NE for 4 hr. 5µM gp91ds-tat was added 30 min before NE treatment wherever marked. Cell lysates were assayed for reporter luciferase activity. Normalization of luminescence was done against total protein concentration. Fold differences of promoter activity over control were calculated. $$$$P $\leq$ 0.0001 vs p22-phox-Wt untreated; $$$P $\leq$ 0.001 vs p22-phox-Wt untreated; &P $\leq$ 0.05 vs p22-phox-DN untreated.

Discussion:

While the specificity of kinase signaling is directed by protein-protein interactions, that of redox signaling depends on multiple factors like the localization of the reactive species in subcellular microdomain, the pKa of neighboring cysteine thiols, surrounding antioxidants and the presence of free transition metals etc (Schaar *et al.*, 2015; Dey *et al.*, 2016). Redox signaling in mammalian cell is thus highly nuanced, calibrated and difficult to dissect.

Among the three Noxes present in heart, function of Nox4 is better investigated. Its activation by multiple stimuli including ischemia-reperfusion, pressure overload and energy starvation vis-à-vis its location in the mitochondria, ER and the nucleus; exemplifies the complexity of redox signaling in cardiac pathobiology (Maejima *et al.*, 2011). On the contrary, the role of Nox2, the prototype Nox; in cardiac function is lesser understood, even though its activation by pressure volume overload and early preconditioning has been reported (Bell *et al.*, 2005; Maejima *et al.*, 2011). The functioning of the cardiovascular system is modulated by a plethora of growth factors, cytokines and hormones; but adrenergic signaling play a nodal role in these processes. Therefore, our observation that in cardiac myoblasts, the activation of adrenergic receptors co-stimulates Nox2 is novel and significant as it gives a new dimension to the adrenergic signaling.

Although ROS have been implicated in all major pathological conditions in heart, its sources and potential targets are largely unknown (Sawyer, 2011; Lassègue *et al.*, 2012; Zhang *et al.*, 2012; Ho *et al.*, 2013; Montezano & Touyz, 2014; Murray *et al.*, 2014; Granger & Kvietys, 2015). We have documented earlier that once the ROS generation is stimulated by NE, it sustains independently, presumably by some yet unknown downstream mechanisms (Gupta *et al.*, 2006; Thakur *et al.*, 2015). As the present study shows that the ROS generated by NE treatment is completely attenuated by the selective inhibition of Nox2, it is thus the only source of ROS at the onset. Though the primary product of Nox2 is $O_2^{\bullet-}$, it can be immediately converted into H_2O_2 by intra- and extracellular SOD (superoxide dismutase), and the chemistry of signaling by these two ROS are quite different. We therefore tested the nature of ROS generated by Nox2 and the presence of both $O_2^{\bullet-}$ and H_2O_2 were detected in NE treated cells. These results are in full agreement with our earlier observation that upon NE treatment, H9c2 cardiac myoblasts generate a complex mixture of $O_2^{\bullet-}$, H_2O_2 and other secondary ROS, although their sources were unknown in earlier study (Thakur *et al.*, 2015). In this study, we also for the first time

demonstrated that H_2O_2 generated by Nox2 is primarily localized in the cytosol, to some extent in the ER but completely absent in the mitochondria. Amongst various organelles, mitochondria have generally been viewed as the principal source of ROS in heart, especially under pathological conditions (Bell *et al.*, 2005; Maejima *et al.*, 2011), although cytosolic, endoplasmic reticular and nuclear ROS have also been attributed to the cardiac pathobiology (Qin *et al.*, 2014; Granger & Kvietys, 2015; Jang *et al.*, 2016; Matsushima *et al.*, 2016). Further study on the targets of cytosolic H_2O_2 in mediating the downstream signals will be of immense interest.

Although the cross-talk between the redox and kinase signaling has long been envisaged, the mechanistic insights are highly inadequate (Burgoyne *et al.*, 2015; Latimer & Veal, 2016). We had demonstrated earlier how kinase and redox signals generated in NE treated cardiac myoblasts are integrated at multiple *cis* regulatory elements in the target genes (Jindal & Goswami, 2011). In reiteration, we now demonstrate that three prototype genes for hypertrophic response viz., ANP, β- and α-MHC, modulated by NE remained to their baseline levels by the selective inhibition of Nox2. This observation further exemplifies the seamless integration of the ROS and kinase signaling we had demonstrated earlier (Jindal & Goswami, 2011). Such integration is further confirmed by the prevention of the induction of the one promoter exclusively regulated by the transcription factors AP-1, and two others i.e of ANP and FosB, considered as the prototype of adrenergic signaling; upon selective inhibition of Nox2. Although the specific inhibition of Nox2 by the peptide inhibitor gp-91-ds-tat has been shown by numerous studies (Derochette *et al.*, 2015), considering our emphasis on the pivotal role of Nox2 in adrenergic signaling, we also validated our claim by using a dominant negative mutant of p22phox which hampers the generation of ROS from Nox2 isoform only. This mutant also completely blocked the induction of FosB, ANP and AP-1 promoters induced by NE. The rational for using these promoters for the validation of Nox2 signaling is, these are at the end points of the kinase and ROS signals generated at the cell surface by the ligand i.e NE.

Taken together, our study firmly establishes the close interaction between the conventional kinase signaling from the adrenergic receptors and the emergent ROS signaling from Nox2 as the key mediator of adrenergic responses in the cardiac myoblasts.

Chapter II

Apocynin prevents isoproterenol induced cardiac hypertrophy in rats

Introduction:

Cardiac hypertrophy is a pathophysiological response to increased cardiac workload, resulting in increase in heart size (Maillet *et al.*, 2013). While physiological hypertrophy is associated with normal cardiac function and occurs during development, pregnancy and sustained exercise; pathological hypertrophy is promoted by hypertension, myocardial injury, excessive neurohumoral activation etc, eventually leading to heart failure (Shimizu & Minamino, 2016). High and sustained β-adrenergic activity with elevated level of blood catecholamines is a hallmark of pathological hypertrophy in heart failure patients (Ciccarelli *et al.*, 2013; Ferrara *et al.*, 2014). Pathological hypertrophy is characterized by increase in myocyte size, increased rate of protein synthesis and reinduction of fetal genes through multiple signaling pathways viz., MAP-, PI3-, Akt kinases and Ca^{++}-calcineurin (Heineke & Molkentin, 2006; Hou & Kang, 2012; Tham *et al.*, 2015). Transcription factors NFκB, NFAT, MEF2, GATA 4 etc has also been associated with the reprogramming of gene expression in the hypertrophied heart (Dirkx *et al.*, 2013). Besides these canonical signal transduction pathways, reactive oxygen species has also been attributed to the hypertrophic responses, but mechanisms are obscure (Chen & Zweier, 2014; Sag *et al.*, 2014).

In recent years, NADPH oxidases (Noxes) have emerged as the major source of intracellular reactive oxygen species (ROS) generation under various pathophysiological setups (Nabeebaccus *et al.*, 2011; Zhang *et al.*, 2013; Sag *et al.*, 2014). Out of seven isoforms of mammalian Noxes, Nox1/2/4 are expressed in heart (Brandes *et al.*, 2010). While tightly regulated ROS generation is essential for the maintenance of various cardiac functions; over production of ROS leads to conditions like interstitial fibrosis, contractile dysfunction, ischemia-reperfusion injury and cardiac remodeling (Lassègue *et al.*, 2012). Therapeutic targeting of Nox mediated generation of ROS is currently an area of intense research (Streeter *et al.*, 2013). We have shown that the stimulation of β-adrenergic receptor co-stimulates Nox and the cross-talk between the kinase and the redox (Nox) signaling determines the downstream responses. In the present study, we demonstrate that apocynin (Apo), a widely used inhibitor of Nox, attenuates the hypertrophic response elicited by the β adrenergic receptor agonist isoproterenol (Iso). Apocynin prevents the upregulation of a number of marker genes induced by Iso. It also substantially alters the rat cardiac proteome affected by the treatment with Iso.

Results:

Isoproterenol induced cardiac hypertrophy parameters are prevented by apocynin

Sustained activation of β-adrenergic receptors is an important hallmark of pathological cardiac hypertrophy. Isoproterenol (Iso), a non-selective β-adrenergic receptor agonist, is widely used for inducing cardiac hypertrophy in experimental rats (Grimm *et al.*, 2015). To explore the role of Noxes, if any, in β-agonist induced cardiac hypertrophy; we injected male Wister rats with Iso (5 mg/kg body weight, subcutaneous) for 14 days. Apocynin, a nontoxic inhibitor of Nox, was also co-administered (10 mg/kg body weight, intraperitonial, 30 min prior to the injection of Iso) (Ismail *et al.*, 2014). Iso induced cardiac hypertrophy, as evident from increase in heart weight to body weight ratio (HW/BW), heart weight to tail length ratio (HW/TL) and the echocardiogram, was prevented by Apo (Figure II.1A, B & C). As summarized in Table.1 and shown in Figure II.1C, Iso increased the IVSDd, LVPWd by ~2 and ~1.5 fold respectively, indicating concentric hypertrophy. There were no significant changes in Apo groups. There was no significant change in LVIDd, LVIDs, FS, EF and SV (stroke volume) in Iso treated heart, suggesting absence of any cardiac dysfunction (Table.1). Taken together, it suggests the involvement of Noxes in inducing cardiac hypertrophy due to sustained adrenergic stimulation.

Apocynin pretreatment prevents isoproterenol induced alteration in transcripts level

To further validate the establishment of cardiac hypertrophy by Iso, and its prevention by Apo; we assayed the mRNA levels of a number of well-established markers of hypertrophy. The total RNA were extracted from the LV section of hearts and the expression of markers genes were assayed by Real-time PCR (Taegtmeyer *et al.*, 2010). As shown in Figure II.2A & B, in Iso treated hearts, the level of transcripts for β-MHC, ANP, BNP and ACTA-1 were increased by ~5.2, ~2.5, ~5.3 and ~2.2 fold respectively, that were prevented either partially (ANP, and BNP) or completely (β-MHC and ACTA-1) by the Apo treatment. We also confirmed the induction of ANP at the protein level by Western blot. As shown in Figure II.2C, Iso treatment increased the level of ANP by ~1.25 fold that was attenuated in Apo treated heart.

Apocynin prevents isoproterenol induced activation of Akt and Erk

Cardiac hypertrophy involves upregulation of key signaling kinases including PKA, Akt and Erk (Tham *et al.*, 2015). To understand if the regression of hypertrophy by Apo involves these kinase, we measured their levels by western blotting (Figure II.3A & B).

(A)

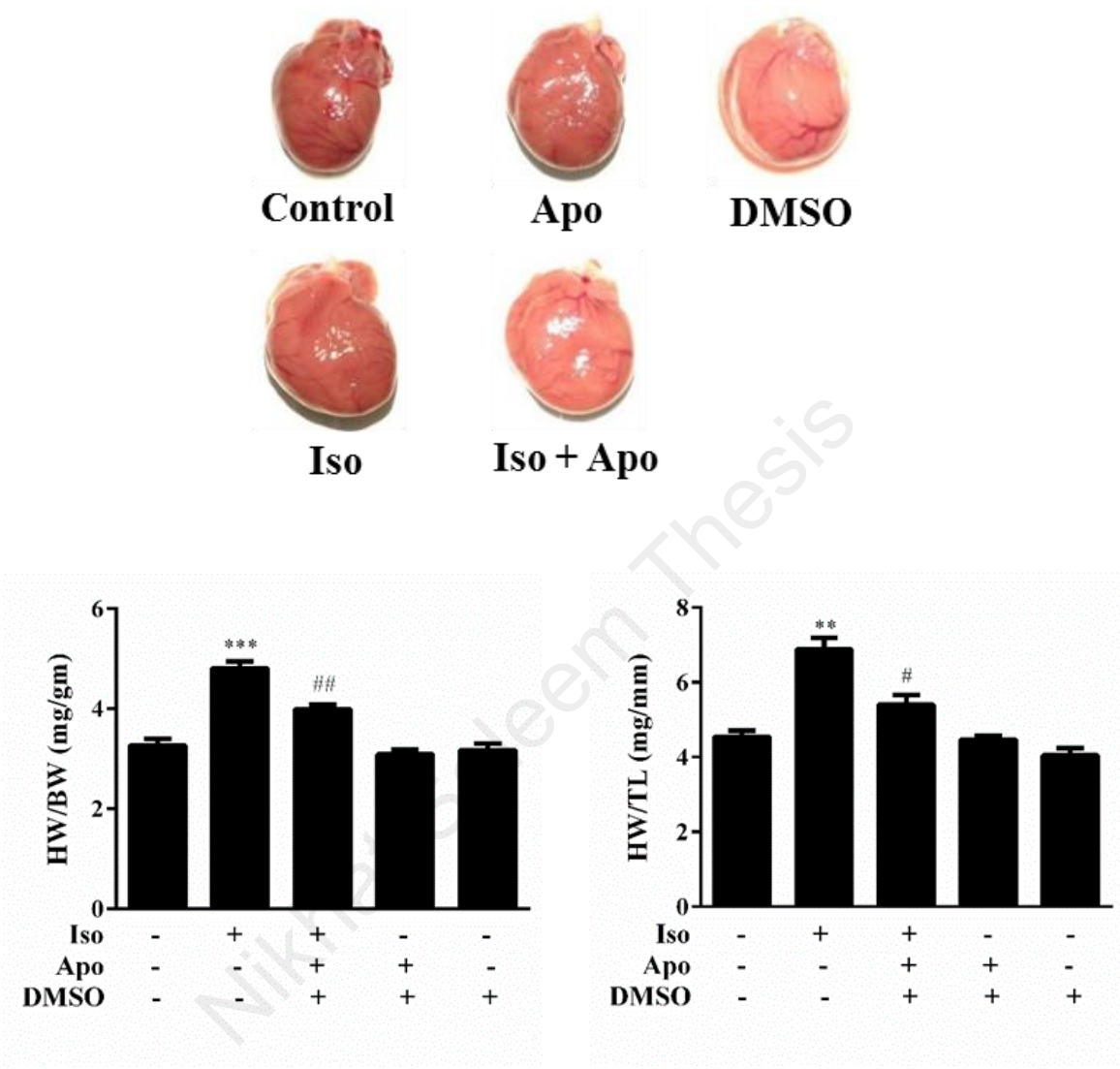

Figure II.1 Isoproterenol induced cardiac hypertrophy in rat is prevented by the Nox inhibitor apocynin: (A) Wistar rats were administered with Iso (5 mg/kg body weight, subcutaneous) and Apo (10 mg/kg body weight, intraperitoneal) for 14 days. Upon completion of treatments, Rats were sacrificed and the heart was excised. Upper panel: representative images of whole heart excised from treated rats. Lower panel: ratio of HW/BW (heart weight to body weight) and HW/TL (heart weight to tail length). **P $\leq$ 0.01 vs Control; ***P $\leq$ 0.001 vs Control; #P $\leq$0.05 vs Iso; ##P $\leq$ 0.01 vs Iso.

(B)

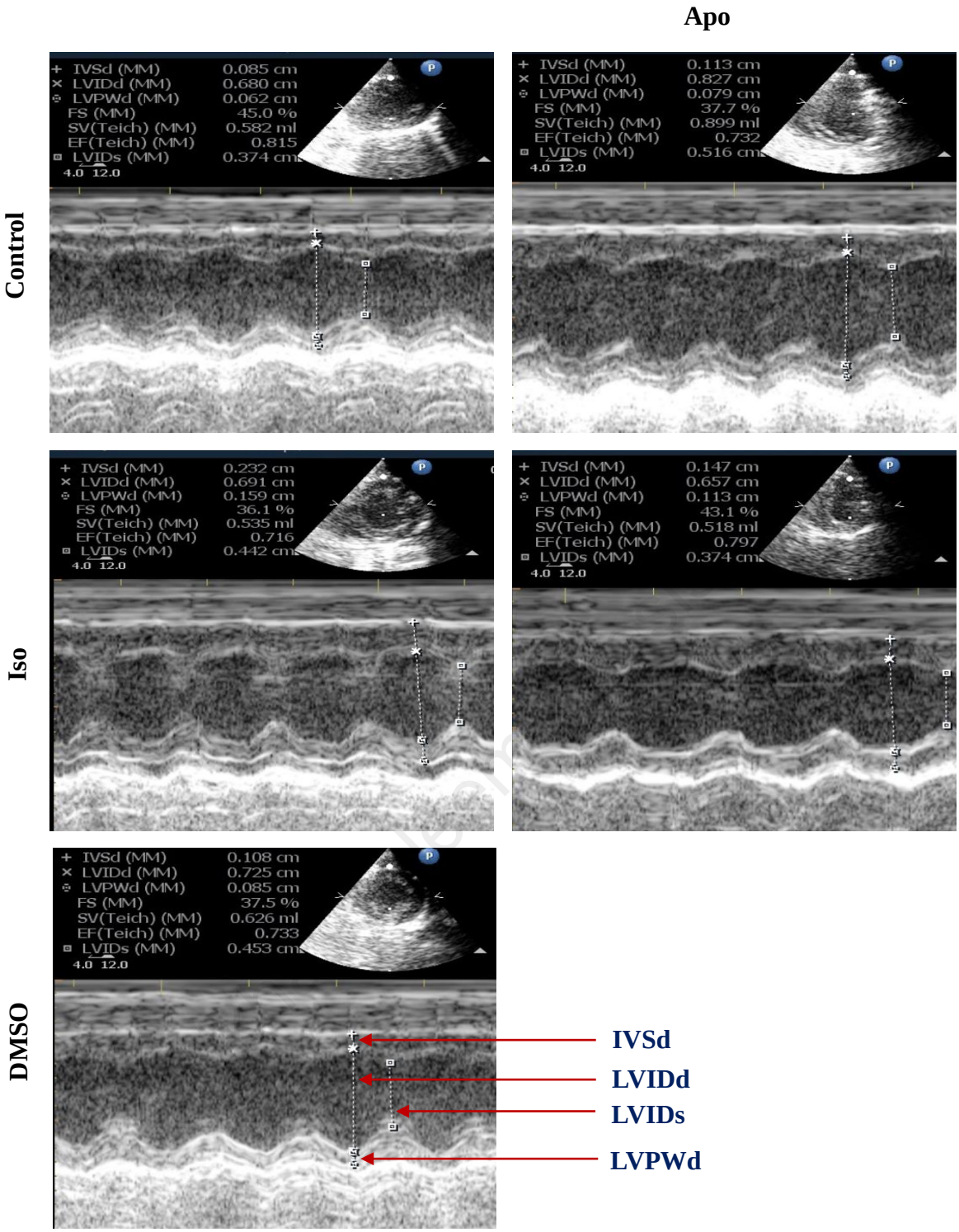

(B) Wistar rats were administered with Iso (5 mg/kg body weight, subcutaneous) and Apo (10 mg/kg body weight, intraperitoneal) for 14 days. Upon completion of treatments. M-mode echocardiography was done on treated rats. Representative echocardiogram of different groups on day 14.

LVIDd, left ventricular internal dimensions at diastole; LVIDs, left ventricular internal dimensions at systole; IVSd, interventricular septal thickness at diastole; LVPWd, Left ventricular posterior wall thickness at diastole.

Table.1 Echocardiography parameters evaluated from M-mode recording on day 14.

Parameters	Control	Iso	Iso+Apo	Apo	DMSO
LVIDd (cm)	0.722±0.027	0.687±0.013	0.680±0.032	0.786±0.059	0.677±0.048
LVIDs (cm)	0.421±0.036	0.431±0.027	0.348±0.018	0.516±0.075	0.428±0.025
IVSd (cm)	0.104±0.014	0.208±0.012	0.115±0.016	0.098±0.008	0.124±0.012
LVPWd (cm)	0.072±0.005	0.151±0.011	0.102±0.006	0.081±0.008	0.095±0.005
FS (%)	38.15±6.85	37.46±2.71	48.43±0.79	35.03±5.19	36.75±0.75
EF (%)	78.8±7.14	73.07±3.26	84.00±3.72	68.97±7.27	75.00±1.70
SV (ml)	0.655±0.040	0.536±0.005	0.613±0.110	0.730±0.105	0.519±0.107
LVM (gm)	0.888±0.030	1.283±0.029	0.939±0.024	0.954±0.073	0.955±0.051

LVIDd, left ventricular internal dimensions at diastole; LVIDs, left ventricular internal dimensions at systole; IVSd, interventricular septal thickness at diastole; LVPWd, Left ventricular posterior wall thickness at diastole; FS, fractional shortening; EF, ejection fraction; SV, stroke volume; LVM, left ventricular mass.

(C)

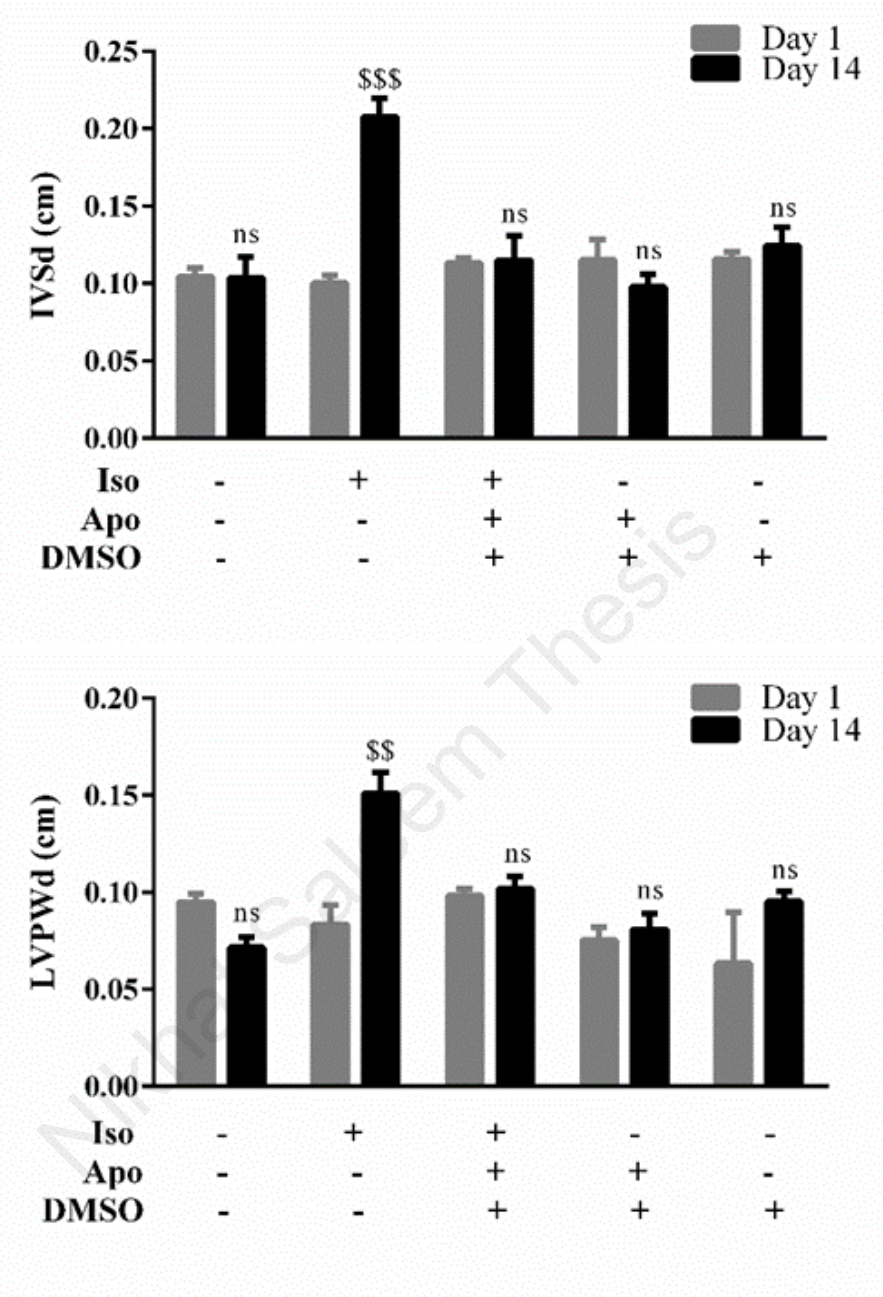

(C) Wistar rats were administered with Iso (5 mg/kg body weight, subcutaneous) and Apo (10 mg/kg body weight, intraperitoneal) for 14 days. M-mode echocardiography was done on day 1 and on completion of treatments i.e. day 14. Quantitative representation of LVIDd and LVPWd on day 1 (baseline) and day 14. $$P $\leq$ 0.01 vs Day 1; $$$P $\leq$ 0.001 vs Day 1.

LVIDd, left ventricular internal dimensions at diastole; LVPWd, Left ventricular posterior wall thickness at diastole.

(A)

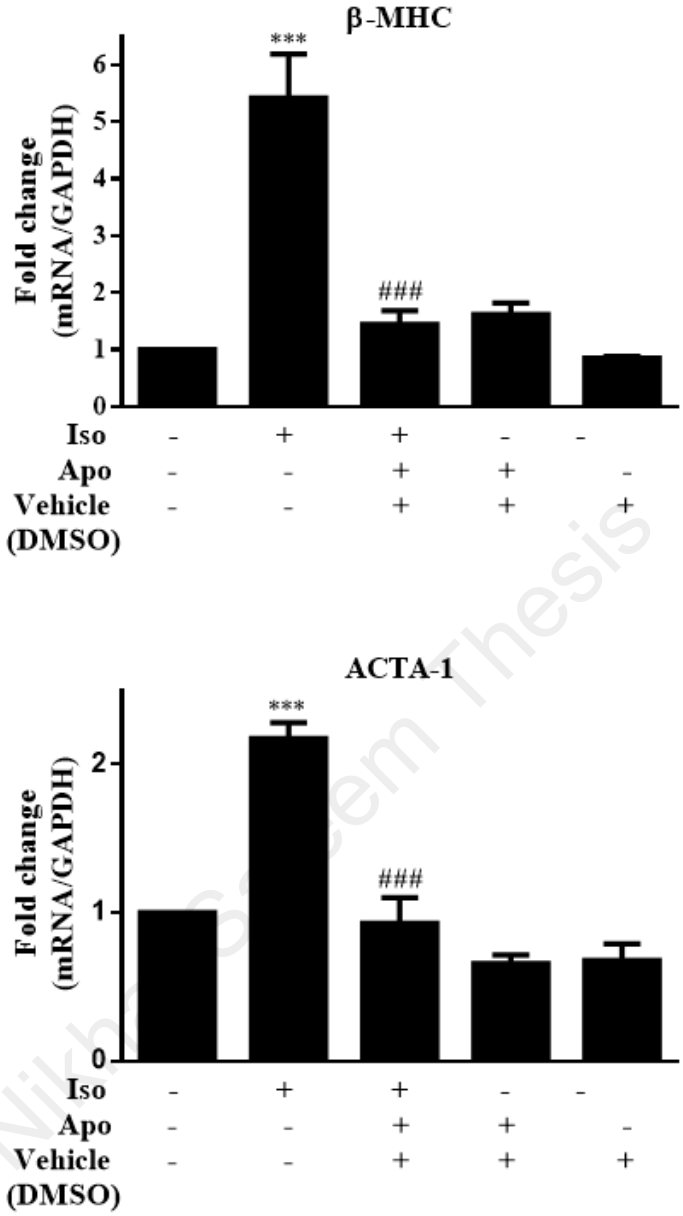

Figure II.2 Apocynin pretreatment prevents isoproterenol induced alteration in transcripts level: (A) Wistar rats were administered with 5 mg/kg BW (subcutaneous) of Iso and 10 mg/kg BW of Apo (intraperitoneal). After 14 days, rats were sacrificed and heart was excised. Total RNA was isolated from the left ventricle and assayed for β-MHC and ACTA-1 transcripts using gene specific primers by Real-time PCR. Normalization of input RNA was done by using GAPDH level as an internal control. Fold differences of mRNA levels over control were calculated. ***P $\leq$ 0.001 vs control; ###P $\leq$ 0.001 vs Iso.

(B)

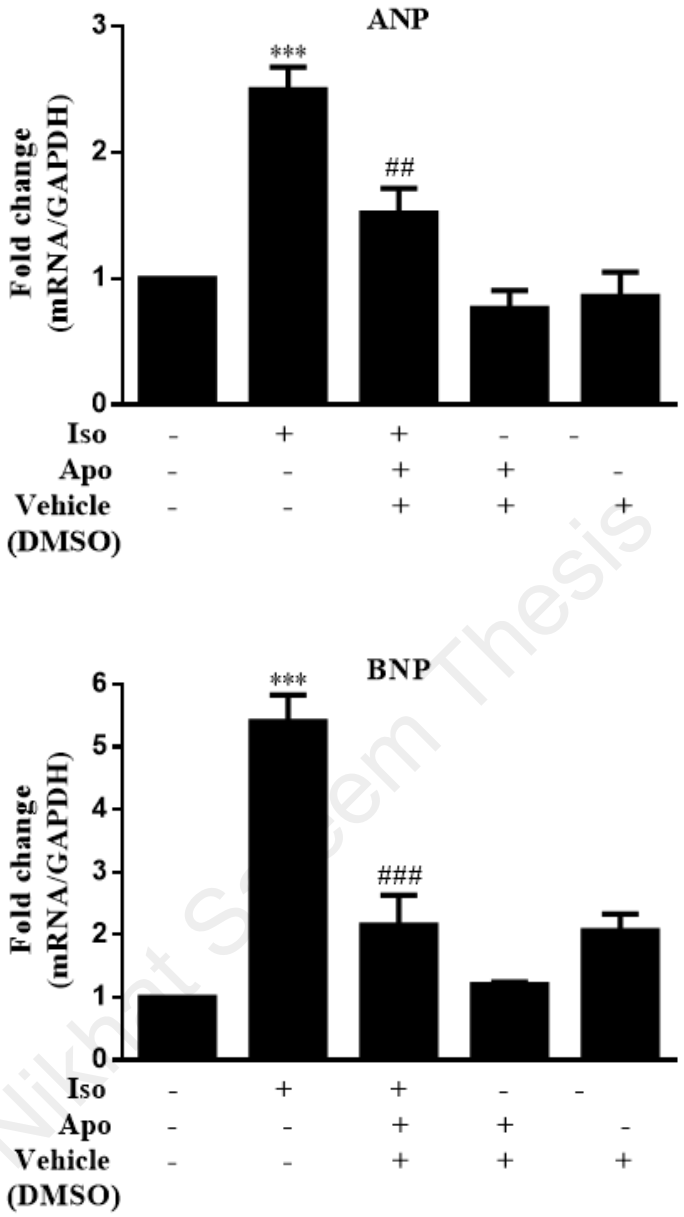

(B) Wistar rats were administered with 5 mg/kg BW (subcutaneous) of Iso and 10 mg/kg BW of Apo (intraperitoneal). After 14 days, rats were sacrificed and heart was excised. Total RNA was isolated from the left ventricle and assayed for ANP and BNP transcripts using gene specific primers by Real-time PCR. Normalization of input RNA was done by using GAPDH level as an internal control. Fold differences of mRNA levels over control were calculated. ***P $\leq$ 0.001 vs control; ##P $\leq$ 0.01 vs Iso; ###P $\leq$ 0.001 vs Iso.

(C)

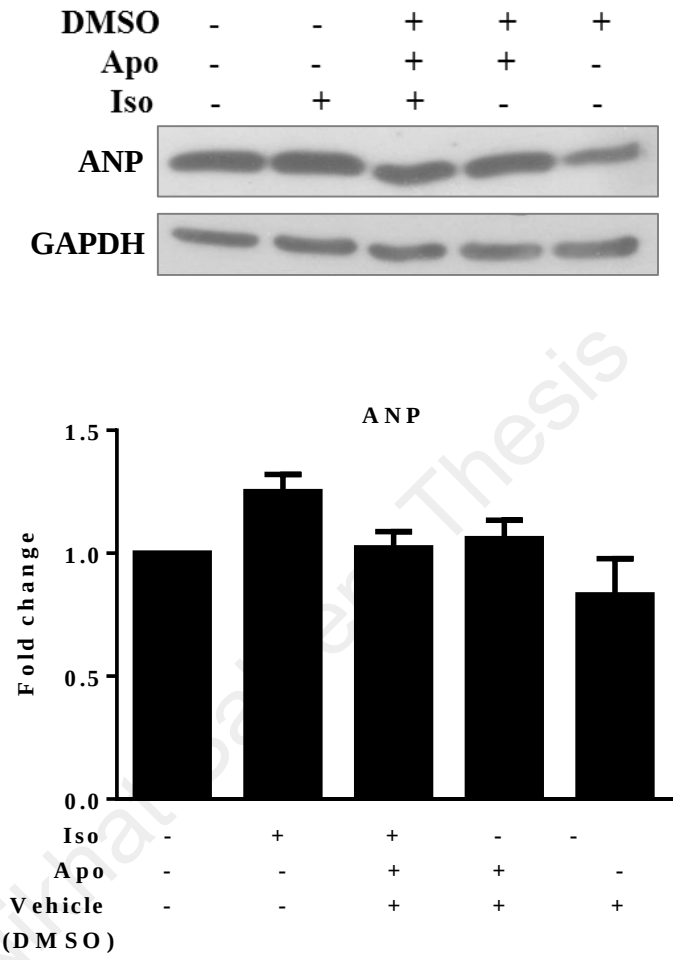

(C) Wistar rats were administered with 5 mg/kg BW (subcutaneous) of Iso and 10 mg/kg BW of Apo (intraperitoneal). After 14 days, rats were sacrificed and heart was excised. Total protein was isolated from the left ventricle and equal amounts (80µg) of lysates were assayed by Western blot analysis using antibodies specific for ANP. GAPDH level was the loading control. Fold differences of protein levels over control were calculated.

Iso treatment increased pPKA level by ~1.4 fold and pretreatment with Apo prevented that increase. We also assayed the level of the transcription factor CREB, a downstream target of PKA, which was unaffected under Iso treatment (Figure II.3A). The level of pAkt increased by ~2.0 fold under Iso treatment and Apo brought it to ~1.2 fold to the baseline. Similarly, in Iso treated rats, pErk1/2 level was increased by ~1.2 fold and pretreatment with Apo abrogated the induction (Figure II.3B). Taken together, these data suggest that the activation of PKA, Akt and Erk by the stimulation of β-adrenergic receptor is attenuated by the inhibition of Nox by apocynin.

Apocynin alters the Iso treated Cardiac proteome

To further understand the wider mechanisms of the reversal of Iso induced cardiac hypertrophy by Apo, we performed a comparative proteome analysis of the left ventricle section of the Iso and Iso plus Apo treated hearts. The total protein extracts were resolved by 2D gel electrophoresis followed by silver staining to visualize the spots. Representative 2D images of different groups are shown in Figure II.4A. The gel images were analysed and several differentially expressed protein spots were randomly identified. The spots were then excised, identified by MALDI-TOF/MS analysis and were tabulated based on the nature of modulation by Iso and Iso plus Apo. As shown in Table.2, we identified ten proteins which were upregulated by Iso and apocynin restored them. These ten proteins are involved in cardiac pathobiology in general. In particular, two were involved in cell signaling (Calsequestrin 2 and Arginine vasopressin-induced protein 1); two in vascular function (Renin precursor protein and Fibroblast growth factor 12); five in energy metabolism (Prohibitin, NADH dehydrogenase (ubiquinone) Fe-S protein, Cytosolic aspartate aminotransferase, Enoyl-CoA hydratase, Mito precursor, Short-chain specific acyl-CoA dehydrogenase), and one in cardiac development (T-box 3). Similarly, four proteins were found to be downregulated by Iso and restored by Apo; out of which, two were gene regulatory proteins (Transcription elongation factor SPT5, Zinc finger protein 2 homolog), one was chaperone (Heat shock protein-90) and one contractile protein (Myosin regulatory light chain 2). Four proteins were also identified that were upregulated by Iso and further increased by Apo. Among them, one was a chaperone (Heat shock protein β-6), one was a Ca^{++} signaling protein (Myozenin-2) and two were involved in metabolism (β-enolase and Nucleoside diphosphate kinase B). Two proteins were downregulated by Iso but Apo further reduced it (Myosin light chain 3 and Troponin T). Four proteins were unaffected by Iso, but Apo modulated their expression. Those were

(A)

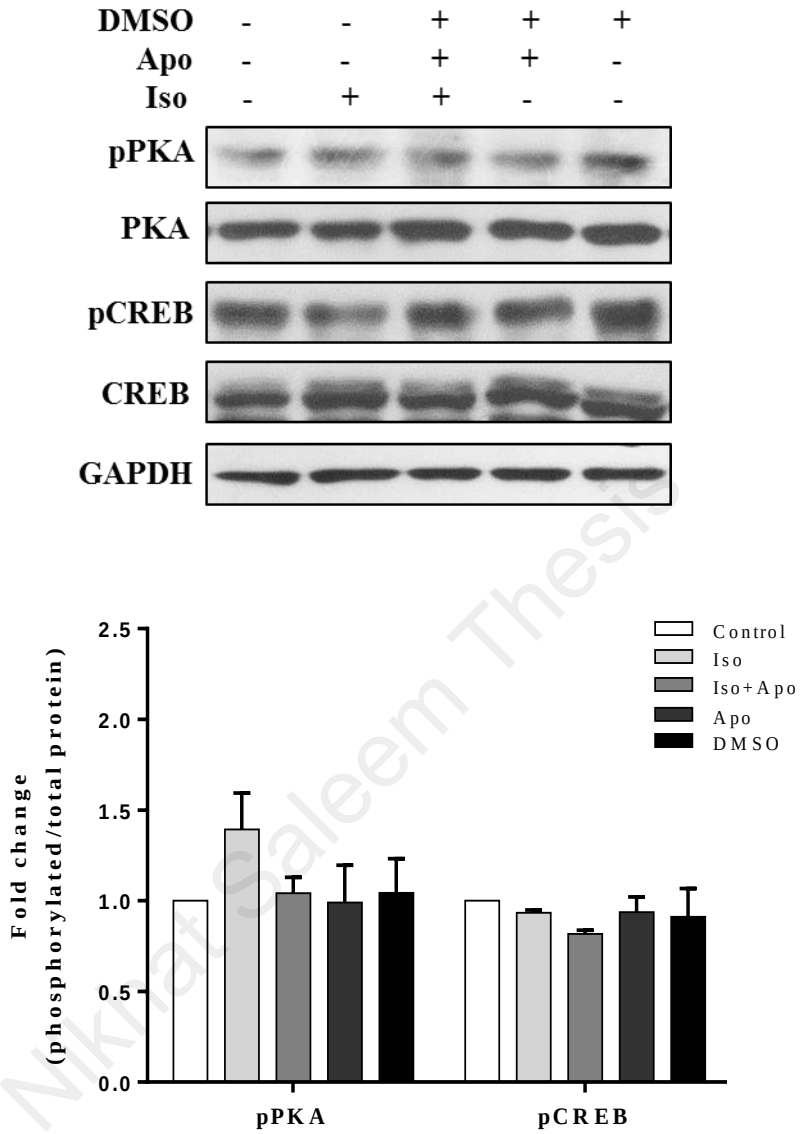

Figure II.3 Apocynin prevents isoproterenol induced activation of downstream kinases: (A) Wistar rats were administered with 5 mg/kg BW (subcutaneous) of Iso and 10 mg/kg BW of Apo (intraperitoneal). After 14 days, rats were sacrificed and heart was excised. Total protein was isolated from the left ventricle and equal amounts (80µg) of lysates were assayed by Western blot analysis using antibodies specific for phospho PKA and phospho CREB. Total PKA and total CREB were used as respective controls. Also GAPDH level was the loading control. The mean density values of pPKA and pCREB were evaluated as a ratio relative to that of total PKA and total CREB respectively. Fold differences of relative ratio of protein levels over control were calculated.

(B)

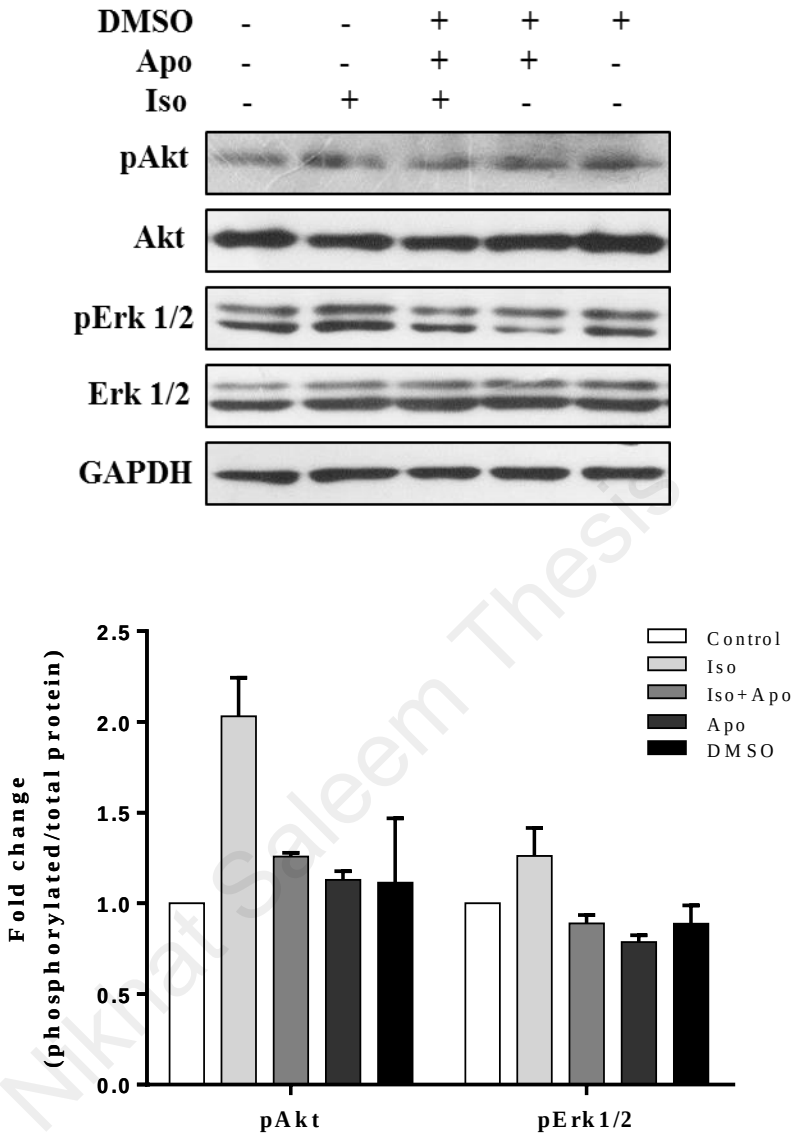

(B) Wistar rats were administered with 5 mg/kg BW (subcutaneous) of Iso and 10 mg/kg BW of Apo (intraperitoneal). After 14 days, rats were sacrificed and heart was excised. Total protein was isolated from the left ventricle and equal amounts (80µg) of lysates were assayed by Western blot analysis using antibodies specific for phospho Akt and phospho ERK1/2. Total Akt and total ERK1/2 were used as respective controls. Also GAPDH level was the loading control. The mean density values of pAkt and pERK were evaluated as a ratio relative to that of total Akt and total ERK respectively. Fold differences of relative ratio of protein levels over control were calculated.

(A)

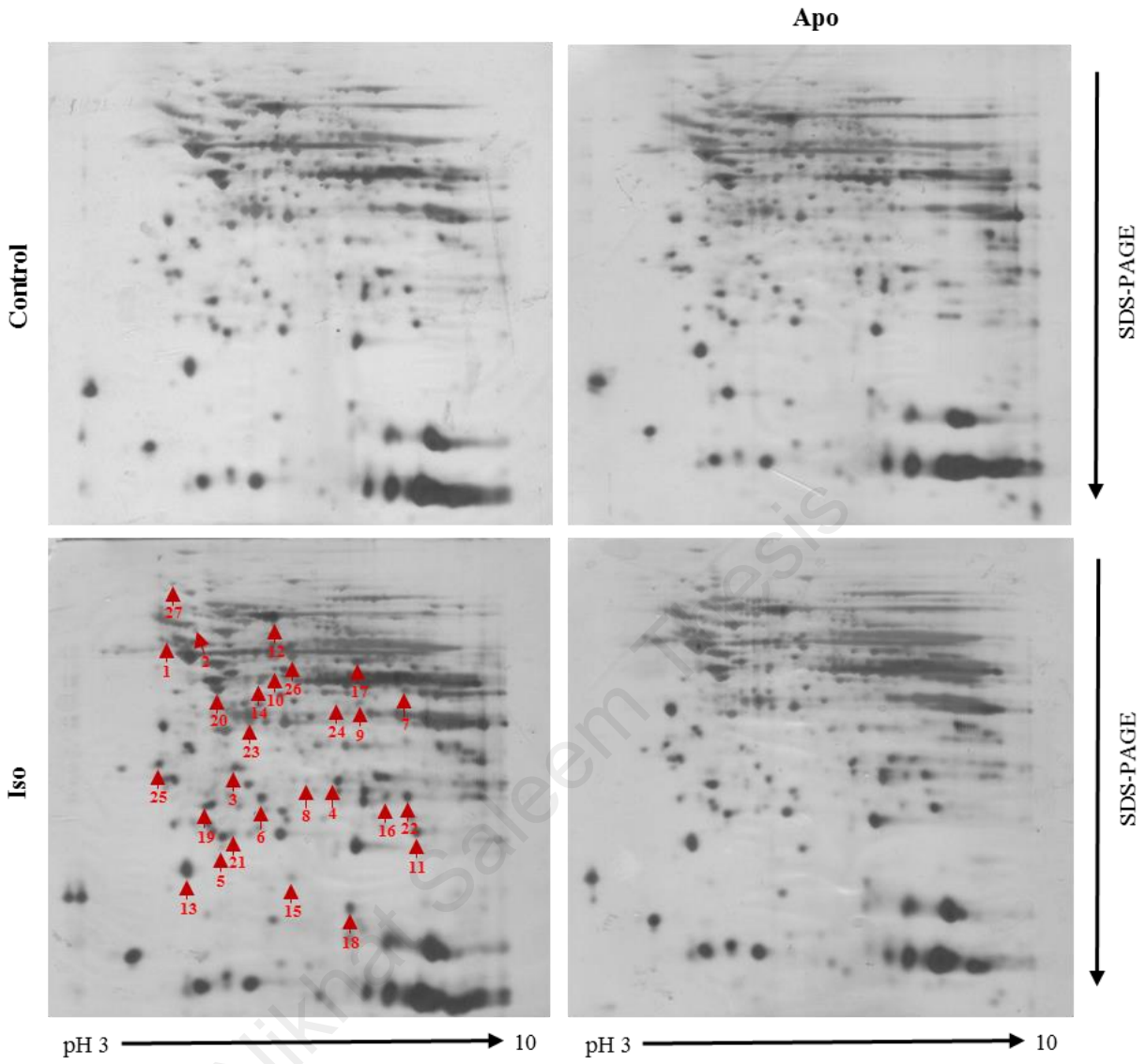

Figure II.4 Analysis of the effects of apocynin on isoproterenol modulated cardiac proteome: Wistar rats were administered with 5 mg/kg BW of Iso and 10 mg/kg BW of Apo. After 14 days, rats were sacrificed, hearts were excised and lysates were prepared from the left ventricle. Two hundred fifty microgram of lysate was resolved on a 13 cm IPG strip with pH gradient 3-10 (linear) followed by second dimension separation on 12% SDS PAGE. Then silver staining was performed to visualize the protein spots. (**A)** Representative 2D images of different groups. Gel images were analysed by using SameSpots software from totallab, UK. All the differentially expressed spots were marked (red arrow) and identified by MALDI-TOF analysis.

(B)

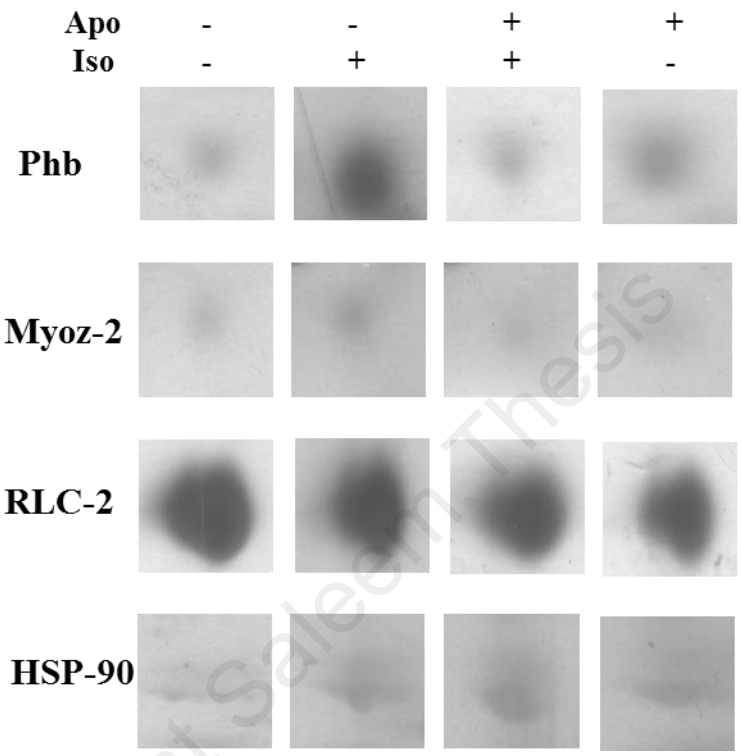

(**B)** Close up areas of the gels showing variation in the intensity of the four representative (randomly chosen) differentially expressed proteins viz., Prohibitin (Phb), Myozenin-2 (Myoz-2), Myosin regulatory light chain-2 (RLC-2) and Heat Shock Protein-90 (HSP-90) spots are also shown.

Table.2 Grouping of modulated proteins identified from 2D gel analysis followed by its MALDI-TOF/MS.

Group	Spot No.	Name of the protein	Relative level of expression*	
Upregulated by Iso, restored by Apo	1.	Calsequestrin 2	1 1.2146 0.9429	1. Ca^{2+}-binding protein in the sarcoplasmic reticulum of cardiac myocytes. Senses changes in the luminal Ca^{2+} concentration and communicates to ryanodine receptor channel.
	2.	Renin precursor protein	1 1.4760 1.0017	2. The precursor of renin protein, a endopeptidase which generate angiotensin I from angiotensinogen in the plasma. Plays a critical role in adverse left ventricular remodeling and chronic heart failure.
	3.	Prohibitin	1 1.7556 1.0903	3. Highly conserved group of protein family involved in energy metabolism, proliferation, apoptosis, and senescence. Significantly increased in I/R rats. Protects cardiomyocytes from oxidative stress induced damage.
	4.	Arginine vasopressin-induced protein 1	1 1.5969 1.0832	4. Involved in MAP kinase activation, epithelial sodium channel (ENaC) down-regulation and cell cycling. Elevated during cardiac stress, have role in the regulation of blood pressure and the pathogenesis of hypertension.
	5.	Fibroblast growth factor 12	1 2.0472 1.2473	5. Master regulator of VSMC plasticity, induces the quiescent and differentiated phenotypes.
	6.	NADH dehydrogenase (ubiquinone) Fe-S protein	1 1.1835 0.9161	6. Core subunit of the mitochondrial ETC complex I, transfers electrons from NADH to the respiratory chain.
	7.	Cytosolic aspartate aminotransferase	1 1.1942 0.9633	7. Biosynthesis of L-glutamate from L-aspartate or L-cysteine. Elevated level is found in myocardial infarction.
	8.	Enoyl-CoA hydratase, Mito	1	8. Catalyzes the second step of β-oxidation in fatty acid metabolism to

		precursor	1.3968 0.8411	produce acetyl CoA and energy.
	9.	Short-chain specific acyl-CoA dehydrogenase	1 1.2745 0.9788	9. Catalyzes the dehydrogenation of acyl CoA derivatives in β-oxidation.
	10.	T-box 3	1 1.5196 1.1684	10. Transcription factor required for pacemaker and conduction system development in the embryonic. Also reprogram adult cardiomyocytes into pacemaker cells.
Downregulated by Iso, restored by Apo.	11.	Transcription elongation factor SPT5	1 0.8357 1.0130	1. Conserved throughout evolution, regulates mRNA processing and transcription elongation by RNA polymerase II and I.
	12.	Heat shock protein-90	1 0.5761 1.0298	2. Molecular chaperone. Have pathogenic role in atherosclerosis and cardiac hypertrophy.
	13.	Myosin regulatory light chain 2	1 0.5056 0.7434	3. Contractile protein.
	14.	Zinc finger protein 2 homolog	1 0.8758 1.1522	4. Transcription factor involved in neuronal differentiation and phenotypic maintenance.
Upregulated by Iso and further increased by Apo	15.	Heat shock protein β-6	1 1.1949 1.8073	1 Small molecular chaperone that maintains denatured proteins in a folding-competent state. Regulate smooth muscle vasorelaxation and cardiac myocyte contractility. Overexpression mediates cardioprotection and angiogenesis after induced damage.
	16.	Myozenin-2	1 1.2116 1.3035	2. Cardiac specificZ-disc protein. Involved in modulation of calcineurin signaling and in myofibrillogenesis.
	17.	β-enolase	1	3. Glycolytic enzyme that catalyzes the reversible conversion of 2-

			1.3199 2.2623	phosphoglycerate to phosphoenolpyruvate. Involved in striated muscle development and regeneration.
	18.	Nucleoside diphosphate kinase B	1 1.1709 1.2679	4. Catalyzes the synthesis of nucleoside triphosphates. Negatively regulates Rho activity by interacting with AKAP13/LBC.
Downregulated by Iso and further reduced by Apo	19.	Myosin light chain 3	1 0.8769 0.7970	1. Regulatory light chain of myosin referred as cardiac ventricular/ slow skeletal muscle isoform. Mutations in MYL3 is associated to the familial hypertrophic cardiomyopathy.
	20.	Troponin T, cardiac isoform	1 0.7891 0.7074	2. Tropomyosin binding subunit of troponin, regulate muscle contraction. Serve as a marker of heart muscle damage.
No change with Iso, but modulated by Iso+Apo	21.	Phosphatidylethanolamine-binding protein 1	1 1.0644 1.4561	1. Novel effector of signal transduction pathways vis-à-vis physiological modulator of Raf kinase, GPCR signaling and NFκB activation, thereby control cellular growth, motility, apoptosis, genomic integrity, and therapeutic resistance.
	22.	Homolog of zebra fish ES1	1 1.1158 1.3383	2. Conserved across E.coli. to human and are expressed in diverse tissues having high metabolic demands. Involved in mitochondrial biogenesis.
	23.	Zinc finger CCCH domain-containing protein	1 1.0451 0.8955	3. Involved in cell cycle and growth phase related regulation.
	24.	Sodium channel Nav1.7	1 0.9799 0.7587	4. Voltage gated sodium channel involved in generation and conduction of action potentials majorly contributing to pain signaling.
	25.	Polymerase, delta 2, regulatory subunit	1 1.0757 0.8023	5. Component of DNA polymerase delta complex, involved in DNA replication and repair.
	26.	α-enolase isoform X1	1 0.8985 0.9072	1. Key glycolytic enzyme involved in multiple functions, considered as a marker of pathological stress in number of diseases. Induced expression under I/R and myocardial infarction.

No change	27.	Stathmin-4 isoform b	1 1.0616 1.0119	2. Microtubule destabilizers, regarded as intracellular signaling relay center. Involved in the regulation of neurogenesis.

* In the descending order: Control, Iso, Iso plus Apo

Phosphatidylethanolamine-binding protein 1, a signaling protein; Homolog of zebra fish ES1, involved in mitochondrial biogenesis; Zinc finger CCCH domain-containing protein involved in cell cycle regulation; a sodium channel; and Polymerase, delta 2, regulatory subunit, a component of DNA polymerase delta complex, involved in DNA replication and repair. Taken together, these results strongly suggest that Apo has broader effects on cardiac proteome under Iso stress.

Discussion:

Cardiac hypertrophy is the common manifestation of several cardiovascular disorders. At the cellular level, there are several hallmarks like increased protein synthesis, increase in myocyte volume but not in number, and partial reactivation of fetal gene expression programs. Although oxidative stress has been attributed to it, failure of antioxidants in ameliorating those conditions necessitated a revisit of the concept of the cause and effect relationship (Sawyer, 2011). Such reexamination has also been necessitated by the emergence of reactive oxygen species like superoxide and hydrogen peroxide as the mediators of physiological signals (Zhang *et al.*, 2012).

Noxes are the enzymes solely dedicated to the generation of intracellular superoxide and hydrogen peroxide. With the emerging evidences on their pivotal role in the pathophysiology of various diseases, therapeutic inhibitors of Noxes are also being explored (Brandes *et al.*, 2014b; Altenhöfer *et al.*, 2015). Apocynin, a non-toxic plant metabolite, has been in use for treating respiratory, metabolic and cardiovascular disorders even before its mode of action were known (’t Hart *et al.*, 2014). Later studies had described it as an inhibitor of Nox (Altenhöfer *et al.*, 2015). Recent years there has been a flurry of reports showing its beneficial effects under several pathobiological setups (Altenhöfer *et al.*, 2015; Rastogi *et al.*, 2016). Despite the ambiguities regarding the specificity of its actions, its beneficial effects have largely been well appreciated (Simonyi *et al.*, 2012). Based on our earlier study showing the involvement of Nox2 in mediating adrenergic signaling (manuscript under revision in Molecular and Cellular Biochemistry), we have tested whether Apo can ameliorate the hypertrophic response elicited by the adrenergic agonist Iso in male rats. As evident from the gross morphological parameters (HW/BW and HW/TL ratio), echocardiography, and expression levels of the transcripts of the established markers of hypertrophy (β-MHC, ANP, BNP and ACTA-1), Apo was quite effective in preventing the hypertrophic responses measured after two weeks of treatment. In full agreement, the activation of key nodal kinases mediating adrenergic signaling viz., PKA, ERK and Akt by Iso were also prevented by Apo; reiterating the well anticipated cross talk between the redox and kinase pathways. Noticeably, transcription factor CREB, one of the downstream targets of PKA and a regulator of cardiac functions (Liu *et al.*, 2006), was affected neither by Iso nor by Iso + Apo, suggesting specificity of their effects. Although CREB is known to be the downstream target of β-AR/PKA signaling, no alteration in its activity by Iso has earlier been reported (Yin *et al.*, 2016).

Adrenergic signaling is highly complex that substantially modulates the cardiac proteome (Kumar *et al.*, 2017). Our observation that Apo further alters the proteome in Iso treated heart is significant as it suggests a far wider role of Noxes in cardiac function. Although a counter argument in favor of a pleiotropic effect of Apo might be put forward, the proteomic data still argues well in view of the fast emerging role of Noxes in cardiac function (Santos *et al.*, 2016).

Summary and Conclusions

Cardiac cells have multiple adrenergic receptors (α and β with several subtypes) and sustained adrenergic stimulation under increased cardiac load and decreased contractile function result in pathological hypertrophy, apoptosis and autophagy (Capote *et al.*, 2015). Such responses initially induce cardiac remodeling that involves a complex series of structural, functional, transcriptional, electrophysiological, and signaling events leading to change in shape and volume of the heart. Although remodeling is an adaptive process, it often leads to maladaptation, causing heart failure (Hill & Olson, 2008; Burchfield *et al.*, 2013).

Oxidative stress, the pathological imbalance towards excess generation of ROS relative to the antioxidant defense system of the cell, is one of the most evidenced marker of many of the cardiovascular dysfunctions (Elahi *et al.*, 2009; Sawyer, 2011; Ho *et al.*, 2013; Münzel *et al.*, 2015). Different patho-physiological stimuli generate different combinations of ROS leading to different biological effects. Controlled generation of ROS is crucial for physiological processes thus maintaining the cellular homeostatsis (Santos *et al.*, 2011; Madamanchi & Runge, 2013). Excessive generation of ROS causes nonspecific damage to cellular protein, membranes and DNA, thereby disturb a wide range of cellular events. A number of studies have suggested the importance of the source(s) and spatiotemporal distribution of ROS in determining the pathobiological outcomes. However, their mechanisms of actions is largely unknown (Chen & Zweier, 2014). Earlier we have demonstrated that in H9c2 cardiac myoblasts, hypertrophic and apoptotic responses elicited by NE are initiated by generation of distinct but comparable repertoire of ROS at the onset, followed by respective gene expression programs (Gupta *et al.*, 2006; Jindal & Goswami, 2011; Thakur *et al.*, 2015). Major intracellular sources of ROS in cardiac cells include mitochondrial ETC, NOX (1/2 and 4), NOS and xanthine oxidase (Burgoyne *et al.*, 2012). Recently Noxes have come forth as crucial source of ROS in cardiovascular pathophysiology (Brandes *et al.*, 2010; Sirokmány *et al.*, 2016). Despite recent advances on the role of specific Nox isoforms; their involvement in mediating distinct downstream responses are poorly understood as yet.

In this study, we treated H9c2 cardiac myoblasts with norepinephrine (NE, 2µM), inducing generation of ROS in general (DCFH-DA positive) and superoxide (DHE positive) in particular that was inhibited by Nox2 specific peptide inhibitor gp91ds-tat. Live cell imaging using organelle specific H_2O_2 sensitive genetically encoded fluoroprobe HyPer showed that the site of ROS generation is primarily in the cytosol, to some extent the ER

but not the mitochondria. Transcript analysis of marker genes of cardiac hypertrophy viz., ANP, β-MHC and α-MHC have revealed that the increase in the level of ANP and β-MHC and decrease in α-MHC level by NE treatment was prevented by specific inhibition of Nox2 by gp91ds-tat. Immunostaining have also established that the induction of ANP and β-MHC at the protein level were attenuated by the inhibition of Nox2. Induction of c-Jun and FosB, the two members of the transcription factor family AP-1, were also blocked by the inhibition of Nox2 by gp91ds-tat. Although, there was decrease in the phospho-c-Jun level with NE treatment, Nox2 inhibition restored it near to baseline suggesting Nox2 mediated modulation. Induction of promoter reporter constructs harboring multiple AP-1 elements and the upstream of FosB and ANP genes by NE were also blocked by the inhibition of Nox2 by gp91ds-tat. Similar results were also obtained by using a dominant negative mutant of p22phox, a constituent of Nox2 to prevent its activation.

Thus, this study for the first time establishes the significant role of Nox2 in mediating the NE induced pathological adrenergic signaling in cardiac myoblasts.

Although, the implication of oxidative stress in the pathogenesis of cardiovascular diseases is known for decades, the antioxidant therapies targeting oxidative stress in the progression of those diseases have largely been unsuccessful (Sawyer, 2011). The current study also evaluated the effects of a NADPH oxidase inhibitor, apocynin (Apo) on the production of reactive oxygen species and the development of pathological cardiac hypertrophy under sustained β-adrenergic stimulation in male Wister rats. As evident from the HW/BW ratio, HW/Tl ratio and echocardiography, hypertrophic responses induced by isoproterenol (Iso; 5 mg/Kg body weight, subcutaneous), were blocked by Apo (10 mg/Kg body weight, intraperitoneal). Increase in mRNA levels of a number of markers of hypertrophy viz., ANP, BNP, β-MHC and ACTA-1 by Iso were also partially or completely prevented by Apo. Iso stimulated activation of key signaling kinases such as PKA, Erk and Akt, was also prevented by Apo treatment. Proteomic analysis revealed that pretreatment of Apo restored a subset of proteins up- and down- regulated in the Iso induced hypertrophied hearts.

Our study thus provide hemodynamic and molecular evidence supporting the therapeutic value of Apo in ameliorating adrenergic stress induced cardiac hypertrophy.

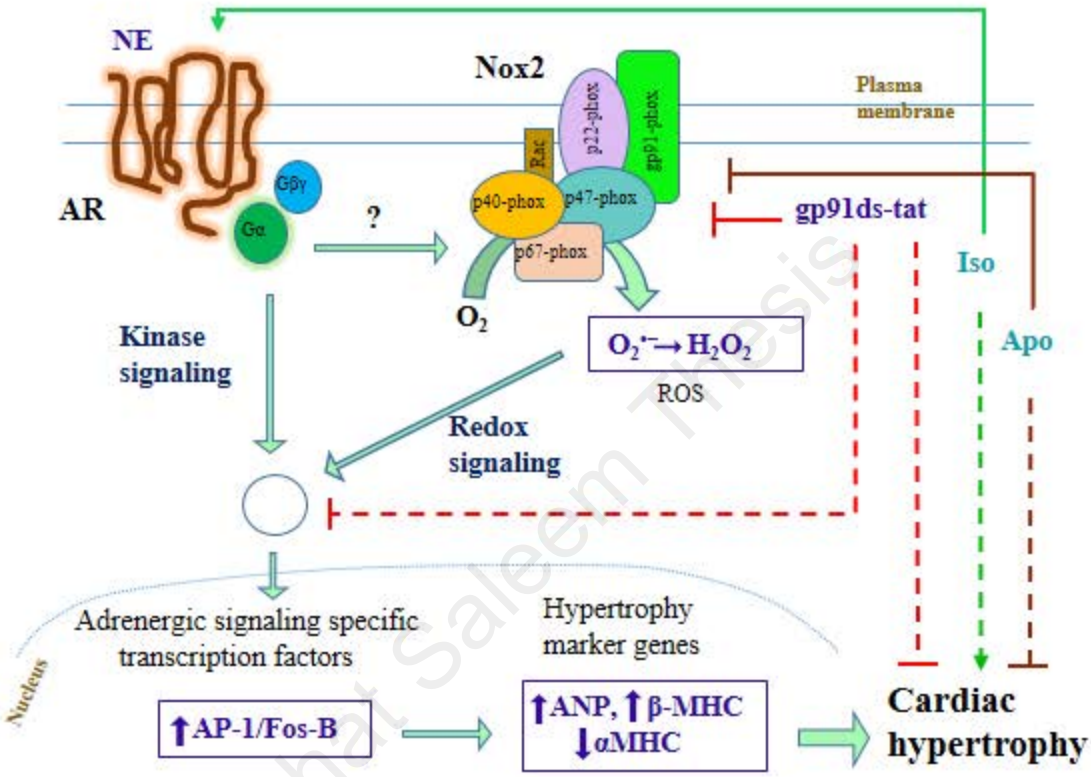

Schematic representation of the observation of this study: Adrenergic receptor stimulation with NE (2 μM) induces ROS generation by Nox2 resulting in cardiac hypertrophy by modulating adrenergic signaling specific transcription factors and downstream target genes. gp91ds-tat (5 μM) blocks the activation of Nox2 which result in attenuation of downstream events. Isoproterenol (β-AR agonist) induces cardiac hypertrophy and apocynin prevent the hypertrophy by inhibiting Nox activity.

Continuous arrow/blunt headed lines mean direct targets while dotted arrow/blunt headed lines mean downstream indirect targets. AR, adrenergic receptor; NE, norepinephrine; Iso, isoproterenol; Apo, apocynin

References

Abate, C., Patel, L., Rauscher, F.J., and Curran, T. (1990) Redox regulation of fos and jun DNA-binding activity in vitro. *Science* **249**: 1157–1161.

Adachi, T., Pimentel, D.R., Heibeck, T., Hou, X., Lee, Y.J., Jiang, B., *et al.* (2004) S-glutathiolation of Ras mediates redox-sensitive signaling by angiotensin II in vascular smooth muscle cells. *J Biol Chem* **279**: 29857–29862.

Adachi, T., Weisbrod, R.M., Pimentel, D.R., Ying, J., Sharov, V.S., Schöneich, C., and Cohen, R.A. (2004) S-Glutathiolation by peroxynitrite activates SERCA during arterial relaxation by nitric oxide. *Nat Med* **10**: 1200–1207.

Ago, T., Kuribayashi, F., Hiroaki, H., Takeya, R., Ito, T., Kohda, D., and Sumimoto, H. (2003) Phosphorylation of p47phox directs phox homology domain from SH3 domain toward phosphoinositides, leading to phagocyte NADPH oxidase activation. *Proc Natl Acad Sci U S A* **100**: 4474–4479.

Ago, T., Kuroda, J., Pain, J., Fu, C., Li, H., and Sadoshima, J. (2010) Upregulation of Nox4 by hypertrophic stimuli promotes apoptosis and mitochondrial dysfunction in cardiac myocytes. *Circ Res* **106**: 1253–1264.

Aguirre, J., and Lambeth, J.D. (2010) Nox enzymes from fungus to fly to fish and what they tell us about Nox function in mammals. *Free Radic Biol Med* **49**: 1342–1353.

Ai, X., Curran, J.W., Shannon, T.R., Bers, D.M., and Pogwizd, S.M. (2005) Ca2+/calmodulin-dependent protein kinase modulates cardiac ryanodine receptor phosphorylation and sarcoplasmic reticulum Ca2+ leak in heart failure. *Circ Res* **97**: 1314–1322.

Alkaitis, M.S., and Crabtree, M.J. (2012) Recoupling the cardiac nitric oxide synthases: tetrahydrobiopterin synthesis and recycling. *Curr Heart Fail Rep* **9**: 200–210.

Altenhöfer, S., Radermacher, K.A., Kleikers, P.W.M., Wingler, K., and Schmidt, H.H.H.W. (2015) Evolution of NADPH Oxidase Inhibitors: Selectivity and Mechanisms for Target Engagement. *Antioxid Redox Signal* **23**: 406–427.

Amirahmadi, F., Turnbull, L., Du, X.-J., Graham, R.M., and Woodcock, E.A. (2008) Heightened alpha1A-adrenergic receptor activity suppresses ischaemia/reperfusion-induced Ins(1,4,5)P3 generation in the mouse heart: a comparison with ischaemic preconditioning. *Clin Sci Lond Engl 1979* **114**: 157–164.

Aon, M.A., Cortassa, S., and O'Rourke, B. (2010) Redox-optimized ROS balance: a unifying hypothesis. *Biochim Biophys Acta* **1797**: 865–877.

Arad, M., Seidman, C.E., and Seidman, J.G. (2007) AMP-activated protein kinase in the heart: role during health and disease. *Circ Res* **100**: 474–488.

Asrih, M., Mach, F., Nencioni, A., Dallegri, F., Quercioli, A., and Montecucco, F. (2013) Role of mitogen-activated protein kinase pathways in multifactorial adverse cardiac remodeling associated with metabolic syndrome. *Mediators Inflamm* **2013**: 367245.

Auman, J.T., Seidler, F.J., Tate, C.A., and Slotkin, T.A. (2002) Are developing beta-adrenoceptors able to desensitize? Acute and chronic effects of beta-agonists in neonatal heart and liver. *Am J Physiol Regul Integr Comp Physiol* **283**: R205-217.

Bache, R.J., and Chen, Y. (2014) NOX2-induced myocardial fibrosis and diastolic dysfunction: role of the endothelium. *J Am Coll Cardiol* **63**: 2742–2744.

Backs, J., Song, K., Bezprozvannaya, S., Chang, S., and Olson, E.N. (2006) CaM kinase II selectively signals to histone deacetylase 4 during cardiomyocyte hypertrophy. *J Clin Invest* **116**: 1853–1864.

Baker, A.J. (2014) Adrenergic signaling in heart failure: a balance of toxic and protective effects. *Pflugers Arch* **466**: 1139–1150.

Balligand, J.-L. (2016) Cardiac salvage by tweaking with beta-3-adrenergic receptors. *Cardiovasc Res* **111**: 128–133.

Banerjee, A., Locke-Winter, C., Rogers, K.B., Mitchell, M.B., Brew, E.C., Cairns, C.B., *et al.* (1993) Preconditioning against myocardial dysfunction after ischemia and reperfusion by an alpha 1-adrenergic mechanism. *Circ Res* **73**: 656–670.

Banerjee, P., and Bandyopadhyay, A. (2014) Cytosolic dynamics of annexin A6 trigger feedback regulation of hypertrophy via atrial natriuretic peptide in cardiomyocytes. *J Biol Chem* **289**: 5371–5385.

Bánfi, B., Clark, R.A., Steger, K., and Krause, K.-H. (2003) Two novel proteins activate superoxide generation by the NADPH oxidase NOX1. *J Biol Chem* **278**: 3510–3513.

Barak, L.S., Warabi, K., Feng, X., Caron, M.G., and Kwatra, M.M. (1999) Real-time visualization of the cellular redistribution of G protein-coupled receptor kinase 2 and beta-arrestin 2 during homologous desensitization of the substance P receptor. *J Biol Chem* **274**: 7565–7569.

Barcellos-Hoff, M.H., and Dix, T.A. (1996) Redox-mediated activation of latent transforming growth factor-beta 1. *Mol Endocrinol Baltim Md* **10**: 1077–1083.

Bar-Sagi, D., and Hall, A. (2000) Ras and Rho GTPases: a family reunion. *Cell* **103**: 227–238.

Bartelds, B., Knoester, H., Smid, G.B., Takens, J., Visser, G.H., Penninga, L., *et al.* (2000) Perinatal changes in myocardial metabolism in lambs. *Circulation* **102**: 926–931.

Basuroy, S., Bhattacharya, S., Leffler, C.W., and Parfenova, H. (2009) Nox4 NADPH oxidase mediates oxidative stress and apoptosis caused by TNF-alpha in cerebral vascular endothelial cells. *Am J Physiol Cell Physiol* **296**: C422-432.

Bayer, A.L., Heidkamp, M.C., Patel, N., Porter, M., Engman, S., and Samarel, A.M. (2003) Alterations in protein kinase C isoenzyme expression and autophosphorylation during the progression of pressure overload-induced left ventricular hypertrophy. *Mol Cell Biochem* **242**: 145–152.

Bedard, K., and Krause, K.-H. (2007) The NOX family of ROS-generating NADPH oxidases: physiology and pathophysiology. *Physiol Rev* **87**: 245–313.

Belch, J.J., Bridges, A.B., Scott, N., and Chopra, M. (1991) Oxygen free radicals and congestive heart failure. *Br Heart J* **65**: 245–248.

Bell, R.M., Cave, A.C., Johar, S., Hearse, D.J., Shah, A.M., and Shattock, M.J. (2005) Pivotal role of NOX-2-containing NADPH oxidase in early ischemic preconditioning. *FASEB J Off Publ Fed Am Soc Exp Biol* **19**: 2037–2039.

Belousov, V.V., Fradkov, A.F., Lukyanov, K.A., Staroverov, D.B., Shakhbazov, K.S., Terskikh, A.V., and Lukyanov, S. (2006) Genetically encoded fluorescent indicator for intracellular hydrogen peroxide. *Nat Methods* **3**: 281–286.

Bendall, J.K., Cave, A.C., Heymes, C., Gall, N., and Shah, A.M. (2002) Pivotal role of a gp91(phox)-containing NADPH oxidase in angiotensin II-induced cardiac hypertrophy in mice. *Circulation* **105**: 293–296.

Berry: Models of cardiac hypertrophy and transition... - Google Scholar https://scholar.google.com/scholar_lookup?title=Models+of+cardiac+hypertrophy+and+transition+to+heart+failure.&year=2007&author=Berry&journal=Drug+Discovery+Today%3A+Disease+Models.&volume=4&issue=4&pages=197-206&doi=10.1016%2Fj.ddmod.2007.06.003. Accessed January 16, 2017.

Biberstine-Kinkade, K.J., DeLeo, F.R., Epstein, R.I., LeRoy, B.A., Nauseef, W.M., and Dinauer, M.C. (2001) Heme-ligating histidines in flavocytochrome b(558): identification of specific histidines in gp91(phox). *J Biol Chem* **276**: 31105–31112.

Block, K., Eid, A., Griendling, K.K., Lee, D.-Y., Wittrant, Y., and Gorin, Y. (2008) Nox4 NAD(P)H oxidase mediates Src-dependent tyrosine phosphorylation of PDK-1 in response to angiotensin II: role in mesangial cell hypertrophy and fibronectin expression. *J Biol Chem* **283**: 24061–24076.

Bodiga, S., Zhong, J.C., Wang, W., Basu, R., Lo, J., Liu, G.C., *et al.* (2011) Enhanced susceptibility to biomechanical stress in ACE2 null mice is prevented by loss of the p47(phox) NADPH oxidase subunit. *Cardiovasc Res* **91**: 151–161.

Boivin, B., Yang, M., and Tonks, N.K. (2010) Targeting the reversibly oxidized protein tyrosine phosphatase superfamily. *Sci Signal* **3**: pl2.

Borges, F., Fernandes, E., and Roleira, F. (2002) Progress towards the discovery of xanthine oxidase inhibitors. *Curr Med Chem* **9**: 195–217.

Bossuyt, J., Helmstadter, K., Wu, X., Clements-Jewery, H., Haworth, R.S., Avkiran, M., *et al.* (2008) Ca2+/calmodulin-dependent protein kinase IIdelta and protein kinase D overexpression reinforce the histone deacetylase 5 redistribution in heart failure. *Circ Res* **102**: 695–702.

Boularan, C., and Kehrl, J.H. (2014) Implications of non-canonical G-protein signaling for the immune system. *Cell Signal* **26**: 1269–1282.

Bradford, M.M. (1976) A rapid and sensitive method for the quantitation of microgram quantities of protein utilizing the principle of protein-dye binding. *Anal Biochem* **72**: 248–254.

Brand, M.D. (2010) The sites and topology of mitochondrial superoxide production. *Exp Gerontol* **45**: 466–472.

Brandes, R.P., Viedt, C., Nguyen, K., Beer, S., Kreuzer, J., Busse, R., and Görlach, A. (2001) Thrombin-induced MCP-1 expression involves activation of the p22phox-containing NADPH oxidase in human vascular smooth muscle cells. *Thromb Haemost* **85**: 1104–1110.

Brandes, R.P., Weissmann, N., and Schröder, K. (2010) NADPH oxidases in cardiovascular disease. *Free Radic Biol Med* **49**: 687–706.

Brandes, R.P., Weissmann, N., and Schröder, K. (2014a) Redox-mediated signal transduction by cardiovascular Nox NADPH oxidases. *J Mol Cell Cardiol* **73**: 70–79.

Brandes, R.P., Weissmann, N., and Schröder, K. (2014b) Nox family NADPH oxidases: Molecular mechanisms of activation. *Free Radic Biol Med* **76**: 208–226.

Braun, M.U., LaRosée, P., Simonis, G., Borst, M.M., and Strasser, R.H. (2004) Regulation of protein kinase C isozymes in volume overload cardiac hypertrophy. *Mol Cell Biochem* **262**: 135–143.

Braz, J.C., Bueno, O.F., De Windt, L.J., and Molkentin, J.D. (2002) PKC alpha regulates the hypertrophic growth of cardiomyocytes through extracellular signal-regulated kinase1/2 (ERK1/2). *J Cell Biol* **156**: 905–919.

Brennan, J.P., Bardswell, S.C., Burgoyne, J.R., Fuller, W., Schröder, E., Wait, R., *et al.* (2006) Oxidant-induced activation of type I protein kinase A is mediated by RI subunit interprotein disulfide bond formation. *J Biol Chem* **281**: 21827–21836.

Bristow, M.R., Ginsburg, R., Umans, V., Fowler, M., Minobe, W., Rasmussen, R., *et al.* (1986) Beta 1- and beta 2-adrenergic-receptor subpopulations in nonfailing and failing human ventricular myocardium: coupling of both receptor subtypes to muscle contraction and selective beta 1-receptor down-regulation in heart failure. *Circ Res* **59**: 297–309.

Brodde, O.E., and Michel, M.C. (1999) Adrenergic and muscarinic receptors in the human heart. *Pharmacol Rev* **51**: 651–690.

Brown, D.I., and Griendling, K.K. (2015) Regulation of signal transduction by reactive oxygen species in the cardiovascular system. *Circ Res* **116**: 531–549.

Buetler, T.M., Krauskopf, A., and Ruegg, U.T. (2004) Role of superoxide as a signaling molecule. *News Physiol Sci Int J Physiol Prod Jointly Int Union Physiol Sci Am Physiol Soc* **19**: 120–123.

Burch, P.M., Yuan, Z., Loonen, A., and Heintz, N.H. (2004) An extracellular signal-regulated kinase 1- and 2-dependent program of chromatin trafficking of c-Fos and Fra-1 is required for cyclin D1 expression during cell cycle reentry. *Mol Cell Biol* **24**: 4696–4709.

Burchfield, J.S., Xie, M., and Hill, J.A. (2013) Pathological ventricular remodeling: mechanisms: part 1 of 2. *Circulation* **128**: 388–400.

Burgoyne, J.R., and Eaton, P. (2009) Transnitrosylating nitric oxide species directly activate type I protein kinase A, providing a novel adenylate cyclase-independent cross-talk to beta-adrenergic-like signaling. *J Biol Chem* **284**: 29260–29268.

Burgoyne, J.R., Madhani, M., Cuello, F., Charles, R.L., Brennan, J.P., Schröder, E., *et al.* (2007) Cysteine redox sensor in PKGIa enables oxidant-induced activation. *Science* **317**: 1393–1397.

Burgoyne, J.R., Mongue-Din, H., Eaton, P., and Shah, A.M. (2012) Redox signaling in cardiac physiology and pathology. *Circ Res* **111**: 1091–1106.

Burgoyne, J.R., Rudyk, O., Cho, H., Prysyazhna, O., Hathaway, N., Weeks, A., *et al.* (2015) Deficient angiogenesis in redox-dead Cys17Ser PKARIα knock-in mice. *Nat Commun* **6**: 7920.

Bylund, D.B., Eikenberg, D.C., Hieble, J.P., Langer, S.Z., Lefkowitz, R.J., Minneman, K.P., *et al.* (1994) International Union of Pharmacology nomenclature of adrenoceptors. *Pharmacol Rev* **46**: 121–136.

Byon, C.H., Heath, J.M., and Chen, Y. (2016) Redox signaling in cardiovascular pathophysiology: A focus on hydrogen peroxide and vascular smooth muscle cells. *Redox Biol* **9**: 244–253.

Cai, H., Griendling, K.K., and Harrison, D.G. (2003) The vascular NAD(P)H oxidases as therapeutic targets in cardiovascular diseases. *Trends Pharmacol Sci* **24**: 471–478.

Cantor, E.J.F., Babick, A.P., Vasanji, Z., Dhalla, N.S., and Netticadan, T. (2005) A comparative serial echocardiographic analysis of cardiac structure and function in rats subjected to pressure or volume overload. *J Mol Cell Cardiol* **38**: 777–786.

Capote, L.A., Mendez Perez, R., and Lymperopoulos, A. (2015) GPCR signaling and cardiac function. *Eur J Pharmacol* **763**: 143–148.

Cappola, T.P., Kass, D.A., Nelson, G.S., Berger, R.D., Rosas, G.O., Kobeissi, Z.A., *et al.* (2001) Allopurinol improves myocardial efficiency in patients with idiopathic dilated cardiomyopathy. *Circulation* **104**: 2407–2411.

Cave, A.C., Brewer, A.C., Narayanapanicker, A., Ray, R., Grieve, D.J., Walker, S., and Shah, A.M. (2006) NADPH oxidases in cardiovascular health and disease. *Antioxid Redox Signal* **8**: 691–728.

Chabot, C., Spring, K., Gratton, J.-P., Elchebly, M., and Royal, I. (2009) New role for the protein tyrosine phosphatase DEP-1 in Akt activation and endothelial cell survival. *Mol Cell Biol* **29**: 241–253.

Chen, F., Pandey, D., Chadli, A., Catravas, J.D., Chen, T., and Fulton, D.J.R. (2011) Hsp90 regulates NADPH oxidase activity and is necessary for superoxide but not hydrogen peroxide production. *Antioxid Redox Signal* **14**: 2107–2119.

Chen, K., Craige, S.E., and Keaney, J.F. (2009) Downstream targets and intracellular compartmentalization in Nox signaling. *Antioxid Redox Signal* **11**: 2467–2480.

Chen, K., Kirber, M.T., Xiao, H., Yang, Y., and Keaney, J.F. (2008) Regulation of ROS signal transduction by NADPH oxidase 4 localization. *J Cell Biol* **181**: 1129–1139.

Chen, W., and Frangogiannis, N.G. (2010) The role of inflammatory and fibrogenic pathways in heart failure associated with aging. *Heart Fail Rev* **15**: 415–422.

Chen, X., Zeng, S., Zou, J., Chen, Y., Yue, Z., Gao, Y., *et al.* (2014) Rapamycin attenuated cardiac hypertrophy induced by isoproterenol and maintained energy homeostasis via inhibiting NF-κB activation. *Mediators Inflamm* **2014**: 868753.

Chen, Y.-R., and Zweier, J.L. (2014) Cardiac mitochondria and reactive oxygen species generation. *Circ Res* **114**: 524–537.

Chignalia, A.Z., Schuldt, E.Z., Camargo, L.L., Montezano, A.C., Callera, G.E., Laurindo, F.R., *et al.* (2012) Testosterone induces vascular smooth muscle cell migration by NADPH oxidase and c-Src-dependent pathways. *Hypertens Dallas Tex 1979* **59**: 1263–1271.

Choi, M.H., Lee, I.K., Kim, G.W., Kim, B.U., Han, Y.-H., Yu, D.-Y., *et al.* (2005) Regulation of PDGF signalling and vascular remodelling by peroxiredoxin II. *Nature* **435**: 347–353.

Chruscinski, A.J., Rohrer, D.K., Schauble, E., Desai, K.H., Bernstein, D., and Kobilka, B.K. (1999) Targeted disruption of the beta2 adrenergic receptor gene. *J Biol Chem* **274**: 16694–16700.

Ciccarelli, M., Santulli, G., Pascale, V., Trimarco, B., and Iaccarino, G. (2013) Adrenergic receptors and metabolism: role in development of cardiovascular disease. *Front Physiol* **4**: 265.

Cipak Gasparovic, A., Zarkovic, N., Zarkovic, K., Semen, K., Kaminskyy, D., Yelisyeyeva, O., and Bottari, S.P. (2017) Biomarkers of oxidative and nitro-oxidative stress: conventional and novel approaches. *Br J Pharmacol* **174**: 1771–1783.

Claing, A., Laporte, S.A., Caron, M.G., and Lefkowitz, R.J. (2002) Endocytosis of G protein-coupled receptors: roles of G protein-coupled receptor kinases and beta-arrestin proteins. *Prog Neurobiol* **66**: 61–79.

Clempus, R.E., Sorescu, D., Dikalova, A.E., Pounkova, L., Jo, P., Sorescu, G.P., *et al.* (2007) Nox4 is required for maintenance of the differentiated vascular smooth muscle cell phenotype. *Arterioscler Thromb Vasc Biol* **27**: 42–48.

Clerk, A. (2003) The radical balance between life and death. *J Mol Cell Cardiol* **35**: 599–602.

Corcoran, A., and Cotter, T.G. (2013) Redox regulation of protein kinases. *FEBS J* **280**: 1944–1965.

Craige, S.M., Chen, K., Pei, Y., Li, C., Huang, X., Chen, C., *et al.* (2011) NADPH oxidase 4 promotes endothelial angiogenesis through endothelial nitric oxide synthase activation. *Circulation* **124**: 731–740.

Cucoranu, I., Clempus, R., Dikalova, A., Phelan, P.J., Ariyan, S., Dikalov, S., and Sorescu, D. (2005) NAD(P)H oxidase 4 mediates transforming growth factor-beta1-induced differentiation of cardiac fibroblasts into myofibroblasts. *Circ Res* **97**: 900–907.

Dai, D.-F., Johnson, S.C., Villarin, J.J., Chin, M.T., Nieves-Cintrón, M., Chen, T., *et al.* (2011) Mitochondrial oxidative stress mediates angiotensin II-induced cardiac hypertrophy and Galphaq overexpression-induced heart failure. *Circ Res* **108**: 837–846.

Derochette, S., Serteyn, D., Mouithys-Mickalad, A., Ceusters, J., Deby-Dupont, G., Neven, P., and Franck, T. (2015) EquiNox2: A new method to measure NADPH oxidase activity and to study effect of inhibitors and their interactions with the enzyme. *Talanta* **144**: 1252–1259.

Dey, S., Sidor, A., and O'Rourke, B. (2016) Compartment-specific Control of Reactive Oxygen Species Scavenging by Antioxidant Pathway Enzymes. *J Biol Chem* **291**: 11185–11197.

Dhalla, N.S., and Müller, A.L. (2010) Protein Kinases as Drug Development Targets for Heart Disease Therapy. *Pharm Basel Switz* **3**: 2111–2145.

Dhingra, R., Shaw, J.A., Aviv, Y., and Kirshenbaum, L.A. (2010) Dichotomous actions of NF-kappaB signaling pathways in heart. *J Cardiovasc Transl Res* **3**: 344–354.

Diatchuk, V., Lotan, O., Koshkin, V., Wikstroem, P., and Pick, E. (1997) Inhibition of NADPH oxidase activation by 4-(2-aminoethyl)-benzenesulfonyl fluoride and related compounds. *J Biol Chem* **272**: 13292–13301.

Diekmann, D., Abo, A., Johnston, C., Segal, A.W., and Hall, A. (1994) Interaction of Rac with p67phox and regulation of phagocytic NADPH oxidase activity. *Science* **265**: 531–533.

Dietrich, S., Uppalapati, R., Seiwert, T.Y., and Ma, P.C. (2005) Role of c-MET in upper aerodigestive malignancies--from biology to novel therapies. *J Environ Pathol Toxicol Oncol Off Organ Int Soc Environ Toxicol Cancer* **24**: 149–162.

Dikalov, S.I., Dikalova, A.E., Bikineyeva, A.T., Schmidt, H.H.H.W., Harrison, D.G., and Griendling, K.K. (2008) Distinct roles of Nox1 and Nox4 in basal and angiotensin II-stimulated superoxide and hydrogen peroxide production. *Free Radic Biol Med* **45**: 1340–1351.

Dikalova, A., Clempus, R., Lassègue, B., Cheng, G., McCoy, J., Dikalov, S., *et al.* (2005) Nox1 overexpression potentiates angiotensin II-induced hypertension and vascular smooth muscle hypertrophy in transgenic mice. *Circulation* **112**: 2668–2676.

Ding, W., Dong, M., Deng, J., Yan, D., Liu, Y., Xu, T., and Liu, J. (2014) Polydatin attenuates cardiac hypertrophy through modulation of cardiac Ca2+ handling and calcineurin-NFAT signaling pathway. *Am J Physiol Heart Circ Physiol* **307**: H792-802.

Dirkx, E., Costa Martins, P.A. da, and De Windt, L.J. (2013) Regulation of fetal gene expression in heart failure. *Biochim Biophys Acta* **1832**: 2414–2424.

Doerries, C., Grote, K., Hilfiker-Kleiner, D., Luchtefeld, M., Schaefer, A., Holland, S.M., *et al.* (2007) Critical role of the NAD(P)H oxidase subunit p47phox for left ventricular remodeling/dysfunction and survival after myocardial infarction. *Circ Res* **100**: 894–903.

Dorn, G.W. (2009) Apoptotic and non-apoptotic programmed cardiomyocyte death in ventricular remodelling. *Cardiovasc Res* **81**: 465–473.

Dorn, G.W., Robbins, J., and Sugden, P.H. (2003) Phenotyping hypertrophy: eschew obfuscation. *Circ Res* **92**: 1171–1175.

Dreger, H., Westphal, K., Weller, A., Baumann, G., Stangl, V., Meiners, S., and Stangl, K. (2009) Nrf2-dependent upregulation of antioxidative enzymes: a novel pathway for proteasome inhibitor-mediated cardioprotection. *Cardiovasc Res* **83**: 354–361.

Elahi, M.M., Kong, Y.X., and Matata, B.M. (2009) Oxidative stress as a mediator of cardiovascular disease. *Oxid Med Cell Longev* **2**: 259–269.

Eleuteri, E., Di Stefano, A., Ricciardolo, F.L.M., Magno, F., Gnemmi, I., Colombo, M., *et al.* (2009) Increased nitrotyrosine plasma levels in relation to systemic markers of inflammation and myeloperoxidase in chronic heart failure. *Int J Cardiol* **135**: 386–390.

Ellmark, S.H.M., Dusting, G.J., Fui, M.N.T., Guzzo-Pernell, N., and Drummond, G.R. (2005) The contribution of Nox4 to NADPH oxidase activity in mouse vascular smooth muscle. *Cardiovasc Res* **65**: 495–504.

Engelhardt, S., Hein, L., Wiesmann, F., and Lohse, M.J. (1999) Progressive hypertrophy and heart failure in beta1-adrenergic receptor transgenic mice. *Proc Natl Acad Sci U S A* **96**: 7059–7064.

Erickson, J.R. (2014) Mechanisms of CaMKII Activation in the Heart. *Front Pharmacol* **5**: 59.

Erickson, J.R., Joiner, M.A., Guan, X., Kutschke, W., Yang, J., Oddis, C.V., *et al.* (2008) A dynamic pathway for calcium-independent activation of CaMKII by methionine oxidation. *Cell* **133**: 462–474.

Esler, M., Kaye, D., Lambert, G., Esler, D., and Jennings, G. (1997) Adrenergic nervous system in heart failure. *Am J Cardiol* **80**: 7L–14L.

Fawell, S., Seery, J., Daikh, Y., Moore, C., Chen, L.L., Pepinsky, B., and Barsoum, J. (1994) Tat-mediated delivery of heterologous proteins into cells. *Proc Natl Acad Sci U S A* **91**: 664–668.

Ferguson, S.S. (2001) Evolving concepts in G protein-coupled receptor endocytosis: the role in receptor desensitization and signaling. *Pharmacol Rev* **53**: 1–24.

Fernandes, T., Soci, U.P.R., and Oliveira, E.M. (2011) Eccentric and concentric cardiac hypertrophy induced by exercise training: microRNAs and molecular determinants. *Braz J Med Biol Res Rev Bras Pesqui Medicas E Biol* **44**: 836–847.

Ferrara, N., Komici, K., Corbi, G., Pagano, G., Furgi, G., Rengo, C., *et al.* (2014) β-adrenergic receptor responsiveness in aging heart and clinical implications. *Front Physiol* **4**: 396.

Fisher, A.B. (2009) Redox signaling across cell membranes. *Antioxid Redox Signal* **11**: 1349–1356.

Florea, V.G., and Cohn, J.N. (2014) The autonomic nervous system and heart failure. *Circ Res* **114**: 1815–1826.

Forman, H.J., Ursini, F., and Maiorino, M. (2014) An overview of mechanisms of redox signaling. *J Mol Cell Cardiol* **73**: 2–9.

Freedman, N.J., Liggett, S.B., Drachman, D.E., Pei, G., Caron, M.G., and Lefkowitz, R.J. (1995) Phosphorylation and desensitization of the human beta 1-adrenergic receptor. Involvement of G protein-coupled receptor kinases and cAMP-dependent protein kinase. *J Biol Chem* **270**: 17953–17961.

Frey, N., Katus, H.A., Olson, E.N., and Hill, J.A. (2004) Hypertrophy of the heart: a new therapeutic target? *Circulation* **109**: 1580–1589.

Fu, Y.-C., Chi, C.-S., Yin, S.-C., Hwang, B., Chiu, Y.-T., and Hsu, S.-L. (2004) Norepinephrine induces apoptosis in neonatal rat cardiomyocytes through a reactive oxygen species-TNF alpha-caspase signaling pathway. *Cardiovasc Res* **62**: 558–567.

Fukui, T., Yoshiyama, M., Hanatani, A., Omura, T., Yoshikawa, J., and Abe, Y. (2001) Expression of p22-phox and gp91-phox, essential components of NADPH oxidase, increases after myocardial infarction. *Biochem Biophys Res Commun* **281**: 1200–1206.

Galés, C., Rebois, R.V., Hogue, M., Trieu, P., Breit, A., Hébert, T.E., and Bouvier, M. (2005) Real-time monitoring of receptor and G-protein interactions in living cells. *Nat Methods* **2**: 177–184.

Gianni, D., Bohl, B., Courtneidge, S.A., and Bokoch, G.M. (2008) The involvement of the tyrosine kinase c-Src in the regulation of reactive oxygen species generation mediated by NADPH oxidase-1. *Mol Biol Cell* **19**: 2984–2994.

Goodwin, G.W., Taylor, C.S., and Taegtmeyer, H. (1998) Regulation of energy metabolism of the heart during acute increase in heart work. *J Biol Chem* **273**: 29530–29539.

Gordon, J.W., Shaw, J.A., and Kirshenbaum, L.A. (2011) Multiple facets of NF-κB in the heart: to be or not to NF-κB. *Circ Res* **108**: 1122–1132.

Granger, D.N., and Kvietys, P.R. (2015) Reperfusion injury and reactive oxygen species: The evolution of a concept. *Redox Biol* **6**: 524–551.

Grassi, G., Seravalle, G., Quarti-Trevano, F., Dell'Oro, R., Arenare, F., Spaziani, D., and Mancia, G. (2009) Sympathetic and baroreflex cardiovascular control in hypertension-related left ventricular dysfunction. *Hypertens Dallas Tex 1979* **53**: 205–209.

Gray, S.P., and Jandeleit-Dahm, K.A.M. (2015) The role of NADPH oxidase in vascular disease--hypertension, atherosclerosis & stroke. *Curr Pharm Des* **21**: 5933–5944.

Grimm, M., Ling, H., Willeford, A., Pereira, L., Gray, C.B.B., Erickson, J.R., *et al.* (2015) CaMKIIδ mediates β-adrenergic effects on RyR2 phosphorylation and SR Ca(2+) leak and the pathophysiological response to chronic β-adrenergic stimulation. *J Mol Cell Cardiol* **85**: 282–291.

Grobe, A.C., Wells, S.M., Benavidez, E., Oishi, P., Azakie, A., Fineman, J.R., and Black, S.M. (2006) Increased oxidative stress in lambs with increased pulmonary blood flow and pulmonary hypertension: role of NADPH oxidase and endothelial NO synthase. *Am J Physiol Lung Cell Mol Physiol* **290**: L1069-1077.

Groitl, B., and Jakob, U. (2014) Thiol-based redox switches. *Biochim Biophys Acta* **1844**: 1335–1343.

Gu, X., and Bishop, S.P. (1994) Increased protein kinase C and isozyme redistribution in pressure-overload cardiac hypertrophy in the rat. *Circ Res* **75**: 926–931.

Gupta, M.K., Neelakantan, T.V., Sanghamitra, M., Tyagi, R.K., Dinda, A., Maulik, S., *et al.* (2006) An assessment of the role of reactive oxygen species and redox signaling in norepinephrine-induced apoptosis and hypertrophy of H9c2 cardiac myoblasts. *Antioxid Redox Signal* **8**: 1081–1093.

Hamid, T., Guo, S.Z., Kingery, J.R., Xiang, X., Dawn, B., and Prabhu, S.D. (2011) Cardiomyocyte NF-κB p65 promotes adverse remodelling, apoptosis, and endoplasmic reticulum stress in heart failure. *Cardiovasc Res* **89**: 129–138.

Handayaningsih, A.-E., Iguchi, G., Fukuoka, H., Nishizawa, H., Takahashi, M., Yamamoto, M., *et al.* (2011) Reactive oxygen species play an essential role in IGF-I signaling and IGF-I-induced myocyte hypertrophy in C2C12 myocytes. *Endocrinology* **152**: 912–921.

Hanna, I.R., Hilenski, L.L., Dikalova, A., Taniyama, Y., Dikalov, S., Lyle, A., *et al.* (2004) Functional association of nox1 with p22phox in vascular smooth muscle cells. *Free Radic Biol Med* **37**: 1542–1549.

Hart, B.A. 't, Copray, S., and Philippens, I. (2014) Apocynin, a low molecular oral treatment for neurodegenerative disease. *BioMed Res Int* **2014**: 298020.

Harzand, A., Tamariz, L., and Hare, J.M. (2012) Uric acid, heart failure survival, and the impact of xanthine oxidase inhibition. *Congest Heart Fail Greenwich Conn* **18**: 179–182.

Haworth, R.S., Stathopoulou, K., Candasamy, A.J., and Avkiran, M. (2012) Neurohormonal regulation of cardiac histone deacetylase 5 nuclear localization by phosphorylation-dependent and phosphorylation-independent mechanisms. *Circ Res* **110**: 1585–1595.

Hayden, M.S., and Ghosh, S. (2008) Shared principles in NF-kappaB signaling. *Cell* **132**: 344–362.

He, B.J., Joiner, M.-L.A., Singh, M.V., Luczak, E.D., Swaminathan, P.D., Koval, O.M., *et al.* (2011) Oxidation of CaMKII determines the cardiotoxic effects of aldosterone. *Nat Med* **17**: 1610–1618.

He, M., Siow, R.C.M., Sugden, D., Gao, L., Cheng, X., and Mann, G.E. (2011) Induction of HO-1 and redox signaling in endothelial cells by advanced glycation end products: a role for Nrf2 in vascular protection in diabetes. *Nutr Metab Cardiovasc Dis NMCD* **21**: 277–285.

Heineke, J., and Molkentin, J.D. (2006) Regulation of cardiac hypertrophy by intracellular signalling pathways. *Nat Rev Mol Cell Biol* **7**: 589–600.

Heo, J., and Campbell, S.L. (2005) Superoxide anion radical modulates the activity of Ras and Ras-related GTPases by a radical-based mechanism similar to that of nitric oxide. *J Biol Chem* **280**: 12438–12445.

Heppner, D.E., and Vliet, A. van der (2016) Redox-dependent regulation of epidermal growth factor receptor signaling. *Redox Biol* **8**: 24–27.

Heumüller, S., Wind, S., Barbosa-Sicard, E., Schmidt, H.H.H.W., Busse, R., Schröder, K., and Brandes, R.P. (2008) Apocynin is not an inhibitor of vascular NADPH oxidases but an antioxidant. *Hypertens Dallas Tex 1979* **51**: 211–217.

Higgins, P., Dawson, J., and Walters, M. (2009) The potential for xanthine oxidase inhibition in the prevention and treatment of cardiovascular and cerebrovascular disease. *Cardiovasc Psychiatry Neurol* **2009**: 282059.

Hill, J.A., and Olson, E.N. (2008) Cardiac plasticity. *N Engl J Med* **358**: 1370–1380.

Hill, M.F., and Singal, P.K. (1996) Antioxidant and oxidative stress changes during heart failure subsequent to myocardial infarction in rats. *Am J Pathol* **148**: 291–300.

Hingtgen, S.D., Tian, X., Yang, J., Dunlay, S.M., Peek, A.S., Wu, Y., *et al.* (2006) Nox2-containing NADPH oxidase and Akt activation play a key role in angiotensin II-induced cardiomyocyte hypertrophy. *Physiol Genomics* **26**: 180–191.

Hirotani, S., Otsu, K., Nishida, K., Higuchi, Y., Morita, T., Nakayama, H., *et al.* (2002) Involvement of nuclear factor-kappaB and apoptosis signal-regulating kinase 1 in G-protein-coupled receptor agonist-induced cardiomyocyte hypertrophy. *Circulation* **105**: 509–515.

Ho, E., Karimi Galougahi, K., Liu, C.-C., Bhindi, R., and Figtree, G.A. (2013) Biological markers of oxidative stress: Applications to cardiovascular research and practice. *Redox Biol* **1**: 483–491.

Hook, S.S., and Means, A.R. (2001) Ca(2+)/CaM-dependent kinases: from activation to function. *Annu Rev Pharmacol Toxicol* **41**: 471–505.

Hosoya, T., Maruyama, A., Kang, M.-I., Kawatani, Y., Shibata, T., Uchida, K., *et al.* (2005) Differential responses of the Nrf2-Keap1 system to laminar and oscillatory shear stresses in endothelial cells. *J Biol Chem* **280**: 27244–27250.

Hou, J., and Kang, Y.J. (2012) Regression of pathological cardiac hypertrophy: signaling pathways and therapeutic targets. *Pharmacol Ther* **135**: 337–354.

Hoyle, N.P., and O'Neill, J.S. (2015) Oxidation-reduction cycles of peroxiredoxin proteins and nontranscriptional aspects of timekeeping. *Biochemistry (Mosc)* **54**: 184–193.

Hudmon, A., and Schulman, H. (2002) Structure-function of the multifunctional Ca2+/calmodulin-dependent protein kinase II. *Biochem J* **364**: 593–611.

Hwang, J., Ing, M.H., Salazar, A., Lassègue, B., Griendling, K., Navab, M., *et al.* (2003) Pulsatile versus oscillatory shear stress regulates NADPH oxidase subunit expression: implication for native LDL oxidation. *Circ Res* **93**: 1225–1232.

Ide, T., Tsutsui, H., Kinugawa, S., Utsumi, H., Kang, D., Hattori, N., *et al.* (1999) Mitochondrial electron transport complex I is a potential source of oxygen free radicals in the failing myocardium. *Circ Res* **85**: 357–363.

Ismail, H.M., Scapozza, L., Ruegg, U.T., and Dorchies, O.M. (2014) Diapocynin, a dimer of the NADPH oxidase inhibitor apocynin, reduces ROS production and prevents force loss in eccentrically contracting dystrophic muscle. *PloS One* **9**: e110708.

Itoh, K., Wakabayashi, N., Katoh, Y., Ishii, T., Igarashi, K., Engel, J.D., and Yamamoto, M. (1999) Keap1 represses nuclear activation of antioxidant responsive elements by Nrf2 through binding to the amino-terminal Neh2 domain. *Genes Dev* **13**: 76–86.

Itoh, K., Wakabayashi, N., Katoh, Y., Ishii, T., O'Connor, T., and Yamamoto, M. (2003) Keap1 regulates both cytoplasmic-nuclear shuttling and degradation of Nrf2 in response to electrophiles. *Genes Cells Devoted Mol Cell Mech* **8**: 379–391.

Iwanaga, Y., Aoyama, T., Kihara, Y., Onozawa, Y., Yoneda, T., and Sasayama, S. (2002) Excessive activation of matrix metalloproteinases coincides with left ventricular remodeling during transition from hypertrophy to heart failure in hypertensive rats. *J Am Coll Cardiol* **39**: 1384–1391.

Izumiya, Y., Kim, S., Izumi, Y., Yoshida, K., Yoshiyama, M., Matsuzawa, A., *et al.* (2003) Apoptosis signal-regulating kinase 1 plays a pivotal role in angiotensin II-induced cardiac hypertrophy and remodeling. *Circ Res* **93**: 874–883.

Jang, S., Lewis, T.S., Powers, C., Khuchua, Z., Baines, C.P., Wipf, P., and Javadov, S. (2016) Elucidating Mitochondrial Electron Transport Chain Supercomplexes in the Heart During Ischemia-Reperfusion. *Antioxid Redox Signal* .

Janiszewski, M., Lopes, L.R., Carmo, A.O., Pedro, M.A., Brandes, R.P., Santos, C.X.C., and Laurindo, F.R.M. (2005) Regulation of NAD(P)H oxidase by associated protein disulfide isomerase in vascular smooth muscle cells. *J Biol Chem* **280**: 40813–40819.

Jiang, S., Streeter, J., Schickling, B.M., Zimmerman, K., Weiss, R.M., and Miller, F.J. (2014) Nox1 NADPH oxidase is necessary for late but not early myocardial ischaemic preconditioning. *Cardiovasc Res* **102**: 79–87.

Jindal, E., and Goswami, S.K. (2011) In cardiac myoblasts, cellular redox regulates FosB and Fra-1 through multiple cis-regulatory modules. *Free Radic Biol Med* **51**: 1512–1521.

Johnson, G.L., and Lapadat, R. (2002) Mitogen-activated protein kinase pathways mediated by ERK, JNK, and p38 protein kinases. *Science* **298**: 1911–1912.

Johnston, A.S., Lehnart, S.E., and Burgoyne, J.R. (2015) Ca(2+) signaling in the myocardium by (redox) regulation of PKA/CaMKII. *Front Pharmacol* **6**: 166.

Jones, P.P., Meng, X., Xiao, B., Cai, S., Bolstad, J., Wagenknecht, T., *et al.* (2008) Localization of PKA phosphorylation site, Ser(2030), in the three-dimensional structure of cardiac ryanodine receptor. *Biochem J* **410**: 261–270.

Kaludercic, N., Mialet-Perez, J., Paolocci, N., Parini, A., and Di Lisa, F. (2014) Monoamine oxidases as sources of oxidants in the heart. *J Mol Cell Cardiol* **73**: 34–42.

Kaludercic, N., Takimoto, E., Nagayama, T., Feng, N., Lai, E.W., Bedja, D., *et al.* (2010) Monoamine oxidase A-mediated enhanced catabolism of norepinephrine contributes to adverse remodeling and pump failure in hearts with pressure overload. *Circ Res* **106**: 193–202.

Kass, D.A., Champion, H.C., and Beavo, J.A. (2007) Phosphodiesterase type 5: expanding roles in cardiovascular regulation. *Circ Res* **101**: 1084–1095.

Kawahara, T., Ritsick, D., Cheng, G., and Lambeth, J.D. (2005) Point mutations in the proline-rich region of p22phox are dominant inhibitors of Nox1- and Nox2-dependent reactive oxygen generation. *J Biol Chem* **280**: 31859–31869.

Kelly, E., Bailey, C.P., and Henderson, G. (2008) Agonist-selective mechanisms of GPCR desensitization. *Br J Pharmacol* **153 Suppl 1**: S379-388.

Kimura, K., Kanazawa, H., Ieda, M., Kawaguchi-Manabe, H., Miyake, Y., Yagi, T., *et al.* (2010) Norepinephrine-induced nerve growth factor depletion causes cardiac sympathetic denervation in severe heart failure. *Auton Neurosci Basic Clin* **156**: 27–35.

Knowlton, K.U., Baracchini, E., Ross, R.S., Harris, A.N., Henderson, S.A., Evans, S.M., *et al.* (1991) Co-regulation of the atrial natriuretic factor and cardiac myosin light chain-2 genes during alpha-adrenergic stimulation of neonatal rat ventricular cells. Identification of cis sequences within an embryonic and a constitutive contractile protein gene which mediate inducible expression. *J Biol Chem* **266**: 7759–7768.

Kovacic, P., Pozos, R.S., Somanathan, R., Shangari, N., and O'Brien, P.J. (2005) Mechanism of mitochondrial uncouplers, inhibitors, and toxins: focus on electron transfer, free radicals, and structure-activity relationships. *Curr Med Chem* **12**: 2601–2623.

Krijnen, P. a. J., Meischl, C., Hack, C.E., Meijer, C.J.L.M., Visser, C.A., Roos, D., and Niessen, H.W.M. (2003) Increased Nox2 expression in human cardiomyocytes after acute myocardial infarction. *J Clin Pathol* **56**: 194–199.

Kruger, N.J. (1994) The Bradford method for protein quantitation. *Methods Mol Biol Clifton NJ* **32**: 9–15.

Kumar, S., Jahangir Alam, M., Prabhakar, P., Ahmad, S., Maulik, S.K., Sharma, M., and Goswami, S.K. (2017) Proteomic analysis of the protective effects of aqueous bark extract

of Terminalia arjuna (Roxb.) on isoproterenol-induced cardiac hypertrophy in rats. *J Ethnopharmacol* **198**: 98–108.

Kuroda, J., Ago, T., Matsushima, S., Zhai, P., Schneider, M.D., and Sadoshima, J. (2010) NADPH oxidase 4 (Nox4) is a major source of oxidative stress in the failing heart. *Proc Natl Acad Sci U S A* **107**: 15565–15570.

Kwon, J., Lee, S.-R., Yang, K.-S., Ahn, Y., Kim, Y.J., Stadtman, E.R., and Rhee, S.G. (2004) Reversible oxidation and inactivation of the tumor suppressor PTEN in cells stimulated with peptide growth factors. *Proc Natl Acad Sci U S A* **101**: 16419–16424.

Lancel, S., Qin, F., Lennon, S.L., Zhang, J., Tong, X., Mazzini, M.J., *et al.* (2010) Oxidative posttranslational modifications mediate decreased SERCA activity and myocyte dysfunction in Galphaq-overexpressing mice. *Circ Res* **107**: 228–232.

Lancel, S., Zhang, J., Evangelista, A., Trucillo, M.P., Tong, X., Siwik, D.A., *et al.* (2009) Nitroxyl activates SERCA in cardiac myocytes via glutathiolation of cysteine 674. *Circ Res* **104**: 720–723.

Lanzafame, A.A., Turnbull, L., Amiramahdi, F., Arthur, J.F., Huynh, H., and Woodcock, E.A. (2006) Inositol phospholipids localized to caveolae in rat heart are regulated by alpha1-adrenergic receptors and by ischemia-reperfusion. *Am J Physiol Heart Circ Physiol* **290**: H2059-2065.

Lassègue, B., and Clempus, R.E. (2003) Vascular NAD(P)H oxidases: specific features, expression, and regulation. *Am J Physiol Regul Integr Comp Physiol* **285**: R277-297.

Lassègue, B., San Martín, A., and Griendling, K.K. (2012) Biochemistry, physiology, and pathophysiology of NADPH oxidases in the cardiovascular system. *Circ Res* **110**: 1364–1390.

Latimer, H.R., and Veal, E.A. (2016) Peroxiredoxins in Regulation of MAPK Signalling Pathways; Sensors and Barriers to Signal Transduction. *Mol Cells* **39**: 40–45.

Lee, J.-G., Baek, K., Soetandyo, N., and Ye, Y. (2013) Reversible inactivation of deubiquitinases by reactive oxygen species in vitro and in cells. *Nat Commun* **4**: 1568.

Lee, Y.-M., Kim, B.-J., Chun, Y.-S., So, I., Choi, H., Kim, M.-S., and Park, J.-W. (2006) NOX4 as an oxygen sensor to regulate TASK-1 activity. *Cell Signal* **18**: 499–507.

Leenen, F.H., White, R., and Yuan, B. (2001) Isoproterenol-induced cardiac hypertrophy: role of circulatory versus cardiac renin-angiotensin system. *Am J Physiol Heart Circ Physiol* **281**: H2410-2416.

Lefkowitz, R.J. (2000) The superfamily of heptahelical receptors. *Nat Cell Biol* **2**: E133-136.

Leineweber, K., Wangemann, T., Giessler, C., Bruck, H., Dhein, S., Kostelka, M., *et al.* (2002) Age-dependent changes of cardiac neuronal noradrenaline reuptake transporter (uptake1) in the human heart. *J Am Coll Cardiol* **40**: 1459.

Levonen, A.-L., Inkala, M., Heikura, T., Jauhiainen, S., Jyrkkänen, H.-K., Kansanen, E., *et al.* (2007) Nrf2 gene transfer induces antioxidant enzymes and suppresses smooth muscle cell growth in vitro and reduces oxidative stress in rabbit aorta in vivo. *Arterioscler Thromb Vasc Biol* **27**: 741–747.

Li, J., Bigelow, D.J., and Squier, T.C. (2004) Conformational changes within the cytosolic portion of phospholamban upon release of Ca-ATPase inhibition. *Biochemistry (Mosc)* **43**: 3870–3879.

Li, J.-M., Gall, N.P., Grieve, D.J., Chen, M., and Shah, A.M. (2002) Activation of NADPH oxidase during progression of cardiac hypertrophy to failure. *Hypertens Dallas Tex 1979* **40**: 477–484.

Li, Y.Y., McTiernan, C.F., and Feldman, A.M. (2000) Interplay of matrix metalloproteinases, tissue inhibitors of metalloproteinases and their regulators in cardiac matrix remodeling. *Cardiovasc Res* **46**: 214–224.

Liang, Q., De Windt, L.J., Witt, S.A., Kimball, T.R., Markham, B.E., and Molkentin, J.D. (2001) The transcription factors GATA4 and GATA6 regulate cardiomyocyte hypertrophy in vitro and in vivo. *J Biol Chem* **276**: 30245–30253.

Liang, Q., Wiese, R.J., Bueno, O.F., Dai, Y.S., Markham, B.E., and Molkentin, J.D. (2001) The transcription factor GATA4 is activated by extracellular signal-regulated kinase 1- and 2-mediated phosphorylation of serine 105 in cardiomyocytes. *Mol Cell Biol* **21**: 7460–7469.

Liu, H., Nishitoh, H., Ichijo, H., and Kyriakis, J.M. (2000) Activation of apoptosis signal-regulating kinase 1 (ASK1) by tumor necrosis factor receptor-associated factor 2 requires prior dissociation of the ASK1 inhibitor thioredoxin. *Mol Cell Biol* **20**: 2198–2208.

Liu, X., Sun, S.Q., Hassid, A., and Ostrom, R.S. (2006) cAMP inhibits transforming growth factor-beta-stimulated collagen synthesis via inhibition of extracellular signal-regulated kinase 1/2 and Smad signaling in cardiac fibroblasts. *Mol Pharmacol* **70**: 1992–2003.

Löhneysen, K. von, Noack, D., Wood, M.R., Friedman, J.S., and Knaus, U.G. (2010) Structural insights into Nox4 and Nox2: motifs involved in function and cellular localization. *Mol Cell Biol* **30**: 961–975.

Looi, Y.H., Grieve, D.J., Siva, A., Walker, S.J., Anilkumar, N., Cave, A.C., *et al.* (2008) Involvement of Nox2 NADPH oxidase in adverse cardiac remodeling after myocardial infarction. *Hypertens Dallas Tex 1979* **51**: 319–325.

Lucia, C. de, Femminella, G.D., Gambino, G., Pagano, G., Allocca, E., Rengo, C., *et al.* (2014) Adrenal adrenoceptors in heart failure. *Front Physiol* **5**: 246.

Lyle, A.N., Deshpande, N.N., Taniyama, Y., Seidel-Rogol, B., Pounkova, L., Du, P., *et al.* (2009) Poldip2, a novel regulator of Nox4 and cytoskeletal integrity in vascular smooth muscle cells. *Circ Res* **105**: 249–259.

Lymperopoulos, A., Rengo, G., and Koch, W.J. (2012) GRK2 inhibition in heart failure: something old, something new. *Curr Pharm Des* **18**: 186–191.

Lymperopoulos, A., Rengo, G., and Koch, W.J. (2013) Adrenergic nervous system in heart failure: pathophysiology and therapy. *Circ Res* **113**: 739–753.

Ma, Q. (2013) Role of nrf2 in oxidative stress and toxicity. *Annu Rev Pharmacol Toxicol* **53**: 401–426.

Mackey, A.M., Sanvicens, N., Groeger, G., Doonan, F., Wallace, D., and Cotter, T.G. (2008) Redox survival signalling in retina-derived 661W cells. *Cell Death Differ* **15**: 1291–1303.

Madamanchi, A. (2007) Beta-adrenergic receptor signaling in cardiac function and heart failure. *McGill J Med MJM Int Forum Adv Med Sci Stud* **10**: 99–104.

Madamanchi, N.R., and Runge, M.S. (2013) Redox signaling in cardiovascular health and disease. *Free Radic Biol Med* **61**: 473–501.

Maejima, Y., Kuroda, J., Matsushima, S., Ago, T., and Sadoshima, J. (2011) Regulation of myocardial growth and death by NADPH oxidase. *J Mol Cell Cardiol* **50**: 408–416.

Mahadev, K., Zilbering, A., Zhu, L., and Goldstein, B.J. (2001) Insulin-stimulated hydrogen peroxide reversibly inhibits protein-tyrosine phosphatase 1b in vivo and enhances the early insulin action cascade. *J Biol Chem* **276**: 21938–21942.

Maillet, M., Berlo, J.H. van, and Molkentin, J.D. (2013) Molecular basis of physiological heart growth: fundamental concepts and new players. *Nat Rev Mol Cell Biol* **14**: 38–48.

Malinouski, M., Zhou, Y., Belousov, V.V., Hatfield, D.L., and Gladyshev, V.N. (2011) Hydrogen peroxide probes directed to different cellular compartments. *PloS One* **6**: e14564.

Martyn, K.D., Frederick, L.M., Loehneysen, K. von, Dinauer, M.C., and Knaus, U.G. (2006) Functional analysis of Nox4 reveals unique characteristics compared to other NADPH oxidases. *Cell Signal* **18**: 69–82.

Matsumoto, E., Sasaki, S., Kinoshita, H., Kito, T., Ohta, H., Konishi, M., *et al.* (2013) Angiotensin II-induced cardiac hypertrophy and fibrosis are promoted in mice lacking Fgf16. *Genes Cells Devoted Mol Cell Mech* **18**: 544–553.

Matsuno, K., Iwata, K., Matsumoto, M., Katsuyama, M., Cui, W., Murata, A., *et al.* (2012) NOX1/NADPH oxidase is involved in endotoxin-induced cardiomyocyte apoptosis. *Free Radic Biol Med* **53**: 1718–1728.

Matsushima, S., Kuroda, J., Ago, T., Zhai, P., Park, J.Y., Xie, L.-H., *et al.* (2013) Increased oxidative stress in the nucleus caused by Nox4 mediates oxidation of HDAC4 and cardiac hypertrophy. *Circ Res* **112**: 651–663.

Matsushima, S., Kuroda, J., Zhai, P., Liu, T., Ikeda, S., Nagarajan, N., *et al.* (2016) Tyrosine kinase FYN negatively regulates NOX4 in cardiac remodeling. *J Clin Invest* **126**: 3403–3416.

Matthews, J.R., Wakasugi, N., Virelizier, J.L., Yodoi, J., and Hay, R.T. (1992) Thioredoxin regulates the DNA binding activity of NF-kappa B by reduction of a disulphide bond involving cysteine 62. *Nucleic Acids Res* **20**: 3821–3830.

Maulik, N., Sasaki, H., Addya, S., and Das, D.K. (2000) Regulation of cardiomyocyte apoptosis by redox-sensitive transcription factors. *FEBS Lett* **485**: 7–12.

McCloskey, D.T., Turnbull, L., Swigart, P., O'Connell, T.D., Simpson, P.C., and Baker, A.J. (2003) Abnormal myocardial contraction in alpha(1A)- and alpha(1B)-adrenoceptor double-knockout mice. *J Mol Cell Cardiol* **35**: 1207–1216.

Medzikovic, L., Schumacher, C.A., Verkerk, A.O., Deel, E.D. van, Wolswinkel, R., Made, I. van der, *et al.* (2015) Orphan nuclear receptor Nur77 affects cardiomyocyte calcium homeostasis and adverse cardiac remodelling. *Sci Rep* **5**: 15404.

Meerson, F.Z. (1961) On the mechanism of compensatory hyperfunction and insufficiency of the heart. *Cor Vasa* **3**: 161–177.

Meng, Q., and Xia, Y. (2011) c-Jun, at the crossroad of the signaling network. *Protein Cell* **2**: 889–898.

Meredith, I.T., Eisenhofer, G., Lambert, G.W., Dewar, E.M., Jennings, G.L., and Esler, M.D. (1993) Cardiac sympathetic nervous activity in congestive heart failure. Evidence for increased neuronal norepinephrine release and preserved neuronal uptake. *Circulation* **88**: 136–145.

Milano, C.A., Allen, L.F., Rockman, H.A., Dolber, P.C., McMinn, T.R., Chien, K.R., *et al.* (1994) Enhanced myocardial function in transgenic mice overexpressing the beta 2-adrenergic receptor. *Science* **264**: 582–586.

Miller, F.J., Filali, M., Huss, G.J., Stanic, B., Chamseddine, A., Barna, T.J., and Lamb, F.S. (2007) Cytokine activation of nuclear factor kappa B in vascular smooth muscle cells requires signaling endosomes containing Nox1 and ClC-3. *Circ Res* **101**: 663–671.

Minhas, K.M., Saraiva, R.M., Schuleri, K.H., Lehrke, S., Zheng, M., Saliaris, A.P., *et al.* (2006) Xanthine oxidoreductase inhibition causes reverse remodeling in rats with dilated cardiomyopathy. *Circ Res* **98**: 271–279.

Misra, A., Haudek, S.B., Knuefermann, P., Vallejo, J.G., Chen, Z.J., Michael, L.H., *et al.* (2003) Nuclear factor-kappaB protects the adult cardiac myocyte against ischemia-induced apoptosis in a murine model of acute myocardial infarction. *Circulation* **108**: 3075–3078.

Mitchell, L., Hobbs, G.A., Aghajanian, A., and Campbell, S.L. (2013) Redox regulation of Ras and Rho GTPases: mechanism and function. *Antioxid Redox Signal* **18**: 250–258.

Mollova, M.Y., Katus, H.A., and Backs, J. (2015) Regulation of CaMKII signaling in cardiovascular disease. *Front Pharmacol* **6**: 178.

Mondol, A.S., Tonks, N.K., and Kamata, T. (2014) Nox4 redox regulation of PTP1B contributes to the proliferation and migration of glioblastoma cells by modulating tyrosine phosphorylation of coronin-1C. *Free Radic Biol Med* **67**: 285–291.

Moniotte, S., Kobzik, L., Feron, O., Trochu, J.N., Gauthier, C., and Balligand, J.L. (2001) Upregulation of beta(3)-adrenoceptors and altered contractile response to inotropic amines in human failing myocardium. *Circulation* **103**: 1649–1655.

Montesano, A., Luzi, L., Senesi, P., Mazzocchi, N., and Terruzzi, I. (2013) Resveratrol promotes myogenesis and hypertrophy in murine myoblasts. *J Transl Med* **11**: 310.

Montezano, A.C., and Touyz, R.M. (2014) Reactive oxygen species, vascular Noxs, and hypertension: focus on translational and clinical research. *Antioxid Redox Signal* **20**: 164–182.

Montgomery, M.D., Chan, T., Swigart, P.M., Myagmar, B.-E., Dash, R., and Simpson, P.C. (2017) An Alpha-1A Adrenergic Receptor Agonist Prevents Acute Doxorubicin Cardiomyopathy in Male Mice. *PloS One* **12**: e0168409.

Morris, M.J., Cox, H.S., Lambert, G.W., Kaye, D.M., Jennings, G.L., Meredith, I.T., and Esler, M.D. (1997) Region-specific neuropeptide Y overflows at rest and during sympathetic activation in humans. *Hypertens Dallas Tex 1979* **29**: 137–143.

Mozaffarian, D., Benjamin, E.J., Go, A.S., Arnett, D.K., Blaha, M.J., Cushman, M., *et al.* (2016) Heart Disease and Stroke Statistics-2016 Update: A Report From the American Heart Association. *Circulation* **133**: e38-60.

Mudd, J.O., and Kass, D.A. (2008) Tackling heart failure in the twenty-first century. *Nature* **451**: 919–928.

Munagala, V.K., Hart, C.Y.T., Burnett, J.C., Meyer, D.M., and Redfield, M.M. (2005) Ventricular structure and function in aged dogs with renal hypertension: a model of experimental diastolic heart failure. *Circulation* **111**: 1128–1135.

Münzel, T., Gori, T., Keaney, J.F., Maack, C., and Daiber, A. (2015) Pathophysiological role of oxidative stress in systolic and diastolic heart failure and its therapeutic implications. *Eur Heart J* **36**: 2555–2564.

Murdoch, C.E., Chaubey, S., Zeng, L., Yu, B., Ivetic, A., Walker, S.J., *et al.* (2014) Endothelial NADPH oxidase-2 promotes interstitial cardiac fibrosis and diastolic dysfunction through proinflammatory effects and endothelial-mesenchymal transition. *J Am Coll Cardiol* **63**: 2734–2741.

Murray, T.V.A., Ahmad, A., and Brewer, A.C. (2014) Reactive oxygen at the heart of metabolism. *Trends Cardiovasc Med* **24**: 113–120.

Murray, T.V.A., Smyrnias, I., Shah, A.M., and Brewer, A.C. (2013) NADPH oxidase 4 regulates cardiomyocyte differentiation via redox activation of c-Jun protein and the cis-regulation of GATA-4 gene transcription. *J Biol Chem* **288**: 15745–15759.

Nabeebaccus, A., Hafstad, A., Eykyn, T., Yin, X., Brewer, A., Zhang, M., *et al.* (2015) Cardiac-targeted NADPH oxidase 4 in the adaptive cardiac remodelling of the murine heart. *Lancet Lond Engl* **385 Suppl 1**: S73.

Nabeebaccus, A., Zhang, M., and Shah, A.M. (2011) NADPH oxidases and cardiac remodelling. *Heart Fail Rev* **16**: 5–12.

Najafi, A., Sequeira, V., Kuster, D.W.D., and Velden, J. van der (2016) β-adrenergic receptor signalling and its functional consequences in the diseased heart. *Eur J Clin Invest* **46**: 362–374.

Nakanishi, A., Wada, Y., Kitagishi, Y., and Matsuda, S. (2014) Link between PI3K/AKT/PTEN Pathway and NOX Proteinin Diseases. *Aging Dis* **5**: 203–211.

Nandi, S.S., and Mishra, P.K. (2015) Harnessing fetal and adult genetic reprograming for therapy of heart disease. *J Nat Sci* **1**.

Neves, S.R., Ram, P.T., and Iyengar, R. (2002) G protein pathways. *Science* **296**: 1636–1639.

O'Connell, T.D., Ishizaka, S., Nakamura, A., Swigart, P.M., Rodrigo, M.C., Simpson, G.L., *et al.* (2003) The alpha(1A/C)- and alpha(1B)-adrenergic receptors are required for physiological cardiac hypertrophy in the double-knockout mouse. *J Clin Invest* **111**: 1783–1791.

O'Connell, T.D., Jensen, B.C., Baker, A.J., and Simpson, P.C. (2014) Cardiac alpha1-adrenergic receptors: novel aspects of expression, signaling mechanisms, physiologic function, and clinical importance. *Pharmacol Rev* **66**: 308–333.

O'Connell, T.D., Swigart, P.M., Rodrigo, M.C., Ishizaka, S., Joho, S., Turnbull, L., *et al.* (2006) Alpha1-adrenergic receptors prevent a maladaptive cardiac response to pressure overload. *J Clin Invest* **116**: 1005–1015.

Parajuli, N., Patel, V.B., Wang, W., Basu, R., and Oudit, G.Y. (2014) Loss of NOX2 (gp91phox) prevents oxidative stress and progression to advanced heart failure. *Clin Sci Lond Engl 1979* **127**: 331–340.

Park, S.K., Kim, J., Seomun, Y., Choi, J., Kim, D.H., Han, I.O., *et al.* (2001) Hydrogen peroxide is a novel inducer of connective tissue growth factor. *Biochem Biophys Res Commun* **284**: 966–971.

Patten, R.D., and Hall-Porter, M.R. (2009) Small animal models of heart failure: development of novel therapies, past and present. *Circ Heart Fail* **2**: 138–144.

Periasamy, M., and Kalyanasundaram, A. (2007) SERCA pump isoforms: their role in calcium transport and disease. *Muscle Nerve* **35**: 430–442.

Perrelli, M.-G., Pagliaro, P., and Penna, C. (2011) Ischemia/reperfusion injury and cardioprotective mechanisms: Role of mitochondria and reactive oxygen species. *World J Cardiol* **3**: 186–200.

Perry, S.J., and Lefkowitz, R.J. (2002) Arresting developments in heptahelical receptor signaling and regulation. *Trends Cell Biol* **12**: 130–138.

Petrônio, M.S., Zeraik, M.L., Fonseca, L.M. da, and Ximenes, V.F. (2013) Apocynin: chemical and biophysical properties of a NADPH oxidase inhibitor. *Mol Basel Switz* **18**: 2821–2839.

Phrommintikul, A., and Chattipakorn, N. (2006) Roles of cardiac ryanodine receptor in heart failure and sudden cardiac death. *Int J Cardiol* **112**: 142–152.

Pierce, K.L., Premont, R.T., and Lefkowitz, R.J. (2002) Seven-transmembrane receptors. *Nat Rev Mol Cell Biol* **3**: 639–650.

Pietrowski, E., Bender, B., Huppert, J., White, R., Luhmann, H.J., and Kuhlmann, C.R.W. (2011) Pro-inflammatory effects of interleukin-17A on vascular smooth muscle cells involve NAD(P)H- oxidase derived reactive oxygen species. *J Vasc Res* **48**: 52–58.

Pimentel, D.R., Amin, J.K., Xiao, L., Miller, T., Viereck, J., Oliver-Krasinski, J., *et al.* (2001) Reactive oxygen species mediate amplitude-dependent hypertrophic and apoptotic responses to mechanical stretch in cardiac myocytes. *Circ Res* **89**: 453–460.

Prejbisz, A., Lenders, J.W.M., Eisenhofer, G., and Januszewicz, A. (2011) Cardiovascular manifestations of phaeochromocytoma. *J Hypertens* **29**: 2049–2060.

Prosser, B.L., Ward, C.W., and Lederer, W.J. (2010) Subcellular Ca2+ signaling in the heart: the role of ryanodine receptor sensitivity. *J Gen Physiol* **136**: 135–142.

Prosser, B.L., Ward, C.W., and Lederer, W.J. (2011) X-ROS signaling: rapid mechano-chemo transduction in heart. *Science* **333**: 1440–1445.

Prysyazhna, O., Rudyk, O., and Eaton, P. (2012) Single atom substitution in mouse protein kinase G eliminates oxidant sensing to cause hypertension. *Nat Med* **18**: 286–290.

Pu, W.T., Ma, Q., and Izumo, S. (2003) NFAT transcription factors are critical survival factors that inhibit cardiomyocyte apoptosis during phenylephrine stimulation in vitro. *Circ Res* **92**: 725–731.

Purushothaman, S., and Nair, R.R. (2016) Mitoprotective antioxidant EUK-134 stimulates fatty acid oxidation and prevents hypertrophy in H9C2 cells. *Mol Cell Biochem* **420**: 185–194.

Qi, M., and Elion, E.A. (2005) MAP kinase pathways. *J Cell Sci* **118**: 3569–3572.

Qin, F., Siwik, D.A., Pimentel, D.R., Morgan, R.J., Biolo, A., Tu, V.H., *et al.* (2014) Cytosolic H2O2 mediates hypertrophy, apoptosis, and decreased SERCA activity in mice with chronic hemodynamic overload. *Am J Physiol Heart Circ Physiol* **306**: H1453-1463.

Rajabi, M., Kassiotis, C., Razeghi, P., and Taegtmeyer, H. (2007) Return to the fetal gene program protects the stressed heart: a strong hypothesis. *Heart Fail Rev* **12**: 331–343.

Rastogi, R., Geng, X., Li, F., and Ding, Y. (2016) NOX Activation by Subunit Interaction and Underlying Mechanisms in Disease. *Front Cell Neurosci* **10**: 301.

Reinkober, J., Tscheschner, H., Pleger, S.T., Most, P., Katus, H.A., Koch, W.J., and Raake, P.W.J. (2012) Targeting GRK2 by gene therapy for heart failure: benefits above β-blockade. *Gene Ther* **19**: 686–693.

Remondino, A., Kwon, S.H., Communal, C., Pimentel, D.R., Sawyer, D.B., Singh, K., and Colucci, W.S. (2003) Beta-adrenergic receptor-stimulated apoptosis in cardiac myocytes

is mediated by reactive oxygen species/c-Jun NH2-terminal kinase-dependent activation of the mitochondrial pathway. *Circ Res* **92**: 136–138.

Rey, F.E., Cifuentes, M.E., Kiarash, A., Quinn, M.T., and Pagano, P.J. (2001) Novel competitive inhibitor of NAD(P)H oxidase assembly attenuates vascular O(2)(-) and systolic blood pressure in mice. *Circ Res* **89**: 408–414.

Rhee, S.G., Kang, S.W., Jeong, W., Chang, T.-S., Yang, K.-S., and Woo, H.A. (2005) Intracellular messenger function of hydrogen peroxide and its regulation by peroxiredoxins. *Curr Opin Cell Biol* **17**: 183–189.

Rockman, H.A., Ross, R.S., Harris, A.N., Knowlton, K.U., Steinhelper, M.E., Field, L.J., *et al.* (1991) Segregation of atrial-specific and inducible expression of an atrial natriuretic factor transgene in an in vivo murine model of cardiac hypertrophy. *Proc Natl Acad Sci U S A* **88**: 8277–8281.

Rose, B.A., Force, T., and Wang, Y. (2010) Mitogen-activated protein kinase signaling in the heart: angels versus demons in a heart-breaking tale. *Physiol Rev* **90**: 1507–1546.

Rothermel, B.A., Berenji, K., Tannous, P., Kutschke, W., Dey, A., Nolan, B., *et al.* (2005) Differential activation of stress-response signaling in load-induced cardiac hypertrophy and failure. *Physiol Genomics* **23**: 18–27.

Rysä, J., Leskinen, H., Ilves, M., and Ruskoaho, H. (2005) Distinct upregulation of extracellular matrix genes in transition from hypertrophy to hypertensive heart failure. *Hypertens Dallas Tex 1979* **45**: 927–933.

Saavedra, W.F., Paolocci, N., St John, M.E., Skaf, M.W., Stewart, G.C., Xie, J.-S., *et al.* (2002) Imbalance between xanthine oxidase and nitric oxide synthase signaling pathways underlies mechanoenergetic uncoupling in the failing heart. *Circ Res* **90**: 297–304.

Sag, C.M., Köhler, A.C., Anderson, M.E., Backs, J., and Maier, L.S. (2011) CaMKII-dependent SR Ca leak contributes to doxorubicin-induced impaired Ca handling in isolated cardiac myocytes. *J Mol Cell Cardiol* **51**: 749–759.

Sag, C.M., Santos, C.X.C., and Shah, A.M. (2014) Redox regulation of cardiac hypertrophy. *J Mol Cell Cardiol* **73**: 103–111.

Salazar, N.C., Chen, J., and Rockman, H.A. (2007) Cardiac GPCRs: GPCR signaling in healthy and failing hearts. *Biochim Biophys Acta* **1768**: 1006–1018.

Salazar-Cantú, A., Pérez-Treviño, P., Montalvo-Parra, D., Balderas-Villalobos, J., Gómez-Víquez, N.L., García, N., and Altamirano, J. (2016) Role of SERCA and the sarcoplasmic reticulum calcium content on calcium waves propagation in rat ventricular myocytes. *Arch Biochem Biophys* **604**: 11–19.

Santos, C.X.C., Anilkumar, N., Zhang, M., Brewer, A.C., and Shah, A.M. (2011) Redox signaling in cardiac myocytes. *Free Radic Biol Med* **50**: 777–793.

Santos, C.X.C., Raza, S., and Shah, A.M. (2016) Redox signaling in the cardiomyocyte: From physiology to failure. *Int J Biochem Cell Biol* **74**: 145–151.

Sawicki, G. (2013) Intracellular regulation of matrix metalloproteinase-2 activity: new strategies in treatment and protection of heart subjected to oxidative stress. *Scientifica* **2013**: 130451.

Sawyer, D.B. (2011) Oxidative stress in heart failure: what are we missing? *Am J Med Sci* **342**: 120–124.

Sawyer, D.B., and Colucci, W.S. (2000) Mitochondrial oxidative stress in heart failure: "oxygen wastage" revisited. *Circ Res* **86**: 119–120.

Schaar, C.E., Dues, D.J., Spielbauer, K.K., Machiela, E., Cooper, J.F., Senchuk, M., *et al.* (2015) Mitochondrial and cytoplasmic ROS have opposing effects on lifespan. *PLoS Genet* **11**: e1004972.

Schröder, K., Helmcke, I., Palfi, K., Krause, K.-H., Busse, R., and Brandes, R.P. (2007) Nox1 mediates basic fibroblast growth factor-induced migration of vascular smooth muscle cells. *Arterioscler Thromb Vasc Biol* **27**: 1736–1743.

Schuchardt, M., Herrmann, J., Tölle, M., and Giet, M. van der (2017) Xanthine oxidase and its role as target in cardiovascular disease: cardiovascular protection by enzyme inhibition? *Curr Pharm Des* .

Schulz, E., Jansen, T., Wenzel, P., Daiber, A., and Münzel, T. (2008) Nitric oxide, tetrahydrobiopterin, oxidative stress, and endothelial dysfunction in hypertension. *Antioxid Redox Signal* **10**: 1115–1126.

Schwartz, K., Boheler, K.R., Bastie, D. de la, Lompre, A.M., and Mercadier, J.J. (1992) Switches in cardiac muscle gene expression as a result of pressure and volume overload. *Am J Physiol* **262**: R364-369.

Sciarretta, S., Volpe, M., and Sadoshima, J. (2014) NOX4 regulates autophagy during energy deprivation. *Autophagy* **10**: 699–701.

Sciarretta, S., Zhai, P., Shao, D., Zablocki, D., Nagarajan, N., Terada, L.S., *et al.* (2013) Activation of NADPH oxidase 4 in the endoplasmic reticulum promotes cardiomyocyte autophagy and survival during energy stress through the protein kinase RNA-activated-like endoplasmic reticulum kinase/eukaryotic initiation factor 2α/activating transcription factor 4 pathway. *Circ Res* **113**: 1253–1264.

Sedeek, M., Gutsol, A., Montezano, A.C., Burger, D., Nguyen Dinh Cat, A., Kennedy, C.R.J., *et al.* (2013) Renoprotective effects of a novel Nox1/4 inhibitor in a mouse model of Type 2 diabetes. *Clin Sci Lond Engl 1979* **124**: 191–202.

Serrander, L., Cartier, L., Bedard, K., Banfi, B., Lardy, B., Plastre, O., *et al.* (2007) NOX4 activity is determined by mRNA levels and reveals a unique pattern of ROS generation. *Biochem J* **406**: 105–114.

Seshiah, P.N., Weber, D.S., Rocic, P., Valppu, L., Taniyama, Y., and Griendling, K.K. (2002) Angiotensin II stimulation of NAD(P)H oxidase activity: upstream mediators. *Circ Res* **91**: 406–413.

Sharma, P., Chakraborty, R., Wang, L., Min, B., Tremblay, M.L., Kawahara, T., *et al.* (2008) Redox regulation of interleukin-4 signaling. *Immunity* **29**: 551–564.

Shimizu, I., and Minamino, T. (2016) Physiological and pathological cardiac hypertrophy. *J Mol Cell Cardiol* **97**: 245–262.

Simon, J.N., Duglan, D., Casadei, B., and Carnicer, R. (2014) Nitric oxide synthase regulation of cardiac excitation-contraction coupling in health and disease. *J Mol Cell Cardiol* **73**: 80–91.

Simonyi, A., Serfozo, P., Lehmidi, T.M., Cui, J., Gu, Z., Lubahn, D.B., *et al.* (2012) The neuroprotective effects of apocynin. *Front Biosci Elite Ed* **4**: 2183–2193.

Sirker, A., Murdoch, C.E., Protti, A., Sawyer, G.J., Santos, C.X.C., Martin, D., *et al.* (2016) Cell-specific effects of Nox2 on the acute and chronic response to myocardial infarction. *J Mol Cell Cardiol* **98**: 11–17.

Sirokmány, G., Donkó, Á., and Geiszt, M. (2016) Nox/Duox Family of NADPH Oxidases: Lessons from Knockout Mouse Models. *Trends Pharmacol Sci* **37**: 318–327.

Siwik, D.A., Kuster, G.M., Brahmbhatt, J.V., Zaidi, Z., Malik, J., Ooi, H., and Ghorayeb, G. (2008) EMMPRIN mediates beta-adrenergic receptor-stimulated matrix metalloproteinase activity in cardiac myocytes. *J Mol Cell Cardiol* **44**: 210–217.

Spencer, N.Y., and Engelhardt, J.F. (2014) The basic biology of redoxosomes in cytokine-mediated signal transduction and implications for disease-specific therapies. *Biochemistry (Mosc)* **53**: 1551–1564.

Spinale, F.G. (2007) Myocardial matrix remodeling and the matrix metalloproteinases: influence on cardiac form and function. *Physiol Rev* **87**: 1285–1342.

Stangherlin, A., and Reddy, A.B. (2013) Regulation of circadian clocks by redox homeostasis. *J Biol Chem* **288**: 26505–26511.

Steinberg, S.F. (2012) Cardiac actions of protein kinase C isoforms. *Physiol Bethesda Md* **27**: 130–139.

Steinberg, S.F. (2015) Mechanisms for redox-regulation of protein kinase C. *Front Pharmacol* **6**: 128.

Stolk, J., Hiltermann, T.J., Dijkman, J.H., and Verhoeven, A.J. (1994) Characteristics of the inhibition of NADPH oxidase activation in neutrophils by apocynin, a methoxy-substituted catechol. *Am J Respir Cell Mol Biol* **11**: 95–102.

Streeter, J., Thiel, W., Brieger, K., and Miller, F.J. (2013) Opportunity nox: the future of NADPH oxidases as therapeutic targets in cardiovascular disease. *Cardiovasc Ther* **31**: 125–137.

Sturrock, A., Cahill, B., Norman, K., Huecksteadt, T.P., Hill, K., Sanders, K., *et al.* (2006) Transforming growth factor-beta1 induces Nox4 NAD(P)H oxidase and reactive oxygen species-dependent proliferation in human pulmonary artery smooth muscle cells. *Am J Physiol Lung Cell Mol Physiol* **290**: L661–L673.

Sumimoto, H. (2008) Structure, regulation and evolution of Nox-family NADPH oxidases that produce reactive oxygen species. *FEBS J* **275**: 3249–3277.

Suzuki, Y.J. (2011) Cell signaling pathways for the regulation of GATA4 transcription factor: Implications for cell growth and apoptosis. *Cell Signal* **23**: 1094–1099.

Swaminathan, P.D., Purohit, A., Soni, S., Voigt, N., Singh, M.V., Glukhov, A.V., *et al.* (2011) Oxidized CaMKII causes cardiac sinus node dysfunction in mice. *J Clin Invest* **121**: 3277–3288.

Szanto, I., Rubbia-Brandt, L., Kiss, P., Steger, K., Banfi, B., Kovari, E., *et al.* (2005) Expression of NOX1, a superoxide-generating NADPH oxidase, in colon cancer and inflammatory bowel disease. *J Pathol* **207**: 164–176.

Taegtmeyer, H., Sen, S., and Vela, D. (2010) Return to the fetal gene program: a suggested metabolic link to gene expression in the heart. *Ann N Y Acad Sci* **1188**: 191–198.

Takac, I., Schröder, K., Zhang, L., Lardy, B., Anilkumar, N., Lambeth, J.D., *et al.* (2011) The E-loop is involved in hydrogen peroxide formation by the NADPH oxidase Nox4. *J Biol Chem* **286**: 13304–13313.

Takimoto, E., and Kass, D.A. (2007) Role of oxidative stress in cardiac hypertrophy and remodeling. *Hypertens Dallas Tex 1979* **49**: 241–248.

Terentyev, D., Györke, I., Belevych, A.E., Terentyeva, R., Sridhar, A., Nishijima, Y., *et al.* (2008) Redox modification of ryanodine receptors contributes to sarcoplasmic reticulum Ca2+ leak in chronic heart failure. *Circ Res* **103**: 1466–1472.

Thakur, A., Alam, M.J., Ajayakumar, M.R., Ghaskadbi, S., Sharma, M., and Goswami, S.K. (2015) Norepinephrine-induced apoptotic and hypertrophic responses in H9c2 cardiac myoblasts are characterized by different repertoire of reactive oxygen species generation. *Redox Biol* **5**: 243–252.

Tham, Y.K., Bernardo, B.C., Ooi, J.Y.Y., Weeks, K.L., and McMullen, J.R. (2015) Pathophysiology of cardiac hypertrophy and heart failure: signaling pathways and novel therapeutic targets. *Arch Toxicol* **89**: 1401–1438.

Theccanat, T., Philip, J.L., Razzaque, A.M., Ludmer, N., Li, J., Xu, X., and Akhter, S.A. (2016) Regulation of cellular oxidative stress and apoptosis by G protein-coupled receptor kinase-2; The role of NADPH oxidase 4. *Cell Signal* **28**: 190–203.

Tilley, D.G. (2011) G protein-dependent and G protein-independent signaling pathways and their impact on cardiac function. *Circ Res* **109**: 217–230.

Tocchetti, C.G., Wang, W., Froehlich, J.P., Huke, S., Aon, M.A., Wilson, G.M., *et al.* (2007) Nitroxyl improves cellular heart function by directly enhancing cardiac sarcoplasmic reticulum Ca2+ cycling. *Circ Res* **100**: 96–104.

Tombes, R.M., Faison, M.O., and Turbeville, J.M. (2003) Organization and evolution of multifunctional Ca(2+)/CaM-dependent protein kinase genes. *Gene* **322**: 17–31.

Traenckner, E.B., Pahl, H.L., Henkel, T., Schmidt, K.N., Wilk, S., and Baeuerle, P.A. (1995) Phosphorylation of human I kappa B-alpha on serines 32 and 36 controls I kappa B-alpha proteolysis and NF-kappa B activation in response to diverse stimuli. *EMBO J* **14**: 2876–2883.

Triposkiadis, F., Karayannis, G., Giamouzis, G., Skoularigis, J., Louridas, G., and Butler, J. (2009) The sympathetic nervous system in heart failure physiology, pathophysiology, and clinical implications. *J Am Coll Cardiol* **54**: 1747–1762.

Tsutsui, H., Kinugawa, S., and Matsushima, S. (2011) Oxidative stress and heart failure. *Am J Physiol Heart Circ Physiol* **301**: H2181-2190.

Turnbull, L., McCloskey, D.T., O'Connell, T.D., Simpson, P.C., and Baker, A.J. (2003) Alpha 1-adrenergic receptor responses in alpha 1AB-AR knockout mouse hearts suggest the presence of alpha 1D-AR. *Am J Physiol Heart Circ Physiol* **284**: H1104-1109.

Turner, R., and Tjian, R. (1989) Leucine repeats and an adjacent DNA binding domain mediate the formation of functional cFos-cJun heterodimers. *Science* **243**: 1689–1694.

Uhlinger, D.J., Taylor, K.L., and Lambeth, J.D. (1994) p67-phox enhances the binding of p47-phox to the human neutrophil respiratory burst oxidase complex. *J Biol Chem* **269**: 22095–22098.

Ukai, T., Cheng, C.P., Tachibana, H., Igawa, A., Zhang, Z.S., Cheng, H.J., and Little, W.C. (2001) Allopurinol enhances the contractile response to dobutamine and exercise in dogs with pacing-induced heart failure. *Circulation* **103**: 750–755.

Vassalle, C., Pratali, L., Boni, C., Mercuri, A., and Ndreu, R. (2008) An oxidative stress score as a combined measure of the pro-oxidant and anti-oxidant counterparts in patients with coronary artery disease. *Clin Biochem* **41**: 1162–1167.

Viedt, C., Soto, U., Krieger-Brauer, H.I., Fei, J., Elsing, C., Kübler, W., and Kreuzer, J. (2000) Differential activation of mitogen-activated protein kinases in smooth muscle cells by angiotensin II: involvement of p22phox and reactive oxygen species. *Arterioscler Thromb Vasc Biol* **20**: 940–948.

Vockel, M., and Vestweber, D. (2013) How T cells trigger the dissociation of the endothelial receptor phosphatase VE-PTP from VE-cadherin. *Blood* **122**: 2512–2522.

Vorbach, C., Harrison, R., and Capecchi, M.R. (2003) Xanthine oxidoreductase is central to the evolution and function of the innate immune system. *Trends Immunol* **24**: 512–517.

Wadley, A.J., Aldred, S., and Coles, S.J. (2016) An unexplored role for Peroxiredoxin in exercise-induced redox signalling? *Redox Biol* **8**: 51–58.

Wang, J., Paradis, P., Aries, A., Komati, H., Lefebvre, C., Wang, H., and Nemer, M. (2005) Convergence of protein kinase C and JAK-STAT signaling on transcription factor GATA-4. *Mol Cell Biol* **25**: 9829–9844.

Wang, R., Wang, Y., Lin, W.K., Zhang, Y., Liu, W., Huang, K., *et al.* (2014) Inhibition of angiotensin II-induced cardiac hypertrophy and associated ventricular arrhythmias by a p21 activated kinase 1 bioactive peptide. *PloS One* **9**: e101974.

Wang, W., Fang, H., Groom, L., Cheng, A., Zhang, W., Liu, J., *et al.* (2008) Superoxide flashes in single mitochondria. *Cell* **134**: 279–290.

Watkins, S.J., Borthwick, G.M., and Arthur, H.M. (2011) The H9C2 cell line and primary neonatal cardiomyocyte cells show similar hypertrophic responses in vitro. *In Vitro Cell Dev Biol Anim* **47**: 125–131.

Weinberg, E.O., Schoen, F.J., George, D., Kagaya, Y., Douglas, P.S., Litwin, S.E., *et al.* (1994) Angiotensin-converting enzyme inhibition prolongs survival and modifies the transition to heart failure in rats with pressure overload hypertrophy due to ascending aortic stenosis. *Circulation* **90**: 1410–1422.

Welch, H.C.E., Coadwell, W.J., Ellson, C.D., Ferguson, G.J., Andrews, S.R., Erdjument-Bromage, H., *et al.* (2002) P-Rex1, a PtdIns(3,4,5)P3- and Gbetagamma-regulated guanine-nucleotide exchange factor for Rac. *Cell* **108**: 809–821.

White, C.N., Figtree, G.A., Liu, C.-C., Garcia, A., Hamilton, E.J., Chia, K.K.M., and Rasmussen, H.H. (2009) Angiotensin II inhibits the Na+-K+ pump via PKC-dependent activation of NADPH oxidase. *Am J Physiol Cell Physiol* **296**: C693-700.

Widmann, C., Gibson, S., Jarpe, M.B., and Johnson, G.L. (1999) Mitogen-activated protein kinase: conservation of a three-kinase module from yeast to human. *Physiol Rev* **79**: 143–180.

Williams, H.C., and Griendling, K.K. (2007) NADPH oxidase inhibitors: new antihypertensive agents? *J Cardiovasc Pharmacol* **50**: 9–16.

Windak, R., Müller, J., Felley, A., Akhmedov, A., Wagner, E.F., Pedrazzini, T., *et al.* (2013) The AP-1 transcription factor c-Jun prevents stress-imposed maladaptive remodeling of the heart. *PloS One* **8**: e73294.

Winyard, P.G., Moody, C.J., and Jacob, C. (2005) Oxidative activation of antioxidant defence. *Trends Biochem Sci* **30**: 453–461.

Woo, A.Y.H., and Xiao, R. (2012) β-Adrenergic receptor subtype signaling in heart: from bench to bedside. *Acta Pharmacol Sin* **33**: 335–341.

Wright, C.D., Chen, Q., Baye, N.L., Huang, Y., Healy, C.L., Kasinathan, S., and O'Connell, T.D. (2008) Nuclear alpha1-adrenergic receptors signal activated ERK localization to caveolae in adult cardiac myocytes. *Circ Res* **103**: 992–1000.

Wu, R.F., Ma, Z., Myers, D.P., and Terada, L.S. (2007) HIV-1 Tat activates dual Nox pathways leading to independent activation of ERK and JNK MAP kinases. *J Biol Chem* **282**: 37412–37419.

Xiao, L., Pimental, D.R., Amin, J.K., Singh, K., Sawyer, D.B., and Colucci, W.S. (2001) MEK1/2-ERK1/2 mediates alpha1-adrenergic receptor-stimulated hypertrophy in adult rat ventricular myocytes. *J Mol Cell Cardiol* **33**: 779–787.

Xiao, L., Pimentel, D.R., Wang, J., Singh, K., Colucci, W.S., and Sawyer, D.B. (2002) Role of reactive oxygen species and NAD(P)H oxidase in alpha(1)-adrenoceptor signaling in adult rat cardiac myocytes. *Am J Physiol Cell Physiol* **282**: C926-934.

Xu, L., Eu, J.P., Meissner, G., and Stamler, J.S. (1998) Activation of the cardiac calcium release channel (ryanodine receptor) by poly-S-nitrosylation. *Science* **279**: 234–237.

Yamaguchi, O., Higuchi, Y., Hirotani, S., Kashiwase, K., Nakayama, H., Hikoso, S., *et al.* (2003) Targeted deletion of apoptosis signal-regulating kinase 1 attenuates left ventricular remodeling. *Proc Natl Acad Sci U S A* **100**: 15883–15888.

Yan, L., Zhang, J.D., Wang, B., Lv, Y.J., Jiang, H., Liu, G.L., *et al.* (2013) Quercetin inhibits left ventricular hypertrophy in spontaneously hypertensive rats and inhibits angiotensin II-induced H9C2 cells hypertrophy by enhancing PPAR-γ expression and suppressing AP-1 activity. *PloS One* **8**: e72548.

Yariswamy, M., Yoshida, T., Valente, A.J., Kandikattu, H.K., Sakamuri, S.S.V.P., Siddesha, J.M., *et al.* (2016) Cardiac-restricted Overexpression of TRAF3 Interacting Protein 2 (TRAF3IP2) Results in Spontaneous Development of Myocardial Hypertrophy, Fibrosis, and Dysfunction. *J Biol Chem* **291**: 19425–19436.

Yin, Q., Yang, C., Wu, J., Lu, H., Zheng, X., Zhang, Y., *et al.* (2016) Downregulation of β-Adrenoceptors in Isoproterenol-Induced Cardiac Remodeling through HuR. *PloS One* **11**: e0152005.

Ying, J., Sharov, V., Xu, S., Jiang, B., Gerrity, R., Schöneich, C., and Cohen, R.A. (2008) Cysteine-674 oxidation and degradation of sarcoplasmic reticulum Ca(2+) ATPase in diabetic pig aorta. *Free Radic Biol Med* **45**: 756–762.

Yoon, S., and Eom, G.H. (2016) HDAC and HDAC Inhibitor: From Cancer to Cardiovascular Diseases. *Chonnam Med J* **52**: 1–11.

Zee, R.S., Yoo, C.B., Pimentel, D.R., Perlman, D.H., Burgoyne, J.R., Hou, X., *et al.* (2010) Redox regulation of sirtuin-1 by S-glutathiolation. *Antioxid Redox Signal* **13**: 1023–1032.

Zelarayan, L., Renger, A., Noack, C., Zafiriou, M.-P., Gehrke, C., Nagel, R. van der, *et al.* (2009) NF-kappaB activation is required for adaptive cardiac hypertrophy. *Cardiovasc Res* **84**: 416–424.

Zhang, G., Zhang, F., Muh, R., Yi, F., Chalupsky, K., Cai, H., and Li, P.-L. (2007) Autocrine/paracrine pattern of superoxide production through NAD(P)H oxidase in coronary arterial myocytes. *Am J Physiol Heart Circ Physiol* **292**: H483-495.

Zhang, M., Brewer, A.C., Schröder, K., Santos, C.X.C., Grieve, D.J., Wang, M., *et al.* (2010) NADPH oxidase-4 mediates protection against chronic load-induced stress in mouse hearts by enhancing angiogenesis. *Proc Natl Acad Sci U S A* **107**: 18121–18126.

Zhang, M., Perino, A., Ghigo, A., Hirsch, E., and Shah, A.M. (2013) NADPH oxidases in heart failure: poachers or gamekeepers? *Antioxid Redox Signal* **18**: 1024–1041.

Zhang, X., and Kim, K.-M. (2017) Multifactorial Regulation of G Protein-Coupled Receptor Endocytosis. *Biomol Ther* **25**: 26–43.

Zhang, Y., Tocchetti, C.G., Krieg, T., and Moens, A.L. (2012) Oxidative and nitrosative stress in the maintenance of myocardial function. *Free Radic Biol Med* **53**: 1531–1540.

Zhu, W., Woo, A.Y.-H., Yang, D., Cheng, H., Crow, M.T., and Xiao, R.-P. (2007) Activation of CaMKIIdeltaC is a common intermediate of diverse death stimuli-induced heart muscle cell apoptosis. *J Biol Chem* **282**: 10833–10839.

Zima, A.V., and Blatter, L.A. (2006) Redox regulation of cardiac calcium channels and transporters. *Cardiovasc Res* **71**: 310–321.

Zor, U., Ferber, E., Gergely, P., Szücs, K., Dombrádi, V., and Goldman, R. (1993) Reactive oxygen species mediate phorbol ester-regulated tyrosine phosphorylation and phospholipase A2 activation: potentiation by vanadate. *Biochem J* **295 (Pt 3)**: 879–888.

Zorov, D.B., Filburn, C.R., Klotz, L.O., Zweier, J.L., and Sollott, S.J. (2000) Reactive oxygen species (ROS)-induced ROS release: a new phenomenon accompanying induction of the mitochondrial permeability transition in cardiac myocytes. *J Exp Med* **192**: 1001–1014.

PUBLICATIONS IN JOURNALS:

1. **Saleem, N.** and Goswami, S.K. *Activation of adrenergic receptor in H9c2 cardiac myoblasts co-stimulates Nox2 and the derived ROS mediate the downstream responses.* Mol Cell Biochem (2017). doi:10.1007/s11010-017-3088-8.
2. **Saleem, N.** and Goswami, S.K. *Apocynin prevents isoproterenol-induced cardiac hypertrophy in rat* [Communicated].
3. Jain BP, Pandey S, **Saleem N**, Tanti GK, Mishra S and Goswami SK. *SG2NA is a regulator of Endoplasmic Reticulum (ER) homeostasis as its depletion leads to ER stress*. Cell Stress and Chaperones (2017) [In Press].

PRESENTATIONS AT CONFERENCES:

1. **Nikhat Saleem** and S. K. Goswami. *Adrenergic Signaling in Cardiac Myocytes Involve Activation of NADPH Oxidase.* Oral talk at **"Cardiovascular Research Convergence-2"** held at All India Institute of Medical Sciences, New Delhi on January 17th, 2015.
2. **Nikhat Saleem** and S. K. Goswami. *Nor-epinephrine Signaling in Cardiac Myocytes Involve Activation of NADPH Oxidase*. Poster presentation at "83rd Annual Meeting of "Society of Biological Chemists, India (SBCI) and Symposium on Evolution: Molecules to Life and Workshop on Quantitative Biology" held at Bhubaneswar, Odisha, from December 17-21, 2014.
3. **Nikhat Saleem** and S. K. Goswami. *NOX Activation upon Adrenergic Receptor Stimulation and its Effect on Downstream Signaling Events.* Poster presentation at "38th All India Cell Biology Conference and International Symposium on Cellular Response to Drugs" held at CSIR-CDRI, Lucknow from December 10-12, 2014.
4. **Nikhat Saleem** and S. K. Goswami. *Redox signalling in cardiac myoblasts under adrenergic stress: Cross talk between β2-adrenergic receptor and NADPH Oxidase* Poster presentation at "82nd Annual Meeting of Society of Biological Chemists, India (SBCI) and International conference on Genomics: Mechanism and Function" held at School of Life Sciences, University of Hyderabad, Hyderabad, from December 2-5, 2013.
5. **Nikhat Saleem** and Shyamal K. Goswami. *Study of redox signalling in cardiac myoblasts under adrenergic stress by redox-sensitive fluorescence protein probes.* Poster presentation at "National Research Scholars meet in Life Sciences" held at Advanced Centre for Treatment, Research and Education in Cancer (ACTREC), Kharghar, Navi Mumbai from December 21st -22nd, 2012.

Mol Cell Biochem
DOI 10.1007/s11010-017-3088-8

Activation of adrenergic receptor in H9c2 cardiac myoblasts co-stimulates Nox2 and the derived ROS mediate the downstream responses

Nikhat Saleem[1] · Shyamal K. Goswami[1]

Received: 26 December 2016 / Accepted: 1 June 2017

Abstract In recent years, NADPH oxidases (Noxes) have emerged as an important player in cardiovascular pathophysiology. Despite the growing evidences on the role of specific Nox isoforms, mechanisms of their activation, targets of reactive oxygen species (ROS) generated, and their downstream effects are poorly understood as yet. In this study, we treated H9c2 cardiac myoblasts with norepinephrine (NE, 2 μM), inducing ROS generation that was inhibited by Nox2-specific peptide inhibitor gp91ds-tat. Organelle-specific hydrogen peroxide-sensitive probe HyPer showed that the site of ROS generation is primarily in the cytosol, to some extent in the endoplasmic reticulum (ER) but not the mitochondria. Modulation of mRNAs of marker genes of cardiac hypertrophy i.e. induction in ANP and β-MHC, and reduction in α-MHC by NE treatment was prevented by specific inhibition of Nox2 by gp91ds-tat. Induction of ANP and β-MHC at the protein level were also attenuated by the inhibition of Nox2. Induction of c-Jun and FosB, the two members of the transcription factor family AP-1, were also blocked by the inhibition of Nox2 by gp91ds-tat. Induction of promoter-reporter constructs harboring multiple AP-1 elements and the upstream of FosB and ANP genes by NE were also blocked by the inhibition of Nox2 by gp91ds-tat and a dominant negative mutant of p22phox, a constituent of Nox2 that prevents its activation. This study for the first time establishes the significant role of Nox2 in mediating the NE-induced pathological adrenergic signaling in cardiac myoblasts.

Keywords Redox signaling · Reactive oxygen species · NADPH oxidase · Cardiac hypertrophy · Norepinephrine · gp91ds-tat

Introduction

Oxidative stress has long been attributed to cardiovascular diseases like endothelial dysfunction, cardiac hypertrophy, cardiomyocyte apoptosis, ischemia–reperfusion injury, and heart failure [1–3]. Paradoxically, alleviating those conditions by antioxidants has largely been unsuccessful [4]. Recent years have seen paradigm shifts wherein apart from their deleterious effects, reactive oxygen species (ROS) have emerged as the mediator of intracellular signals [5]. Such regulatory roles of ROS are fast evolving [6, 7]. Superoxide ($O_2^{\cdot-}$), a prevalent ROS, is generated from a number of redox enzymes and mitochondrial electron transport complexes in distinct cellular locations. It is also converted into hydrogen peroxide (H_2O_2), a potent signaling molecule [7]. Their effects on the cellular constituents depend on the duration of generation, steady-state concentrations, subcellular locations, and surrounding antioxidants [8, 9]. $O_2^{\cdot-}$ and H_2O_2 may oxidize, nitrosylate, or glutathionylate the cysteine thiols in adjoining proteins, affecting their conformation, stability, and functions [6, 10].

The response of the cardiovascular system to the pathological stimuli leading to the development of hypertrophy and heart failure is complex and involves all known modes of regulations including phosphorylation–dephosphorylation, intracellular trafficking, protein and mRNA

Electronic supplementary material The online version of this article (doi:10.1007/s11010-017-3088-8) contains supplementary material, which is available to authorized users.

✉ Shyamal K. Goswami
skgoswami@mail.jnu.ac.in; shyamal.goswami@gmail.com

[1] School of Life Sciences, Jawaharlal Nehru University, New Delhi 110067, India

Published online: 07 June 2017

turnover, and oxidative modifications of the cellular proteome [11]. While the other modes of regulation are better understood, those by the oxidative and nitrosative modifications of various proteins are least investigated till date [6, 11].

Norepinephrine (NE) is released from the sympathetic nervous system and targets α- and β-adrenergic receptors, regulating cardiac performance [12, 13]. Cardiac myocytes in culture when treated with a lower dose of NE (≤10 μM NE) elicit hypertrophic response, while at a higher dose (≥50 μM NE) induces apoptosis. These two responses are the hallmark of heart failure [14, 15]. We have demonstrated earlier that although ROS are the common denominators of both the responses, its mechanism of actions is far more nuanced and complex than simple threshold-dependent effects as perceived earlier [16, 17].

NADPH oxidases (Nox1-5) are enzymes solely dedicated for the production of $O_2^{\cdot-}$ and H_2O_2 in various tissues in a context-specific manner [18]. Except Nox4 which is constitutive, all other Noxes are activated by various mechanisms [19]. Apart from their activation by intracellular mechanisms like calcium flux and by protein–protein interactions, they are also co-activated by the engagement of various growth factors, peptide hormones, and cytokines to their cognate receptors, though the mechanisms are not fully understood [20–22]. Three of its isoforms viz., Nox1/2/4 are expressed in heart and ROS generated from them have been attributed to interstitial fibrosis, contractile dysfunction, ischemia–reperfusion injury, and cardiac remodeling [6, 11, 23, 24].

Nox2, the prototype member of the family, is primarily localized in the plasma membrane and it is involved in redox signaling from cell exterior to interior [25]. In heart, several pathophysiological stimuli, i.e., hypoxia, membrane depolarization (endothelial cells), induction of platelet activating factor (PAF), arachidonic acid, tumor necrosis factor-α (TNF-α), and interleukin-1β (IL-1β), activate Nox2 [23].

Despite evidences that generation of ROS is an integral part of adrenergic signaling, their source, nature, and mode of actions are largely unknown [16, 17, 26]. In the present study, we demonstrate that in H9c2 cardiac myoblasts, stimulation of adrenergic receptor by NE co-stimulates Nox2 generating $O_2^{\cdot-}$ and H_2O_2. ROS generated from Nox2 is an integral part of the adrenergic signaling as the inhibition of Nox2 prevents the activation of transcription factors mediating hypertrophic response and the induction of a number of marker genes considered as the hallmarks of hypertrophy.

Materials and methods

Reagents

All chemicals were purchased from Sigma-Aldrich, USA unless otherwise specified. Peptide inhibitor gp91ds-tat (*RKKRRQRRRCSTRIRRQL-NH2)* was obtained from AnaSpec, Inc. pHyPer-Cyto and pHyPer-Mito constructs were obtained from Evrogen (Moscow, Russia). p22-phox-Wt and p22-phox-DN constructs were kind gift from Dr. Jaharul Haque, Cleveland Clinic, USA [27]. Rabbit monoclonal antibodies against Fos-B, c-Jun, p–c-Jun, and GAPDH were purchased from Cell Signaling Technologies, USA. Rabbit polyclonal antibody against β-MHC was purchased from Biorbyt, UK. Mouse monoclonal antibody against ANP and Horseradish peroxidase-conjugated anti-mouse and anti-rabbit IgG antibodies were obtained from Santa Cruz Biotechnology, USA. Alexa fluor-555 goat anti-rabbit and Alexa fluor-488 goat anti-mouse secondary antibodies were procured from Thermo Fisher Scientific, US. All the oligonucleotides used for cloning and transcript level measurement were synthesized from Sigma-Aldrich (Supplemental Table 1).

Cell culture

H9c2 cardiac myoblasts were procured from Sigma-Aldrich, USA (originally from ECACC, UK) and were cultured as monolayer in Dulbecco's modified Eagle medium (DMEM) supplemented with 10% fetal bovine serum (FBS), 90 U/ml Penicillin, 90 μg/ml streptomycin and 5 μg/ml amphotericin B in humidified, 5% CO_2 containing incubator at 37 °C.

ROS/$O_2^{\cdot-}$ measurement

H9c2 cells were grown in 35-mm dish to 70% confluence and kept in serum-free media for 12–14 h followed by treatment with 2 μM NE for 10 min. Wherever necessary, cells were pretreated with gp91ds-tat peptide (5 μM), 30 min prior to NE treatment. Thirty minutes prior to imaging, cells were treated with the fluoroprobes Dichlorodihydro-fluorescein diacetate (DCFH-DA, 5 μM) or Dihydroethidium (DHE, 10 μM), kept in dark at 37 °C, and washed in PBS (phosphate buffer saline), and the images were captured in Nikon Eclipse Ti-E fluorescence microscope using excitation/emission at 504/529 and 535/610 nm, respectively. For quantification, the mean intensity of fluorescence was measured by NIS-Elements software (Nikon).

Construction of pHyPer-ER

For targeting HyPer to endoplasmic reticulum (ER), the HyPer-ER was reconstituted from HyPer-Cyto essentially as described by Malinouski et al. [28]. Briefly, an 87-nucleotide-long oligonucleotide harboring the ER signal peptide sequence of 29 amino acids was generated from the total RNA isolated from the pituitary gland of rat by using appropriate primers (supplemental Table 1). The PCR product was then cloned in frame at the N-terminal of pHyPer-Cyto. Also, in the C-terminal, a synthetic 12-nucleotide-long sequence harboring the ER retention signal (KDEL) was inserted. The strategy details are given in Supplemental Fig. 1s.

Measurement of cell compartment-specific H_2O_2 generation

H9c2 cells were grown in 35-mm glass bottom dish to 70% confluence followed by transient transfection using Escort IV transfection reagent according to the manufacturer's instructions. After 24 h of transfection, cells were kept in serum-free media for 12–14 h followed by treatment with 2 μM NE in phenol red free DMEM. Fluorescence of live cells was captured while in a live cell chamber with 5% CO_2 at 37 °C by Andor spinning disc confocal microscope (Olympus) with excitation using 488 nm laser line. The intensity of fluorescence was quantified by NIS-Elements AR-ver 4.000 software.

Gene expression analysis

H9c2 cells were grown to 70% confluence and kept in serum-free media for 12–14 h followed by 2 μM NE treatment. Wherever necessary, cells were also treated with gp91ds-tat peptide (5 μM) 30 min prior to NE treatment. After 24 h, total RNA was isolated using TRI reagent according to the manufacturer's instructions. One microgram of RNA was reverse transcribed using Applied Biosystems reverse transcription kit as per the manufacturer's protocol. Gene-specific primers were used to analyze the transcript level using SYBR green master mix (Applied Biosystems) in an Applied Biosystems 7500 real-time PCR system. Modulation of transcript levels was quantified using Ct values and normalization was done with the transcript level of the house keeping gene GAPDH.

Immunofluorescence analysis

H9c2 cells were grown on poly-L-lysine-coated coverslips in 12-well culture plate. Cells were treated with 2 μM NE and 5 μM gp91ds-tat peptide (30 min prior to NE treatment) wherever marked for indicated time point. After treatment time, cells were fixed with chilled methanol for 20 min followed by PBS washes and blocked with PBS containing 1% BSA, 1% bovine serum, and 0.1% Triton-X-100 for 60 min. Then, after PBS washes, the coverslips were incubated overnight at 4 °C with 1:100 rabbit-anti-β-MHC or mouse-anti-ANP or rabbit-anti-FosB antibodies diluted in blocking solution. Next day, after washing three times with PBS, cells were incubated with 1:500 Alexa fluor-555 goat anti-rabbit secondary antibody (red fluorescence) or Alexa fluor-488 goat anti-mouse secondary antibody (green fluorescence) for 60 min. After three washes in PBS, the coverslips were sealed with glass slides in 80% glycerol (in PBS) containing cell nuclei stain Hoechst (1:1000). The images were captured in Nikon Eclipse Ti-E fluorescence microscope at 60X magnification.

Immunoblot analysis

H9c2 cells were grown to 70% confluence and kept in serum-free media for 12–14 h followed by 2 μM NE treatment. Wherever necessary, cells were also treated with gp91ds-tat peptide (5 μM) 30 min prior to NE treatment. After indicated time points, cells were harvested in cold PBS followed by centrifuge at 3000 rpm for 15 min. The pellet obtained was lysed in RIPA buffer (50 mM Tris; pH 7.4, 150 mM NaCl, 1% Triton X-100, 1% sodium deoxycholate, 0.1% SDS, 1 mM EDTA) with phosphatase inhibitor cocktail, 1 mM phenylmethylsulfonyl fluoride (PMSF), and protease inhibitor cocktail followed by sonication. The homogenates were centrifuged and supernatant was assessed for protein concentration by the Bradford method using BSA as standard. Proteins were separated (50 μg per well) on 10 or 12% SDS-polyacrylamide gel and transferred onto PVDF membrane (Millipore, USA). Membranes were blocked with 3% BSA in 0.1% TBST for 2 h at room temperature followed by incubation with specific primary antibodies (diluted in 3% BSA in 0.1% TBST) at 4 °C overnight. Then the membrane was incubated with anti-rabbit or anti-mouse IgG secondary antibody conjugated to peroxidase (HRP) at 1:10,000 dilution in 0.1% TBST for 1 h at room temperature. Membranes were exposed to enhanced chemiluminescence reagent and visualized on X-ray film (Kodak, USA). Quantification of band intensities was performed with the Image-J software system. The signal intensity of each protein band was normalized with the corresponding GAPDH signal and fold change over control was calculated.

Analysis of promoter-reporter activity

H9c2 cells were grown to 70% confluence followed by transient transfection with reporter plasmids with or without

the co-transfection with p22-phox constructs using Escort IV transfection reagent as directed by the manufacturer. Cells were kept in serum-free medium for 12–14 h and treated with 2 μM NE and 5 μM gp91ds-tat peptide (30 min prior to NE treatment) wherever marked. The cells were harvested after 4 h of NE treatment in 1× lysis buffer (Promega), lysates were then analyzed for luciferase activity using the Luciferase Reagent Assay Kit (Promega) in accordance with the manufacturer's instructions in a GLOMAX Multi JR detection system (Promega). Normalization of transfection efficiency was done by the estimation of total protein used for the luciferase assay [29, 30].

Statistical analysis

Statistical analyses were performed using GraphPad Prism, PC version 5 (GraphPad software). Data are expressed as mean ± SEM. Each experiment was performed at least in triplicate. Experimental groups were compared with the use of one-way ANOVA if there was one independent variable (Tukey's test) or two-way ANOVA if there were two independent variables. Values of $P < 0.05$ were considered statistically significant.

Results

NE-treated cardiac myoblast generates ROS from Nox2

We have demonstrated earlier that cardiac myoblasts upon stimulation with NE generates a complex repertoire of ROS that contribute towards the downstream responses viz., hypertrophy and apoptosis [16, 17, 30]. Since such generation of ROS is an immediate (<1 min) response and includes both $O_2^{\cdot-}$ and H_2O_2, involvement of Nox2 is anticipated. To test this possibility, H9c2 cardiac myoblasts were kept in serum-free medium overnight and stimulated with NE (2 μM) for 10 min. Generation of ROS was monitored by the general ROS-sensitive fluoroprobe Dichloro-dihydro-fluorescein diacetate (DCFH-DA) and $O_2^{\cdot-}$-specific fluoroprobe Dihydroethidium (DHE). To test the involvement of Nox2, its specific peptide inhibitor gp91ds-tat (5 μM) was added. As shown in Fig. 1a, NE-induced ROS (DCFH-DA) generation was completely blocked by the specific inhibition of Nox2. In agreement with our previous report, part of the ROS was $O_2^{\cdot-}$ (DHE sensitive) that was also completely blocked by

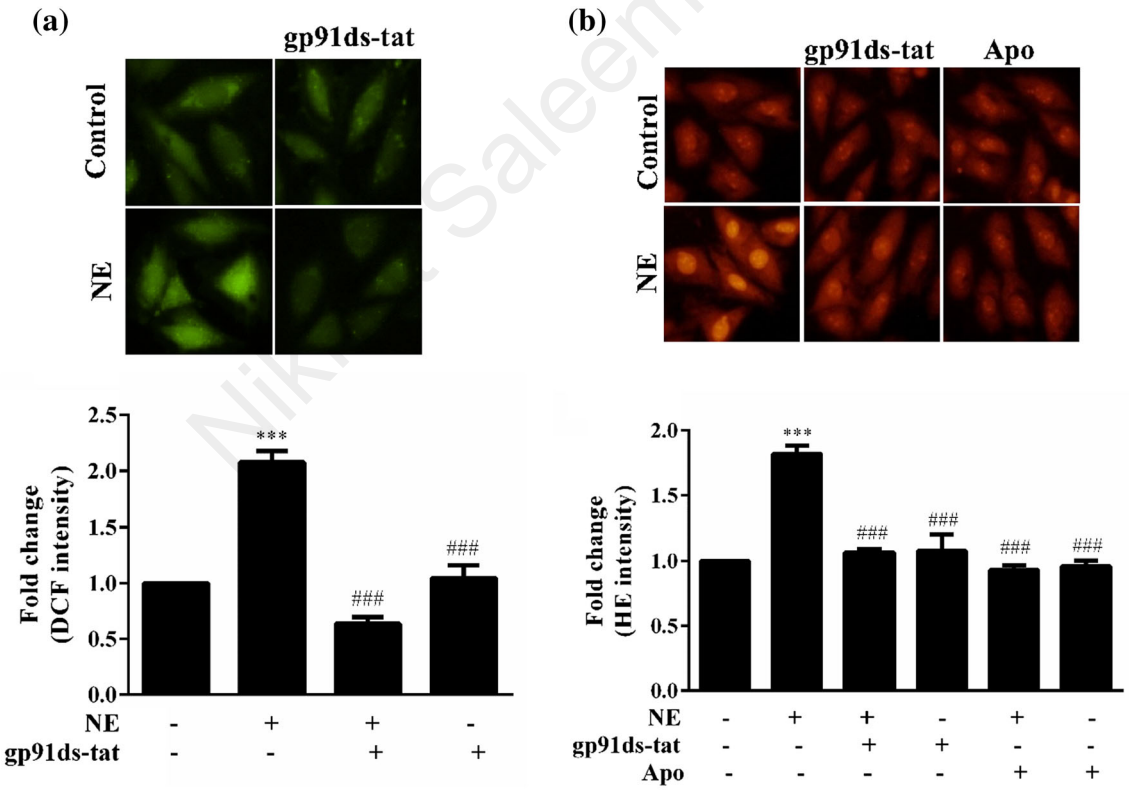

Fig. 1 Nox2 is the source of ROS in NE-treated cardiac myoblasts Upper panel: H9c2 cells were serum starved overnight followed by treatment with 2 μM NE for 10 min. 5 μM gp91ds-tat or 10 μM Apo was added 30 min before NE treatment wherever marked. Cells were labeled with **a** redox-sensitive fluoroprobe DCFH-DA (5 μM) or **b** superoxide-sensitive fluoroprobe DHE (10 μM), 30 min prior to imaging. *Lower Panel* quantification of the fluorescence intensity normalized to control. $^{***}P \leq 0.001$ versus control; $^{###}P \leq 0.001$ versus NE

the specific inhibition of Nox2 by gp91ds-tat as well as the general inhibition of all Noxes by apocynin (Fig. 1b). These results strongly corroborated with our hypothesis that stimulation of adrenergic receptor by NE co-activates Nox2 and generates $O_2^{\cdot-}$ and other associated ROS.

NE induces ROS generation primarily in the cytosol

We have demonstrated earlier that treatment of H9c2 cardiac myoblasts with 2 μM of NE leads to the sustained but oscillating generation of ROS [16, 17, 30]. Since redox signaling is specified by the cellular microdomain where it is generated, we also tested the subcellular location of the ROS generated by NE. Cells were transfected with the H_2O_2-sensitive cpYFP (circularly permuted-yellow fluorescent protein)-based ratiometric fluorescent probe HyPer plasmids [31] that monitors the H_2O_2 generation in the cytoplasm, mitochondria, and endoplasmic reticulum (ER). After 24 h of transfection, cells were kept overnight in serum-free media followed by treatment with 2 μM NE and live cell imaging was done for 1 h at Ex_{max} 488 nm. As shown in Fig. 2a, snapshots of a single living cell showed treatment with NE resulted in a sharp and rapid increase in H_2O_2 generation in the cytosol, that sustained till 1 h, the last time point tested (further analysis was not possible as the cells started crumbling, presumably due to the repeated exposure to the light). Although there was a gradual decrease (∼20%) in fluorescence with time, it was still well above the baseline (untreated cells). Noticeably, no increase in fluorescence was seen in the mitochondria in NE-treated cells as monitored by the HyPer-Mito (Fig. 2b). Rather, the signal was below the baseline (untreated control) after 30 min, though the reason is not clear. The efficacy of the assay was evident from the increase in fluorescence in cells treated with 20 μM H_2O_2. Unlike the mitochondria, some increase in fluorescence was seen in ER upon NE treatment (Fig. 2c), though the response was not as intense as in cytosol. The higher baseline intensity of HyPer-ER reflects the oxidizing environment of ER. Together, these data suggest that cytosol is the primary and the ER is the secondary location of H_2O_2 generation in NE-treated cells. Due to the lack of organelle-specific probes, similar assay for superoxide generation in those organelles could not be done.

Induction of fetal gene expression by NE is prevented by the inhibition of Nox2

Re-induction of fetal gene expression program is a characteristic feature of cardiac hypertrophy and it is faithfully reproduced by treating cultured myocytes ex vivo with adrenergic agonists [32, 33]. To analyze the role of Nox2-induced ROS in the induction of fetal gene program if any, we estimated the mRNA levels of three established markers viz., ANP (atrial natriuretic peptide), α-MHC (α-myosin heavy chain), and β-MHC (β-myosin heavy chain). As expected, upon treatment with 2μ NE, the transcript levels of ANP and β-MHC increased by ∼1.7 and 2.0 fold, respectively, and that of α-MHC decreased by ∼0.4 fold. Pretreatment of cells with gp91ds-tat (5 μM) prevented the modulation of transcript levels by NE (Fig. 3a). We further confirmed such modulation of hypertrophic markers at the protein levels by immunocytochemistry. As shown in Fig. 3b, treatment with NE (2 μM) increased the levels of both ANP and β-MHC that were attenuated by the inhibition of Nox2 by gp91ds-tat (5 μM). These results not only strengthened our previous observation that ROS induced by NE treatment play a direct role in regulation of gene expression in hypertrophied heart [16, 17, 30], it also established that Nox2 is the primary source of this regulatory ROS (Figs. 1, 2).

Nox2-induced ROS modulate the activities of transcription factors mediating hypertrophic responses

Heterodimeric transcription factor AP-1 has long been identified as the key mediator of hypertrophic signals elicited by several agonists [34]. Also, depending on the pathophysiological stimuli, the role of AP-1 can be divergent [35]. We have demonstrated earlier that in NE-treated cardiac myoblasts, the redox and kinase signals integrate at various transcription factors viz, AP-1, SP-1, and CREB, which then mediate their effects through the cognate *cis*-regulatory elements in the responsive gene promoters, specifying the transcriptional output [16, 30]. To reiterate that observation in the context of ROS generated from Nox2, the expression levels of two members of the AP-1 family that is c-Jun and FosB were assayed by Western analysis. As shown in Fig. 4a (left panel), upon treatment with NE, c-Jun level was induced by 1.25 and 1.38 fold at 2 and 4 h of NE treatment, respectively, and that were attenuated by gp91ds-tat treatment. Although, gp91ds-tat itself also showed some induction of c-Jun, it was less than that able to suppress the c-Jun level below baseline at 4 h. Similar observations were also made for FosB (FBJ murine osteosarcoma viral oncogene homolog B), a member of the AP-1 family and the dimerization partner of c-Jun. As shown in Fig. 4a (left panel), level of FosB was increased by 1.45 fold in NE-treated cells at 2 h but diminished thereafter at 4 h. This kinetic is in agreement with our earlier study with the FosB transcript [30]. As expected, the induction of FosB was also abrogated by treatment with gp91ds-tat. In view with the low intensity of the signal with the FosB antibody in the Western blot (possibly, a reflection of the low abundance), we also confirmed its

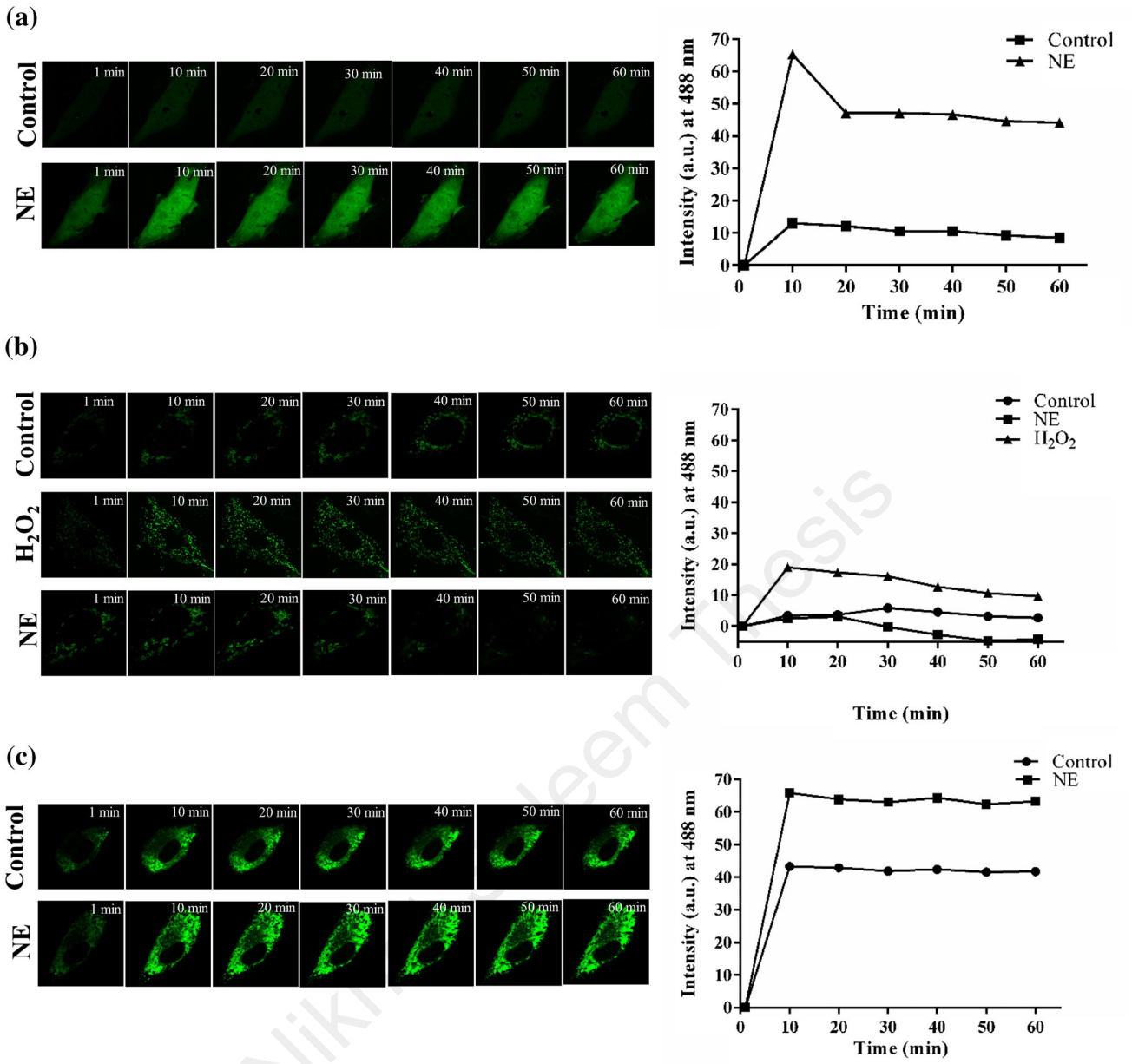

Fig. 2 NE induces generation of hydrogen peroxide primarily in the cytosol Left panel: H9c2 cells were transfected with **a** pHyPer-Cyto, **b** pHyPer-Mito, and **c** pHyPer-ER. After 24 h of transfection, cells were kept overnight in serum-free media followed by treatment with 2 μM NE or 20 μM H_2O_2 treatment as marked. Live single cell imaging was done at 60X for 1 h at Ex_{max} 488 nm and most representative image is shown. *Right panel* quantification of the fluorescence intensity normalized to intensity at 1 min

modulation by immunocytochemistry as shown on the right panel. Immunocytochemistry not only reiterated the pattern of modulation seen in the Western blot, it also showed the nuclear localization of FosB. We also examined the level of phospho-c-Jun in NE-treated cells and its modulation by gp91ds-tat. As shown in Fig. 4a (left panel), treatment with NE rather decreased the level of phospho-c-Jun (thus effectively decreasing the phospho-c-Jun/c-Jun ratio) while treatment with gp91ds-tat partially restored that reduction. Although, phosphorylation of c-jun is known for its activation (in addition to the increase in its expression level), its cellular function is highly context specific with multiple layers of a regulatory networks wherein it integrates different signals [36]. It is thus difficult to assess the implication of increase in c-Jun expression with concurrent decrease in its state of phosphorylation upon NE treatment. Nevertheless, these data unequivocally reiterate that Nox2 plays a role in modulating the AP-1 activity by NE. Subsequent to analyzing the expression of c-Jun and FosB, we also assayed a number of promoter-reporter (luciferase)

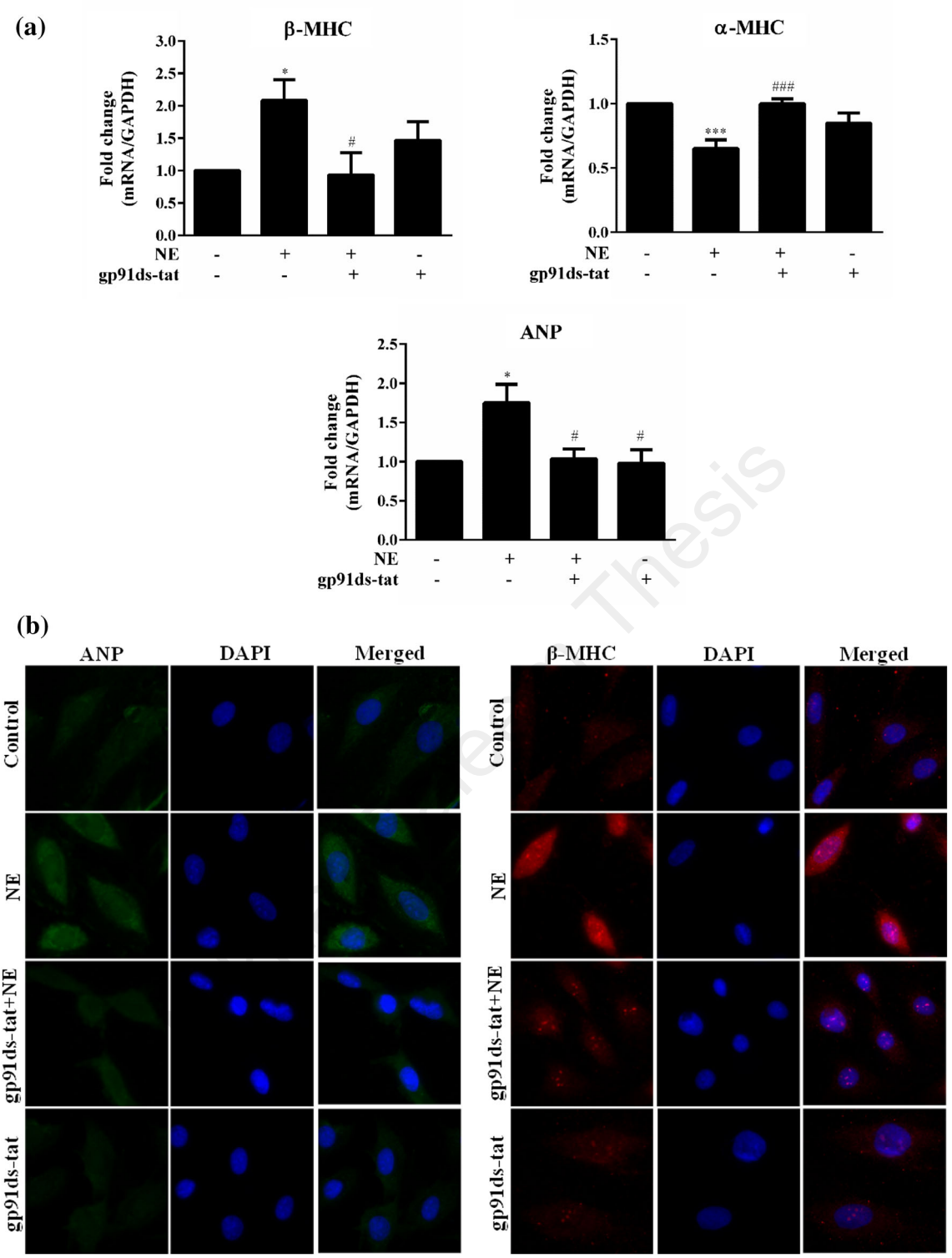

Fig. 3 Induction of fetal gene expression by NE is prevented by the inhibition of Nox2 H9c2 cells were serum starved overnight followed by treatment with 2 μM NE for 24 h. 5 μM gp91ds-tat was added 30 min before NE treatment wherever marked. **a** Total RNA was assayed for ANP, β-MHC, and α-MHC transcripts using gene-specific primers by Real-time PCR. Normalization of input RNA was done by using GAPDH level as an internal control. Fold differences of mRNA levels over control were calculated. **b** Immunostaining was done using antibody specific for ANP (*left panel*) and β-MHC (*right panel*). $^{*}P \leq 0.05$ versus control; $^{***}P \leq 0.001$ versus control; $^{\#}P \leq 0.05$ versus NE; $^{\#\#\#}P \leq 0.001$ versus NE

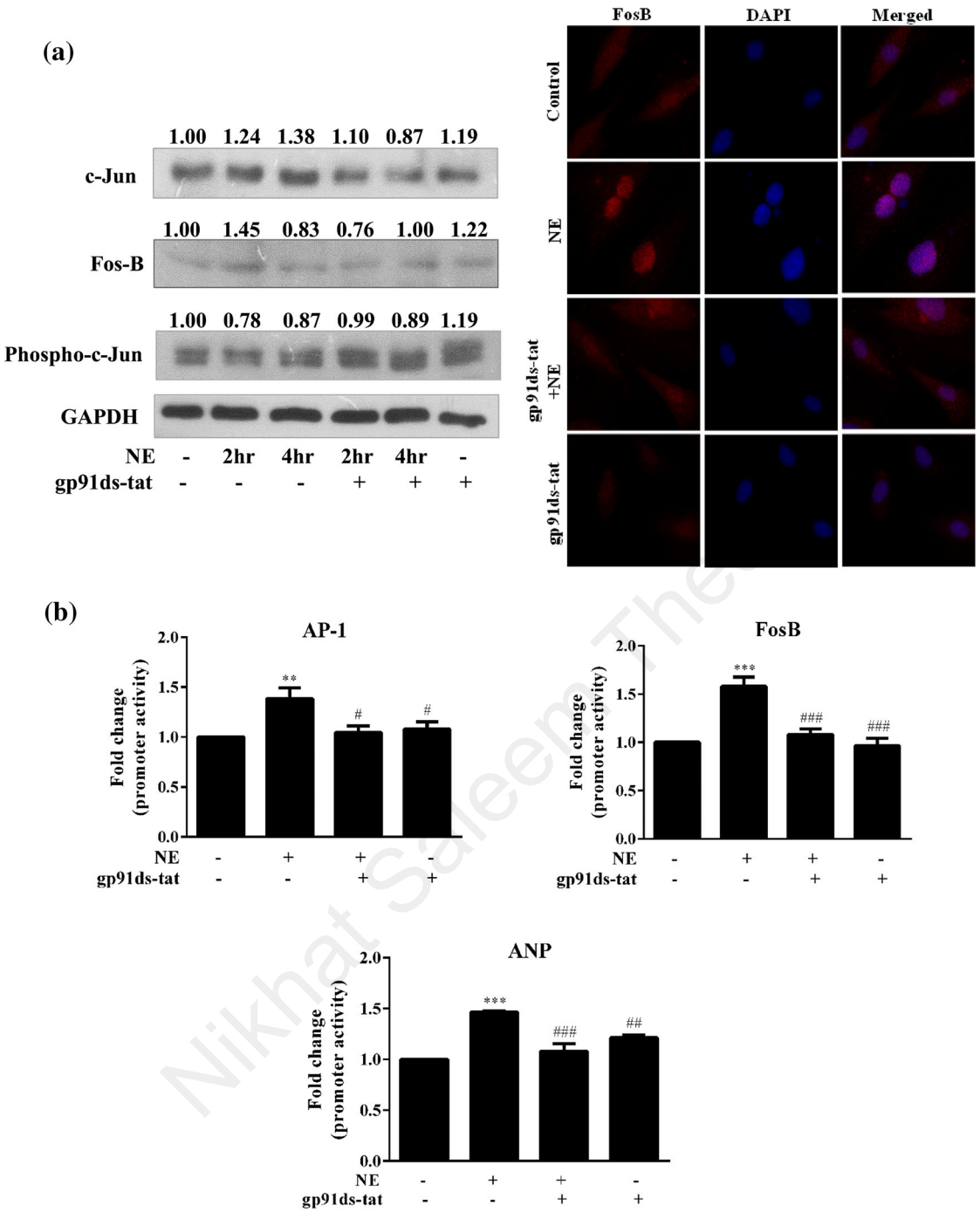

Fig. 4 Nox2-induced ROS modulate the activities of transcription factors mediating the hypertrophic response **a** H9c2 cells were serum starved overnight followed by treatment with 2 μM NE for 2 or 4 h as indicated. 5 μM gp91ds-tat was added 30 min before NE treatment wherever marked. *Left panel* Total protein was isolated and equal amount (50 μg) of lysates were assayed by Western blot analysis using antibody specific for FosB, Phospho-c-Jun, and c-Jun. GAPDH level was the loading control. The intensity of bands was evaluated as a ratio relative to that of GAPDH and values are written above the respective bands. Most representative image out of three independent experiment is shown. *Right panel* Immunostaining was done using antibody specific for FosB. H9c2 cells were **b** transfected with AP-1, FosB, and ANP promoter-reporter constructs either alone **c** or co-transfected with p22-phox-Wt or p22-phox-DN constructs. After 24 h of transfection, cells were kept overnight in serum-free media followed by treatment with 2 μM NE for 4 h. 5 μM gp91ds-tat was added 30 min before NE treatment wherever marked. Cell lysates were assayed for reporter luciferase activity. Normalization of luminescence was done against total protein concentration. Fold differences of promoter activity over control were calculated. $^{**}P \leq 0.01$ versus control; $^{***}P \leq 0.001$ versus control; $^{\#}P \leq 0.05$ versus NE; $^{\#\#}P \leq 0.01$ versus NE; $^{\#\#\#}P \leq 0.001$ versus NE $^{\$\$\$\$}P \leq 0.0001$ versus p22-phox-Wt untreated; $^{\$\$\$}P \leq 0.001$ vs p22-phox-Wt untreated; $^{\$}P \leq 0.05$ versus p22-phox-DN untreated

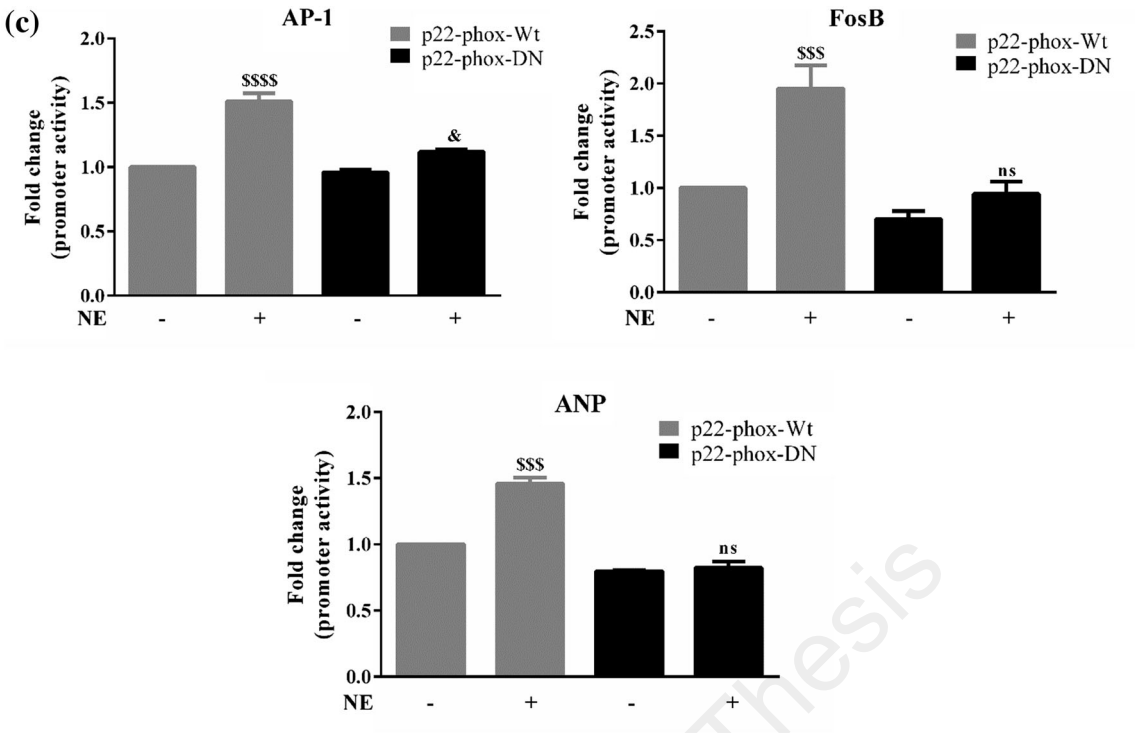

Fig. 4 continued

constructs regulated by AP-1 in cardiac myocytes treated with adrenergic agonists. We tested one synthetic promoter harboring three consecutive AP-1 binding sites, and two endogenous promoters viz that of ANP and FosB genes. The endogenous promoter of ANP gene has been extensively studied for analyzing the signal transduction pathways mediating hypertrophic response [37] and it harbors an AP-1 site along with other cis-elements [38]. Although the FosB promoter has not been studied in details, we have demonstrated that it is selectively activated by the hypertrophic dose of NE and have used it as a paradigm of understanding how redox and kinase signals integrate at the gene level regulating its expression [16, 30]. When we tested the effects of NE on these promoters, there was increase by ~1.45 fold for AP-1, ~1.6 fold for FosB, and ~1.5 fold for ANP. Pretreatment of cells with the Nox2 inhibitor gp91ds-tat (5 μM) prevented the induction of all three (Fig. 4b).

To further confirm the role of Nox2 in regulating the expression of these promoters in NE-treated cells, we co-transfected the wildtype (Wt) and the dominant negative (DN) variants of p22-phox subunit of Nox. Although the activation of both Nox2/4 isoforms requires p22-phox, its DN variant (P156Q) prevents ROS generation from Nox2 only [19, 27]. We argued that if the upregulation of these promoters are Nox2 dependent, it would be compromised by the over-expression by the DN mutant of p22-phox. As shown in Fig. 4c, expression of p22-phox-DN subunit of Nox compromised the stimulatory effect of NE seen in control, that is promoters transfected with the p22-phox-Wt, confirming the involvement of Nox2 in mediating NE response. Taken together, these data reiterate the involvement of Nox2 in modulating the gene network involved in hypertrophic signaling by NE.

Discussion

While the specificity of kinase signaling is directed by protein–protein interactions, that of redox signaling depends on multiple factors like the localization of the reactive species in subcellular microdomain, the pKa of neighboring cysteine thiols, surrounding antioxidants, and the presence of free transition metals [39, 40]. Redox signaling in mammalian cell is thus highly nuanced, calibrated, and difficult to dissect.

Among the three Noxes present in heart, function of Nox4 is better investigated. Its activation by multiple stimuli including ischemia–reperfusion, pressure overload, and energy starvation vis-à-vis its location in the mitochondria, ER, and the nucleus exemplifies the complexity of redox signaling in cardiac pathobiology [41]. On the contrary, the role of Nox2, the prototype Nox, in cardiac function is lesser understood, even though its activation by pressure volume overload and early preconditioning has been reported [41, 42]. The functioning of the cardiovascular system is

modulated by a plethora of growth factors, cytokines, and hormones, but adrenergic signaling plays a nodal role in these processes. Therefore, our observation that in cardiac myoblasts, the activation of adrenergic receptors co-stimulates Nox2 is novel and significant as it gives a new dimension to the adrenergic signaling.

Although ROS have been implicated in all major pathological conditions in heart, its sources and potential targets are largely unknown [1–4, 23, 24, 43]. We have documented earlier that once the ROS generation is stimulated by NE, it sustains independently, presumably by some yet unknown downstream mechanisms [16, 17]. As the present study shows that the ROS generated by NE treatment is completely attenuated by the selective inhibition of Nox2, it is thus the only source of ROS at the onset. Although the primary product of Nox2 is $O_2^{\cdot-}$, it can be immediately converted into H_2O_2 by intra- and extracellular SOD (superoxide dismutase), and the chemistry of signaling by these two ROS is quite different. We therefore tested the nature of ROS generated by Nox2 and the presence of both $O_2^{\cdot-}$ and H_2O_2 were detected in NE-treated cells. These results are in full agreement with our earlier observation that upon NE treatment, H9c2 cardiac myoblasts generate a complex mixture of $O_2^{\cdot-}$, H_2O_2, and other secondary ROS, although their sources were unknown in earlier study [17]. In this study, we also for the first time demonstrated that H_2O_2 generated by Nox2 is primarily localized in the cytosol, to some extent in the ER but completely absent in the mitochondria. Among various organelles, mitochondria have generally been viewed as the principal source of ROS in heart, especially under pathological conditions [41, 42], although cytosolic, endoplasmic reticular, and nuclear ROS have also been attributed to the cardiac pathobiology [23, 44–46]. Further study on the targets of cytosolic H_2O_2 in mediating the downstream signals will be of immense interest.

Although the cross-talk between the redox and kinase signaling has long been envisaged, the mechanistic insights are highly inadequate [7, 47]. We had demonstrated earlier how kinase and redox signals generated in NE-treated cardiac myoblasts are integrated at multiple *cis* regulatory elements in the target genes [30]. In reiteration, we now demonstrate that three prototype genes for hypertrophic response viz., ANP, β-, and α-MHC; modulated by NE remained to their baseline levels by the selective inhibition of Nox2. This observation further exemplifies the seamless integration of the ROS and kinase signaling we had demonstrated earlier [30]. Such integration is further confirmed by the prevention of the induction of the one promoter exclusively regulated by the transcription factors AP-1, and two others, i.e., of ANP and FosB, considered as the prototype of adrenergic signaling; upon selective inhibition of Nox2. Although the specific inhibition of Nox2 by the peptide inhibitor gp-91-ds-tat has been shown by numerous studies [48], considering our emphasis on the pivotal role of Nox2 in adrenergic signaling, we also validated our claim by using a dominant negative mutant of p22phox which hampers the generation of ROS from Nox2 isoform only. This mutant also completely blocked the induction of FosB, ANP, and AP-1 promoters induced by NE. The rational for using these promoters for the validation of Nox2 signaling is that these are at the end points of the kinase and ROS signals generated at the cell surface by the ligand, i.e., NE.

Taken together, our study firmly establishes the close interaction between the conventional kinase signaling from the adrenergic receptors and the emergent ROS signaling from Nox2 as the key mediator of adrenergic responses in the cardiac myoblasts.

Acknowledgements This work was supported by The Department of Biotechnology, Government of India, under Grant (BT/PR4268/BRB/10/1016/2011), awarded to SKG. NS is a recipient of a JRF/SRF from the Indian Council of Medical Research, Government of India.

Compiance with ethical standards

Ethical approval This article does not contain any studies performed with animals.

References

1. Ho E, Karimi Galougahi K, Liu C-C et al (2013) Biological markers of oxidative stress: applications to cardiovascular research and practice. Redox Biol 1:483–491. doi:10.1016/j.redox.2013.07.006
2. Murray TVA, Ahmad A, Brewer AC (2014) Reactive oxygen at the heart of metabolism. Trends Cardiovasc Med 24:113–120. doi:10.1016/j.tcm.2013.09.003
3. Zhang Y, Tocchetti CG, Krieg T, Moens AL (2012) Oxidative and nitrosative stress in the maintenance of myocardial function. Free Radic Biol Med 53:1531–1540. doi:10.1016/j.freeradbiomed.2012.07.010
4. Sawyer DB (2011) Oxidative stress in heart failure: what are we missing? Am J Med Sci 342:120–124. doi:10.1097/MAJ.0b013e3182249fcd
5. Wadley AJ, Aldred S, Coles SJ (2016) An unexplored role for Peroxiredoxin in exercise-induced redox signalling? Redox Biol 8:51–58. doi:10.1016/j.redox.2015.10.003
6. Forman HJ, Ursini F, Maiorino M (2014) An overview of mechanisms of redox signaling. J Mol Cell Cardiol 73:2–9. doi:10.1016/j.yjmcc.2014.01.018
7. Latimer HR, Veal EA (2016) Peroxiredoxins in regulation of MAPK signalling pathways; sensors and barriers to signal transduction. Mol Cells 39:40–45. doi:10.14348/molcells.2016.2327
8. Lee J-G, Baek K, Soetandyo N, Ye Y (2013) Reversible inactivation of deubiquitinases by reactive oxygen species in vitro and in cells. Nat Commun 4:1568. doi:10.1038/ncomms2532

9. Stangherlin A, Reddy AB (2013) Regulation of circadian clocks by redox homeostasis. J Biol Chem 288:26505–26511. doi:10.1074/jbc.R113.457564
10. Groitl B, Jakob U (2014) Thiol-based redox switches. Biochim Biophys Acta 1844:1335–1343. doi:10.1016/j.bbapap.2014.03.007
11. Madamanchi NR, Runge MS (2013) Redox signaling in cardiovascular health and disease. Free Radic Biol Med 61:473–501. doi:10.1016/j.freeradbiomed.2013.04.001
12. Ciccarelli M, Santulli G, Pascale V et al (2013) Adrenergic receptors and metabolism: role in development of cardiovascular disease. Front Physiol 4:265. doi:10.3389/fphys.2013.00265
13. Ferrara N, Komici K, Corbi G et al (2014) β-adrenergic receptor responsiveness in aging heart and clinical implications. Front Physiol 4:396. doi:10.3389/fphys.2013.00396
14. Clerk A (2003) The radical balance between life and death. J Mol Cell Cardiol 35:599–602
15. Fu Y-C, Chi C-S, Yin S-C et al (2004) Norepinephrine induces apoptosis in neonatal rat cardiomyocytes through a reactive oxygen species-TNF alpha-caspase signaling pathway. Cardiovasc Res 62:558–567. doi:10.1016/j.cardiores.2004.01.039
16. Gupta MK, Neelakantan TV, Sanghamitra M et al (2006) An assessment of the role of reactive oxygen species and redox signaling in norepinephrine-induced apoptosis and hypertrophy of H9c2 cardiac myoblasts. Antioxid Redox Signal 8:1081–1093. doi:10.1089/ars.2006.8.1081
17. Thakur A, Alam MJ, Ajayakumar MR et al (2015) Norepinephrine-induced apoptotic and hypertrophic responses in H9c2 cardiac myoblasts are characterized by different repertoire of reactive oxygen species generation. Redox Biol 5:243–252. doi:10.1016/j.redox.2015.05.005
18. Sirokmány G, Donkó Á, Geiszt M (2016) Nox/Duox family of NADPH oxidases: lessons from knockout mouse models. Trends Pharmacol Sci 37:318–327. doi:10.1016/j.tips.2016.01.006
19. von Löhneysen K, Noack D, Wood MR et al (2010) Structural insights into Nox4 and Nox2: motifs involved in function and cellular localization. Mol Cell Biol 30:961–975. doi:10.1128/MCB.01393-09
20. Heppner DE, van der Vliet A (2016) Redox-dependent regulation of epidermal growth factor receptor signaling. Redox Biol 8:24–27. doi:10.1016/j.redox.2015.12.002
21. Spencer NY, Engelhardt JF (2014) The basic biology of redoxosomes in cytokine-mediated signal transduction and implications for disease-specific therapies. Biochemistry (Mosc) 53:1551–1564. doi:10.1021/bi401719r
22. Brandes RP, Weissmann N, Schröder K (2014) Nox family NADPH oxidases: molecular mechanisms of activation. Free Radic Biol Med 76:208–226. doi:10.1016/j.freeradbiomed.2014.07.046
23. Granger DN, Kvietys PR (2015) Reperfusion injury and reactive oxygen species: the evolution of a concept. Redox Biol 6:524–551. doi:10.1016/j.redox.2015.08.020
24. Lassègue B, San Martín A, Griendling KK (2012) Biochemistry, physiology, and pathophysiology of NADPH oxidases in the cardiovascular system. Circ Res 110:1364–1390. doi:10.1161/CIRCRESAHA.111.243972
25. Fisher AB (2009) Redox signaling across cell membranes. Antioxid Redox Signal 11:1349–1356. doi:10.1089/ars.2008.2378
26. Theccanat T, Philip JL, Razzaque AM et al (2016) Regulation of cellular oxidative stress and apoptosis by G protein-coupled receptor kinase-2; The role of NADPH oxidase 4. Cell Signal 28:190–203. doi:10.1016/j.cellsig.2015.11.013
27. Kawahara T, Ritsick D, Cheng G, Lambeth JD (2005) Point mutations in the proline-rich region of p22phox are dominant inhibitors of Nox1- and Nox2-dependent reactive oxygen generation. J Biol Chem 280:31859–31869. doi:10.1074/jbc.M501882200
28. Malinouski M, Zhou Y, Belousov VV et al (2011) Hydrogen peroxide probes directed to different cellular compartments. PLoS One 6:e14564. doi:10.1371/journal.pone.0014564
29. Burch PM, Yuan Z, Loonen A, Heintz NH (2004) An extracellular signal-regulated kinase 1- and 2-dependent program of chromatin trafficking of c-Fos and Fra-1 is required for cyclin D1 expression during cell cycle reentry. Mol Cell Biol 24:4696–4709. doi:10.1128/MCB.24.11.4696-4709.2004
30. Jindal E, Goswami SK (2011) In cardiac myoblasts, cellular redox regulates FosB and Fra-1 through multiple cis-regulatory modules. Free Radic Biol Med 51:1512–1521. doi:10.1016/j.freeradbiomed.2011.07.008
31. Belousov VV, Fradkov AF, Lukyanov KA et al (2006) Genetically encoded fluorescent indicator for intracellular hydrogen peroxide. Nat Methods 3:281–286. doi:10.1038/nmeth866
32. Banerjee P, Bandyopadhyay A (2014) Cytosolic dynamics of annexin A6 trigger feedback regulation of hypertrophy via atrial natriuretic peptide in cardiomyocytes. J Biol Chem 289:5371–5385. doi:10.1074/jbc.M113.514810
33. Yariswamy M, Yoshida T, Valente AJ et al (2016) Cardiac-restricted overexpression of TRAF3 interacting protein 2 (TRAF3IP2) results in spontaneous development of myocardial hypertrophy, fibrosis, and dysfunction. J Biol Chem 291:19425–19436. doi:10.1074/jbc.M116.724138
34. Yan L, Zhang JD, Wang B et al (2013) Quercetin inhibits left ventricular hypertrophy in spontaneously hypertensive rats and inhibits angiotensin II-induced H9C2 cells hypertrophy by enhancing PPAR-γ expression and suppressing AP-1 activity. PLoS One 8:e72548. doi:10.1371/journal.pone.0072548
35. Windak R, Müller J, Felley A et al (2013) The AP-1 transcription factor c-Jun prevents stress-imposed maladaptive remodeling of the heart. PLoS One 8:e73294. doi:10.1371/journal.pone.0073294
36. Meng Q, Xia Y (2011) c-Jun, at the crossroad of the signaling network. Protein Cell 2:889–898. doi:10.1007/s13238-011-1113-3
37. Wang J, Paradis P, Aries A et al (2005) Convergence of protein kinase C and JAK-STAT signaling on transcription factor GATA-4. Mol Cell Biol 25:9829–9844. doi:10.1128/MCB.25.22.9829-9844.2005
38. Knowlton KU, Baracchini E, Ross RS et al (1991) Co-regulation of the atrial natriuretic factor and cardiac myosin light chain-2 genes during alpha-adrenergic stimulation of neonatal rat ventricular cells. Identification of cis sequences within an embryonic and a constitutive contractile protein gene which mediate inducible expression. J Biol Chem 266:7759–7768
39. Dey S, Sidor A, O'Rourke B (2016) Compartment-specific control of reactive oxygen species scavenging by antioxidant pathway enzymes. J Biol Chem 291:11185–11197. doi:10.1074/jbc.M116.726968
40. Schaar CE, Dues DJ, Spielbauer KK et al (2015) Mitochondrial and cytoplasmic ROS have opposing effects on lifespan. PLoS Genet 11:e1004972. doi:10.1371/journal.pgen.1004972
41. Maejima Y, Kuroda J, Matsushima S et al (2011) Regulation of myocardial growth and death by NADPH oxidase. J Mol Cell Cardiol 50:408–416. doi:10.1016/j.yjmcc.2010.12.018
42. Bell RM, Cave AC, Johar S et al (2005) Pivotal role of NOX-2-containing NADPH oxidase in early ischemic preconditioning. FASEB J Off Publ Fed Am Soc Exp Biol 19:2037–2039. doi:10.1096/fj.04-2774fje
43. Montezano AC, Touyz RM (2014) Reactive oxygen species, vascular Noxs, and hypertension: focus on translational and clinical research. Antioxid Redox Signal 20:164–182. doi:10.1089/ars.2013.5302

44. Jang S, Lewis TS, Powers C et al (2016) Elucidating mitochondrial electron transport chain supercomplexes in the heart during ischemia-reperfusion. Antioxid Redox Signal. doi:10.1089/ars.2016.6635
45. Qin F, Siwik DA, Pimentel DR et al (2014) Cytosolic H2O2 mediates hypertrophy, apoptosis, and decreased SERCA activity in mice with chronic hemodynamic overload. Am J Physiol Heart Circ Physiol 306:H1453–H1463. doi:10.1152/ajpheart.00084.2014
46. Matsushima S, Kuroda J, Zhai P et al (2016) Tyrosine kinase FYN negatively regulates NOX4 in cardiac remodeling. J Clin Investig 126:3403–3416. doi:10.1172/JCI85624
47. Burgoyne JR, Rudyk O, Cho H et al (2015) Deficient angiogenesis in redox-dead Cys17Ser PKARIα knock-in mice. Nat Commun 6:7920. doi:10.1038/ncomms8920
48. Derochette S, Serteyn D, Mouithys-Mickalad A et al (2015) EquiNox2: a new method to measure NADPH oxidase activity and to study effect of inhibitors and their interactions with the enzyme. Talanta 144:1252–1259. doi:10.1016/j.talanta.2015.08.007